ΠΑΝΕΠΙΣΤΗΜΙΟ ΚΡΗΤΗΣ-ΙΑΤΡΙΚΗ ΣΧΟΛΗ

ΜΕΤΑΠΤΥΧΙΑΚΟ ΠΡΟΓΡΑΜΜΑ ΚΥΤΤΑΡΙΚΗ ΚΑΙ

ΓΕΝΕΤΙΚΗ ΑΙΤΙΟΛΟΓΙΑ, ΔΙΑΓΝΩΣΤΙΚΗ ΚΑΙ

ΘΕΡΑΠΕΥΤΙΚΗ ΤΩΝ ΑΣΘΕΝΕΙΩΝ ΤΟΥ ΑΝΘΡΩΠΟΥ

ΔΙΔΑΚΤΟΡΙΚΗ ΔΙΑΤΡΙΒΗ

ΜΕΛΕΤΗ ΤΟΥ ΡΟΛΟΥ ΤΗΣ ΠΡΩΤΕΙΝΗΣ BCRP1 ΣΤΑ ΚΥΤΤΑΡΑ ΤΟΥ ΠΛΕΥΡΙΚΟΥ ΠΛΗΘΥΣΜΟΥ ΤΗΣ ΚΑΡΔΙΑΣ

ΚΩΝΣΤΑΝΤΙΝΑ-ΙΩΑΝΝΑ ΣΕΡΕΤΗ

ΙΟΥΝΙΟΣ 2012

UNIVERSITY OF CRETE-SCHOOL OF MEDICINE

GRADUATE PROGRAM IN CELLULAR AND

GENETIC ETIOLOGY, DIAGNOSIS AND

TREATMENT OF HUMAN DISEASES

PhD THESIS

THE ROLE OF BREAST CANCER RESISTANCE PROTEIN 1 (BCRP1) IN THE CARDIAC SIDE POPULATION CELLS

KONSTANTINA-IOANNA SERETI

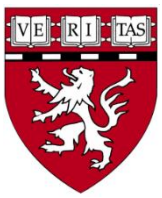

JUNE 2012

Ευχαριστίες

Θα ήθελα να εκφράσω ειλικρινή ευγνωμοσύνη στην επιβλέπουσα καθηγήτρια του διδακτορικού μου Δρ. Roglih Liao για την καθοδήγησή της καθόλη τη διάρκεια των σπουδών μου καθώς και για την υποστήριξή της τόσο σε επαγγελματικό όσο και σε προσωπικό επίπεδο.

Είμαι βαθύτατα ευγνώμων στον Δρ. Βασίλη Ζαννή και στο μεταπτυχιακό πρόγραμμα που μου επέτρεψαν να διευρύνω τους ορίζοντες μου και για τη συνεχή υποστηρίξη καθόλη τη διάρκεια των μεταπτυχιακών μου σπουδών.

Ιδιαίτερες ευχαριστίες σε όλα τα μέλη του εργαστηρίου CMRL που πέρα από συνάδελφοι είναι και φίλοι, για την πολύτιμη βοήθειά τους και τη δημιουργία ενός εξαιρετικού εργασιακού περιβάλλοντος.

Πάνω απ'όλους θέλω να ευχαριστήσω την καλύτερη οικογένεια του κόσμου, τους γονείς μου, Νικήτα και Ντίνα, και τις καλύτερές μου φίλες, τις αδελφές μου Πέννυ και Άντζυ για την αστείρευτη αγάπη και υποστήριξή τους.

Τέλος, ένα μεγάλο ευχαριστώ στη νέα μου οικογένεια και συνοδοιπόρο σε όλο αυτό το ταξίδι, τον Άγγελο. Η αγάπη, η βοήθεια και η συνεχή ενθάρρυνσή του μου δίνουν δύναμη να ξεπερνώ τις δυσκολίες και κάνουν την κάθε μου μέρα ευτυχισμένη.

Acknowledgments

I would like to express my sincerest gratitude to my thesis supervisor Dr Ronglih Liao for her mentorship and guidance throughout my PhD as well as for her support in both professional and personal level.

I'm deeply grateful to Dr Vassilis Zannis and my graduate program for giving me the opportunity to expand my horizons and for their continuous support throughout my graduate studies.

Special thanks to all the members of the CMRL lab for their valuable assistance, for creating a great work environment and for being not just colleagues but friends.

I cannot thank enough the best family in the world, my parents Nikitas and Ntina and my best friends, my sisters Penny and Angie for their unconditional love and support.

Last, I would like to thank my new family and partner throughout this journey, Angelos. His love, help and constant encouragement give me strength to overcome difficulties and make my every day a celebration.

Στην οικογένειά μου

CONTENTS

ΠΕΡΙΛΗΨΗ

Οι καρδιαγγειακές παθήσεις αποτελούν την κύρια αιτία θανάτου στον ανεπτυγμένο κόσμο. Πρόσφατη επιστημονική πρόοδος έχει προσφέρει σημαντική βελτίωση τόσο στις μεθόδους θεραπείας της νόσου όσο και στην ποιότητα ζωής των ασθενών. Ωστόσο, με εξαίρεση τη μεταμόσχευση καρδιάς, η οποία αντιπροσωπεύει την πιο αποτελεσματική θεραπεία, καμία από τις υπάρχουσες θεραπείες δε στοχεύει στην αναγέννηση του κατεστραμμένου καρδιακού ιστού.

Η ανακάλυψη μιτωτικών καρδιομυοκυττάρων και πιο πρόσφατα εξωγενών και κυρίως ενδογενών καρδιακών πρόδρομων κυττάρων, έχει πλέον καταρρίψει την αντίληψη ότι η καρδιά αποτελεί ένα όργανο χωρίς αναγεννητική ικανότητα. Η αναγέννηση του καρδιακού ιστού μέσω κυτταρικής θεραπείας αποτελεί έναν πολλά υποσχόμενο ερευνητικό τομέα και έχει ανοίξει νέους ορίζοντες για τη θεραπεία των καρδιαγγειακών παθήσεων.

Τα «καρδιακά κύτταρα πλευρικού πληθυσμού» (cardiac side population cells, CSP cells) αποτελούν ενδογενή καρδιακά πρόδρομα κύτταρα. Η αναγνώριση των κυττάρων CSP βασίζεται στην ικανότητα μεμβρανικών μεταφορέων ABC, και ειδικότερα των πρωτεϊνών Abcg2 και Mdr1, να εξάγουν από το κυτταρόπλασμα τη χρωστική ουσία Hoechst 33342. Κάτω από κατάλληλες συνθήκες καλλιέργειας, τα κύτταρα CSP, έχουν την ικανότητα να διαφοροποιούνται σε όλους τους κύριους τύπους καρδιακών κυττάρων.

Οι πρωτεΐνες ABC εμπλέκονται στην μεταφορά διαφόρων ουσιών τόσο προς το εξωτερικό του κυττάρου όσο και μεταξύ των κυτταρικών οργανιδίων. Οι πρωτεΐνες Abcg2/Bcrp1 και Mdr1 ανακαλύφθηκαν σε κυτταρικές σειρές που είναι ανθεκτικές στην τοξική δράση αντικαρκινικών ουσιών και έχουν συσχετιστεί με την ανθεκτικότητα σε

φάρμακα χημειοθεραπείας που παρατηρείται σε αρκετούς καρκίνους. Επίσης, η πρωτεΐνη Abcg2/Bcrp1 έχει προστατευτικό ρόλο σε ευαίσθητους ιστούς όπως ο εγκέφαλος και το έμβρυο, εναντίον της εισόδου ξενοβιοτικών ουσιών διαμέσου του αιματοεγκεφαλικού φραγμού και του πλακούντα. Έχει επίσης προταθεί ότι ο μεταφορέας Abcg2 παρέχει προστασία από τον κυτταρικό θάνατο σε συνθήκες υποξίας. Η έκφραση του Abcg2 έχει επίσης συσχετισθεί με τον πολλαπλασιασμό των καρκινικών κυττάρων. Επιπλέον, ο μεταφορέας Abcg2 έχει αναγνωριστεί ως ο καθοριστικός παράγοντας για το φαινότυπο «πλευρικού πληθυσμού» (side population) στο μυελό των οστών (BMSP). Τέλος είναι αξιοσημείωτο ότι σε κύτταρα SP του μυελού των οστών η υπερέκφραση του Abcg2 προώθησε τον πολλαπλασιασμό των κυττάρων, ενώ η αναστολή του εμπόδισε τη διαφοροποίηση και την αιμοποιητική διαδικασία. Στην καρδιά έχει αποδειχθεί ότι ύστερα από τραυματισμό ο Abcg2, προστατεύοντας τα ενδοθηλιακά κύτταρα, έχει ευεργετική δράση στη λειτουργία του μυοκαρδίου. Ωστόσο, η συμβολή του στα καρδιακά SP παραμένει ασαφής.

Το βασικό χαρακτηριστικό των πρόδρομων κυττάρων είναι η ικανότητα τους να αυτο-ανανεώνονται (self-renewal) και να διαφοροποιούνται (differentiation) προς εξειδικευμένα κύτταρα κατά τη διάρκεια μίας κυτταρικής διαίρεσης. Η ομοιόσταση των πρόδρομων κυττάρων επιτυγχάνεται μέσα από μια ισορροπία μεταξύ συμμετρικών και ασύμμετρων κυτταρικών διαιρέσεων. Η ρύθμιση αυτής της ισορροπίας έχει ιδιαίτερη σημασία τόσο για τα πρόδρομα όσο και για τα καρκινικά κύτταρα. Απορρύθμιση των κυτταρικών διαιρέσεων μπορεί να οδηγήσει σε εξάντληση του αριθμού των πρόδρομων κυττάρων ή αντίστοιχα τον υπερπολλαπλασιασμό των καρκινικών κυττάρων. Η μοίρα που θα ακολουθήσει το πρόδρομο κύτταρο αποφασίζεται κατά τη διάρκεια του κυτταρικού κύκλου και πιο συγκεκριμένα κατά τη φάση G1. Συμφώνα με την υπόθεση του «μήκους

του κυτταρικού κύκλου» (“Cell cycle length” hypothesis) η επιμήκυνση της φάσης G1 συνδέεται με την ασύμμετρη διαίρεση και διαφοροποίηση των βλαστικών/πρόδρομων κυττάρων.

Ο στόχος της παρούσας μελέτης είναι η διερεύνηση του ρόλου του μεταφορέα Abcg2 στο φαινότυπο και την ομοιόσταση των κυττάρων CSP, καθώς και στην *in vivo* επίδρασή του στο πλαίσιο εμφράγματος του μυοκαρδίου.

Ποντίκια WT, Abcg2-KO και Mdr1a/b-KO, από διαφορετικά αναπτυξιακά στάδια, χρησιμοποιήθηκαν ώστε να εξεταστεί η σχετική συνεισφορά του Abcg2 στον καρδιακό φαινότυπο SP. Η επίδραση του Abcg2 στον πολλαπλασιασμό και την επιβίωση των κυττάρων CSP μελετήθηκε μέσω διάφορων μεθόδων. Τα αποτελέσματα επιβεβαιώθηκαν περαιτέρω μέσω τεχνικών κέρδους και απώλειας λειτουργίας (gain/loss of function). Η σημασία της ικανότητας εξαγωγής ουσιών από τον Abcg2 στον πολλαπλασιασμό των κυττάρων CSP εξετάστηκε μέσω μεταλλαξιγένεσης. Μέθοδοι όπως ανοσο-κυτταροχημική ανίχνευση πρωτεϊνών του κυτταρικού κύκλου, συστήματα αναφοράς δεικτών του κυτταρικού κύκλου με λεντι-ιούς και RT-PCR χρησιμοποιήθηκαν σε συνδυασμό με ζωντανή απεικόνιση κυττάρων, για τον προσδιορισμό του κυτταρικού κύκλου WT και Abcg2-KO κυττάρων CSP. Ο ρόλος του Abcg2 στην ασύμμετρη διαίρεση και την καρδιακή διαφοροποίηση εξετάστηκε μέσω ανοσο-κυτταροχημικής ανίχνευσης πρωτεϊνών που καθορίζουν την κυτταρική μοίρα και καρδιακών δεικτών αντίστοιχα. Επιπλέον, μοντέλα καρδιακής βλάβης, όπως ισχαιμία-επαναιμάτωση και έμφραγμα του μυοκαρδίου χρησιμοποιήθηκαν ώστε να διερευνηθεί ο *in vivo* ρόλος του Abcg2. Τέλος, αναλύθηκε η έκφραση μεμβρανικών πρωτεϊνών καθώς και η ικανότητα πολλαπλασιασμού και διαφοροποίησης των κυττάρων CSP από διαφορετικά αναπτυξιακά στάδια ποντικού.

Η παρούσα διατριβή αποκαλύπτει για πρώτη φορά ότι η συμβολή του μεταφορέα Abcg2 στο φαινότυπο CSP εξαρτάται από το αναπτυξιακό στάδιο. Επιπρόσθετα, ο μεταφορέας Abcg2 βρέθηκε ότι προστατεύει τα κύτταρα CSP από κυτταρικό θάνατο και προάγει τον κυτταρικό τους κύκλο, ενώ παράλληλα αναστέλλει την ασύμμετρη διαίρεση και τη διαφοροποίησή τους. Τέλος, η εργασία μου παρέχει *in vivo* δεδομένα που υποστηρίζουν ότι ο μεταφορέας Abcg2 έχει σημαντικό προστατευτικό ρόλο μετά από έμφραγμα του μυοκαρδίου.

SUMMARY

Cardiovascular diseases represent the leading cause of death in the industrialized world. Several scientific advances have achieved significant improvement in disease treatment and patient quality of life. However, with the exception of heart transplantation which represents the most efficient treatment, none of the current therapies focus on replacing the lost cardiac tissue.

The identification of mitotic myocytes and more recently, of resident cardiac progenitor cells has abolished the long standing dogma that the heart is a terminally differentiated organ. Cardiac regeneration, through stem cell based therapies has become a promising area of research and has opened new horizons for the treatment of cardiovascular diseases.

Cardiac side population (CSP) cells represent a resident cardiac progenitor cell population. CSP cells are identified based on the ability of ABC-cassette membrane transporters to efflux the DNA-binding dye Hoechst 33342. ABC-transporters Abcg2 and Mdr1 have been shown to efficiently export Hoechst. Upon proper stimulation, CSP cells are able to differentiate into all major cardiac cell types.

Abcg2 and Mdr1 belong to the large family of ABC-transporters. ABC proteins are involved in the trafficking of a large variety of substrates across the cell membrane and intracellular organelles. Abcg2 and Mdr1 were initially identified in cancer drug resistant cells lines and have been associated with chemotherapy drug resistance observed in cancers. In particular, in addition to cancer resistance, Abcg2 has been suggested to play a protective role in crucial tissues such as the brain and fetus against xenobiotic transfer

through the blood-brain and placenta barriers. Abcg2 has also been shown to confer protection from cell death under hypoxic conditions. Most importantly, Abcg2 has been identified as the molecular determinant of the bone marrow SP phenotype. However, its contribution to the cardiac SP phenotype remains unclear.

Abcg2 expression has been further linked to the proliferation of cancer cells. Additionally, in bone marrow SP cells, Abcg2 over-expression promoted cell proliferation while its inhibition resulted in abrogation of hematopoiesis.

In the heart, Abcg2 expression has been demonstrated to be beneficial following injury by protecting microvascular endothelial cell function.

The fundamental characteristic of stem/progenitor cells is the capacity to self-renew and differentiate within one cell division. Stem/progenitor cell homeostasis is achieved through a balance between symmetric and asymmetric cell divisions. Regulation of the switch between these two types of division is of particular importance in normal and cancer stem cells. Deregulated divisions can lead to stem cell pool exhaustion or cancer cell over-proliferation.

Cell fate decisions are made during the cell cycle and particularly during the G1-phase. The "cell cycle length" hypothesis suggests that lengthening of G1 is associated and required for stem/progenitor cell asymmetric division and differentiation.

The goal of my study is to investigate the role of Abcg2 in the CSP phenotype and homeostasis as well as its effects *in vivo*, in a myocardial injury context.

CSP cells from WT, Abcg2-KO and Mdr1a/b-KO mice from different developmental stages were analyzed by flow cytometry to examine the relative contribution of each

transporter. The effects of Abcg2 on CSP cell proliferation and survival were determined through various methods. Gain- and loss-of-function approaches were utilized to confirm the results. Site-mutagenesis allowed the assessment of the role of Abcg2 efflux capacity in CSP proliferation. Cell cycle marker staining, lentiviral cell cycle indicators and RT-PCR based gene arrays were used in combination with live cell imaging, to delineate the cell cycle profile of WT and Abcg2-deficient CSP cells. Immuno-cytochemical staining for cell fate determinants and cardiac markers, revealed the effects of Abcg2 on CSP asymmetric division and cardiomyogenic differentiation. Moreover, ischemia-reperfusion and myocardial infarction were used as myocardial injury models to investigate the *in vivo* role of Abcg2. Lastly, the surface marker expression, proliferation and differentiation capacity of CSP cells from different developmental stages were analyzed.

My work reveals for the first time that Abcg2 has an age-dependent contribution to the CSP phenotype. Moreover, Abcg2 was found to promote CSP cell cycle progression and survival while inhibiting their asymmetric division and differentiation. Finally, my work provides *in vivo* evidence supporting that Abcg2 plays a protective role following myocardial injury.

INTRODUCTION

CARDIOVASCULAR DISEASES

Cardiovascular diseases (CVD) represent the leading cause of death worldwide [9]. Only in the United States, CVD claim one life every 39 seconds, accounting for more deaths (32.8% in 2008) than cancer, respiratory disease (CLRD: Chronic Lower Respiratory disease) and accidents combined. More than one in three individuals suffers from one or more types of CVD. As a consequence the estimated direct and indirect costs for CVD were $297.7 billion in 2008 and are projected to reach $818 billion between 2010 and 2030. Similarly, in Greece, the most recent statistics revealed that in 2009, CVD accounted for 34.86% and 30.43% of total deaths per 100000 male and female individuals respectively [10].

CARDIAC REMODELING

The pathophysiologic response of the heart to injury following loss of cardiac tissue, due to myocardial infarction or pressure overload-induced hypertrophy, leading to chronic heart failure, is called cardiac remodeling. This initially adaptive response involves cardiomyocyte hypertrophy and death as well as fibrosis and activation of matrix metalloproteinases [11]. Following myocardial infarction, the necrotic area is replaced by fibrotic tissue (scar formation) and the infarcted wall becomes thinner. In order to increase

stroke volume and maintain normal cardiac output, the LV chamber dilates. Myocyte hypertrophy in the infarct remote area leads to increased wall thickness and changes in chamber configuration resulting in poor ventricular performance [5] (Figure 1).

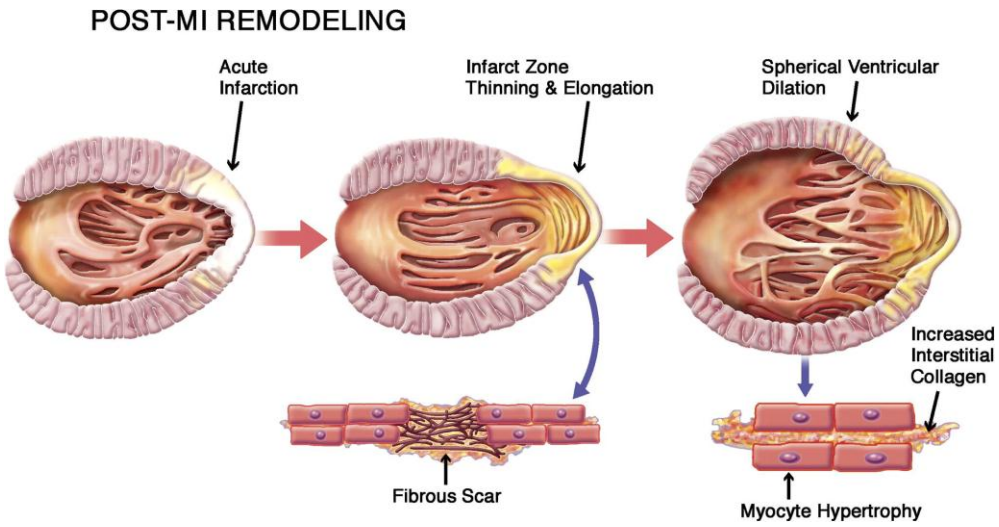

Figure 1: Post-MI cardiac remodeling: upon myocardial infarction a fibrous scar is formed followed by thinning and elongation of the infarcted area. The ventricle is further dilated and acquires a spherical configuration. Myocytes undergoes hypertrophy and production of interstitial collagen is increased [5].

THERAPEUTIC STRATEGIES

The majority of therapeutic strategies are focusing on the causes of heart failure while current treatment options include drugs, such as β-blockers [12], ACE inhibitors (Angiotensin Converting Enzyme), angiotensin receptor antagonists or diuretics [13], and invasive procedures including drug eluting stents [14], coronary artery bypass grafting [15], left ventricular (LV) reconstruction [16], mitral valve repair, pacemakers [17] as well as implantation of left ventricular assist devices (LVAD) [18]. Despite, the remarkable

improvement in heart failure prognosis provided by all available therapies, none of them targets the fundamental issue of the disease which is the loss of myocardial tissue. To date the most effective treatment encompassing cardiomyocyte loss is heart transplantation. Nevertheless, issues such as donor heart availability as well as immune rejection call for the development of new, less invasive therapies.

CELL-BASED THERAPIES

The option of stem cell-based therapies holds great promise and some first clinical trials have already been undertaken. Initial stem cell-based clinical trials involved satellite cells from skeletal muscle. These cells appeared as good candidates for cardiac transplantation since they exhibit increased survival during ischemia [19]. Moreover, animal studies demonstrated that cardiac function was ameliorated and remodeling was limited after administration of the cells to infracted hearts [19, 20]. However, no significant benefit was observed in clinical trials using these cells [21].

Bone marrow-derived stem cells have been widely used in clinical trials for the treatment of heart failure [22]. Based on their ability to differentiate into cardiomyocytes *in vitro* as well as their ease of availability, hematopoietic stem cells have been used in a number of studies. Clinical trials using circulating hematopoietic progenitors or bone marrow mononuclear cells produced some initial encouraging results; however additional studies demonstrated minimal long term beneficial effects [22-26]. Nevertheless, the meta-analysis of a large number of studies revealed an overall benefit of bone marrow cell

administration in ejection fraction (5.4% improvement) and infarct size (5.49% decrease) [23].

Bone marrow-derived mesenchymal (MSC) and endothelial (EPC) stem/progenitor cells have also been used in clinical trials as therapeutic strategies for myocardial infarction (reviewed in [24]. Both populations can generate cardiomyocytes *in vitro* while administration to patients with myocardial infarction resulted in marginal improvement of cardiac function. Their utilization however presents some difficulties due to the wide range of differentiation capacity. Namely, MSCs were shown to generate osteoblasts within the ventricle whereas EPCs have the ability to differentiate into various cell types.

Overall, to date cell-based clinical therapies have provided marginal benefits for heart failure patients and the discovery of new therapeutic approaches is imperative.

CARDIAC CELL TURNOVER

Until recently, the heart was viewed as a terminally differentiated organ with no self-renewal ability [25, 26]. It was widely believed that the heart sustains its function until the death of an individual with the same or less cells present at birth and that the only way of postnatal cardiac growth occurs through cell size growth (hypertrophy) and not proliferation (hyperplasia). This perception was mainly supported by the very low frequency of myocardial tumors in the population as well as the lack of cardiomyocyte DNA synthesis in adult hearts [31, 32]. Analysis of tritiated thymidine incorporation, demonstrated that during embryonic mouse development cardiomyocyte DNA synthesis occurs in two phases. The first peak is observed during fetal life and is followed by a

significant drop early postnatally. The second DNA synthesis wave is observed between post-natal day 4 and 10. Microscopic observation of DAPI stained nuclei revealed that the second DNA synthesis phase is attributed to binucleation and not myocyte proliferation [27]. Further supporting the non-dividing nature of myocytes, Soonpaa and colleagues using a similar approach demonstrated that myocardial injury (cauterization) is unable to activate myocyte DNA synthesis. According to these studies, each cardiomyocyte is as old as the individual and cardiomyocyte cell death should occur scarcely [28].

Myocyte proliferation has been a subject of debate for decades. Studies demonstrating DNA synthesis in adult rats [29-32] as well as myocyte proliferation *in vitro* [33] have challenged the long standing idea of the cardiomyocytes as fully differentiated cells. More recent studies have definitely abolished this old dogma and currently it is widely accepted that the heart is a self renewing organ [7, 34-39]. Beltrami et al demonstrated that new cardiomyocytes are generated following myocardial infarction. Cardiac tissue from patients that succumbed to myocardial infarction was immuno-stained for the mitotic marker Ki67 and compared to tissue from healthy hearts. Interestingly, 4% of the

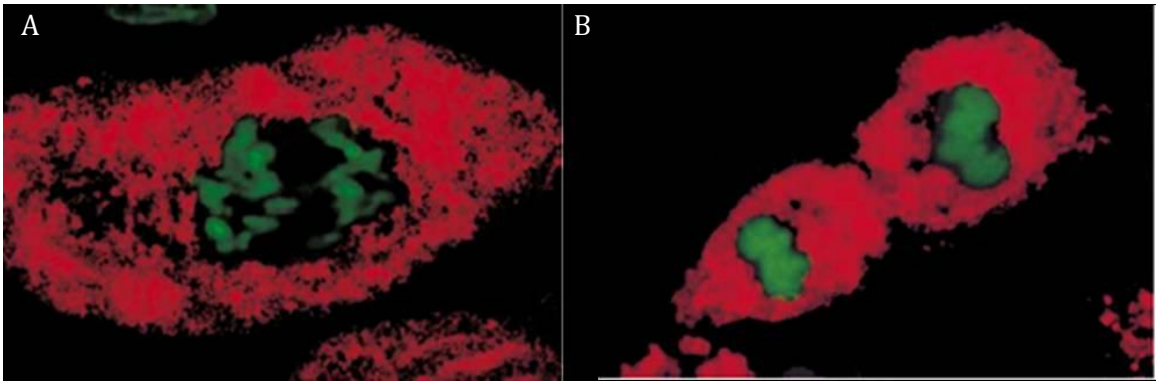

Figure 2: Cycling myocytes in infarcted heart. A) α-sarcomeric actin (red) positive cardiomyocytes in metaphase as evidenced by chromosome organization (propidium iodide, green) and B) dividing myocyte in cytokinesis [7].

cardiomyocytes found in the infarct border zone expressed Ki67 and this percentage was reduced to 1% in the remote area. Moreover, Ki67 labeling was accompanied by cytokinesis further demonstrating myocyte proliferation. Cycling myocytes were also detected in the healthy hearts albeit at lower numbers (0.11%) [7] (Figure 2).

In a seminal study, Bergmann et al used the cellular levels of C^{14} as a cell birth date marker and was able to provide compelling evidence supporting cardiomyocyte proliferation during the lifetime of an individual [1]. Nuclear bomb testing in the 1950s led to an increase in the atmospheric C^{14} levels which dramatically dropped after the Limited Nuclear Test Ban Treaty in 1963. As a consequence C^{14} incorporated in the DNA of each living organism. Based on the fact that C^{14} levels in each cell correspond to the atmospheric levels at the date the cell was born, Bergmann et al analyzed individuals born up to 22 years

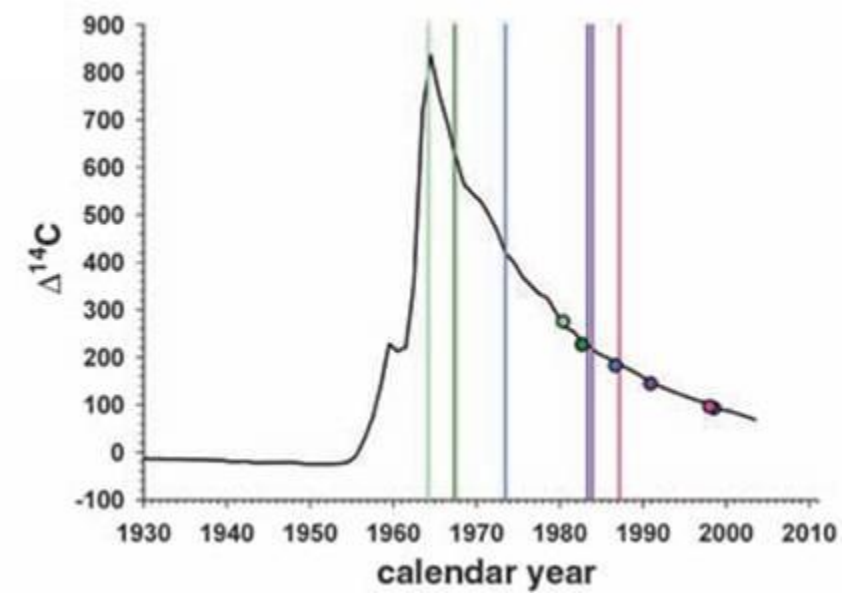

Figure 3: Cardiac cell turnover. The black curve corresponds to the atmospheric C^{14} levels from 1930 to 2010. Each circle represents the C^{14} levels in genomic DNA of the cardiomyocytes of each individual and the corresponding vertical lines indicate the date of birth of the individual. Cellular C^{14} levels correspond to the atmospheric levels the time the cell was born [2].

before the nuclear testing and demonstrated that C^{14} levels in cardiomyocytes were increased compared to the prevalent atmospheric levels before the bombings. These results clearly suggest that cardiomyocytes are able to renew during adulthood. This study further suggests that the cardiomyocyte renewal rate decreases with age and that during an average life span approximately 50% of the cardiomyocytes will be exchanged [1] (Figure 3).

In line with this report, Kajstura et al demonstrated that the cells (myocytes and non-myocytes) of the adult human heart are renewed several times during the lifetime of an individual [40]. The authors utilized post-mortem heart samples from cancer patients who had been treated with the radiosensitiser iododeoxyuridine (IdU). IdU is a nucleotide analogue that incorporates into the DNA during DNA synthesis enabling the detection of newly formed cells. This analysis revealed that approximately 22% of new cardiac-myocytes are produced every year [40].

Overall, these studies point out that the adult heart whether it is human or murine, indeed possesses regenerative potential which decreases with age and increases after injury. Slight discrepancies observed in the reported extent of cardiomyocyte renewal could be due to the experimental settings of each study as well as the models used. It still remains unclear whether these newly generated cardiomyocytes derive from pre-existing cardiomyocytes that re-enter the cell cycle or the differentiation of resident or extra-cardiac progenitor/stem cells.

An elegant study by Hsieh and colleagues, confirmed myocyte turn-over using a fate mapping approach. The authors suggest that cardiomyocytes are able to regenerate from stem/progenitor cells following myocardial injury [41]. A double transgenic mouse was generated by the cross-breeding of a mouse expressing a tamoxifen-inducible Cre recombinase under the control of the cardiomyocyte specific α-myosin heavy chain promoter (MerCreMer mice) with a reporter mouse (ZEG) constitutively expressing β-galactosidase. Upon, tamoxifen treatment and Cre expression, a lox-P flanked stop sequence is removed and β-galactosidase expression is replaced by GFP expression. The strength of this method relies on the fact that following tamoxifen withdrawal, the majority of cardiomyocytes is GFP positive and if new myocyte formation occurs, the percentage of GFP positive cells will be decreased. The authors demonstrated that three months following myocardial infarction the proportion of GFP positive cardiomyocytes decreased significantly. Namely, a 15.3% decrease was detected in the infarct border zone and 7.1% in the area remote from the infarct. Similar effects were observed following pressure-overload induced hypertrophy. These results clearly indicate that the newly formed GFP-negative cardiomyocytes originate from α-myosin heavy chain and thus GFP-negative stem/progenitor cells. In line with this hypothesis is the increased expression of common stem cell markers such as c-kit and Nanog in the infarct border area. It is noteworthy that no significant regeneration was observed during normal aging [41].

The recent identification of resident cells with stem or progenitor cell characteristics that are able to regenerate the adult myocardium further supports the notion of cardiac regeneration and has opened new horizons in the cardiovascular field.

Using a variety of methodologies, several groups have revealed the existence of various populations of cardiac stem/progenitor cells. It still remains unclear whether these populations share a common parental cell and thus represent different stages in the stem cell hierarchy or whether they constitute population with distinct developmental origins. Nonetheless, these cells possess self-renewal and differentiation capacity, the characteristics that define stem/progenitor cells. The methods used to identify and isolate cardiac progenitor cells vary from cell surface marker expression (ckit [35], sca1 [38]) and functional phenotype (Hoechst efflux [41]) to surface marker independent isolation methods such as cardiosphere formation [37] and expression of transcription factors (Islet1 [36], Wt1 [42]). All these populations share a common feature, that is, their ability to generate all cardiac cell types-cardiomyocytes, endothelial cells and smooth muscle cells-upon proper stimulation.

CKIT POSITIVE CELLS

Beltrami et al, first identified and characterized cardiac cells expressing the stem cell marker c-kit [35]. c-kit, a tyrosine kinase receptor is a common stem cell marker of various adult stem cells [43]. In the heart, ckit has been used to identify cardiac stem cells from several model organisms [35, 44, 45] as well as from humans [46] and to date ckit positive cells represent the most well studied cardiac stem cell population. Cardiac ckit stem/progenitor cells is a rare population (0.1%) of cells negative for the blood lineage markers (Lin^-) and positive for other common stem cell markers such as Sca1 and Mdr1. They are mainly found in small clusters in the interstitial space with higher density in the apex and atria. A small number of ckit cells in each cluster express the cardiac transcription

factors Gata4, Nkx2.5 and Mef2c as well as sarcomeric proteins representing cells at early stages of cardiac differentiation. ckit cells were found to be self-renewing, clonogenic and multipotent. Notably, when ckit cells were injected in the injured myocardium of rats they were able to engraft in the infarct area and generate new cardiomyocytes, capillaries and vessels and significantly improve cardiac performance [35]. Similarly, ckit^{+} stem/progenitor cells delivered through intracoronary injection were shown to decrease infarct size while restraining myocardial remodeling following 5 weeks after MI in rats [47]. Most importantly, ckit^{+} cardiac progenitors were isolated from human heart tissue and were found to be clonogenic and able to generate cardiomyocytes as well as endothelial and smooth muscle cells both *in vitro* and *in vivo* after injection in infarcted mouse hearts [46].

More recently, ckit positive stem cells have entered a phase I clinical trial (SCIPIO) [48]. ckit positive stem cells isolated from the atria of patients with post-infarction cardiac dysfunction were expanded in culture and reintroduced (one million cells) to the patient by intracoronary infusion approximately four months following bypass surgery. Initial results from 7-14 patients, revealed that autologous ckit positive stem cell administration improved cardiac function and decreased infarct size. Although preliminary, these results are very encouraging and data from more patients are anticipated with great interest.

SCA1 POSITIVE CELLS

In 2003 another population of resident adult cardiac stem/progenitor cells was described. Oh and colleagues [38] reported the existence of cells expressing the stem cell antigen 1 (Sca1), a glycosyl-phosphatidylinositol-anchored cell surface protein belonging to

the Ly6 antigen family. Sca1 is a common marker for hematopoietic stem cells, however, cardiac Sca1 positive stem/progenitor cells seem to represent a distinct population based on the lack of other hematopoietic marker expression (Lin^-) [38]. Sca1 positive cells express the endothelial marker CD31 but are negative for other endothelial cell markers such as Flt-1, Flk-1, vascular endothelial-cadherin and von Willebrand factor. Similar to ckit cells, Sca1 positive cells express cardiac transcription factors such as Gata4 and Mef2c but lack expression of cardiac structural genes, a characteristic of mature cardiomyocytes. Moreover, Sca1 positive cells are self-renewing and upon stimulation are able to differentiate into cardiomyocytes. Most importantly, when administered intravenously in mice following MI, they are able to home to the injured myocardium and differentiate into myocytes. However, high levels of cellular fusion with endogenous cardiomyocytes were observed [38]. More recent studies have further characterized this progenitor cell population and have confirmed their regenerative capacity both *in vitro* and *in vivo* [49, 50]. Interestingly, although a human homologue for Sca1 has not been identified yet, Smits and colleagues were able to isolate a population of cardiac progenitor cells from human biopsies by utilizing the antibody that recognizes the murine Sca1. These cells similarly to murine Sca1 positive stem/progenitor cell are able to self-renew and differentiate into cardiomyocytes [51].

CARDIOSPHERE-DERIVED STEM/PROGENITOR CELLS

Messina et al, were able to isolate from both mice and humans, another population of cardiac stem/progenitor cells that form clusters named cardiospheres under special culture conditions [37]. Cardiospheres consist of ckit, Sca1, Flk-1 and CD31 positive

proliferating cells mainly found at the center of the sphere and more differentiated cells in the periphery expressing cardiac and endothelial markers. These cardiosphere-derived cells (CDC) are self-renewing and clonogenic while they exhibit cardiac and endothelial cell differentiation capacity both *in vitro* and *in vivo*. Furthermore, intramyocardial injection of cardiospheres to mice following myocardial infarction demonstrated a significant increase in cardiac performance.

Recently, Makkar and colleagues reported the first results from a phase I clinical trial utilizing CDCs [52]. Intracoronary infusion of CDCs in patients having suffered from myocardial infarction resulted in significant decrease of the infarct size and corresponding increase of the viable tissue.

ISL1 AND WT1 POSITIVE CELLS

Laugwitz and colleagues [36] identified a population of cardiac stem cells that contribute to cardiac development. The LIM-homeodomain transcription factor Isl1 is highly expressed during embryonic development and marks a cell population that contributes to the formation of the heart. Islt1 positive stem/progenitors cells were isolated form neonatal mice are self-renewing and under appropriate conditions, exhibit a high cardiomyogenic differentiation capacity (25%). Isl1 positive cells were also detected in neonatal rat and human myocardium. Furthermore, by genetic fate mapping, Moretti et al demonstrated that embryonic Islt1 positive cells contribute to the formation of cardiac, endothelial and smooth muscle cells [53]. Nevertheless, the expression of Isl1 in the adult heart is scarce [36], limiting the usage of this population for cell based therapies.

Interestingly, a recent study by Ye et al, reported the expression of Isl1 cells in Sca1 positive cardiosphere-derived cells from post-MI adult mouse hearts [54]. These cells were able to differentiate into cardiomyocytes, endothelial and smooth muscle cells *in vitro*. When re-introduced to the infarcted myocardium, they were able to promote angiogenesis, generate endothelial and smooth muscle cells and ameliorate cardiac function [54].

Zhou et al, demonstrated the existence of a population of epicardial progenitors expressing the transcription factor Wt1 contributing to the embryonic cardiac development [42]. Similarly, another population of embryonic cardiac stem/progenitor cells of epicardial origin was identified based on the expression of the transcription factor Tbx18 [55]. Interestingly, both populations originate from a common Isl1 and Nkx2.5 double-positive parent population.

CARDIAC SIDE POPULATION CELLS

Hielrihy and colleagues were the first to report in 2002 the existence of resident cardiac progenitor cell in adult mice [41]. These so called cardiac side population (CSP) cells were isolated based on their ability to efflux the DNA binding Hoechst 33342 (Figure 4). Goodell et al first identified in murine bone marrow a population of cells expressing hematopoietic stem cell (HSC) markers and highly enriched in HSC activity. These cells were termed Side Population (SP) as they appear as a Hoechst low/negative population on the side of the main population (MP) of Hoechst retaining cells during dual wavelength FACS analysis. Moreover, bone marrow SP cells were shown to have strong long-term repopulating ability when injected in lethally irradiated mice. SP cells have been since

identified in a variety of tissues such as skeletal muscle, liver, lung, kidney, skin, mammary gland, testis, brain and heart [41, 56-62] as well as in several forms of cancer [63-68]. More recently CSP cells were identified in human left atrium biopsies [69] as well as in developing human hearts [70].

CSP cells isolated from adult mice represent approximately 1% of cardiomyocyte-excluded total mononuclear cells. Importantly, CSP cells are phenotypically different from HSCs since they do not express HSC markers such as CD34, ckit, Sca1, Flk2 and Thy1.1. Hierlihy et al further demonstrated that CSP cells can form colonies under appropriate culture conditions and differentiate into cardiomyocytes as evidenced by connexin-43 expression when co-cultured with mature cardiomyocytes [41]. Since this first report, several other laboratories have confirmed the existence of cardiac stem/progenitor cells with the SP phenotype and have further characterized them [6, 78, 79].

Martin et al demonstrated the existence of Sca1 positive CSP cells during embryonic

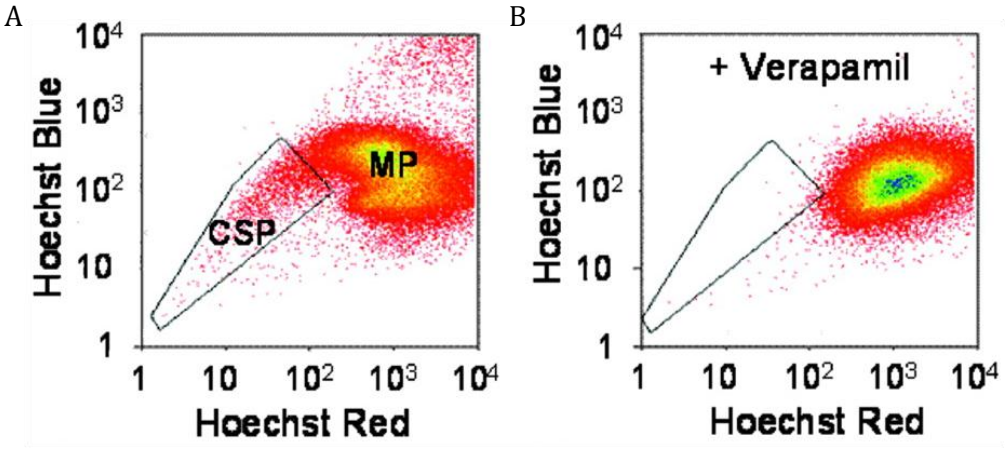

Figure 4: Cardiac side population cells (CSP). A) Characteristic flow cytometric analysis of cardiac mononuclear cells stained with Hoechst 33342 dye. CSP through active efflux of the dye appear as Hoechst low/negative compared to dye retaining main population cells (MP). B) adition of verapamil inhibits Hoechst efflux and is used as a negative control [6].

and post-natal development. The authors further proved that following co-culture with cardiac main population cells, CSP cells were able to express the sarcomeric protein α-actinin while when cultured in methylcellulose medium, CSP cells were able to proliferate and form hematopoietic colonies [71].

Pfister et al further characterized adult mouse CSP cells and demonstrated their self-renewing ability and multipotency [6]. CSP cells are able to proliferate and under proper stimulation can differentiate into cardiomyocytes, smooth muscle cells and endothelial cells. CSP cells are predominantly positive for Sca1 (84±2%), and negative for CD44 as well as the hematopoietic markers CD34 and CD45. It is noteworthy that CSP cells express ckit in the mRNA level but not at the protein level [6]. The lack of ckit protein expression could be due to proteolytic cleavage of the extracellular domain of the ckit receptor during the enzymatic digestion of the heart [72]. CSP cells were also found to express cardiac specific transcription factors such as Gata4, Nkx2.5 and Mef2c while markers of more mature cardiomyocytes such as α-sarcomeric actinin and α-myosin heavy chain were not detected [6]. Smooth muscle actin, desmin and the endothelial marker Tie-2 were only expressed in the mRNA level. Interestingly, within the Sca1 positive CSP population, 75% of the cells were found to be positive for the endothelial marker CD31. In an effort to further characterize CSP cells, the authors examined the cardiomyogenic capacity of $Sca1^{+}CD31^{+}$ CSP cells versus $Sca1^{+}CD31^{-}$ CSP cells. They demonstrated that CSP cells negative for CD31 when cultured in differentiation-promoting medium express early cardiomyogenic markers such as Gata4 and Mef2c as well as cardiomyocyte specific proteins such as α-sarcomeric actinin and Troponin-I albeit at a disorganized manner. Upon co-culture with adult rat ventricular cardiomyocytes CD31 negative CSP cells fully differentiated in mature cardiomyocytes as evidenced by expression of α-sarcomeric

protein in an organized striated manner (Figure 5). Furthermore, differentiated CSP cells exhibited contractile function and calcium transients identical to those of adjacent rat cardiomyocytes (Figure 5). In contrast CD31 positive CSP cells were unable to adhere to the culture dish and were negative for cardiac specific markers. The authors also addressed the possibility of cell fusion between CSP cells and cardiomyocytes. An elegant approach using the Cre/lox technology was followed, where CD31 negative CSP cells containing a loxP-flanked β-galactosidase cassette were co-cultured with cardiomyocytes expressing constitutively active Cre-recombinase. In the event of fusion β-galactosidase would be excised and GFP expression would be activated. No GFP positive cells were observed in co-cultures clearly suggesting that $CD31^{-}Sca1^{+}$ CSP cells exhibit cardiomyogenic capacity without cell fusion [6].

In line with these results, Oyama and colleagues demonstrated that CSP cells in murine post-natal hearts reside in a quiescent state (G0 phase) characteristic of stem cells. Moreover, CSP cells were able to differentiate into beating cardiomyocytes following oxytocin or trichostatin-A treatment and into osteocytes and adipocytes after osteogenic and adipogenic induction respectively [73]. Most importantly, the authors demonstrated that following intravenous transplantation in rats with cryoinjured hearts, CSP cells were able to home to the injured myocardium and generate cardiomyocytes, fibroblasts, endothelial and smooth muscle cells.

Interestingly, Mouquet et al illustrated the dynamic regulation of CSP cells homeostasis following injury [74]. Namely, the authors revealed that MI injury in adult mice results in an acute decrease of CSP cell number at one day post-MI followed by CSP pool restoration within one week. This replenishment of the CSP cell pool is due to active

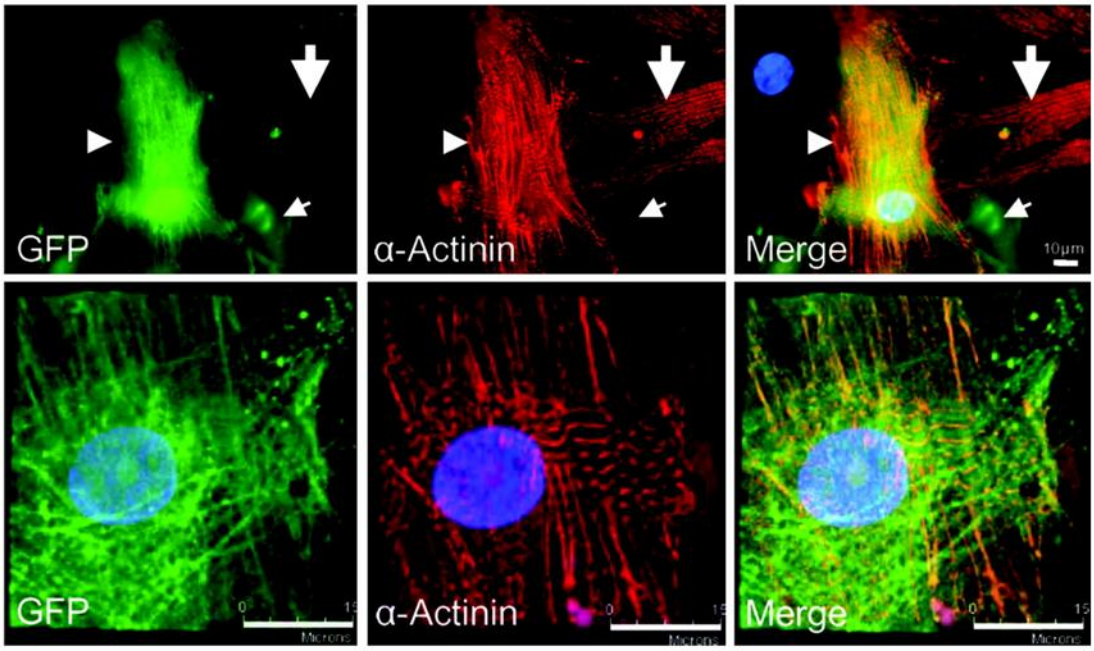

Figure 5: Cardiomyogenic differentiation of CSP cells following co-culture with adult cardiomyocytes. GFP positive CSP cells co-cultured with GFP negative cardiomyocytes express α-sarcomeric actinin (red) and exhibit organized striations [6].

proliferation of resident CSP cells as well as migration of bone marrow SP cells to the heart where they acquire a non-hematopoietic profile [74].

More recently, in an effort to further characterize the mechanisms regulating CSP proliferation and differentiation, Oikonomopoulos et al, revealed that the Wnt signaling pathway through activation of IGFBP3, inhibits CSP cell proliferation both *in vitro* and *in vivo* [75].

Considering the potential of the adult myocardium to regenerate a fact, the question that remains is why following myocardial injury the heart is unable to adequately repair itself and cardiac failure ensues. Resident cardiac stem/progenitor cells constitute a very promising tool for the development of cell based therapies for cardiac failure. However, the

inability to isolate large numbers of cells from patient tissue samples represents a pitfall that hinders their utilization. Further studies are required to decipher the mechanisms that control their homeostasis both *in vitro* as well as *in vivo*.

EMBRYONIC AND INDUCED PLURIPOTENT STEM CELLS

It is widely accepted that the more differentiated a cell is the less plasticity it has. Therefore, problems met with resident cardiac or bone marrow-derived stem cells could be overcome with the use of a more primitive cell population. Embryonic stem cells (ESC) are totipotent and thus represent the ideal therapeutic approach (reviewed in [76]). They are able to proliferate in culture while maintaining an undifferentiated state. ESCs were shown to differentiate into cardiomyocytes, endothelial and smooth muscle cells [77-79], while they engrafted and led to improvement of cardiac function when administered to animal models of MI [80, 81]. Nevertheless, there are several concerns for ESCs use for cardiac repair. Their ability to differentiate in cell lines from all the germ layers increases the possibility for teratoma formation. Moreover, graft rejection is a major concern since ESCs express HLA subclasses and immunosuppression is not an option. Finally, ethical issues concerning the source of ESCs have been raised both within the scientific community as well as in the wider public.

An alternative approach that overcomes several limitations of ESC is the use of induced pluripotent stem cells (iPS) (reviewed in [82]). Reprogramming of fibroblasts by introduction of embryonic genes Oct3/4, Klf4, c-Myc and Sox2 can induce an “embryonic-like” phenotype [73, 83]. Further investigations have limited the transfected genes to two

[84], as well as suggested new transfection methods that do not involve viral transfection, rendering this approach more clinically appropriate [85, 86]. More recently, cardiomyocytes were generated through fibroblast virus-free reprogramming [87]. Although very promising, cell reprogramming studies are still preliminary and additional work addressing the benefits and safety issues of iPS use as a therapeutic means for heart failure are required.

The ability of Side Population cells to efflux Hoechst 33342 is attributed to membrane transporters belonging to the ATP-Binding Cassette (ABC) transporter family [88, 89]. ABC transporters consist one of the largest known protein super-families found in all prokaryotes and eukaryotes. Approximately, 1100 proteins have been described. To date, 49 human ABC transporters have been classified in 7 subfamilies (ABCA, ABCB, ABCC, ABCD, ABCE, ABCF and ABCG). ABC transporters have multiple functions including trafficking (uptake or efflux) across the plasma membrane or intracellular membranes (ER, Golgi, mitochondria, peroxisome, lysosome) of a large variety of substrates such as metabolic products, drugs, toxins, endogenous lipids, peptides, nucleotides and sterols [90-94]. Members of the ABCE and ABCF subfamilies lack a transmembrane domain and play a role in mRNA translation [95-97]. They are also implicated in a number of inherited diseases in humans such as Tangier disease (ABCA1), adrenoleucodystrophy (ABCD1), cystic fibrosis (ABCC7), sitosterolemia (ABCG5, ABCG8) [98] (as well as in multidrug resistance (ABCB1, ABCC1, ABCG2) [90-94].

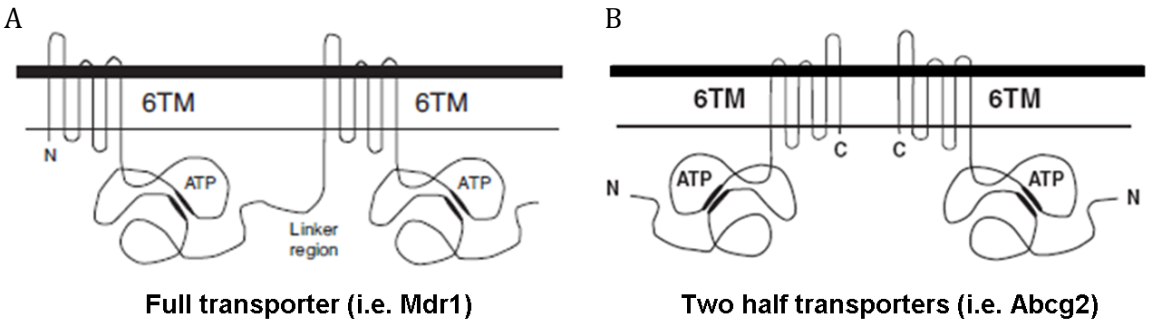

Figure 6: Schematic representation of A) a full and B) a half ABC transporter [adapted from [3]].

ABC proteins are characterized by a highly conserved cytoplasmic ATP-binding domain (ABC for ATP-binding cassette, or NBD for Nucleotide binding domain) usually associated with a hydrophobic TM (transmembrane) domain. The ABC domain consists of three highly conserved motifs: Walker A, B and the "ABC signature" or Walker C motifs. The latter is unique to ABC proteins and distinguishes them from other ATP-binding proteins. The Walker motifs are required for ATP binding and hydrolysis which provides the energy for the transport of the substrates across the membranes. The TM domains consist of 6-11 α-helices and contain the substrate recognition site [90-92].

Active ABC transporters consist of two ABC domains and at least two TM domains. These domains may be present within one polypeptide chain (full transporter) or within two separate proteins (half transporters) which need to either homo- or hetero-dimerize to be biologically functional [152-154] (Figure 8).

ABC TRANSPORTERS AND SIDE POPULATION PHENOTYPE

Two members of the ABC-transporter family, MDR1 and BCRP1, have been found to play a role in stem cell biology [2, 161-164]. The multidrug resistance protein (MDR1) also known as P-glycoprotein (P-gp) or ABCB1 (ABC transporter, family B) identified in drug resistant cancer cell lines, is a full transporter responsible for the efflux of a large number of substrates [99]. The Breast Cancer Resistance Protein 1 (BCRP1), also known as ABCG2 (ABC-transporter, family G), ABCP (placental ABC protein) or MXR (Mitoxantrone Resistance protein) was initially identified as a chemotherapeutic drug efflux pump in drug resistant cancer cell lines and later was found to be expressed in normal tissues [100-102].

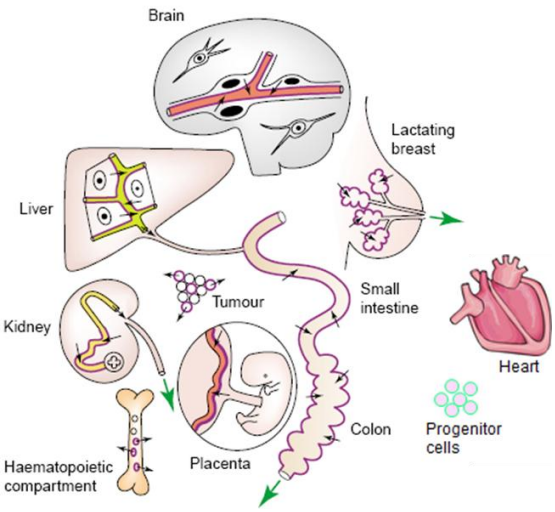

Figure 7: Abcg2 is expressed in a variety of organs and cells (adapted from [4]).

ABCG2 is a half transporter and it is strongly believed to form homo-dimers [103-106] or homo-tetramers [107] through disulfide-bonded cysteins in order to function. ABCG2 is N-glycosylated and unlike other half-transporters, it is predominantly localized to the plasma membrane [108, 109].

Abcg2 is expressed in a variety of tissues with highest expression in the placenta, blood-brain-barrier, kidney, small intestine, liver, testis, ovary and colon and at lower levels in tissues such as the heart and skeletal muscle [110] (Figure 9). Due to its varied tissue expression as well as the large number of Abcg2 substrates, its physiological function has been difficult to define. As mentioned earlier, Abcg2 was initially identified in cancer drug resistant cell lines [100-102]. In normal tissues such as the brain and placenta, Abcg2 has been suggested to play a protective role against xenobiotic transfer through the blood-brain barrier and the maternal-fetal barrier [111]. Abcg2 has been also shown to protect erythrocytes and stem cells from the accumulation of natural dietary compounds. Mice lacking Abcg2 developed sensitivity to a Chlorophyll breakdown product, the phototoxin pheophorbide a (porphyrin). They presented severe phototoxic skin lesions following light exposure as well as a form of protoporphyria [178, 179]. Moreover, other types of porphyrins such as heme and its precursor photoporphyrin IX (PPIX) were found to be Abcg2 substrates. Heme-accumulating Abcg2-KO HSCs were significantly more sensitive under hypoxic conditions

compared to WT cells and had reduced ability to form colonies [112]. More recently Abcg2 was identified as a urate transporter in kidney proximal tubules [113].

Microarray analysis revealed a common molecular signature for SP cells from different tissues that includes several cytoprotective factors related to the response to oxidative stress [114, 115]. Regulation of ROS production is tightly linked to the regulation of cellular homeostasis. Oxidative stress can inhibit or promote cell growth, senescence and death. High levels of ROS are toxic and can induce cell death by damaging DNA, proteins and lipids, whereas, low levels can activate signaling pathways leading to cell survival and proliferation [116-118]. Martin *et al* demonstrated that Abcg2 expression in C2C12 myoblasts activated several genes of the oxidative stress pathway present in the common SP molecular signature [114]. Furthermore, Abcg2 overexpression in mouse embryonic fibroblasts (MEF) resulted in production of low levels of reactive oxygen species which acted as a preconditioning mechanism that protected cells from H_2O_2 induced cell death [114].

Regulation of Abcg2 through hypoxia-induced factors (HIF) could account for the protective effects of the transporter in stress conditions. Several putative hypoxia-response elements (HRE) have been found in the promoter region of Abcg2 [112, 114]. In hematopoietic stem cells HIF-1α was shown to bind and up-regulate Abcg2 under hypoxic conditions [112]. Similarly, another member of the HIF family, HIF-2α, was proven to transcriptionally regulate Abcg2 in C2C12 myoblasts [114]. The anti-cancer drug resistance conferred by ABCG2, as well as its up-regulation under hypoxia are consistent with the fact that many solid tumors consist a hypoxic environment.

The Hoechst dye efflux ability of Side Population cells is attributed to the ABC-transporters Abcg2 and Mdr1. Although both proteins can efficiently efflux the dye, their

contribution in the SP phenotype differs in various tissues. Namely, in bone marrow SP (BMSP), Abcg2 is the molecular determinant of the phenotype. Zhou et al [89] demonstrated that mice lacking Mdr1a/b exhibited normal numbers of SP in their bone marrow. At the same time these cells expressed high levels of Abcg2 suggesting a possible involvement of Abcg2 is the BMSP phenotype [89]. The authors further supported this suggestion by generating Abcg2-KO mice and demonstrating that lack of Abcg2 depletes the bone marrow from SP cells with HSC characteristics [119]. The work by Jonker and colleagues provided further evidence supporting this notion [120]. The authors generated a transgenic mouse carrying deletions of both Abcg2 and Mdr1a/b genes (Abcg2-KO / Mdr1a/b-KO) and demonstrated that the BMSP observed in Mdr1a/b-KO animals (0.35±0.36%) almost completely disappears in the double knockout (0.05±0.08%). Moreover, treatment of cell preparations from WT and Mdr1a/b-KO mice with the Abcg2 specific inhibitor Ko143 abolished the SP phenotype (0.02±0.02% and 0.05±0.06% respectively). In accordance with these observations, the bone marrow of Abcg2-KO mice had a minor SP tail (0.05±0.07%) compared to WT and Mdr1a/b-KO animals.

Interestingly, in mammary gland SP the contribution of the two transporters differs [120]. Abcg2-KO mice exhibited a reduced but clear SP tail (0.04%) as compared to WT (0.22%). However, mammary glands from Abcg2-KO / Mdr1a/b-KO double transgenic mice, had no detectable SP phenotype [120]. These observations clearly suggest that both Abcg2 and Mdr1a/b contribute to the mammary gland SP.

In the first attempt to define the transporter contribution to the cardiac SP phenotype, Martin and colleagues utilized an Abcg2 specific inhibitor, FTC (Fumitremorgin C) that was able to completely abolish the CSP tail. The authors concluded that Abcg2 is the sole molecular determinant of adult CSP cells [71].

While prior work has investigated the role of ABC transporters in regulating the SP phenotype in various tissues, the role of these transporters, particularly Abcg2, in regulating stem cell function remains unclear.

In the cancer field, several groups have provided evidence linking Abcg2 to the proliferation of cancer cells. Patrawala et al, compared Abcg2 positive and Abcg2 negative cells from a variety of cancer cell lines and by BrdU labeling or immunostaining for mitosis and cytokinesis markers demonstrated that cells expressing the transporter were significantly more proliferative [121]. More recently, Chen and colleagues, reported that functional knockdown of Abcg2 by siRNA resulted in inhibition of the proliferation of human breast cancer cell line MCF7/MX and adenocarcinomic human alveolar basal epithelial cell line A549 [122].

Initial evidence supporting a role for Abcg2 in regulating stem cell fate was provided by Zhou and colleagues in 2001 [89]. The authors demonstrated that forced expression of Abcg2 via retroviral transduction of bone marrow cells led to an increase of SP cell numbers while it decreased their ability to form myeloid colonies. Moreover, transplantation of lethally irradiated mice with Abcg2 over-expressing bone marrow cells resulted in defective hematopoietic reconstitution as evidenced by decreased numbers of white blood cells, erythrocytes as well decreased repopulation of peripheral red blood cells (RBC), thymus and bone marrow [89]. Similarly, Scharenberg et al demonstrated that Abcg2 is highly expressed in human pluripotent bone marrow stem cells and its levels sharply decrease during differentiation towards myeloid and lymphoid lineage [65]. Interestingly, Abcg2 expression was found to be up-regulated during erythroid maturation [123]. Overall, these

studies suggest that Abcg2 expression correlates with inhibition of hematopoiesis in early developmental stages.

ABCG2 IN THE HEART

Several reports have suggested a role for Abcg2 in heart failure [192-195]. Expression of Abcg2 was found to be markedly increased in ventricular samples of patients with dilative and ischemic cardiomyopathy [124]. Similarly, Solbach et al, examined the expression pattern of all known ABC transporters in normal and end-stage heart-failure human hearts and revealed that Abcg2 was the transporter with the most apparent up-regulation in samples from failing hearts [125]. Abcg2 was strongly expressed in endothelial cells of arterioles and capillaries as well as in the sarcolemma of cardiomyocytes [124, 125]. Hence, both groups suggested a possible role of Abcg2 as a protective mechanism against cytotoxic drugs such as mitoxantrone and topotecan.

More recent work by Higashikuni and colleagues suggested a role for Abcg2 in promoting endothelial cell survival following MI injury and inducing angiogenesis following pressure overload-induced cardiac hypertrophy [194, 195]. Interestingly, female mice with genetic ablation of Abg2 exhibited increased mortality four to six days post-MI due to cardiac wall rupture. Echocardiographic analysis revealed that lack of Abcg2 increased adverse cardiac remodeling as evidence by increased dilatation and decreased ejection fraction compared to WT mice. Moreover, Abcg2-KO mice exhibited signs of cardiac hypertrophy such as increased heart to body weight ratio and myocyte cross-sectional area as well as increased infarct size. In line with previous reports, the authors identified highly

expressed Abcg2 in endothelial cells of capillaries indicating a role for Abcg2 in these cells. Indeed, lack of Abgc2 resulted in decrease in capillary density and size post-MI. Moreover, Abcg2 inhibition in microvascular endothelial cells resulted in increased oxidative stress-induced cell death as well as migration and tube formation [126]. A more recent work from the same group reported similar results in a pressure overload-induced hypertrophy model [127]. Abcg2-KO mice developed exacerbated cardiac hypertrophy and adverse cardiac remodeling following injury. Furthermore lack of Abcg2 inhibited angiogenesis and increased oxidative stress and inflammation post-injury. Namely, capillary density and number were decreased in Abcg2-KO mice while reactive oxygen species production and inflammatory cytokines levels were elevated. The authors provide evidence suggesting that Abcg2 regulates extracellular levels of the anti-oxidant glutathione in microvascular endothelial cells *in vitro* as well as *in vivo*. Lack of Abcg2 decreased significantly the extracellular glutathione levels following TAC-induced hypertrophy while treatment with a mimetic of the detoxifying enzyme superoxide dismutase resulted in partial rescue of Abcg2-KO cardiac function [127].

SYMMETRIC AND ASYMMETRIC DIVISION

One fundamental characteristic of stem/progenitor cells is the ability to self-renew and simultaneously produce committed progeny [8, 128-130]. During development as well as the adult life of an organism, stem cell homeostasis is controlled through a balance between stem cell number maintenance and generation of differentiated cells. Beside the regulation of the number of cell divisions, this event is defined by the type of cell division. Two types of stem cell division exist; symmetric and asymmetric (Figure 8).

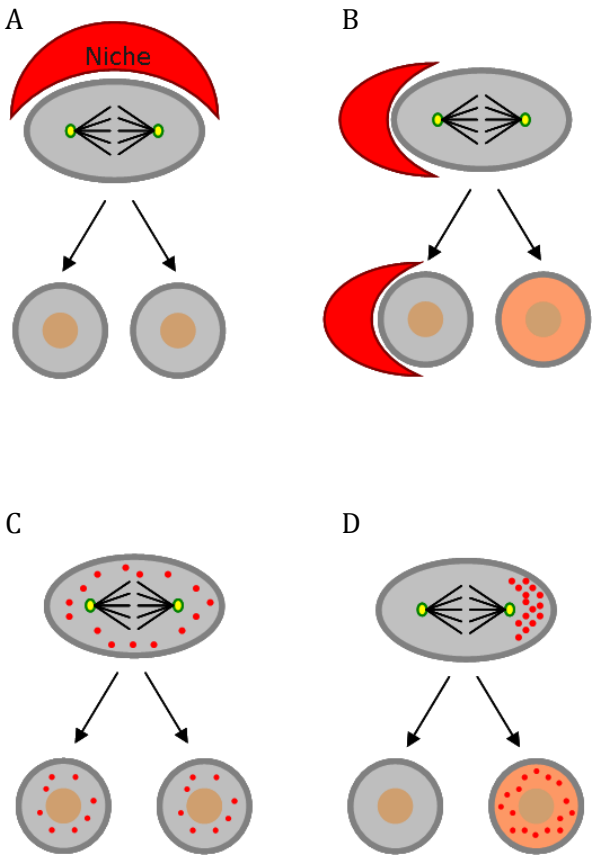

Figure 8: Extrinsic and intrinsic mechanisms regulating cellular division mode. Extrinsic signals originating from the niche (A, B) or intrinsic mechanisms regulating the cell fate determinant partitioning within the cell (C, D), dictate whether the stem cell will divide symmetrically (A, C) or asymmetrically (B, D). Fate determinants are depicted as red dots.

Symmetric divisions produce two daughter cells destined to acquire the same cell fate. A stem/progenitor cell can divide symmetrically to generate two identical stem/progenitor cells which results in the expansion of the stem cell pool, or two identical differentiated cells that will contribute to tissue formation [129]. Symmetric stem cell divisions lead to stem cell expansion during embryonic development as well as well as following injury. Hematopoietic stem cell activation during bone marrow replenishment following transplantation is an excellent example of symmetric division in mammalian cells [131].

Asymmetric stem cell divisions allow the generation of a daughter cell with a stem-cell fate and a differentiated daughter cell in a single division. This type of division ensures a continuous production of differentiated cells while the stem cell pool is maintained. The mechanisms regulating asymmetric stem cell division can be either extrinsic or intrinsic [8, 128-130, 132] (Figure 8).

EXTRINSIC MECHANISMS OF ASYMMETRIC DIVISION: STEM CELL NICHE

Extrinsic mechanisms involve signals originating from the stem/progenitor cell microenvironment also known as niche [133]. First proposed by Schofield in 1978 [134], a niche is an anatomical location within the tissue composed of different cell types and extracellular matrix [135]. Its main role is to maintain stem cells in an undifferentiated state. The mode of division a stem cell residing in the niche will follow is determined by cell-cell communication as well as the positioning of the cell within the niche. Thus the daughter cell that does not receive self-renewal signals from the niche is destined to differentiate

while the daughter that remains attached to its microenvironment will retain the stem cell fate. This is achieved by the positioning of the mitotic spindle perpendicularly to the niche so that the cleavage will result in one cell that leaves and one that stays in the niche [133]. Stem cell niches have been extensively characterized for *Drosophila melanogaster* and *Caenorhabditis elegans* germline stem cells [102-104]. More recently stem cell niches have been identified in several mammalian tissues including the hematopoietic system [136, 137], small intestine and colon [138], skin [139] as well as the heart [140]. Urbanek et al, elegantly demonstrated the existence of stem cell niches for cardiac ckit^{+} stem cells in mouse heart [140]. These niches were primarily located in the atria, base-midregion and apex and consisted of clusters of ckit^{+} cells surrounded by supporting cardiomyocytes, fibroblasts, endothelial and smooth-muscle cells as well as extracellular matrix components such as laminin, fibronectin and integrin [140]. Cell-cell communication was demonstrated by the expression of connexins and cadherens that formed gap and adherens junctions between the cells [140].

INTRINSIC MECHANISMS OF ASYMMETRIC DIVISION

On the other hand, intrinsic mechanisms of asymmetric cell division rely on the asymmetric distribution of cell fate determinants within the cell throughout the cell cycle. During interphase (G1, S and G2 phases) the mother cell loses its symmetry and undergoes polarization [128, 130]. At the beginning of mitosis, cell fate determinants are segregated appropriately and the mitotic spindle is positioned in such way that the cellular cleavage results in the correct segregation of fate determinants.

The first fate determinant, numb, was initially reported in 1994 in *Drosophila's* sensory organ precursor (SOP) cells [141]. Numb is a repressor of Notch signaling [142] and during division it's asymmetric distribution marks the cell destined for differentiation [143]. It has been recently suggested that numb controls intracellular localization of Notch pathway components through binding to the endocytic protein α-adaptin [142, 144, 145]. Since this first report, the mechanisms regulating intrinsic asymmetric division have been widely described in *Drosophila melanogaster* and *Caenorhabditis elegans.*

Several proteins including cell cycle regulators have been implicated in the regulation of asymmetric division [8]. The best characterized example is *Drosophila's* larval neural stem cells or neuroblasts (Figure 9). Apico-basal polarity in neuroblasts is established by the localization of atypical kinase C (aPKC) and Par6 to the apical cortex [146] which is ensured through interactions with the cell division control protein 42 (Cdc42) [147]. aPKC and Par6 are part of the Par complex that also includes Bazooka/Par3 [146]. Through the adaptor protein Inscuteable (Insc), Par complex interacts with a second apical complex composed of the heterotrimeric G protein α_i-subunit (Ga_i), Pins and locomotion defects (Loco) that orients the positioning of the mitotic spindle parallel to the polarity axis [117, 118]. aPKC mediated phosphorylation of cell fate determinants Lgl, Numb and Miranda during mitosis relocates them to the basal cortex where the future differentiated ganglion mother cell (GMC) will be formed. Additional basally located fate determinants such as the transcription factor Prospero and the translation inhibitor Brat together with the adaptor protein for Numb, PON (Partner of Numb) also participate to this asymmetric partitioning [8]. A large number of additional proteins have been implicated in the regulation of the aforementioned steps of asymmetric division [94, 96]. Protein asymmetric localization and cellular polarization are facilitated by the action of actin

myofilaments and microtubules which are polarized polymers [148]. Moreover, the centrosome which is the main microtubule organizing center (MTOC) has been suggested to act as a template for establishing polarity [149, 150].

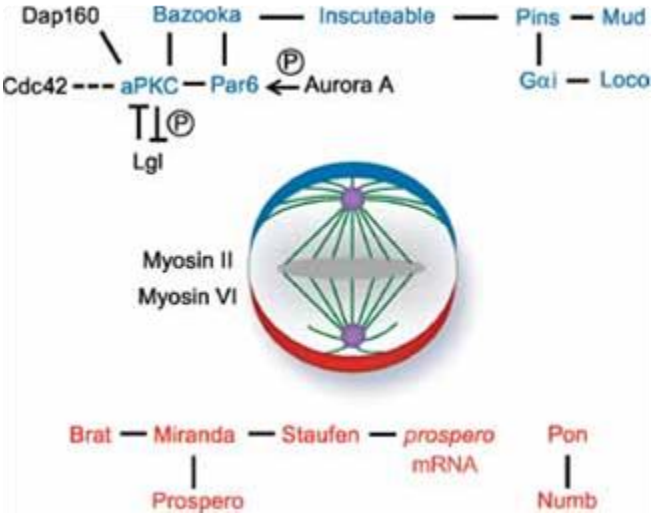

Figure 9: Asymmetric localization of cell fate determinants in drosophila larval neuroblasts. Apical proteins (blue) regulate polarity, basal protein partitioning (red) and spindle orientation [8].

Ⓟ

Similar mechanisms, although not as extensively elucidated, have been found in mammalian stem cells. Most of the molecules controlling asymmetric cell division in *Drosophila* have mammalian homologues with similar roles [128]. Asymmetric division has been primarily studied in mammalian neural [128], hematopoietic [151, 152] and epidermal progenitors [153, 154].

It has recently been suggested that asymmetric localization of misfolded proteins could be a mechanism of cell protection. Aggregates of misfolded proteins (aggresomes) that cannot be processed by the proteasome can be asymmetrically distributed during cell cycle and therefore inherited by only one daughter cell [155, 156].

The importance of asymmetric versus symmetric division regulation has also been highlighted in cancer research. The relatively new concept of cancer stem cells has

suggested that deregulated asymmetric division of a small group of adult stem cells can lead to cancer formation [157]. Several lines of evidence support that the majority of genes controlling cell polarity or fate determination are tumor suppressors. Mutations in such genes lead to uncontrolled self-renewal and over-proliferation that resembles tumor growth [8].

A number of studies have suggested that the tumor suppressor protein p53 is a key regulator of asymmetric cell kinetics in mammalian stem/progenitor cells [158-163]. Up-regulation of p53 in epithelial stem cells [158] as well as restoration of p53 levels in p53-deficient fetal fibroblasts [159] resulted in a switch from symmetric cell divisions to asymmetric divisions. More recently, in ErbB2 mammary cancer stem cells that are characterized by reduced p53 expression, stabilization of p53 by the small molecule nutlin-3 reduced the frequency of symmetric/self-renewing divisions by switching to asymmetric division [162]. It has been further suggested that p53 inhibits proliferation while promoting asymmetric cell divisions, through down-regulation of the rate-limiting enzyme for guanine nucleotide synthesis, IMPDH (inosine 5'-monophosphate dehydrogenase) [160, 164]. Interestingly, guanine nucleotide precursors can override this inhibition and promote symmetric cell kinetics [158, 160, 163]. Similarly, over-expression of IMPDH blocks p53-mediated asymmetric division [159].

CELL CYCLE LENGTH AND ASYMMETRIC DIVISION

As mentioned above, several cell cycle regulators participated in the machinery controlling asymmetric cell division of stem cells. It has been suggested that cell-fate

decisions are made during the G1 cell cycle phase [165]. Moreover, several reports support that the length of G1 plays a crucial role in a cell's decision to undergo symmetric or asymmetric division [166-171]. A number of groups have observed that lengthening of G1 cell cycle phase in stem cells coincides with the onset of differentiation [172-174]. These observations raised the question whether increased G1 duration is a cause or a consequence of differentiation [167]. Calegari and Huttner showed that lengthening of G1 phase through inhibition of cyclin-dependent kinases CDK1 and CDK2 in murine neuroepithelial cells resulted in neurogenesis [166]. The authors proposed the "cell cycle length" hypothesis which is based on the principle that cell fate determinants require a certain amount of time to be produced in sufficient levels and to acquire their position within the cell. Thus a shorter duration of the cell cycle might not allow such processes to take effect and result in symmetric division [166]. In line with this hypothesis, Lange et all, reported that over-expression of Cdk4/cyclinD1 in neural progenitors shortens the G1 phase by 30% and inhibits neurogenesis and asymmetric division while promoting progenitor cell expansion through symmetric divisions [175]. A more direct link between cell cycle and asymmetric cell kinetics was recently provided by Tsunekawa et al. The authors demonstrated that in neural progenitor cells the asymmetric inheritance of the positive regulator of G1 progression, cyclinD2, marks the daughter cell that maintains the stem cell fate while the other daughter exits the cell cycle and eventually differentiates. Genetic manipulation of cyclinD2 expression through over-expression or down-regulation resulted in decreased or increased differentiation respectively [169]. In agreement with the "cell cycle length" hypothesis, the authors propose that the localization of cyclinD2 in the basal process of neural progenitors increases the temporal interval for the protein to reach the nucleus in G1 and similar to G1 lengthening this might promote asymmetric division [140, 141].

The maintenance of stem/progenitor cell homeostasis in cardiac stem cell niches is also achieved through a balance between symmetric and asymmetric divisions [140, 176, 177]. In an elegant study, Urbanek et al were the first to reveal the ability of ckit$^+$ cardiac stem/progenitor cells to divide asymmetrically both *in vivo* and *in vitro* [140]. The authors demonstrated that in cultured ckit$^+$ cardiac stem/progenitor cells the cell-fate determinants numb and α-adaptin segregated primarily asymmetrically to the two daughter cells (62 ± 7%). Furthermore, asymmetric division was accompanied by asymmetric expression of the cardiogenic marker GATA4 indicating that one daughter cell retains the self-renewing ability while the other is committed to cardiomyogenic lineage [140]. As a consequence, the pool of cardiac progenitor cells remains constant. The identification of mechanisms regulating the switch between asymmetric to symmetric cell kinetics is of paramount importance especially in injury conditions such as myocardial infarction where the cardiac stem sell pool needs to be activated, increase in number and concomitantly generate differentiated progeny. In this context, Cottage et al introduced Pim-1 kinase as a possible target molecule [176]. Transgenic mice over-expressing Pim-1 exhibited an increase in cycling ckit$^+$ progenitor cells following myocardial infarction that was not reflected in increased cell number. However, these cells demonstrated increased asymmetric division (65% in transgenic animals versus 26% in WT) that resulted in maintenance of the stem cell pool while enhancing myocardial regeneration [176]. More recently, the adenylate kinase-AMPK pathway was implicated in asymmetric cell kinetics and cardiomyogenic differentiation of embryonic stem cells [178]. Adenylate kinase 1 (AK1) was shown to segregate asymmetrically to one daughter cell and to co-localize with cardiogenic markers while its inhibition resulted in defective cardiogenesis [178].

GOAL OF THE STUDY

The recent identification of resident cardiac progenitor cells has brought great enthusiasm in the cardiovascular field and their potential therapeutic application to treat cardiac diseases holds great promise. Thorough understanding of the biological processes and molecular mechanisms regulating stem cell homeostasis is imperative to enable their use in cardiac regeneration. ABC transporters and specifically Abcg2 have known protective roles in cells of various tissues. However, the role of Abcg2 in cardiac stem/progenitor cell fate and homeostasis is largely unknown. The goal of my study is to delineate the contribution of Abcg2 and Mdr1 in the CSP phenotype. Moreover, I seek to define the role of Abcg2 in the regulation of CSP proliferation, cell cycle progression and survival as well as their asymmetric division and differentiation. Finally, I investigate the role of Abcg2 *in vivo* in a myocardial injury model.

MATERIALS AND METHODS

Animals: Abcg2 and Mdr1 deficient mice were purchased from Taconic (cat. #002767 and 001487 respectively) and bred in our animal facility. Animals were used and analyzed at post-natal day 3, 14, 21 and at 8-12 weeks old. Age matched inbred WT-FVB mice (originally purchased from Taconic) were used as controls. C57BL/6-Tg (ACTBGFP) mice purchased from Jackson laboratories were used to generate FVB-GFP animals. Abcg2-KO mice were cross-bread with FVB-GFP mice for 8 generations to produce Abcg2-KO-GFP mice. C57BL/6 adult (8 weeks) and neonatal (2-3 days) mice were purchased from Charles River laboratory. Transgenic mice expressing GFP under the promoter of Abcg2 were kindly provided by Dr. B. Sorrentino from St. Jude Children's research hospital, Memphis, TN (ref Tadjali M 2006 stem cells). Mice expressing GFP under the control of cardiac specific alpha-myosin heavy chain promoter were kindly provided by Dr. M. Sussman from the San Diego State University. Wistar rats, adult (200g) and neonatal (1-2 days), were purchased from Charles River laboratories. All animal studies were performed according to the guidelines of the Harvard Medical School, the Longwood Medical Area's Institutional Animal Care and Use Committee (IACUC) and the National Society for Medical Research.

Myocardial Infarction (MI): Myocardial infarction was performed via permanent ligation of the coronary artery as described previously [179]. Briefly, 8-10 week old WT-FVB and Abcg2-KO male mice were anesthetized using 65mg/kg pentobarbital and ventilated through a standard rodent ventilator. The descending coronary artery was permanently ligated using a silk suture through an incision performed between the fourth and fifth

intercostal spaces. As control, sham-operated animals underwent a similar procedure without occlusion of the coronary artery. All animals received the analgesic buprenorphine (0.03-0.06mg/kg) for a period of 72 hours to prevent any post-operative discomfort. Animals were sacrificed 4 days post-MI. During the course of the experiment a survival curve was obtained using the GraphPad Prism software.

Ischemia reperfusion injury (IR): Similar to the MI protocol, mice were anesthetized and intubated. The descending coronary artery was ligated for one hour followed by removal of the suture and reperfusion. Sham animals underwent the same procedure devoid of the coronary ligation. Animals were sacrificed one week post-MI.

In vivo **BrdU infusion / labeling:** In both MI and IR injury models, osmotic mini-pumps (Alzet cat #1007D) containing BrdU (40mg/ml, Sigma Cat #B5002) were implanted subcutaneously immediately following the cardiac surgery. The pumps used, deliver 0.5µl of the solution per hour for one week. BrdU was dissolved in 150mM $NaHCO_3$ at 37°C or higher and kept at 37°C until use to avoid precipitation.

Echocardiography: Echocardiography was performed at baseline and one week following IR with a Vevo 2100 Imaging digital ultrasound system from VisualSonics using an 18-38 MHz linear array transducer. Mice were anesthetized with 1% isoflurane in oxygen; their chest was shaved and animals were placed in supine position on a heated platform. Anesthesia was removed and the heart rate returned to normal (~600 beats/min). Data was acquired from the parasternal long axis view followed by the short axis view at the mid-

papillary muscles level. Measurements were obtained from the M-mode images and all data were analyzed in a blinded fashion.

Heart fixation: Mice were anesthetized with intraperitoneal (IP) injection of pentobarbital. To prevent blood coagulation, 100 IU/ml of heparin was administered through IP injection. Hearts were excised and briefly washed in Krebs solution (137mmol/L NaCl, 4.0mmol/L KCl, 1.8mmol/L CaCl, 1.2mmol/L KH_2PO_4, 1.2mmol/L $MgSO_4$, 24.9mmol/L $NaHCO_3$, 11.2mmol/L dextrose (pH 7.4)). A cannula was inserted in the aortic root to initiate retrograde perfusion by the Langerdoff apparatus. In order to vent the besian drain, a thin cannula was pierced through the apex of the left ventricle (LV). An incision in the left atrium allowed the insertion of a balloon into the LV through the mitral valve. A pressure transducer (Statham P23Db, Gould) was connected to the balloon which allowed the recording of LV pressure. Platinum wires placed on the epicardial surface of the right ventricle (RV) were used to pace the hearts (Grass Instruments). All experiments were performed at constant coronary perfusion pressure of 80mmHg. End-diastolic pressure (EDP) was adjusted to 5mmHg by inflating the balloon with saline, hearts were arrested in diastole with KCl and were fixed by perfusing 10% formalin solution at a hydrostatic pressure of 40-50mmHg for 15 min. Hearts were kept overnight in 10% formalin solution at 4^{o}C. Following, the balloon was removed, hearts were cut in three parts (apex, middle, base) and embedded in paraffin. All samples were cut in 4μm thick sections and stained with Masson's trichrome or analyzed by immunohistochemistry.

Wall thickness and Infarct size measurements: Slides stained with Masson's trichrome were used for the following measurements. Wall thickness was measured as previously described [180]. The method is also described in Figure 10. Infarct size was calculated

according to the following equation: (endocardial infarcted circumference / endocardial circumference + epicardial infarcted circumference / epicardial circumference) / 2.

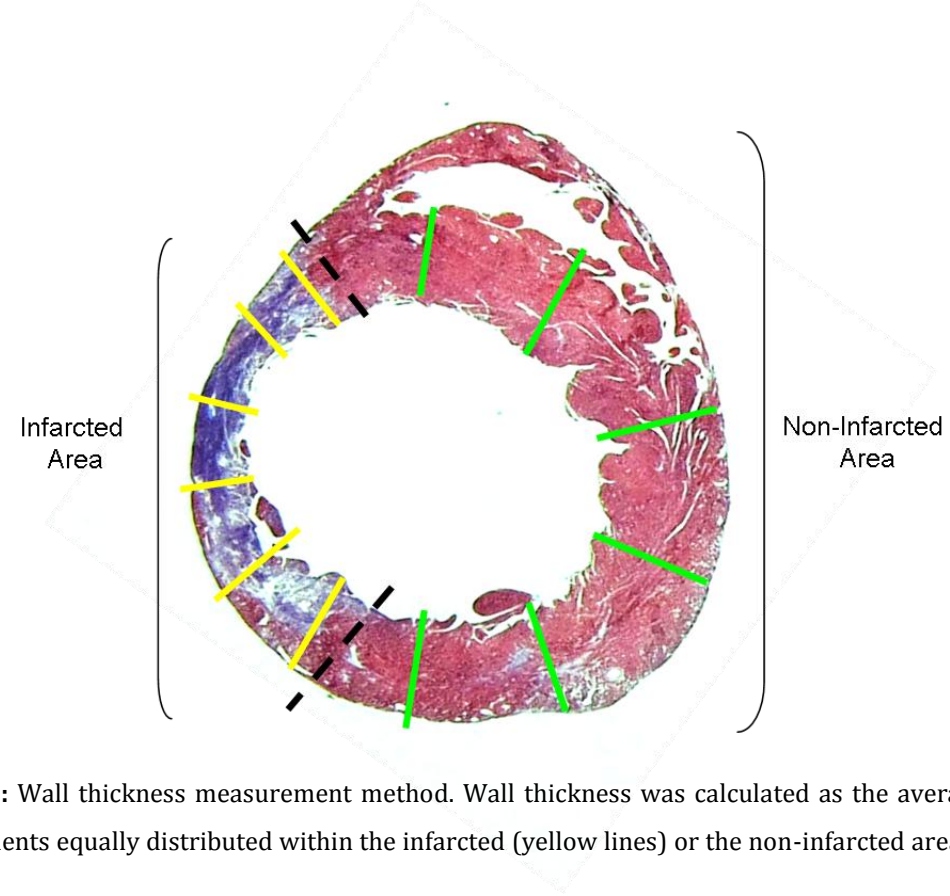

Figure 10: Wall thickness measurement method. Wall thickness was calculated as the average of 6 measurements equally distributed within the infarcted (yellow lines) or the non-infarcted area (green lines).

Immunohistochemistry: Slide preparation for immuno-staining involved de-paraffinization, rehydration and antigen retrieval. Namely, slides were heated for 30 min at 70°C and sequentially immersed into solutions of xylene (2x5 min), ethanol (2x3 min in 96% ethanol, 3 min in 90% and 3 min in 80%) and water (4 min). Slides were then placed in citrate buffer (2.4g/l sodium citrate, sigma #S4641 and 0.35g/l citric acid, sigma #C1909) and micro-waved for 10 min at 100% power. After cooling down, slides were washed in water (2 min) and PBS (4x2 min). Cardiac tissue samples were then stained for α-sarcomeric actinin (1/600, Sigma Cat #A7811), α-sarcomeric actin (1/600, Sigma Cat

#A2172), GFP (1/150, Molecular probes Cat # A11122), BrdU (Roche Cat #11296736001) or WGA (Wheat Germ Agglutinin, Invitrogen Cat #W32465, Alexa 680). For all stainings except BrdU and WGA, primary and secondary antibodies were applied in humid chamber for 1 hour at 37°C and slides were washed in PBS between incubations (5x2 min). BrdU staining was performed according to manufacturer's instructions. When α-sarcomeric actin was used in combination with BrdU the protocol of the latter was used. When myocyte cross-sectional area measurements were needed, antibody stainings were followed by WGA staining (1/100 in PBS for 3 hours at 37°C in a humid chamber, followed by 5x2 min washes in PBS). In the case of high auto-fluorescence, slides were stained with Sudan black solution (0.001g/ml in 70% ethanol) for 30 min at RT followed by extensive washing in PBS (8x2 min). Coverslips were mounted on slides with a DAPI containing mounting medium and signal was detected with the Zeiss epi-fluorescent microscope or LSM-700 confocal microscope.

In situ cell death detection (Tunel assay): Slides were de-parafinized, rehydrated followed by antigen retrieval as described above. Cell death detection was achieved by using the *In situ* cell death detection kit (TMR red) by Roche (Cat #12156792910) according to the manufacturer's instructions.

Capillary size and density: Cardiac tissue sections were stained for CD31 (1/50 dilution, Santa Cruz Cat #sc-1506) and α-sarcomeric actinin following the immunohistochemistry protocol described above. Only vessels with a diameter smaller than 10μm were taken into consideration. More than 500 hundred capillaries (base, middle, apex) were scored for each sample.

Infarct size measurement by the tetrazolium method: Mice were subjected to one hour ischemia followed by reperfusion as described above. The released suture used to induce ischemia was left in place. After 24 hours of reperfusion, mice were again anesthetized, intubated and connected to the ventilator. The chest was opened and the artery was ligated to the same site as before. In order to mark the area at risk fluorescent microspheres were injected through the apex while the carotid artery was occluded. The heart was arrested in diastole with KCl and sectioned from apex to base into approximately 1mm sections. Sections were then incubated in 1% Triphenyltetrazolium chloride (TTC in PBS, Sigma) for 10 min at 37^{o}C and fixed in 10% formalin for 15 min. Necrotic tissue (infarct) was visualized by digital micrographs. The area at risk (% AAR) and initial infarct size were determined based on the following equations: % AAR = 100-(a/r x 100) and % infarct = i/r x 100 (Figure 11).

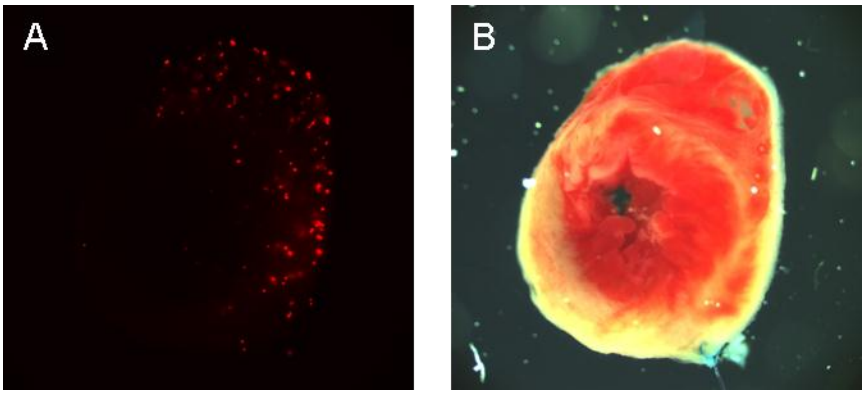

Figure 11: Infarct size and area at risk measurement by the TTC method. A) The area at risk (AAR) and B) the infarct size were calculated according to the equations %AAR = 100-(a/r x 100) and %infarct = i/r x 100 where (a) is the area perfused with fluorescent microspheres (red fluorescence in A), (r) is the total LV area and (i) is the necrotic area (white area in B).

Cardiac and bone marrow SP cell isolation: Mouse hearts were minced with a razor blade and enzymatically digested with a combination of 0.1% collagenase B (Roche), 2.4U/ml dispase II (Roche) and 2.5mmol/L CaCl2 at 37°C for 30 min. They were subsequently filtered through a 70μm and 40μm filters and washed with HANK's solution (HBSS buffer supplemented with 2% FBS HI (Gibco) and 10mmol/L HEPES (Sigma Cat #H7006)). Cells were manually counted and stained with Hoechst 33342 (Sigma Cat #B2261) (5μg/ml, 106 cells/ml) at 37° C for 90 min in DMEM (CellGro) (2% FBS HI, 10mmol/L HEPES). The calcium blocker Verapamil (50 mmol/L) (Sigma, #V4629) was used as a negative control for the detection of the SP population. Bone marrow SP (BMSP) cells were isolated as previously described [88]. For all cell surface antigen stainings, cells were incubated at 4o C for 30 min with fluorochrome-conjugated monoclonal rat anti-mouse antibodies against Sca-1, CD31 and CD45 (Pharmigen). 7-Aminoactinomycin-D (&-AAD) or propidium iodide (PI) were used for dead cell detection.

Flow cytometric analysis and sorting: Flow cytometric analysis was performed with the DXP11 analyzer (Cytek) and the Accuri C6 analyzer (BD Biosciences). Fluorescence activated cell sorting (FACS) was performed with a FACSAria sorter (BD Biosciences). Hoechst was excited by a 20mW UV laser (350nm) and the side population was identified as Hoechst low-negative as previously described [181]. Phycoerythrin (PE), Fluorescein isothiocyanate (FITC), GFP and 7-AAD were detected with a 488nm laser and for detection of Allophycocyanin (APC) a 640nm laser was used. Data were analyzed by the FACSDIVA software (BD Biosciences) and FlowJo (Tree Star).

Sorted CSP cells were placed in culture dishes at a density of 5-8cells/mm^2 in expansion medium (α-MEM, 20% heat-inactivated FBS, 2 mM L-Glutamine and 1%

penicillin/streptomycin (pen/strep). All experiments involving expanded CSP were performed with cells from passages 4-6.

Inhibition of Mdr1a/b-mediated Hoechst 33342 efflux by Fumitremorgin C (FTC): Human neuroblastoma cells, SK-N-FI (ATCC # CRL-2142), were pre-incubated for 30 min at 37°C with or without 50μM verapamil or different concentrations of FTC (10μM, 20μM or 30μM) followed by incubation with 1μg/ml Hoechst for additional 30 min at 37°C. Hoechst efflux was evaluated by flow cytometry.

Determination of CSP proliferation capacity

Proliferation assay: WT and Abcg2-KO CSP cells (20000 cells) were plated in 100mm culture dishes and cultured in expansion medium for 9 days. WT and Abcg2-overexpressing CSP cells (10000 cells) were plated in 60mm dishes and cultured for 6 days. Cells were then trypsinized and counted with a hemocytometer. In all cell culture experiments, CSP cells of passage 4-6 were used and medium was changed every 3 days.

Immunocytochemical staining for phospho-Histone H3 (pH3): CSP cells were plated on coverslips (20mm x 20mm) placed in 60mm dishes and cultured in expansion medium for 5 days. Subsequently, cells were fixed with 4% paraformaldehyde solution for 20-30 min at room temperature (RT), washed 3 times with PBS and permeabilized with 100% methanol for 30 min at -20°C. Cells were then washed to remove methanol and incubated with blocking solution consisting of 1% BSA for one hour at RT. Primary antibody against pH3 (1/200, Abcam Cat #ab32107) was applied for 1-2 hours followed by an anti-rabbit

secondary antibody (1/200, Alexa-555, Molecular probes) for 1-2 hours at RT. Cells were washed 3 times with PBS between antibodies. A drop of DAPI-containing mounting medium (Vector Vectashield) was added on the cells and coverslips were mounted on slides. For visualization of the cells, an epi-fluorescent microscope from Zeiss was used (Zeiss, Axiovert 200M).

Immunocytochemical staining for 5-Bromo-2´-deoxy-Uridine (BrdU): Cells were cultured on coverslips as described above (pH3 staining). BrdU labeling and staining was performed using the 5-Bromo-2´-deoxy-Uridine Labeling and Detection Kit I from Roche (Cat # 11296736001) according to the manufacturer's instructions. Briefly, one hour prior fixation, BrdU labeling solution was added to the culture medium. Cells were then washed with PBS and fixed with ethanol fixative. Anti-BrdU antibody was applied for 30 min at 37^{o}C, followed by a FITC-conjugated secondary antibody, anti-mouse IgG (provided with the kit or from Molecular probes).

Propidium Iodide staining (PI): CSP cells (10000 cells) cultured in 60mm dishes for 5 days were tryspinized and fixed in 70% ethanol overnight. Cells were then washed with PBS and incubated with PI staining solution (0.1% Triton-X100, 2µg/ml PI, 400ng/ml RNase A in PBS) for one hour at 37^{o}C in the dark. Subsequently, cells were washed with PBS and analyzed by FACS. For further data processing, the ModFit Lt software by Verity House was used.

Ki67 staining for FACS analysis: Cells were fixed with 4% paraformaldehyde at 4^{o}C for 30 min and permeabilized with BD Perm/Wash solution (BD Biosciences) at 4^{o}C for 20 min.

The cell suspension was then washed with Perm/Wash solution and the cell pellet was resuspended in 100µl of the same solution. FITC-conjugated Ki67 antibody (Santa Cruz) was added at a concentration of 4ng/µl and cells were incubated at 4^{o}C for 30 min in the dark. Cells were subsequently washed twice with HANK's solution and analyzed with the BD FACS Aria or the Accuri C6 cytometer.

Total protein and DNA measurement: WT and Abcg2-KO CSP cells were plated in clear bottom 96 well plates at a concentration of 2000 cells/well for two days. Cells were then fixed with 4% paraformaldehyde (50µl/well) for 20 min at RT, washed and at the same time permeabilized by three washes with washing solution (0.2% Triton-X in PBS). For total protein detection, succinimidyl ester alexa 680 (Molecular probes, 1:50000 dilution) was added for 15 min at RT in the dark. DNA content was determined by incubation with TO-PRO3 DNA dye (Molecular probes, 1:2500 dilution) for one hour at RT in the dark. Plates were scanned and data was analyzed with a Licor Odyssey infrared imager.

Analysis of CSP cell survival

Annexin and propidium iodide staining: CSP cells were stained for Annexin-V and propidium iodide using an Annexin-V kit (Abcam, Cat #14085) according to the manufacturer's instructions. Briefly, cells were resuspended in 500µl of Annexin-V binding buffer containing 5µl of Annexin-V and 5µl of PI and incubated for 5 min at RT in the dark. Samples were analyzed by flow cytometry using the Accuri C6 analyzer.

CellTiter-Glo and CellTiter-Blue viability assays: The metabolic activity of CSP cells was determined based on ATP production (CellTiter-Glo, Promega Cat #G7573) and reduction of resazurin to fluorescent resorufin (CellTiter-Blue, Promega Cat #G8080) according to manufacturer's instructions. Briefly, 2000 CSP cells were plated in opaque-walled 96-well plates for 2 days in 100μl culture medium. CellTiter-Glo or CellTiter-Blue reagent was then added (100μl and 20μl respectively) and plates were shaken for 2 and 10 min respectively. Cells treated with CellTiter-Glo were incubated for 10 min at RT in the dark and luminescence was measured. Cells treated with CellTiter-Blue were placed in the incubator (37^{o}C, 5% CO_2, 21% O_2) for one hour and fluorescence was recorder at 560/590nm.

Hydrogen peroxide (H_2O_2) treatment: WT and Abcg2-KO CSP cells were plated in 6-well plates at a concentration of 50000 cells/well in regular culture medium for 2 days. To induce stress, cells were incubated for additional 4 hours in the presence of 200μM H_2O_2. Cells were subsequently trypsinized, centrifuged and stained for apoptosis (Annexin-V, as described above) and necrosis (7-AAD, 15μ/sample). Analysis was performed with a FACSAria cytometer.

Adult and neonatal rat ventricular cardiomyocyte isolation: Adult cardiomyocytes were isolated as previously described [6]. Neonatal rat ventricular myocytes (NRVM) were isolated from 1-2 days old Wistar rats. Pups were sacrificed by decapitation; hearts were removed and briefly washed in HBSS. Atria were removed and each heart was cut in smaller pieces (6-8). Hearts were washed twice by transferring in plates with HBSS, then placed in a sterile specimen container containing Trypsin solution (15mg of Trypsin in 25ml HBSS) and incubated for 18 hours at 4^{o}C. The next day, trypsin inactivated by adding the same volume

of pre-culture medium (low glucose DMEM, 7% FBS HI, 1% pen/strep, 100μM BrdU, 1.5mM vitamin B12) and shaking for 3 min at 38°C (150rpm). After the supernatant was removed, the hearts were digested with a series of 5 incubations with collagenase B solution (1mg/ml Collagenase B in HBSS). Each time, tissue was incubated at 38°C with 10ml enzyme under constant shaking for 3.45 min (first incubation), 4.45 min (next 3 incubations) or 5 min (last incubation). After each time point the enzyme solution containing the cells was collected and stored on ice and fresh solution was added to the tissue. Subsequently, the supernatants were centrifuged at 200g (~1000rpm) for 5 min and the cell pellet was resuspended in 20ml medium to wash out the remaining enzyme. Cells were again centrifuged at 50-100g (~700rpm) fro 5 min, then resuspended in 10ml medium and transferred into a T75 flask. After 1 ½ hour incubation at 37°C the medium was gently transferred to a new T75 flask for an additional 1 ½ hour. Myocytes do not attach on plastic very rapidly and therefore this double incubation allows the attachment of non-myocytes (fibroblasts) to the plastic flask and thus the purification of the cell preparation from contaminating cells.

CSP cardiomyogenic differentiation assessment

Co-culture assay: Both adult and neonatal cardiomyocytes were used in the co-culture assays. Adult myocytes were seeded at a low density on coverslips (20mm x 20mm) coated with laminin and cultured for 10 days in long-term culture medium (DMEM, 5 mmol/L creatine, 2mmol/L L-carnitine, 5 mmol/L taurine, 1% pen/strep, 7% FBS HI, 100 μmol/L BrdU). Similarly, NRVM were plated on coverslips at a density of 375cells/mm^2 and cultured in pre-culture medium for 48 hours. For co-culture, CSP cells from WT-GFP and Abcg2-KO-GFP mice as well as CSP cells infected with GFP-expressing (WT and Abcg2-KO

cells) or GFP-Abcg2-overexpressing lentivures (WT cells) were used. CSP cells were added on the cardiomyocytes and maintained for 10-12 days (medium changed every 72 hours) in long-term medium in the case were adult myocytes were used or for 3 days in co-culture medium (DMEM, 5% FBS HI, 1% pen/strep, 10 ug/ml insulin, 10 ug/ml transferrin, 1.5 mM B12, changed every day) when NRVM were used. Subsequently, cells were fixed with 4% paraformaldehyde (30 min, RT), permeabilized with 100% methanol (30 min, 4°C) and incubated with 1% BSA solution (1 hour, RT). Cells were then incubated with anti-α-sarcomeric actinin and anti-GFP (2 hours, RT or 1 hour, 37°C) followed by secondary antibodies anti-mouse IgG alexa 555 (Molecular probes) and anti-rabbit 488 (Molecular probes) (2 hours, RT or 1 hour, 37°C). Coverslips were mounted onto slides using DAPI-containing medium and visualized under a Zeiss epi-fluorescent microscope. α-sarcomeric actinin$^+$, GFP$^+$ CSP cells were scored.

Mono-culture: WT and Abcg2-KO CSP cells were plated in clear bottom 96-well plates at a concentration of 2000 cells/well and cultured in DMEM supplemented with 1% FBS HI and 1% pen/strep for 2 days. The expression of cardiac markers Nkx2.5, Gata4 and Mef2c was evaluated by in cell western. Cells were fixed with 4% paraformaldehyde for 20 min at RT, washed 3 times with 0.2% Triton-X in PBS and incubated with LI-COR blocking buffer for 1 hour at RT. Primary antibodies against Nkx2.5 (Santa Cruz Cat #sc-14033), Gata4 (Santa Cruz Cat #sc-1237) and Mef2c (Santa Cruz Cat #sc-13268) were applied overnight at 4°C at a 1/100 dilution. Gapdh (R&D Cat #2275-PC-100) was used as loading control at a 1/1500 dilution. Next day, plates were placed at RT for 30 min, washed 4 times with 0.2% Triton in PBS and incubated with secondary antibodies (anti-goat alexa 680 and anti-rabbit alexa 800, 1/1000 dilution). Plates were scanned using the Odyssey Infrared Imager (LI-COR).

Immunocytochemistry following cytospin: Freshly isolated WT and Abcg2-KO CSP cells were placed onto slides by cytospin centrifugation (5 min, 500rpm, Shandon Cytopsin 3) at a concentration of 5000 cells/slide. Cells were then fixed with 4% paraformaldehyde, permeabilized with methanol and incubated with blocking buffer as described above. Antibodies against Abcg2 (1/100, Kamiya) and Mdr1 (1/15, Santa Cruz, clone C-19, FITC conjugated) were applied for 2 hours at RT. Alexa-555 anti-rat secondary antibody (for Abcg2 detection) (1/250, Molecular probes) was applied for 2 hours at RT. Coverslips were mounted and cells were visualized with a fluorescence microscope as described above.

RNA isolation: Total RNA was extracted from expanded CSP cells or cardiac tissue using Trizol reagent (Invitrogen Cat# 15596-018). Tissue (using a mortar and pestle) or cells were homogenized in 1ml Trizol and incubated for 5 min at RT. 0.2ml of chloroform per 1ml of Trizol was then added and samples were incubated at RT for 3 min. Subsequently, the samples were centrifugated at 13,000 rpm for 20 min at 4^{o}C and the aqueous phase was transferred to a new tube. Following, 0.5ml of isopropanol was added; samples were mixed gently and incubated for 10 min at RT. Samples were centrifugated again at 13,000 rpm for 30 min at 4^{o}C. The RNA pellet was washed with 0.5ml 70% ethanol followed by a centrifugation at 13,000rpm for 5 min at 4^{o}C. The pellet was air-dried and dissolved in RNase-free water. Further purification was achieved with the RNeasy Mini Kit (Qiagen) according to the manufacturer's instructions. RNA samples were stored at -80^{o}C.

Total RNA was extracted from freshly isolated CSP cells (low amount) with the Absolute RNA Nanoprep kit (Stratagene, Cat #400753) according to manufacturer's instructions.

Genomic DNA removal: Genomic DNA was removed from RNA samples with the Turbo-DNA free kit (Ambion Cat# 1907) according to the manufacturer's instructions. Briefly, samples were incubated with 2-3 units of DNase for 30 min at 37^{o}C. DNase inactivation reagent was added to stop the reaction for 5 min at RT. After centrifugation, the supernatant was transferred a new RNase-free tube and concentration was measured using a Nanodrop1000 instrument (Thermo scientific).

Reverse transcription: For all RT-PCR experiments, except for the qRT-PCR-based gene-arrays, cDNA was synthesized with the iScript cDNA synthesis kit (BIO-RAD Cat #170-8890) according to the manufacturer's instructions. For the gene arrays, the RT2 First Strand synthesis kit (Superarray, SABiosciences, #C-03) was used according to the instructions of the manufacturer. cDNA was stored at -20^{o}C.

Quantitative RT-PCR: The RT-PCR was performed in the MyIQ or CFX instruments from BIO-RAD and the protocol followed for each experiment was as follows:

1. One cycle at 95^{o}C for 3 min

2. 95oC for 15sec followed by 60^{o}C for 1 min. Step2 was repeated for 40 cycles.

3. One cycle at 55^{o}C for 1 min

4. One cycle of 80 steps with starting temperature 55^{o}C, increasing 0.5^{o}C each step.

Primers were designed with the Primer3 software and verified by BLAST. The sequences of the primers used are the following: 5'-TCACCACCATGGAGAAGGC-3'and 3'-GCTAAGCAGTTGGTGGTGCA-5' for GAPDH, 5'-GAACTCCAGAGCCGTTAGGAC-3' and -

CAGAATAGCATTAAGGCCAGG-5' for Abcg2, 5'-TGGGTGCAGCTTTTCTCCTTA-3' and 3'-CAGTGAGCACTTGTCCAATAGAG-5' for Mdr1a, 5'-CTG TTGGCGTATTTGGGATGT-3 and 3'-CAGCATCAAGAGGGGAAGTAATG-5' for Mdr1b. Data analysis was performed according to the standard curve method. GAPDH was used as control.

Quantitative RT-PCR based gene array: RT-PCR arrays were purchased from SABiosciences. The array used in these experiments was the mouse Cell Cycle PCR Array (Cat #PAMM-020). These arrays consist of 96-well plates containing primers for a total of 84 genes representing different signaling pathways, quality control wells for the of reverse transcription (3 wells) and the PCR (3 wells) efficiency as well as wells with primers for housekeeping genes (Gusb, Hprt1, Hsp90ab1, Gapdh, Actb). The PCR program used was as follows:

1. One cycle at 42^{o}C for 10 min

2. 95^{o}C for 15sec followed by 60^{o}C for 1 min. Step2 was repeated for 40 cycles.

3. One cycle at 55^{o}C for 1 min

4. One cycle of 80 steps with starting temperature 55^{o}C, increasing 0.5^{o}C each step.

RT-PCR gene arrays were performed in the MyIQ cycler. Data were analyzed from samples that passed the double quality controls according to the manufacturer's instructions.

DNA isolation

Mini preps: DNA was isolated from 1.5ml of bacterial culture with the Qiagen mini prep kit (QIAprep Spin Miniprep Kit, Cat #27104) according to the manufacturer's instructions.

Midi preps: DNA was isolated from 25ml of bacterial culture with the Qiagen midi prep kit (Cat #12145) according to the manufacturer's instructions.

DNA concentrations were measured with a Nanodrop1000 instrument (Thermo scientific).

Agarose gel electrophoresis: Agarose gels were made with ultra pure agarose in TBE buffer (Tris-base, Boric Acid, EDTA). Agarose concentration varied depending on the size of the DNA analyzed.

Agarose gel extraction: DNA extraction was performed with a DNA Gel extraction kit from Qiagen (Cat #28604 or #28704) according to the manufacturer's instructions.

Statistical analysis: Statistical analysis was performed using Student's unpaired t-test and one way Anova. Data are presented as mean ± SE. P values ≤ 0.05 were considered as statistically significant.

Protein electrophoresis and Western blot: Pelleted cells were lysed in 100µl lysis buffer (Cell signaling) containing 1mM PMSF. For protein isolation from tissue, samples were frozen in liquid nitrogen, crushed with a mortar and pestle and dissolved in lysis buffer with PMSF and sonicated for thorough lysis. All samples were then centrifuged for 15 min at 13000rpm at 4^{o}C and the supernatant containing the protein was transferred in anew tube. The Pierce BCA protein assay kit was used to measure protein concentration according to the manufacturer's instructions. 30-50µg of total protein were loaded into a 4-12% SDS

polyacrylamide gel (Criterion XT, BIO-RAD). Gel electrophoresis was performed at constant voltage of 100V. Proteins were transferred to a PVDF membrane at 15mA overnight at 4^{o}C. Membranes were incubated with Odyssey blocking buffer (LI-COR) for one hour at RT followed by primary (2 hours RT or overnight at 4^{o}C) and secondary antibodies (1 hour RT, Alexa 680, Molecular probes) incubations. Primary antibodies against Abcg2 (1/50, Kamiya Cat # MC980), Gapdh (1/2000, R&D) and appropriate secondary antibodies were used. Membranes were washed between antibody incubations with PBS-T (PBS, 0.1% Tween) and expression signals were detected with the Odyssey infrared system (LI-COR).

Construction of lentiviruses

Abcg2-overexpressing construct (1): Abcg2 cDNA was obtained by enzymatic digestion of pSPORT1 vector (ATCC: American Type Culture Collection, Cat #10471063) with BamHI (New England Biolabs-NEB). The resulting fragment was separated from the vector's backbone by gel extraction and its protruding ends were blunted by Klenow reaction (NEB) according to the manufacturer's instructions. In parallel, the RLV39 vector that promotes gene expression through the constitutively active EF1α promoter was digested with MluI, followed by Klenow. The 5' phosphate groups were removed from the vector by an enzymatic reaction with Antarctic phosphatase (NEB) and the Abcg2 cDNA was cloned (NEB, Quick ligation kit Cat #M2200S) into RLV39. The IRES-GFP cassette was extracted from HPV422 vector by Xba1 and Cla1 double digestion and inserted into RLV39-Abcg2 construct which was digested with the same enzymes. Competent DH5α bacteria (Invitrogen) were transformed with the ligation product according to the manufacturer's instructions and several colonies were tested for the presence and correct orientation of Abcg2 by minipreps. The new RLV39-Abcg2-IRES-GFP construct is a bicistronic vector

constitutively expressing Abcg2 and GFP. Abcg2 overexpression was verified by western blot and RT-PCR.

Abcg2-overexpressing construct (2): The pSPORT vector was digested with HpaI and SalI in order to extract the Abcg2 cDNA. In parallel, the lentiviral vector LSLV83 was digested with MluI, blunted with Klenow and digested again with SalI. 5' phosphate groups were remove from the vector by an enzymatic reaction with Antarctic phosphatase (NEB). Ligation was performed with the Quick ligation kit from NEB (Cat #M2200S). LSLV83 backbone encodes a gene conferring resistance to neomycin, facilitating infected cell selection. Abcg2 expression was driven by the constitutively active promoter EF1α.

Production of control and Abcg2 overexpressing lentivirus.: Confluent HEK293-T cells in 100mm culture plates were split one day before transfection in 5 new 100mm plates. Medium (DMEM, 10% heat-inactivated FBS, 1% pen/strep) was renewed 2 hours before transfection. The vector carrying Abcg2 or the empty backbone (3.2µg, RLV39 or LSLV83) was combined with 4 helper plasmids (4µg HPV275, 0.4µg p633, 0.4µg HPV601, 0.4µg YN15) that encode genes necessary for the virus formation and propagation (gagpol, REV, TAT and VSVg respectively) in a total volume of 40µl (adjusted with water). 160µl of DMEM and 24µl of Fugene were added and the mixture was incubated for 15-45 min at RT. The mixture was then added to the HEK cells (one 100mm dish). Next day, the medium was replaced with 10ml of CSP expansion medium and the virus was collected 24 and 48 hours later, filtered through a 45µm filter and stored at -80°C.

Short-hairpin Abcg2 (shAbcg2) construct: shRNA lentiviral constructs were generated according to the instructions provided by the Stewart lab and Addgene

(http://www.stewartlab.wustl.edu/html/lab_protocols.html). Two shRNA sequences were selected for Abcg2 by using an Invitrogen program and forward and reverse oligos were synthesized as follows:

Forward oligo: 5'CCGG-21bp Sense-CTCGAG-21bp Antisense-TTTTTG 3'

Reverse oligo: 5'AATTCAAAAA-21bp Sense-CTCGAG-21bp Antisense 3'

The two sense and corresponding antisense target sequences are:

1. GGATATTACAGAGTGTCTTCT (sense) and AGAAGACACTCTGTAATATCC (antisense) and

2. GCAACACTTCTCATGACAATC (sense) and GATTGTCATGAGAAGTGTTGC (antisense).

For control virus, a scramble shRNA oligo was generated (CCTAAGGTTAAGTCGCCCTCG (sense) and CGAGGGCGACTTAACCTTAGG (antisense)).

Oligos were resuspended in water at a concentration of 1μg/μl, mixed together (5μl forward oligo + 5μl reverse oligo + 5μl 10x NEB2 buffer + 35μl water) and annealed by incubation at 95^{o}C for 4 min followed by 10 min at 70^{o}C placed in a beaker filled with water to allow gradual cooling down to RT. Subsequently, 9μl of the oligos were ligated (NEB, Quick ligation kit Cat #M2200S) to the pLKOpuro1 vector (digested with AgeI and EcoRI). The ligation product was transformed into DH5α bacteria. Positive clones had only one band of 7.2kb after digestion with NdeI and MluI.

pLKOpuro1 encodes a gene conferring resistance to puromycin, facilitating infected cell selection.

shRNA lentivirus production: A mixture of shRNA-pLKOpuro1 vector (3μg), packaging plasmids pHR'8.2deltaR (3μg) and pCMV-VSV-G (0.375μg), Fugene (18μl) and DMEM (final

volume 300µl) was prepared and incubated at RT for 15-30 min. This mix was then gently applied to approximately 70% confluent HEK293-T cells in a 100mm dish. The following day, the medium was replaced with 10ml of CSP expansion medium and the virus was collected 24 hours later. shRNA viruses were always used freshly made.

CSP cell lentiviral infection: 300000 CSP cells (passage 3-5) were plated in a 100mm plate one day before infection. Medium was then removed and replaced with 3ml of virus and 6µg/ml protamine sulfate (Sigma Cat #P4020). After 3 hours of incubation at 37°C, fresh medium was added. Selection of infected cells was performed 48 hours later either by FACS (GFP+ cells selection) or by drug (puromycin or neomycin) selection. In the case of puromycin and neomycin, selection required 3-4 and 5-10 days respectively.

Asymmetric division assessment: Unsynchronized CSP cells (10000 cells) were cultured on coverslips (20mm x 50mm) for 5 days. Cells were fixed, permeabilized and blocked as described above. Cells were incubated with primary antibodies against pH3 (1/200, Abcam Cat # ab32107) and α-adaptin (1/50, Santa Cruz cat # sc-17771) and appropriate secondary antibodies (1/200, anti rabbit Alexa-488 and anti-mouse Alexa-555, Molecular probes). In symmetrically dividing cells, α-adaptin was evenly distributed in the two daughter cells, whereas in asymmetrically dividing cells α-adaptin segregated preferentially to one of the daughter cells. pH3 staining allowed the identification of mitotic cells. For flow cytometric analysis of numb-expression, CSP cells were lifted from the culture plates, fixed with 4% paraformaldehyde and permeabilized with BD Perm/Wash solution (BD biosciences) at 4°C for 20 min. Cells were blocked with 1% BSA in 1xPBS and incubated with anti-numb (1/500, Abcam Cat #ab4147) for 1 hour at RT. Cells were then washed, incubated with a

secondary goat-anti-rabbit 488 antibody (Molecular probes) for 30 min at RT and analyzed with the Accuri C6 analyzer.

Cell cycle analysis using the Fluorescence Ubiquitination Cell Cycle Indicator (FUCCI) lentiviral system: Plasmids were purchased from RIKEN BRC DNA BANK. $5x10^6$ HEK293-T cells were plated in a 10mm culture dish and cultured for 24 hours at 37°C in 10% CO2. At approximately 75% confluency, cells were used for transfection. The transfection mix consisted of 17µg of the SIN plasmids, mKO2-hCdt1 (30/120, kusadira orange) or mAG-hGeminin (1/110, azami green), 10µg of the packaging plasmid, 10µg of the VSV-G- and Rev-expressing plasmid, DMEM to reach a volume of 450µl, 50µl of 2.5M CaCl2 and 500µl 2x BBS solution (50mM BES, 280mM NaCl, 1.5mM Na_2HPO_4). After 15-20 min incubation at RT, the mix was added drop wise to the cells. Plates were placed at 37°C for 12-16 hours in 3% CO2. Medium was then renewed and cells were incubated for an additional 48 hours at 37°C in 10% CO2. Finally, the medium containing the lentivirus was collected, filtered through a 0.45 µm filter, frozen in liquid nitrogen and stored at -80°C. Medium was added to the remaining cells and more virus was collected 24 hours later. Cells were infected as described above and selection was achieved by FACS sorting.

CSP cells infected with both lentiviruses (mKO2 and mAG) were synchronized for 24 hours at 37°C (α-MEM, 0.1% FBS HI, 2 mM L-Glutamine and 1% pen/strep). Cells were then split into 60mm culture plates and cultured in CSP expansion medium for up to 40 hours. Sampling of the cells was performed at several time points and cells were analyzed by flow cytometry or confocal imaging for the expression of Cdt1 (kusadira orange 548/559nm) or Geminin (azami green, 492/505nm).

RESULTS

ABCG2 REGULATES THE CSP PHENOTYPE IN AN AGE-DEPENDENT MANNER

LACK OF ABCG2 DOES NOT ABOLISH THE CSP PHENOTYPE

Abcg2 is the molecular determinant of the BMSP phenotype. In order to establish the contribution of Abcg2 in the CSP phenotype, mononuclear cell suspensions from WT and Abcg2-KO mouse hearts and bone marrow were isolated and stained with Hoechst 33342. Flow cytometric analysis showed that the SP fraction in the bone marrow of WT mice consisted of approximately 0.2% of the cells (0.2±0.05) while in Abcg2-KO mice the BMSP fraction had completely disappeared (0.02±0.02%) (Figure 10A). Interestingly, Abcg2-KO heart samples, exhibited a reduced but clearly detectable CSP fraction (0.46±0.1%) compared to WT (0.8±0.2%), indicating that Abcg2 is not the sole determinant

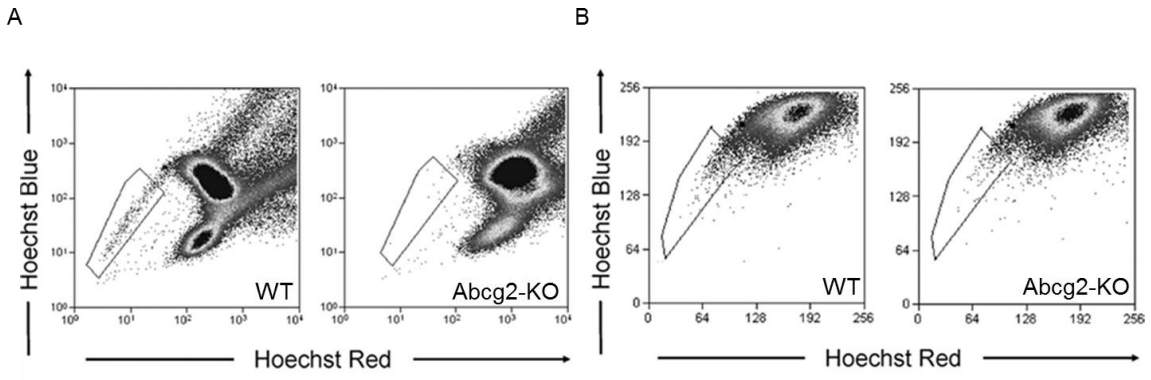

Figure 12: Abcg2 contribution to the SP phenotype of adult murine bone marrow (BM) and heart. Representative flow cytometric analyses of Hoechst-stained A) BM and B) cardiac cells from WT and Abcg2-KO mice. SP cells appear as Hoechst-low/negative cells in the boxed area.

of the SP phenotype in the heart (Figure 10B). As a negative control, two known ABC transporter inhibitors, verapamil and FTC, were used. Both WT and Abcg2-KO CSP tails were completely abolished after addition of these two inhibitors (Figure 11A-F).

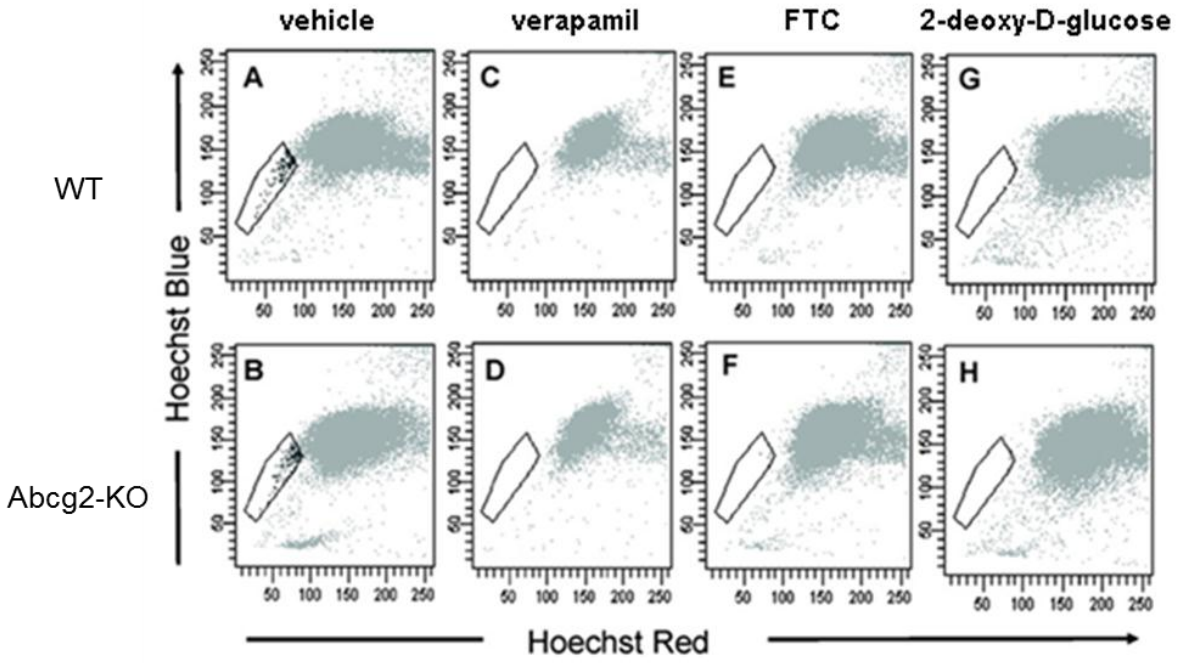

Figure 13: Abcg2-KO CSP cells export Hoechst through a second ABC-transporter. A-H) Representative flow cytometric analyses of WT and Abcg2-KO CSP cells pre-treated with vehicle (A, B), verapamil (C, D), FTC (E, F) and 2-deoxy-D-glucose (G, H). ABC-transporter inhibition or ATP depletion, inhibits the CSP phenotype in both WT and Abcg2-KO CSP. I-Q) Fluorescent microscope images of WT (I-K) and Abcg2-KO (L-N) CSP stained for Mdr1a/b (green) and DAPI (blue). Mdr1a/bko main population (MP) cells serve as negative control (O-Q).

ANOTHER ABC TRANSPORTER IS INVOLVED IN THE REGULATION OF CSP PHENOTYPE IN ADULT MICE.

In order to verify whether the remaining CSP cells in the Abcg2-KO hearts actively export Hoechst through the action of another ABC transporter, WT and Abcg2-KO cardiac cell suspensions were pre-incubated with 2-deoxy-D-glucose instead of glucose to deplete the medium from ATP and thus inactivate any ATP-dependent transport. ATP depletion led to a total elimination of the SP tail indicating the Hoechst efflux in Abcg2-KO CSP is ATP-dependent (Figure 11G, H).

Bunting et al, have shown that P-glycoprotein (or Mdr1or Mdr1a/b in mice), another ABC transporter is also able to efflux Hoechst [182]. Hence, I hypothesized that

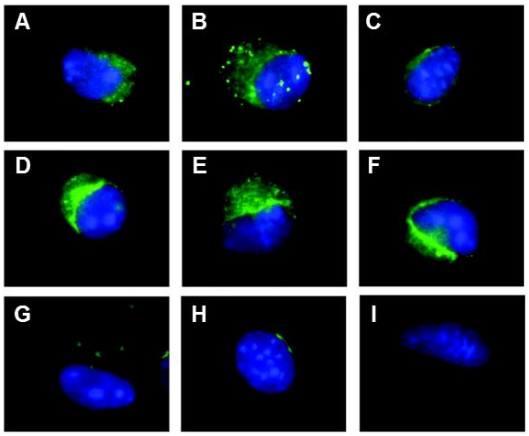

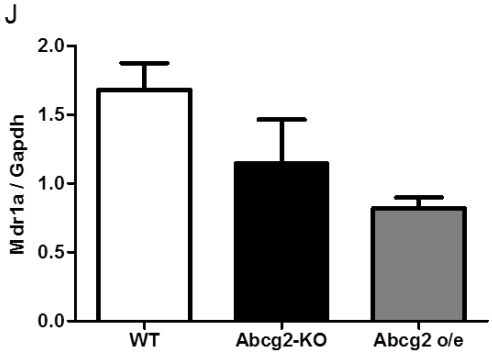

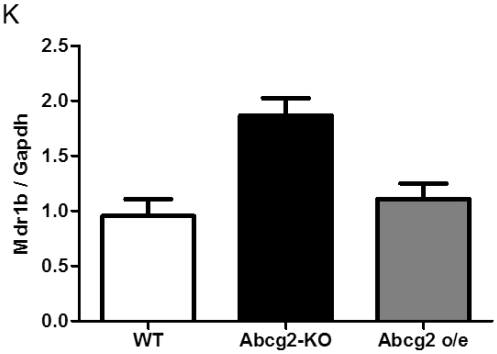

Figure 14: Mdr1a/b is expressed in CSP cells. A-I) Fluorescent microscopy images of WT (A-C) and Abcg2-KO (D-F) CSP cells stained for Mdr1a/b (green) and DAPI (blue). Mdr1a/bko main population (MP) cells serve as negative control (G-I). J and K) Gene expression analysis of Mdr1a and Mdr1b respectively in WT Abcg2-KO and Abcg2 over-expressing (o/e) CSP. Data are mean ± s.e.m.

Mdr1 could be a contributor to the CSP phenotype. The expression of Mdr1 in CSP cells was verified by immuno-cytochemistry (Figure 12 A-I) and RT-PCR (Figure 12J, K). Both methods revealed that CSP cells express Mdr1, in both gene and protein levels.

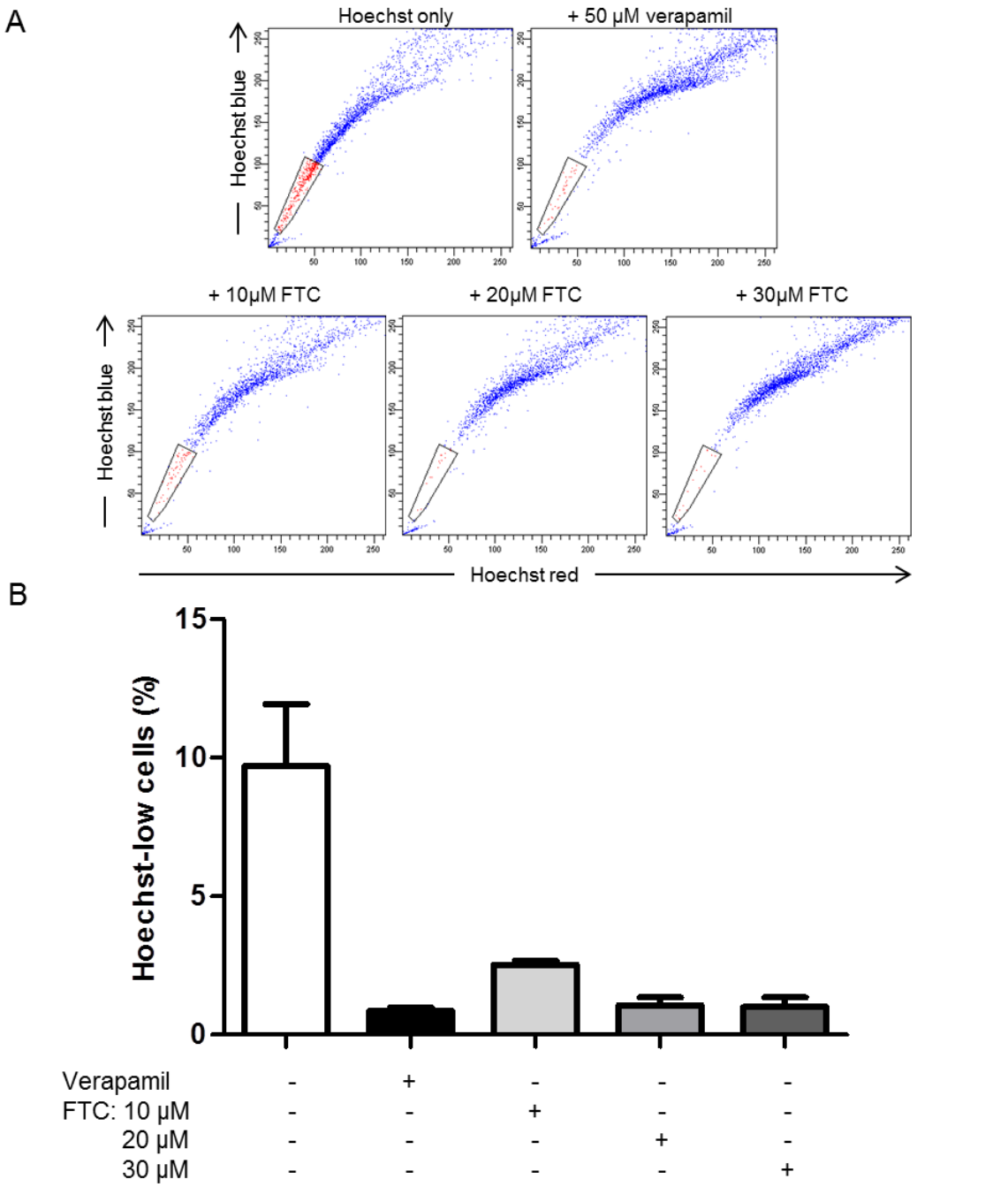

Figure 15: FTC inhibits Mdr1a/b-mediated Hoechst efflux. A) Representative flow cytometric analysis of SK-N-FI cells stained for Hoechst and treated with either verapamil or different concentrations of FTC. B) FTC inhibits Hoechst efflux in a dose dependent manner. Data are mean ± s.e.m.

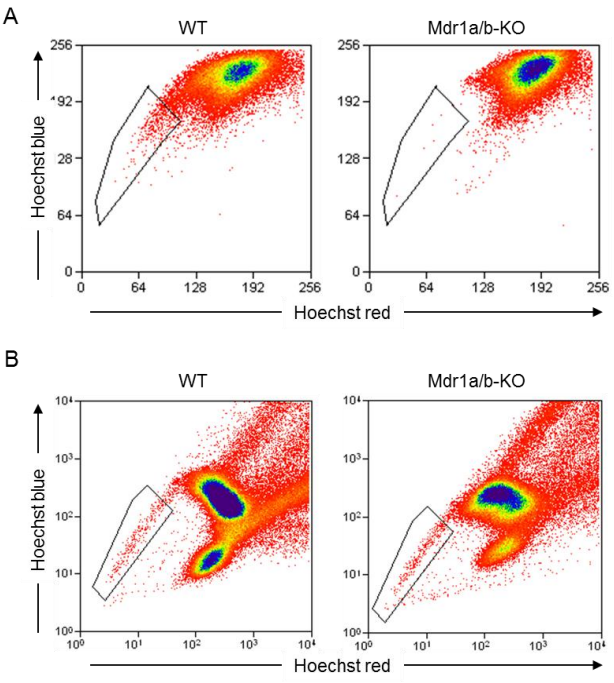

Figure 16: Mrd1a/b contribution to the adult SP phenotype in heart and bone marrow (BM). Representative flow cytometric analyses of Hoechst-stained A) cardiac and B) BM cells from WT and Mdr1a/bko mice.

As shown earlier, the residual CSP cells in the Abcg2-KO hearts were inhibited by addition of FTC. Several reports have indicated that FTC is a specific inhibitor of Abcg2 [183-185], thus before determining the contribution of Mdr1a/b to the CSP phenotype I sought to verify the whether FTC can inhibit Mdr1a/b. For this purpose the Mdr1 over-expressing human neuroblastoma cell line SK-N-F1 was used [186]. Cells were pre-incubated with verapamil (negative control) or increasing concentrations of FTC followed by Hoechst staining. Analysis by flow cytometry revealed that FTC blocks Mdr1-mediated dye efflux in a dose dependent manner (Figure 13). Therefore, the inhibition of Abcg2-KO CSP cells by FTC is likely due to inhibition of Mdr1 efflux.

The contribution of Mdr1a/b to the CSP phenotype was determined by staining of Mdr1a/b-KO cardiac cell suspensions with Hoechst dye. Surprisingly, CSP cells were completely depleted from Mdr1a/b-KO hearts (Figure 14A). It is noteworthy, that the bone marrow of Mdr1a/b-KO animals had similar BMSP levels as the WT animals (Figure 14B).

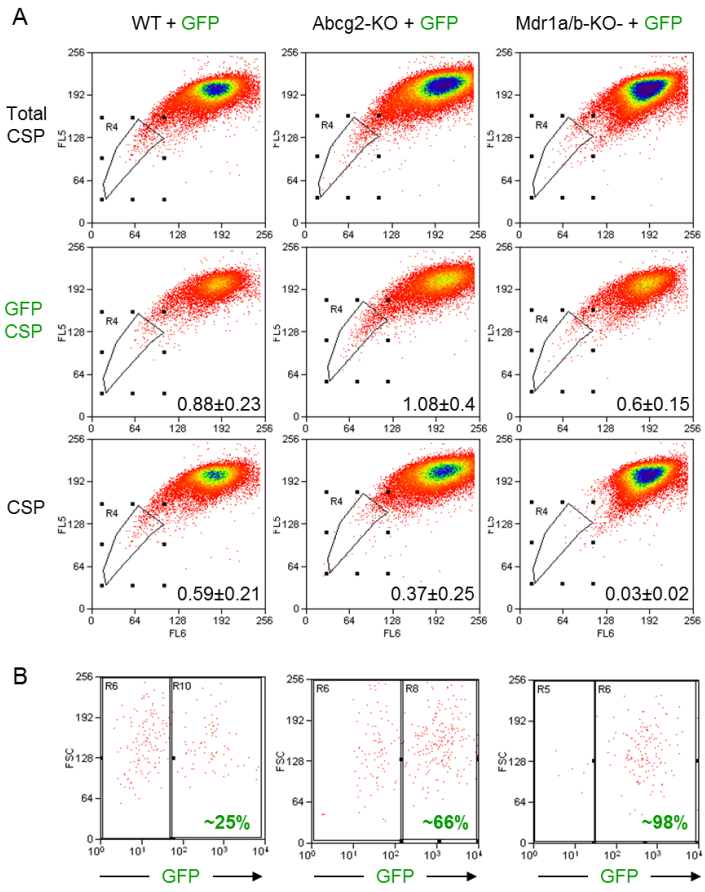

Figure 17: Hoechst staining internal control. A) Flow cytometric analyses of mononuclear cell mixtures containing one part of GFP^+ WT CSP cells and three parts of either WT, Abcg2-KO or Mdr1a/b CSP cells. GFP^+ CSP fraction is within normal levels. GFP^- CSP fractions correspond to previously observed levels. B) In WT cell mixtures approximately 25% of the cells are GFP^+ reflecting the 3:1 ratio of the mixture. In Abcg2-KO cell mixtures ~66% of the cells are GFP^+ while Mdr1a/bko mixtures consist entirely of GFP^+

Several experimental variables, such as cell counting, dye concentration and staining duration, can affect the amount of SP cells in each sample. In order to exclude the possibility that the observed phenotypes are attributed to experimental variations, an internal staining control was used. One million cardiac mononuclear cells from WT-GFP animals were mixed with three million cardiac mononuclear cells from WT, Abcg2-KO or Mdr1a/b-KO animals and stained with Hoechst. Flow cytometric analysis revealed that as expected in all samples the percentages of GFP^+ CSP cells were within the normal WT CSP levels (0.8±0.2%) and the GFP^- WT, Abcg2-KO and Mdr1a/b-KO CSP fractions were within the levels previously observed (0.7±0.2%, 0.37±0.25% and 0.03±0.02% respectively) (Figure 15A). To better demonstrate the accuracy of cell counting and staining both GFP^+ and GFP^- cell populations

were analyzed together. This analysis shows that one third of the CSP cells expressed GFP in the WT sample, approximately 66% of the cells were GFP^+ in Abcg2-KO sample and in the Mdr1a/b-KO sample the CSP tail consisted almost entirely of GFP^+ CSP cells (Figure 15B). These numbers agree with the initial cell mixing ratio (3:1 GFP^- vs GFP^+ cells).

ABCG2-KO CSP CELLS SHARE THE SAME SURFACE MARKER EXPRESSION PATTERN WITH WT CSP CELLS

Although, no specific marker exists for CSP cell identification, they are characterized by high levels of the Stem cell antigen 1 (Sca1) and the endothelial marker CD31. However, CSP cells do not express the hemopoietic marker CD45, which clearly distinguishes them from BMSP. In an effort to characterize the Abcg2 deficient population, Abcg2-KO CSP cells were analyzed for the expression of these markers and were found to express similar levels as the WT cells (Table 1). This result indicates that lack of Abcg2 does not alter the cell surface marker expression of CSP cells and therefore both WT and Abcg2-KO populations share similar characteristics.

Surface marker	WT CSP (%)	Abcg2-KO CSP (%)
Sca1	90±1	89±2
CD31	80±2	79±3
CD45	≤1	≤1

Table 1: Cell surface marker expression in WT and Abcg2-KO CSP cells.

ABCG2 HAS AN AGE-DEPENDENT CONTRIBUTION TO THE CSP PHENOTYPE

Abcg2 has been shown to be highly expressed in embryonic hearts and gradually decrease in the adult [71]. To examine whether the contribution of Abcg2 to the CSP phenotype changes with age, CSP analyses where performed in neonatal (P3), two week old (p14), three week old (p21) and adult mouse hearts (Figure 16). I observed that the CSP cell fraction is significantly increased in early postnatal life and gradually decreases with age. Interestingly, neonatal Abcg2-KO hearts exhibited very limited CSP numbers, whereas WT and Mdrko hearts showed similar levels of CSP cells (Figure 18A). At two weeks of age, CSP

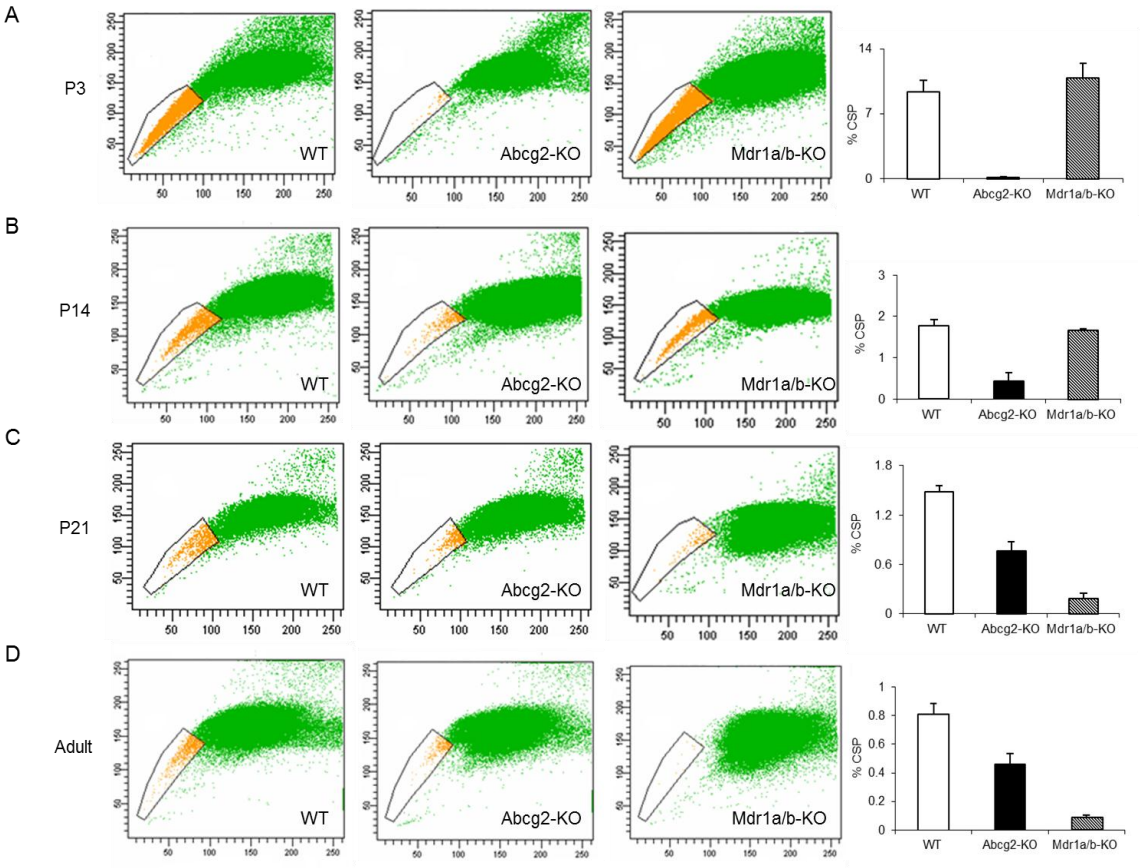

Figure 18: Age-dependent contribution of Abcg2 and Mdr1a/b to the CSP phenotype. CSP flow cytometric analyses of A) neonatal (P3), B) two week old (P14), C) three week old (P21) and D) adult mice. Data are mean ± s.e.m.

cells started to appear in Abcg2-KO samples while WT and Mdr1a/b-KO populations decreased (Figure 18B). A similar pattern was observed at three weeks (Figure 18C) with CSP cells almost reaching the numbers observed in adult animals (Figure 18D).

In order to determine whether the phenotype observed was due to differential expression of Abcg2 and Mdr1 in different developmental stages, Abcg2 gene expression was verified in CSP cells from adult and neonatal mice. Indeed, Abcg2 was highly expressed in neonatal CSP cells compared to adult, while Mdr1a and Mdr1b were predominantly expressed in the adult CSP cells (Figure 19).

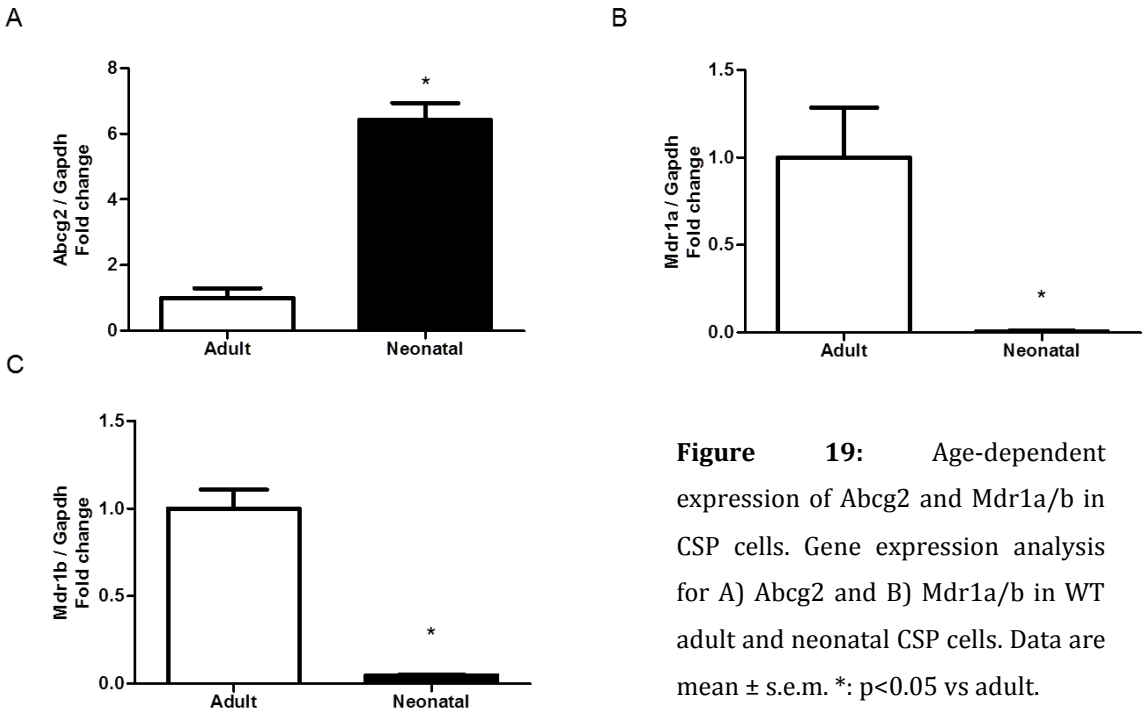

Figure 19: Age-dependent expression of Abcg2 and Mdr1a/b in CSP cells. Gene expression analysis for A) Abcg2 and B) Mdr1a/b in WT adult and neonatal CSP cells. Data are mean ± s.e.m. *: $p<0.05$ vs adult.

ABCG2-KO CSP CELLS EXHIBIT LIMITED PROLIFERATION CAPACITY

My next step was to investigate the cause of the decrease in CSP cells observed in

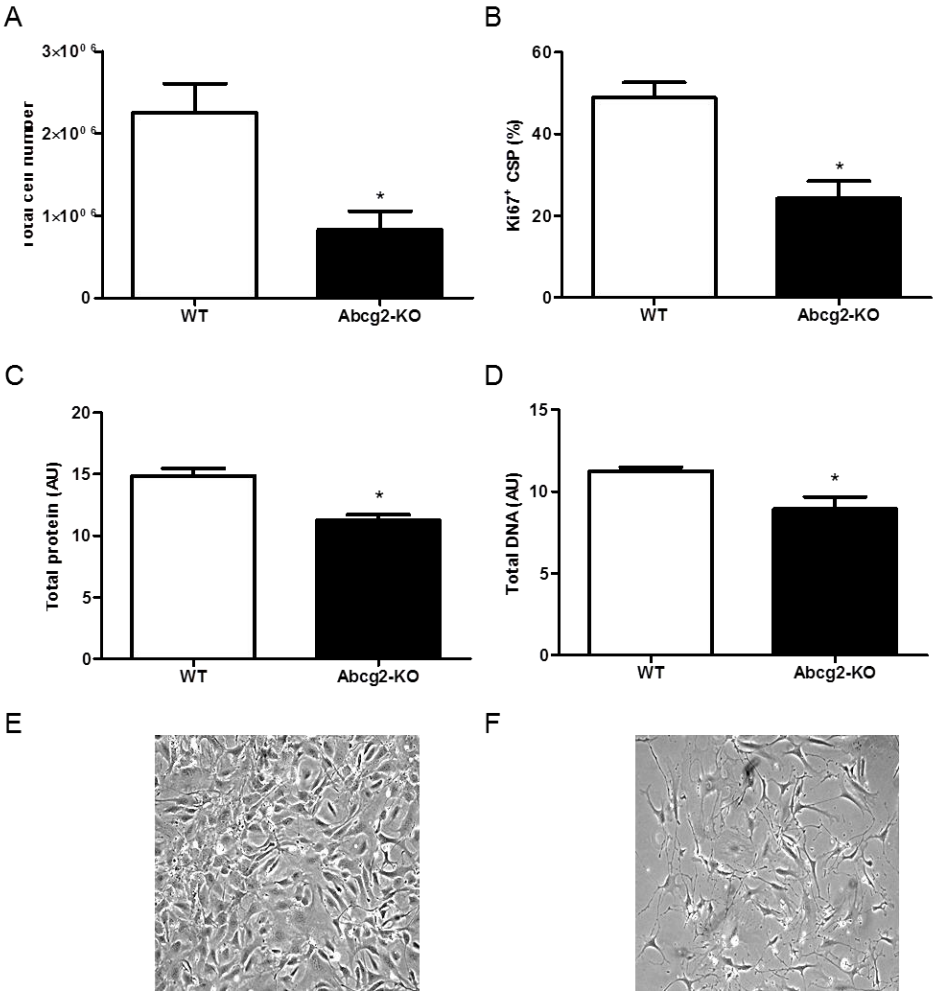

Figure 20: Abcg2 regulates CSP proliferation. Lack of Abcg2 decreases CSP proliferation capacity as shown by A) proliferation assays evaluating the total cell number, B) flow cytometric analysis of Ki67 expression, C) total protein and D) DNA content determined by in cell western. E and F) Representative bright field images of expanded WT and Abcg2-KO CSP respectively. Data are mean ± s.e.m. *:<0.05 vs WT.

Abcg2-KO hearts. Several studies in cancer cell lines have linked Abcg2 to the regulation of proliferation. Namely, Abcg2 over-expressing cells have been shown to be over-proliferative [121]. I therefore decided to examine if and how Abcg2 affects CSP cell proliferation. Proliferation assays demonstrated that CSP cells lacking Abcg2 exhibited decreased cell numbers after several days in culture, compared to WT CSP cells (Figure 20A).

In line with this result, the fraction of cells expressing the proliferation marker Ki67 was markedly decreased in Abcg2-KO CSP cells compared to WT cells (Figure 20B). Furthermore, Abcg2-KO CSP cells had significantly reduced total protein and DNA content compared to WT cells (Figure 20C, D). To determine whether the decreased proliferation observed was due to lack of Abcg2 and not intrinsic differences between WT and Abcg2-KO cells, a lentivirus expressing a shRNA directed against Abcg2 was generated (Figure 21A). A 17-fold decrease of Abcg2 gene expression was achieved in WT CSP cells infected with

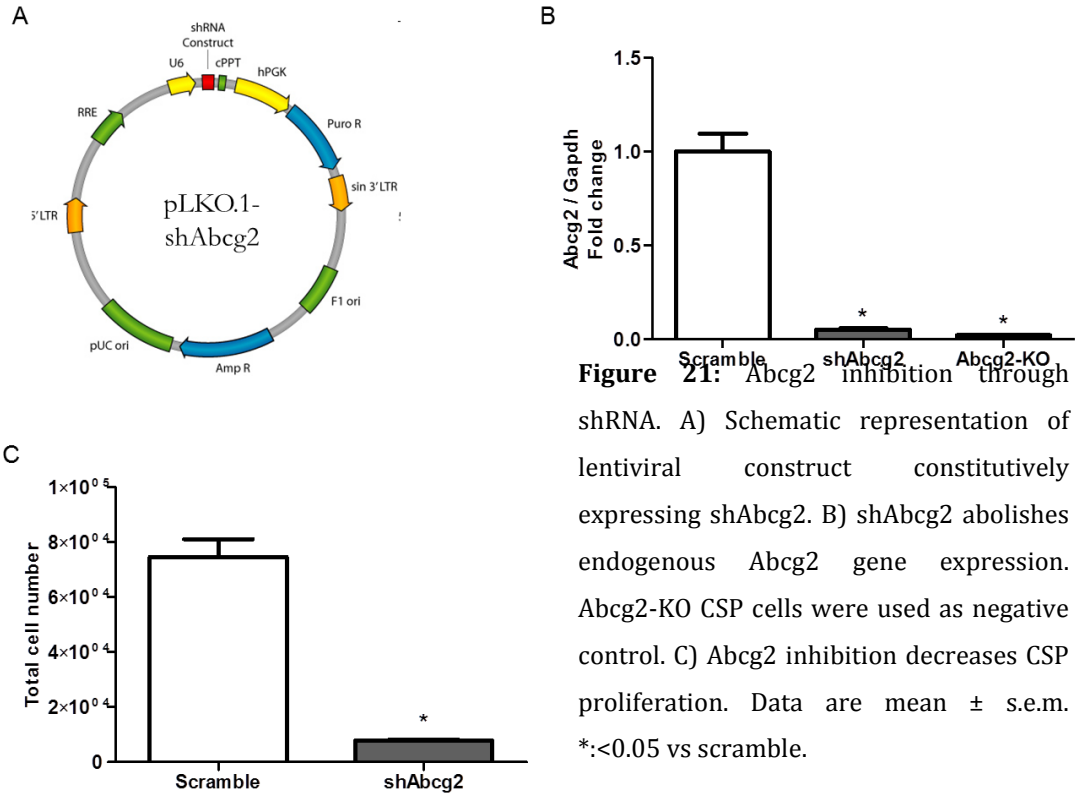

Figure 21: Abcg2 inhibition through shRNA. A) Schematic representation of lentiviral construct constitutively expressing shAbcg2. B) shAbcg2 abolishes endogenous Abcg2 gene expression. Abcg2-KO CSP cells were used as negative control. C) Abcg2 inhibition decreases CSP proliferation. Data are mean ± s.e.m. *:<0.05 vs scramble.

shAbcg2 compared to Scramble infected cells (Figure 21B). This decrease represents a complete inhibition of Abcg2 expression similar to that observed in Abcg2-KO CSP cells (Figure 21B). As anticipated, Abcg2 inhibition by shRNA led to an approximately 9-fold decrease of cell proliferation (Figure 21C).

ABCG2 OVER-EXPRESSION INCREASES CSP PROLIFERATION

In order to establish Abcg2 as a regulator of CSP proliferation, a gain-of-function approach was followed. CSP cells infected with Abcg2 over-expressing lentivirus (Figure 22A, B) demonstrated significantly increased proliferation rates compared with CSP cells infected with control virus (Figure 22C).

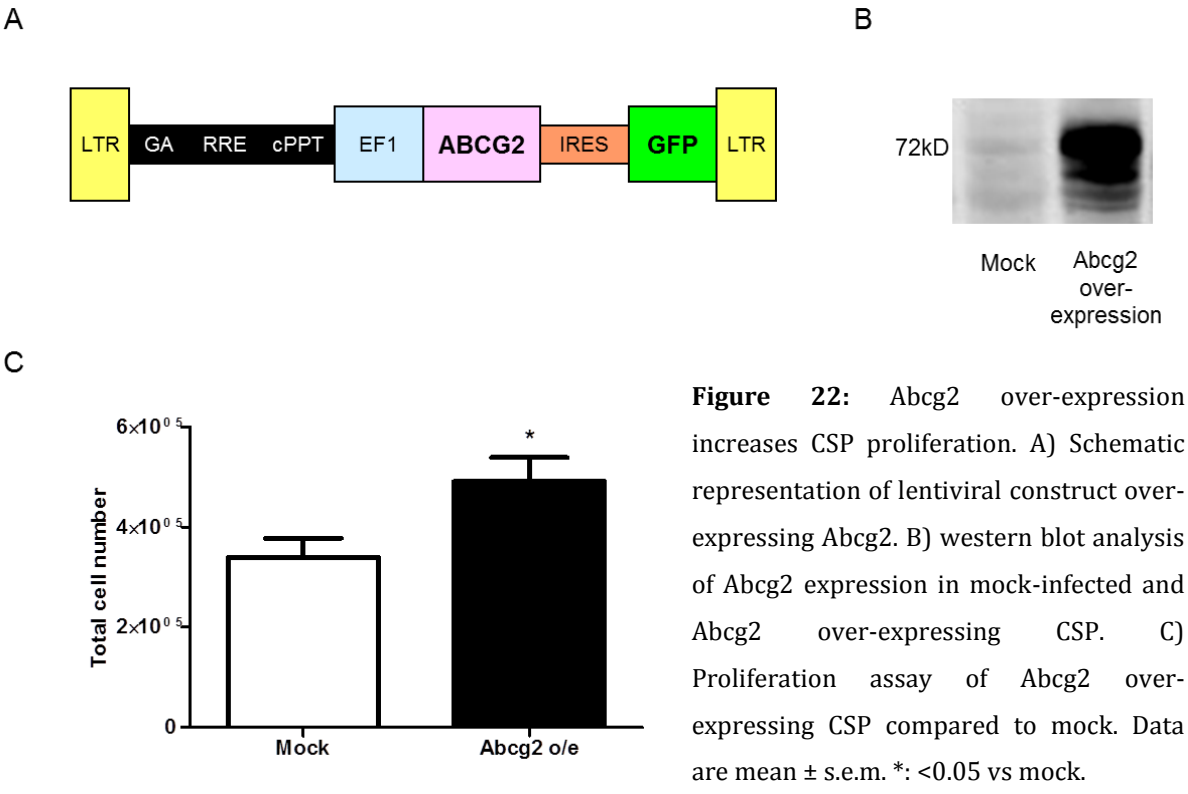

Figure 22: Abcg2 over-expression increases CSP proliferation. A) Schematic representation of lentiviral construct over-expressing Abcg2. B) western blot analysis of Abcg2 expression in mock-infected and Abcg2 over-expressing CSP. C) Proliferation assay of Abcg2 over-expressing CSP compared to mock. Data are mean ± s.e.m. *: <0.05 vs mock.

The primary function of Abcg2 is the export of numerous substances. To investigate whether the transporter function of Abcg2 is required for its effects on CSP proliferation, a mutant/efflux defective form of the protein was generated. A lysine to methionine substitution at amino acid 86 (K86M) within the ATP-binding domain of human Abcg2 has been shown to abolish Abcg2 efflux activity and membrane localization without affecting protein expression and dimerization [187]. The corresponding lysine in the mouse protein is found at amino acid 85 (Figure 23).

To verify the function defect of the mutant, Abcg2-KO CSP cells were infected with lentiviruses over-expressing wild-type (Abcg2^{WT}) and mutant Abcg2 (Abcg2^{mut}) and their Hoechst efflux capacity was assessed. CSP cells expressing Abcg2^{mut} were unable to efflux the dye similar to mock virus infected cells (Figure 24). On the contrary, Abcg2^{WT} expressing CSP exhibited high efflux capacity. We next examined whether Abcg2^{mut} affects

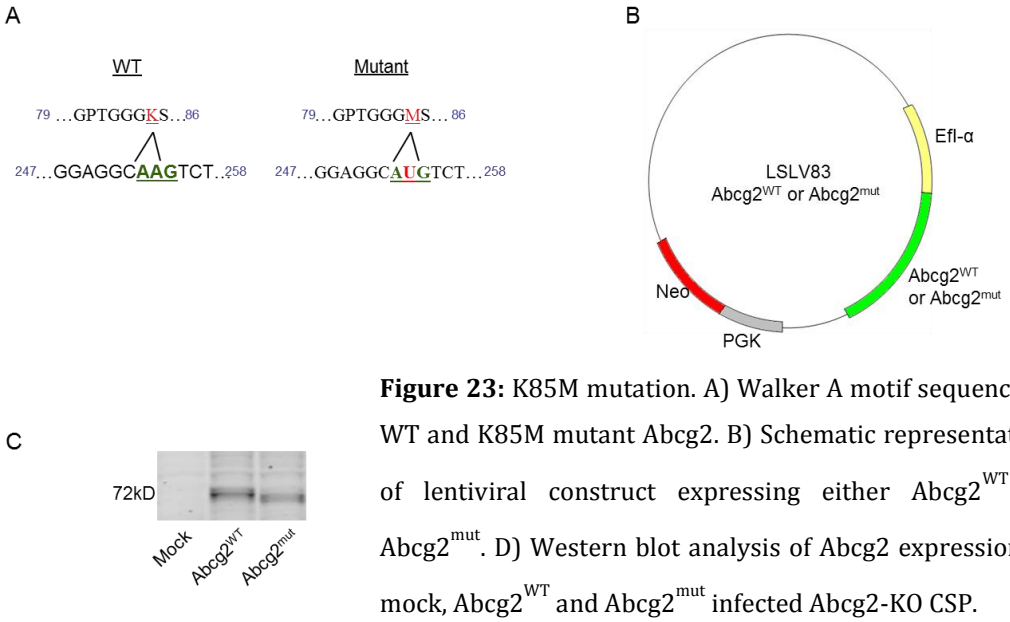

Figure 23: K85M mutation. A) Walker A motif sequence of WT and K85M mutant Abcg2. B) Schematic representation of lentiviral construct expressing either Abcg2^{WT} or Abcg2^{mut}. D) Western blot analysis of Abcg2 expression in mock, Abcg2^{WT} and Abcg2^{mut} infected Abcg2-KO CSP.

the proliferation of CSP cells. As expected, over-expression of Abcg2^{WT} increased significantly the proliferation capacity of Abcg2 null CSP cells (Figure 25). In contrast, Abcg2^{mut}-over-expressing CSP cells demonstrated similar proliferation capacity with Abcg2 null CSP cells (Figure 25). These results clearly suggest that Abcg2 regulates CSP proliferation via its function as a transporter.

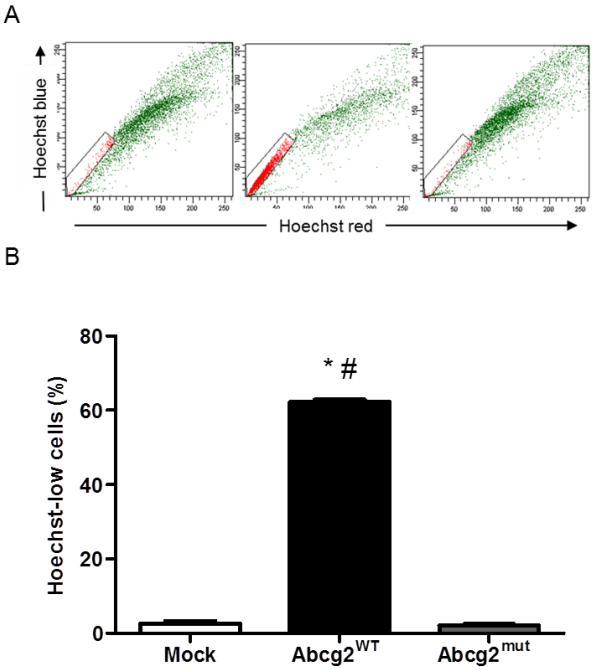

Figure 24: K85M mutation abolishes Abcg2 Hoechst efflux capacity. A) Representative flow cytometric analysis of CSP cells infected with mock, Abcg2^{WT} and Abcg2^{mut}. B) Abcg2 over-expressing CSP cells (Abcg2^{WT})exhibit high efflux capacity while CSP cells expressing the K85M mutant (Abcg2^{mut}) demonstrate similar efflux capacity to Abcg2-KO mock-infected CSP cells. Data are mean ± s.e.m. *,#: p<0.05 vs mock and Abcg2^{mut}.

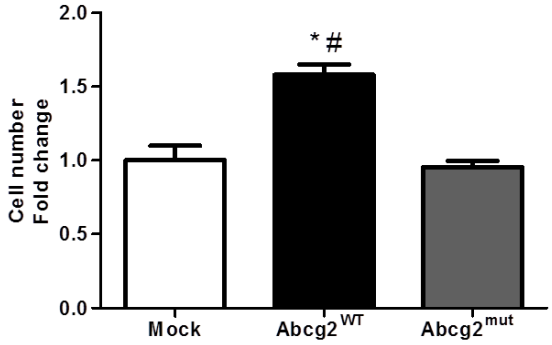

Figure 25: Abcg2 transporter activity is required for its effect on proliferation. Over-expression of Abcg2^{WT} in Abcg2-KO CSP increases their proliferation capacity while Abcg2^{mut} expressing CSP cells exhibit similar cell numbers to Abcg2-KO-Mock cells. Data are mean ± s.e.m. *,#: p<0.05 vs mock and

To further dissect the role of Abcg2 on CSP cell homeostasis, its effects on the cell cycle were investigated. Immuno-cytochemical staining revealed that expression of phospho-histone H3 and BrdU incorporation were decreased in CSP cells lacking Abcg2, indicating that less cells reside in G2/M and S cell cycle phases respectively (Figure 26 A-E). This result was further confirmed by DNA content analysis (propidium iodide staining) (Figure 27).

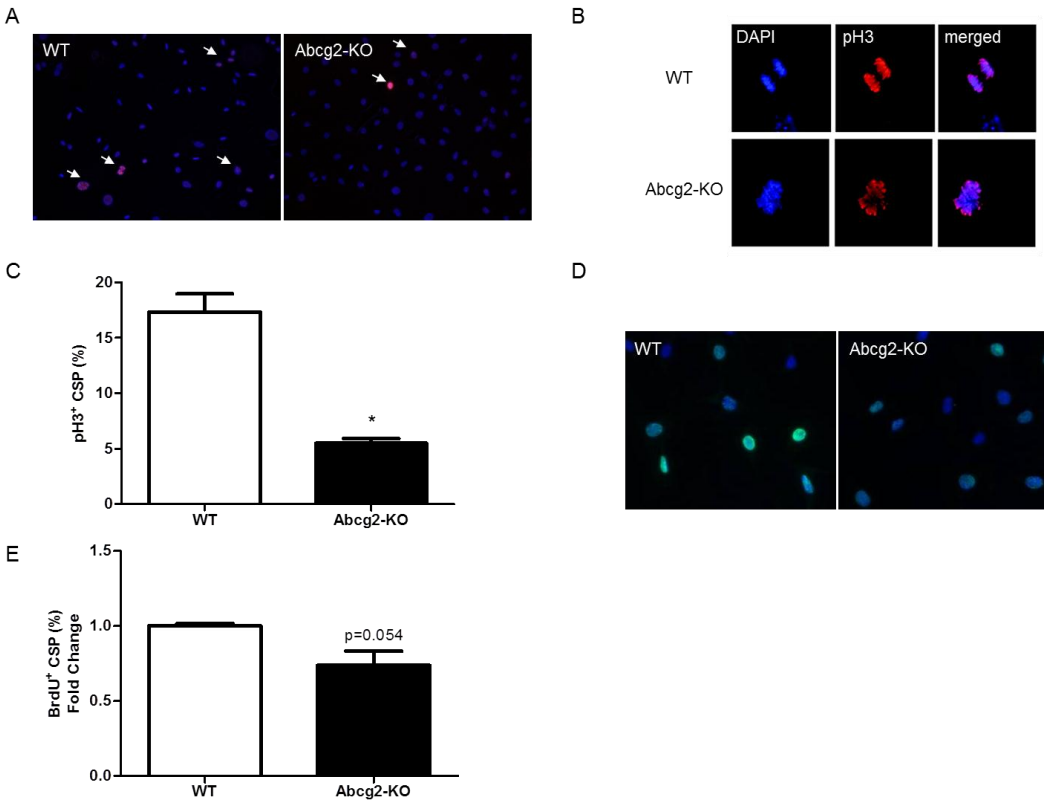

Figure 26: Abcg2 affects CSP cell cycle progression. A and B) Representative fluorescent microscopy images of WT and Abcg2-KO CSP stained for phospho-histone H3 (pH3) in low and high magnification respectively. C) pH3 expression decreases in cells lacking Abcg2. D) Fluorescent microscopy images of WT and Abcg2-KO CSP stained for BrdU (green) and DAPI (blue). E) BrdU incorporating cells are decreased in Abcg2-KO samples. Data are mean ± s.e.m. *,#: $p<0.05$ vs WT.

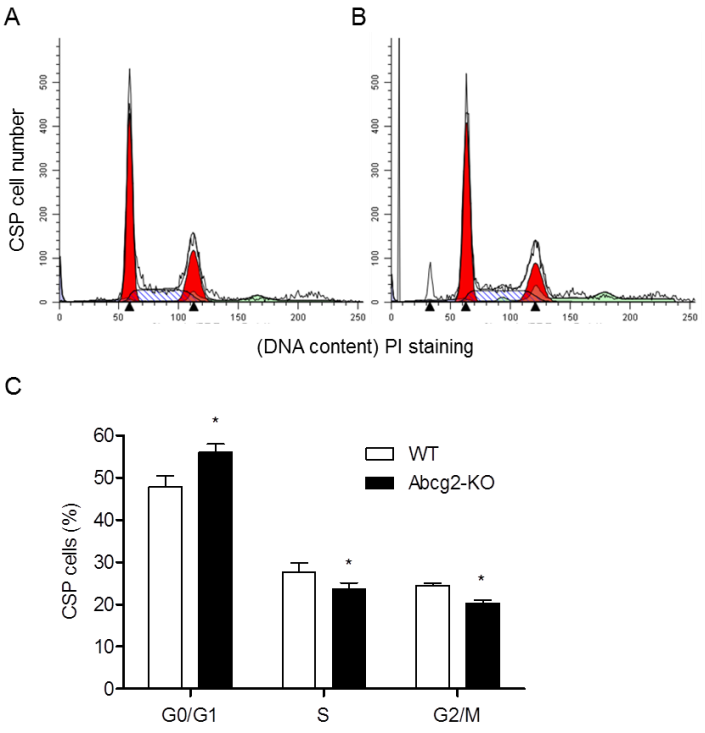

Figure 27: Abcg-2 KO CSP cells exhibit altered cell cycle profile. A and B, representative flow cytometric analyses of WT and Abcg-2 KO CSP cells respectively, stained with propidium iodide (PI). C) Abcg-2 KO CSP cells demonstrated an increase in cells residing in G0/G1 cell cycle phases and a corresponding decrease in S and G2/M compared to WT CSP cells. Data are mean ± s.e.m. *: $p<0.05$

ABCG2 REGULATES G1 TO S CELL CYCLE PHASE TRANSITION IN CSP CELLS

To thoroughly characterize the cell cycle kinetics (duration and distribution) of WT and Abcg2-KO CSP cells a cell cycle fluorescence-based reporter system, the Fluorescence Ubiquitination Cell Cycle Indicator (FUCCI) was used [1]. This system consists of two lentiviruses each expressing a fluorescent protein, Kusabira-orange or azami-green, fused to cell cycle regulators Ctd1 and geminin respectively. These two proteins are temporally regulated by ubiquitin E3 ligases APC^{Cdh1} and SCF^{Skp2} that target them for proteasomal degradation resulting in a biphasic cycling through the cell cycle. Cdt1 is activated during G1 cell cycle phase and its expression sustains through G1-S transition while Geminin is activated during G1-S transition and remains expressed during S, G2 and M phases. Both proteins are silenced shortly after division (Figure 28).

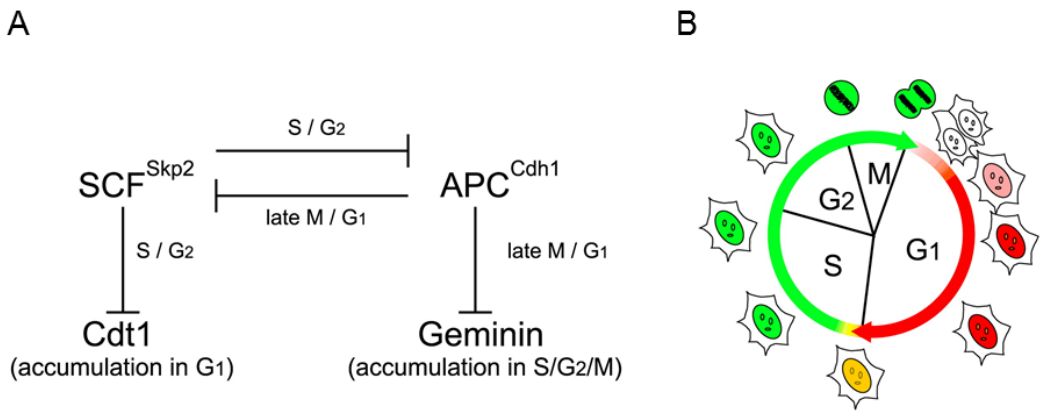

Figure 28: Fluorescent Ubiquitination-based Cell Cycle Indicator. A) Regulation of the cell cycle by SCF^{Skp2} and APC^{Cdh1} maintains a balance between G1 and S/G2/M phases. B) Fluorescent proteins label cells in G1 in red and cells in S-G2-M in green [1].

Flow cytometric analysis of WT and Abcg2-KO CSP cells infected with the two lentiviruses 24 hours post-synchronization revealed that WT CSP cells were actively cycling with 15.7% ± 0.36% of cells residing in G1, 69.2% ± 1.1% in G1-S transition phase, 13.1% ± 0.66% in S-G2-M and 1.55% ± 0.17% of CSP cells appeared as negative for the two proteins. Interestingly, Abcg2-KO CSP cells exhibited a completed different profile. The majority of the cells (54.5% ± 0.28%) appeared as negative for both cell cycle indicators, 37.25% ± 0.07% were in G1 and only a small fraction was in G1-S transition and S-G2-M phases (1.03% ± 0.09% and 2.48% ± 0.05% respectively) (Figure 29A, B).

Monitoring of the cell cycle distribution in WT and Abcg2-KO CSP cells from 18 hours to 28 hours or 40 hours post-synchronization respectively revealed a significant defect in cell cycle progression in Abcg2-KO CSP cells. At the 18 hours timepoint 76.1% ± 0.65% of WT cells resided in G1 and 22% ± 0.79% had already entered S phase (G1-S transition). Progressively, WT cells exited the G1 phase followed by a corresponding increase in cells residing in G1-S transition phase. Between 22 hours and 24 hours, cells in

G1-S reached a peak followed by a progressive decrease. Concomitantly, WT cells started to appear in the S-G2-M quadrant. Entry in G2-M phase was quickly followed by an increase in cells negative for both fluorescent probes indicating cell division (Figure 29C). On the contrary, the majority of Abcg2-KO CSP cells seemed unable to progress in the cell cycle even after 40 hours post-synchronization. At the 18 hours time point the majority of Abcg2-KO CSP cells appeared as negative for the two cell cycle indicators (55.6% ± 0.41%) and remained negative for up to 40 hours. Cells residing in G1 phase (37.8% ± 0.32% 18 hours) remained stable up to 24 hours and decreased modestly thereafter. The amount of Abcg2-KO CSP cells in G1-S transition and S-G2-M phases was negligible at 18 hours post-synchronization and slowly reached approximately 4% and 12% respectively (Figure 29D).

The fraction of cells residing in G1 during the time course of the experiment was fit to a "plateau followed by decay" model and the $T_{50\%}$ was calculated. The $T_{50\%}$ for WT CSP cells was calculated at 20 hours while Abcg2-KO CSP cells had a $T_{50\%}$ at 33 hours post synchronization (Figure 29E). These data clearly suggest that lack of Abcg2 results in prolonged G1 phase and cell cycle exit. Our results were further confirmed by live cell imaging confocal microscopy from 18 hours to 40 hours post-synchronization (Figure 29 F, G). WT CSP cells oscillated between cell cycle phases (red to green to negative daughter cells) while the large majority of Abcg2-KO CSP cells remained in G1 (red). Overall, these results demonstrate that Abcg2 controls the cell cycle progression of CSP cells.

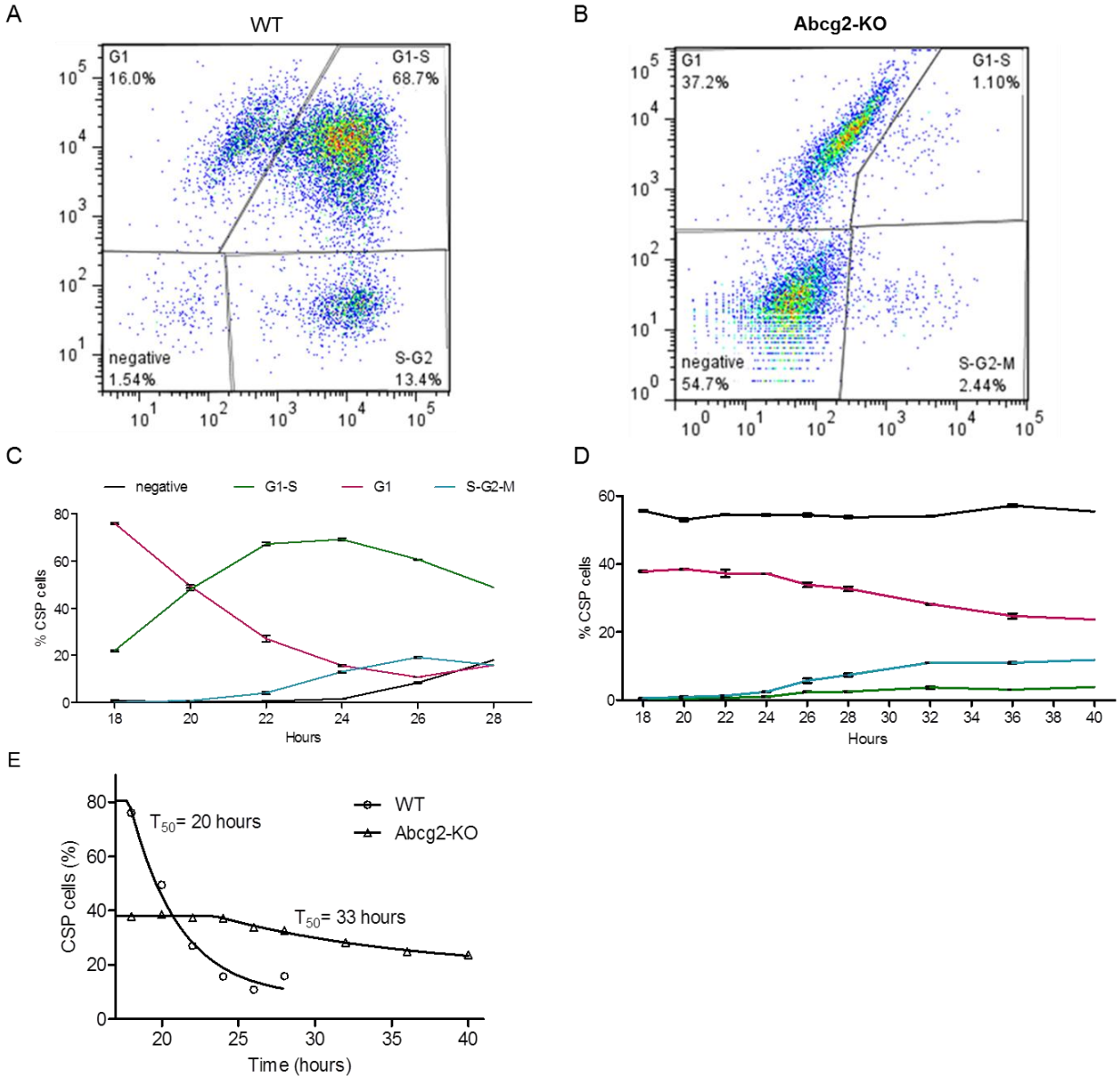

Figure 29: Lack of Abcg2 prolongs cell cycle duration in CSP cells. A-B) Flow cytometric analysis of WT and Abcg-2 KO CSP cells respectively expressing the FUCCI cell cycle indicators 24 hours post-synchronization. Abcg-2 KO CSP appear mainly in the negative and G1 quadrants. C) WT and D) Abcg-2 KO cell cycle progression monitoring from 18 hours to 28 hours and 40 hours respectively post synchronization. E) Calculation of WT and Abcg-2 KO CSP G1 phase $T_{50\%}$ following a "plateau followed by decay" model. F-G) Gallery of pictures derived from live cell imaging confocal microscopy of WT and Abcg-2 KO CSP respectively between 18 hours and 40 hours post-synchronization. Data are mean ± s.e.m.

F

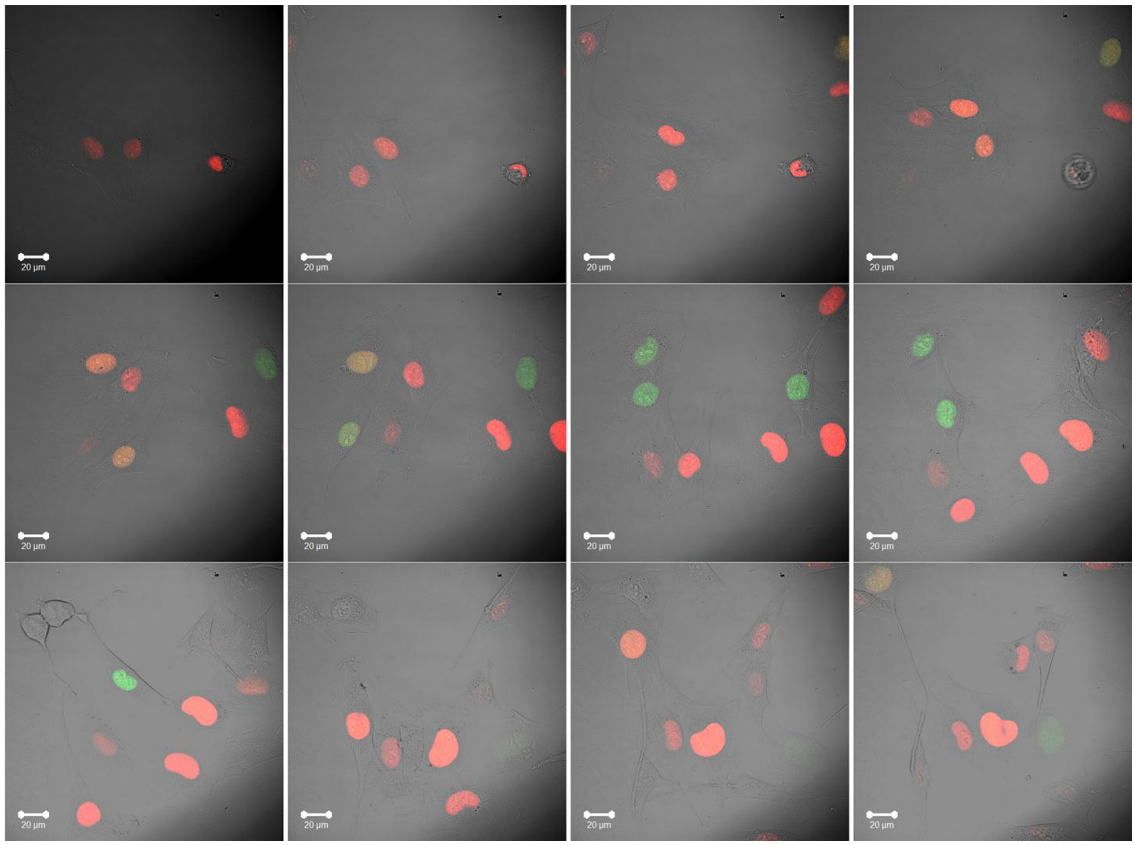

G

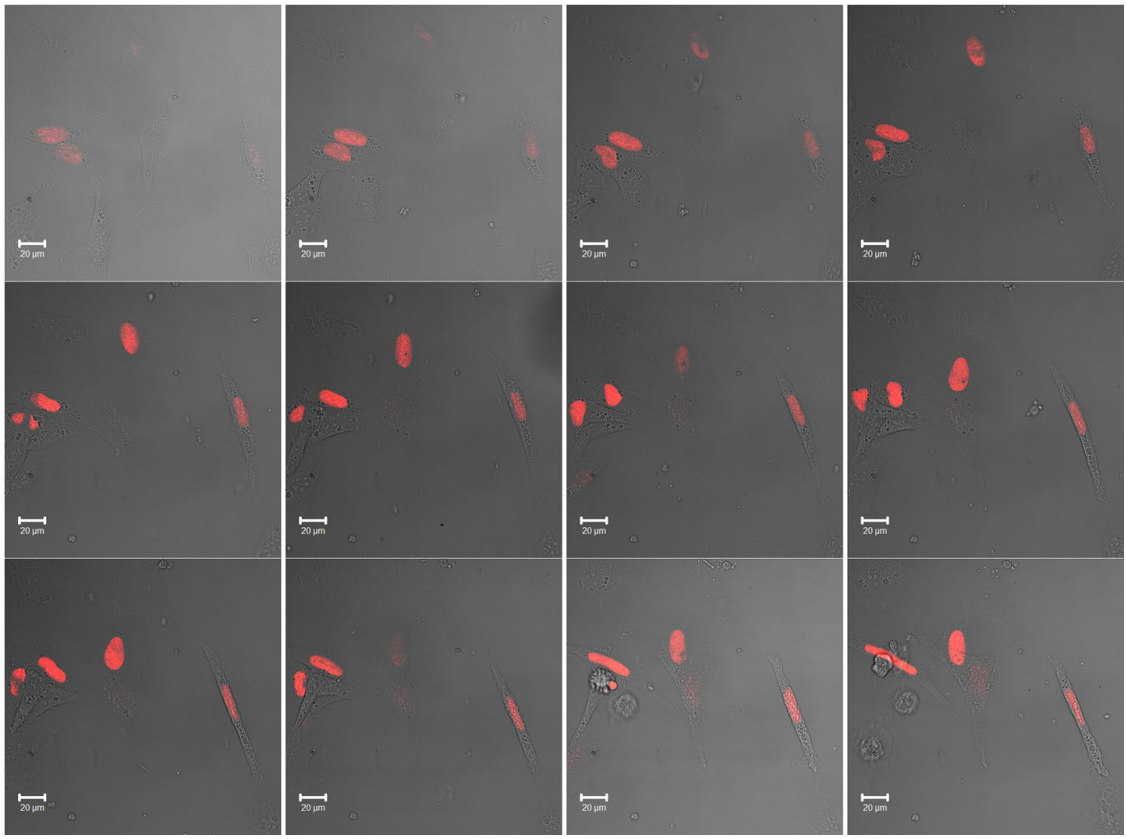

LACK OF ABCG2 ALTERS THE CELL CYCLE GENE EXPRESSION PROFILE OF CSP CELLS

The effect of Abcg2 on the expression of cell cycle molecular regulators was determined by a RT-PCR cell cycle-focused array. In line with the delay in cell cycle progression observed, lack of Abcg2 in CSP cells (shAbcg2) resulted in down-regulation of several cell cycle activators and up-regulation of cell cycle inhibitors (Figure 30A). Interestingly, several DNA damage related genes were also activated in shAbcg2-expressing CSP cells (Figure 30B).

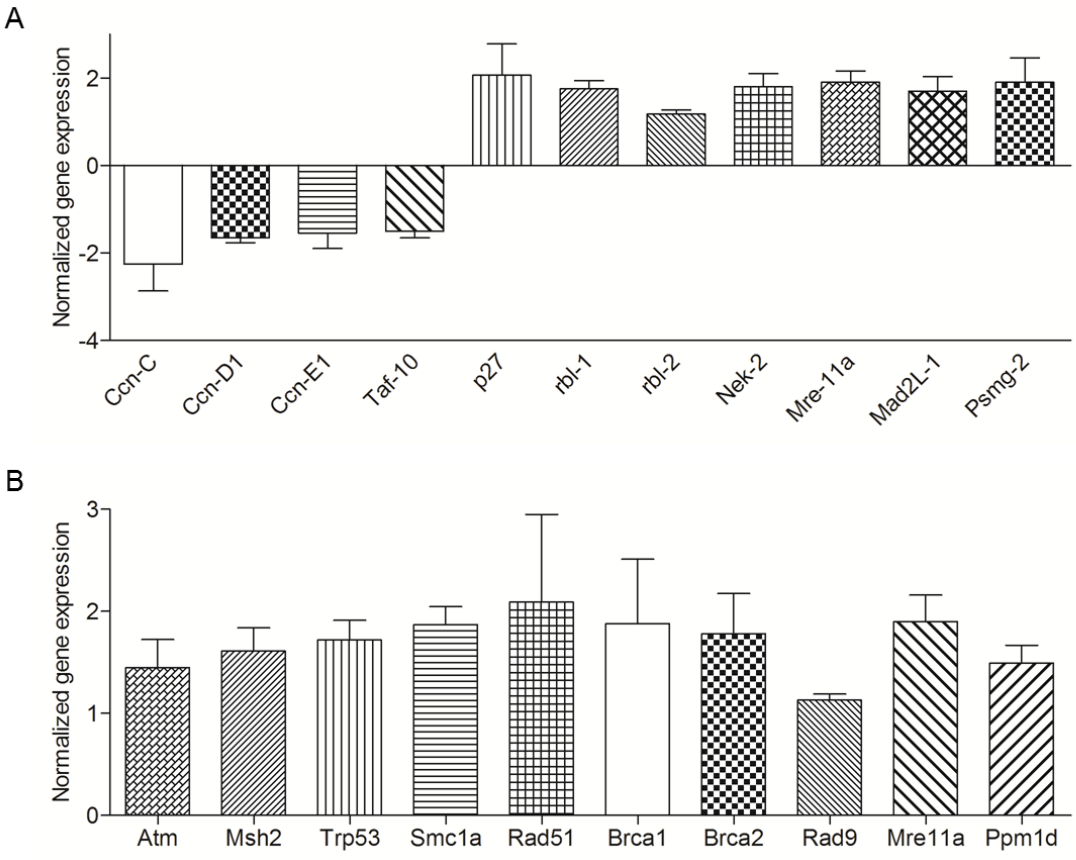

Figure 30: Abcg2 deficiency alters the expression profile of cell cycle regulators and DNA damage-related genes. Significantly altered genes regulating A) cell cycle and B) DNA damage in shAbcg2 infected CSP cells compared to scramble. Data are mean ± s.e.m.

Abcg2 is an exporter of a large variety of compounds including cancer drugs and toxins. It has often been implicated in cell protection from injury [112, 114]. To examine whether Abcg2 affects CSP cell survival, cell apoptosis and necrosis were evaluated by annexin-V and PI staining. CSP cells lacking Abcg2 exhibited increased levels of both apoptotic and necrotic cell death (Figure 31A-D). Further confirmation was obtained by the

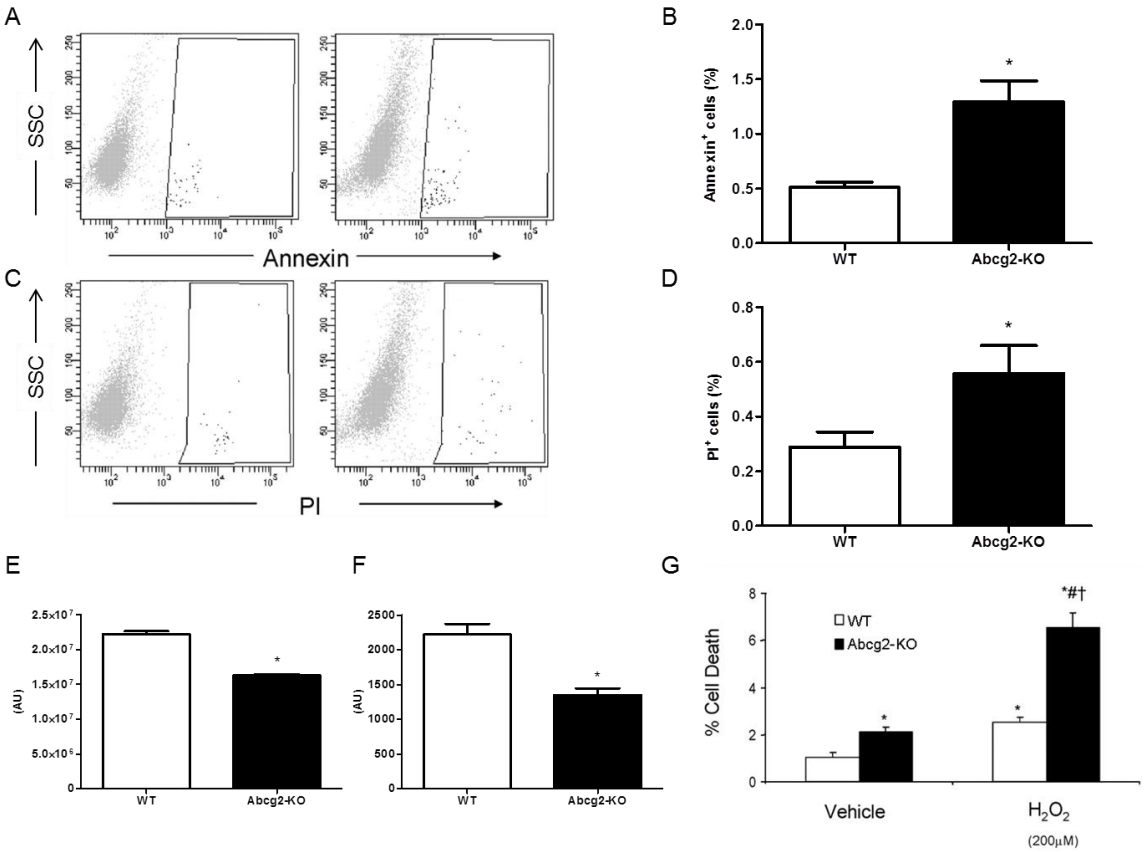

Figure 31: Abcg2 plays a protective role in CSP cells. Lack of Abcg2 increased both apoptotic and necrotic cell death as evidenced by flow cytometric analysis of A-B) Annexin and C-D) Propidium iodide (PI) respectively. E) CellTiter-Glo and F) CellTiter-Blue viability assays reveal decreased metabolic activity in Abcg2-KO CSP compared to WT. G) Abcg2-KO CSP exhibit higher cell death in the presence of both vehicle and 200μM H_2O_2. Data are mean ± s.e.m. *: $p<0.05$ vs WT or WT vehicle, #: $p<0.05$ vs Abcg2-KO vehicle, †: $p<0.05$ vs WT+H_2O_2.

use of cell viability assays measuring ATP production (CellTiter-Glo) or conversion of resazurin to resorufin (CellTiter-Blue). Both methods revealed that Abcg2-KO CSP cells have decreased metabolic activity (Figure 31E, F). The protective role of Abcg2 was further examined under stress conditions. Abcg2-KO CSP cells treated with H_2O_2 exhibited significantly increased cell death compared to WT (Figure 31G).

As mentioned in the introduction, accumulating evidence supports a correlation between prolonged G1 phase and asymmetric cell division [166-171]. To test whether this theory applies to the phenotype observed in Abcg2-KO CSP cells, their cell division mode was assessed. Immuno-cytochemical staining for the cell fate determinant α-adaptin and pH3 demonstrated that shAbcg2 CSP cells divide predominantly asymmetrically (70% of cells in late mitosis) while the majority of divisions in control cells (Scramble) were symmetric (30% of cells in late mitosis) (Figure 32A, B). Moreover, flow cytometric analysis of scramble and shAbcg2 CSP cells revealed that lack of Abcg2 results in a decrease in the

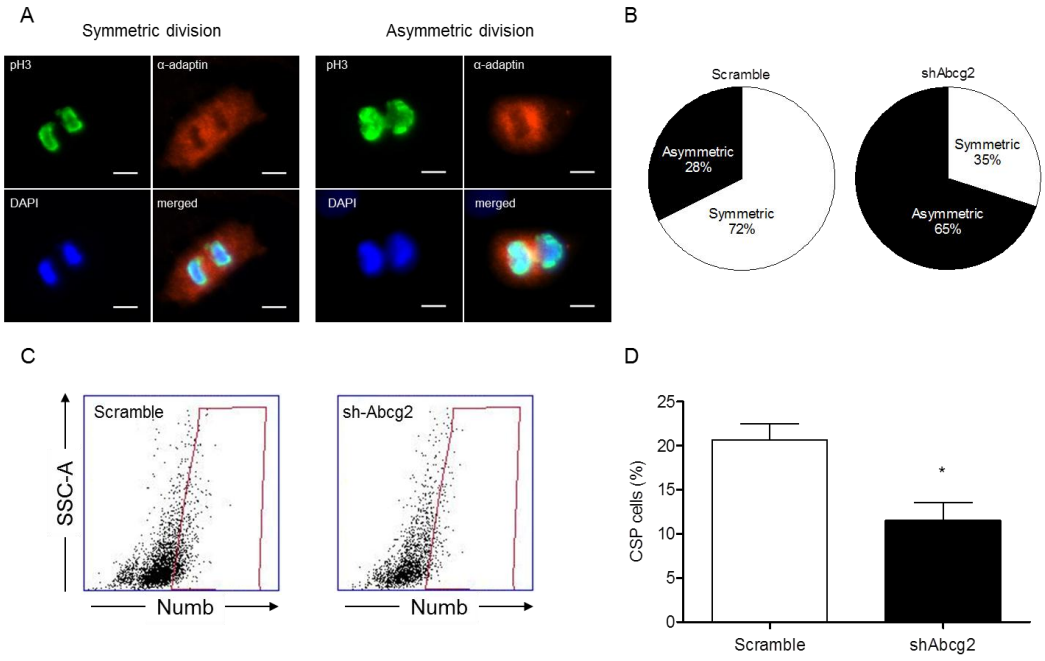

Figure 32: Lack of Abcg-2 favors asymmetric cell division. A) Representative immunofluorescent images of CSP cells stained for pH3 (green), α-adaptin (red) and DAPI (blue). Scale bar 10μm. B) Analysis of the division mode of late mitotic scramble and sh-Abcg-2 CSP cells based on α-adaptin distribution. C) Representative flow cytometric analysis of scramble and sh-Abcg2 CSP stained with numb. D) A decreased fraction of sh-Abcg-2 CSP express numb. Data are mean ± s.e.m. *: $p<0.05$

fraction of cells expressing the cell fate determinant numb (Figure 32C, D) further supporting that during division of Abcg2-deficient cells only one daughter inherits numb.

LACK OF ABCG2 PROMOTES CARDIOMYOGENIC DIFFERENTIATION OF CSP CELLS

In order to examine whether lack of Abcg2 favors cardiomyogenic differentiation, WT and Abcg2-KO CSP cells were cultured in low serum medium and the protein expression of three cardiac markers, Nkx2.5, Gata4 and Mef2c, was determined. As expected, a larger fraction of Abcg2-KO CSP cells expressed these markers compared to WT cells (Figure 33A). Co-culture of WT and Abcg2-KO CSP cells with neonatal rat ventricular myocytes (NRVM) further confirmed this observation (Figure 33B). Preliminary experiments revealed that Abcg2-KO CSP cells exhibited higher structural and functional cardiomyogenic differentiation ability compared to WT cells (Figure 33C-H). Interestingly, over-expression of Abcg2 resulted in a complete loss of CSP differentiation capacity (Figure 33I-K).

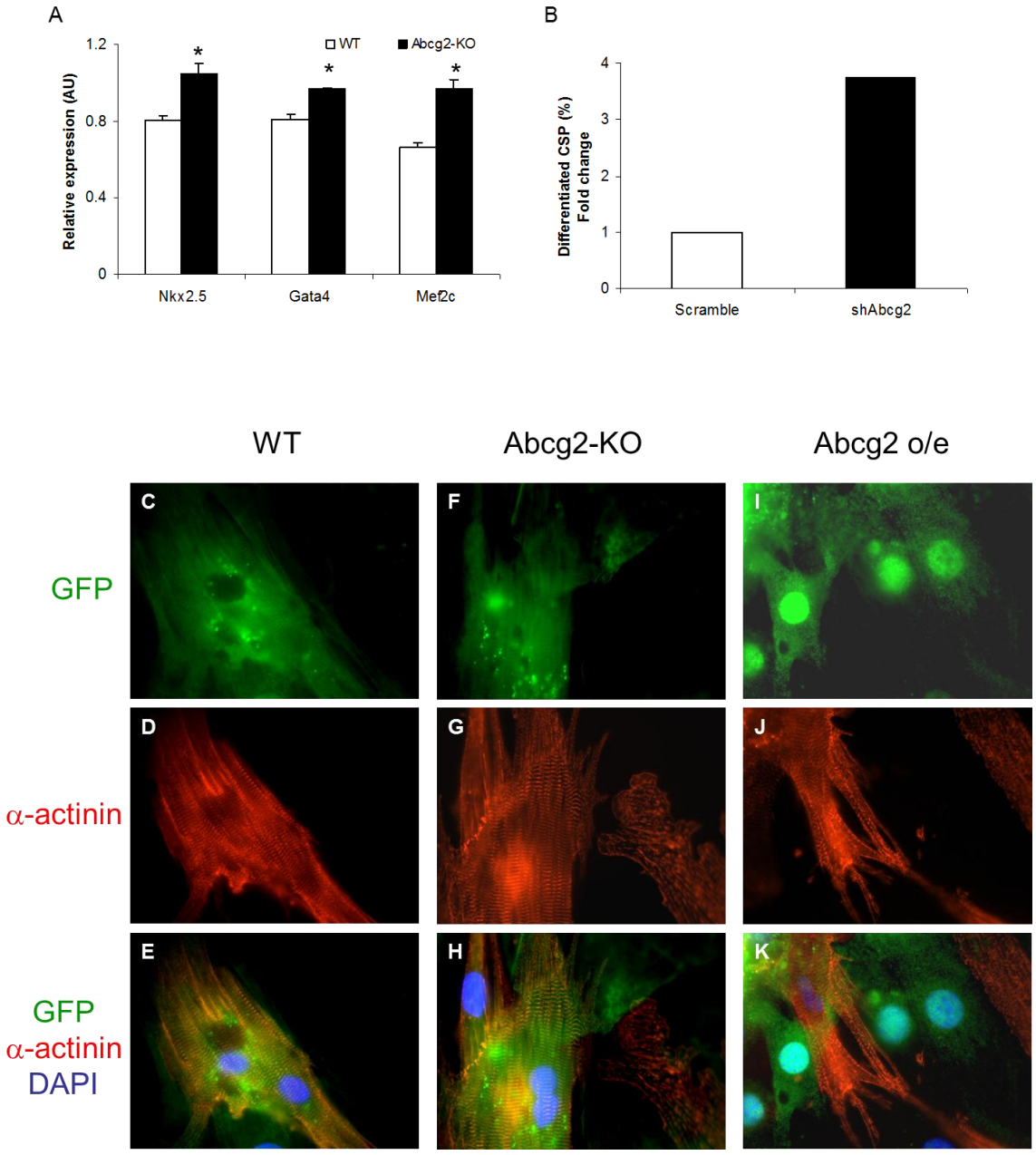

Figure 33: Abcg2 regulates CSP cardiomyogenic differentiation. A) In-cell western blot analysis for the expression of cardiac proteins Nkx2.5, Gata4 and Mef2c in WT and Abcg2-KO CSP. B) Lack of Abcg2 increases CSP cardiomyogenic differentiation in co-culture with NRVM. C-K) Representative immunofluorescent images of GFP^{+} CSP cells co-cultured with NRVM. α-sarcomeric actinin (red), GFP (green), DAPI (blue). Data are mean ± s.e.m. *: $p<0.05$ vs WT.

My next step was to determine the role of Abcg2 in the heart *in vivo* under normal and disease conditions.

ISCHEMIA-REPERFUSION INJURY

Abcg2-KO mice have normal lifespan, breed normally and do not present any adverse phenotype due to lack of Abcg2 under normal conditions. My *in vitro* data, in line with other reports, support a protective role for Abcg2 in basal and stress conditions.

To investigate the impact of Abcg2 deficiency after injury *in vivo*, adult (8 week old) WT and Abcg2-KO mice were subjected to ischemia-reperfusion injury (IR). Animals did not

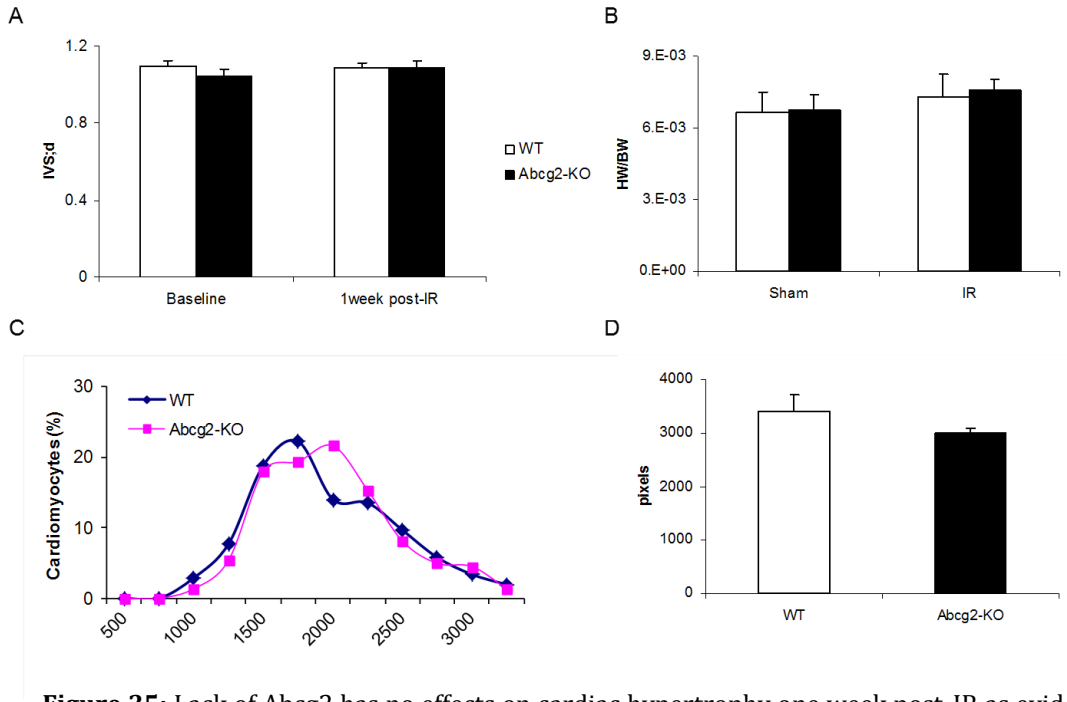

Figure 35: Lack of Abcg2 has no effects on cardiac hypertrophy one week post-IR as evidenced by A) ventricular wall thickness, B) heart weight to body weight ratio (HW/BW), C) cardiomyocyte size distribution and D) cross sectional area. Data are mean ± s.e.m.

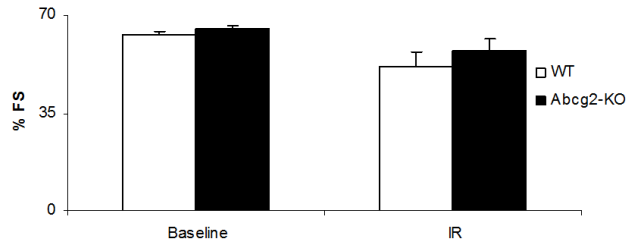

Figure 36: Lack of Abcg2 does not affect fractional shortening one week post-IR. Data are mean ± s.e.m.

show any signs of hypertrophy one week post-IR as evidenced by measurement of left ventricular (LV) wall thickness as well as heart weight (HW) to body weight (BW) ratio (Figure 35A, B). Additionally, lack of Abcg2 had no effect on isolated cardiomyocyte size distribution as well as cardiomyocyte cross-sectional area one week post-IR (Figure 35C, D). Moreover, WT and Abcg2-KO mice exhibited similar decrease in the percentage of fractional shortening after injury (Figure 36).

Interestingly, when heart sections were stained for BrdU, a higher number of cardiomyocytes in Abcg2-KO samples (4.25%) were positive for BrdU incorporation compared to WT (2.75%) (Figure 37). Sham operated samples exhibited limited $BrdU^+$ cells.

The experiment was based on the ability of proliferating / DNA-synthesizing cells to incorporate the nucleotide analogue BrdU. Progenitor cells that participate in the formation of new myocytes synthesize DNA and give rise to one progenitor and one differentiated daughter cell. The identification of the new myocytes can be achieved by immuno-staining for both BrdU in the nucleus and the cardiac marker α-sarcomeric actinin. Each WT and Abcg2-KO heart sample was labeled with BrdU via an osmotic mini-pump introduced subcutaneously at the time of surgery. All proliferating, newly generated cells or cells undergoing DNA repair incorporate the thymidine analogue BrdU allowing their identification.

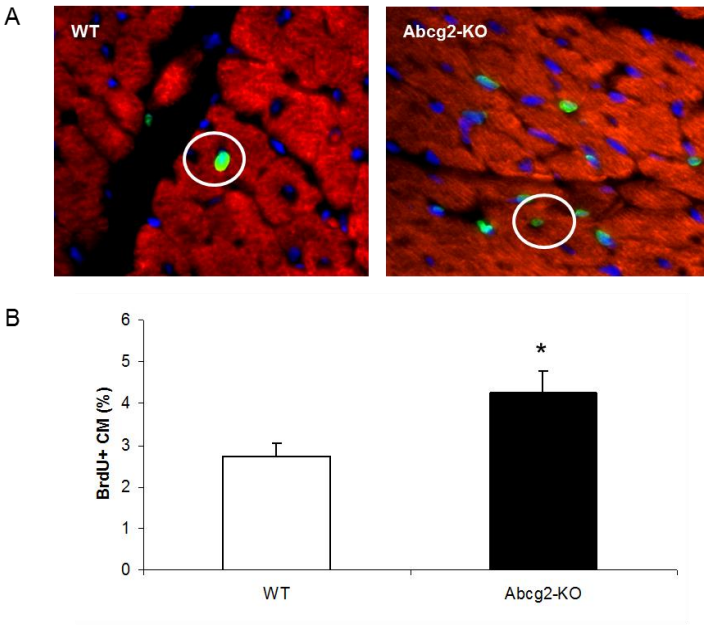

Figure 37: Abcg2-KO mice exhibit higher levels of new cardiomyocyte generation. A) Representative fluorescent microscopy images of WT and Abcg2-KO cardiac tissue sections stained for BrdU (green), α-sarc. actin (red) and DAPI (blue) one week post-IR. B) Percentage of $BrdU^{+}$ cardiomyocytes. Data are mean ± s.e.m.

ABCG2-KO MICE EXHIBIT INCREASED MORTALITY FOLLOWING MYOCARDIAL INFARCTION (MI)

Following the minimal effect of Abcg2 deficiency observed after IR, I sought to examine whether a more severe injury such as myocardial infarction would produce a different outcome. Again, eight week old WT and Abcg2-KO male mice were subjected to acute MI and a BrdU pump was introduced subcutaneously. Surprisingly, Abgc2ko mice demonstrated a significant mortality rate with 50% of the mice dying as early as 2 days after injury and only one third surviving at four days (Figure 38). I therefore chose to perform all analyses at four days post-MI due to the poor survival past this time-point.

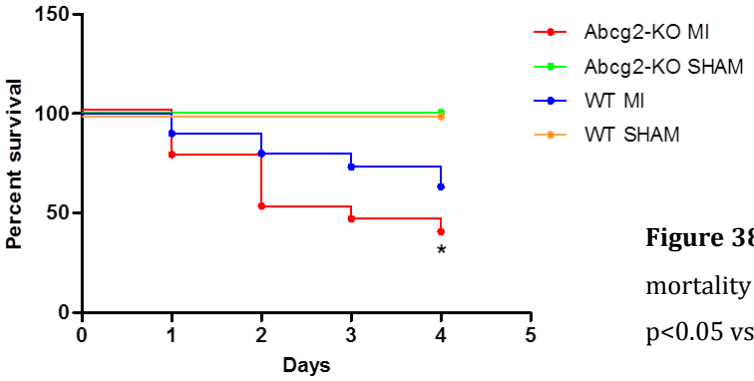

Figure 38: Abcg2-KO mice exhibit increased mortality post-MI compared to WT. *: $p<0.05$ vs WT MI.

ABCG2-KO ANIMALS DEVELOP CARDIAC HYPERTROPHY AND BIGGER INFARCTS POST-MI

In an effort to determine the reason leading to the observed increase in mortality, several parameters were measured. Due to the early time point selected, echocardiographic measurements were difficult to obtain and inconclusive.

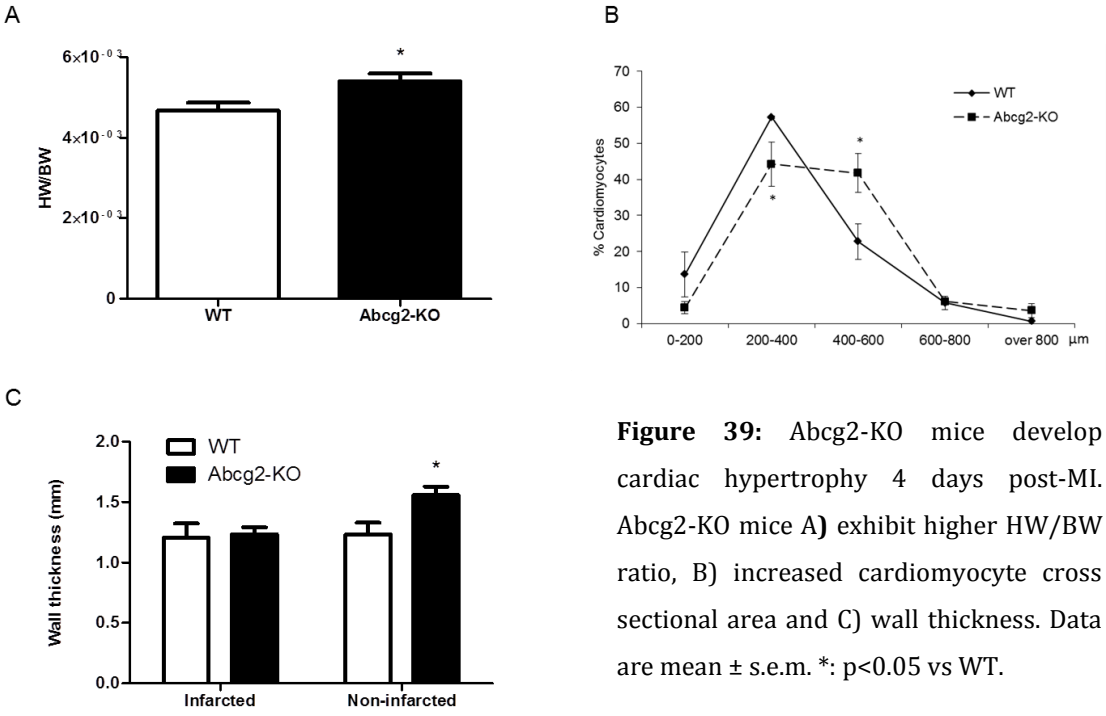

Figure 39: Abcg2-KO mice develop cardiac hypertrophy 4 days post-MI. Abcg2-KO mice A**)** exhibit higher HW/BW ratio, B) increased cardiomyocyte cross sectional area and C) wall thickness. Data are mean ± s.e.m. *: p<0.05 vs WT.

At four days post-MI, surviving Abcg2-KO mice exhibited signs of cardiac hypertrophy as evidenced by increased HW to BW ratio (Figure 39A). Cardiomyocyte cross-sectional area measurement demonstrated that Abcg2 deficient mice exhibit a trend towards cardiomyocyte hypertrophy (Figure 39B). Analysis of Masson's trichrome stained heart sections revealed that Abcg2-KO animals developed significantly bigger infarcts compared to WT mice (Figure 40) as well as increased LV free-wall thickness (Figure 39C).

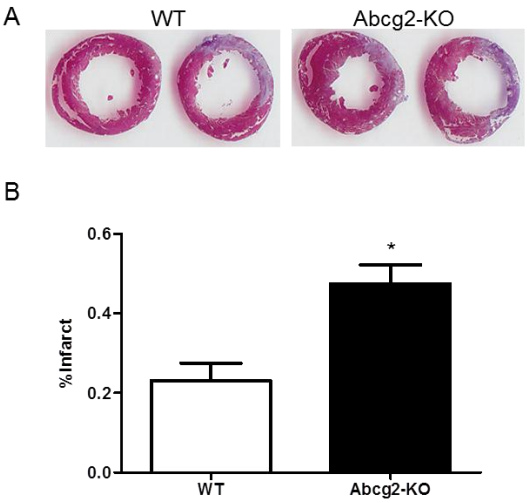

Figure 40: Abcg2-KO mice develop larger infarcts compared to WT 4 days post-MI. A) Masson's trichrome staining. B) Quantification. Data are mean ± s.e.m. *: p<0.05 vs WT.

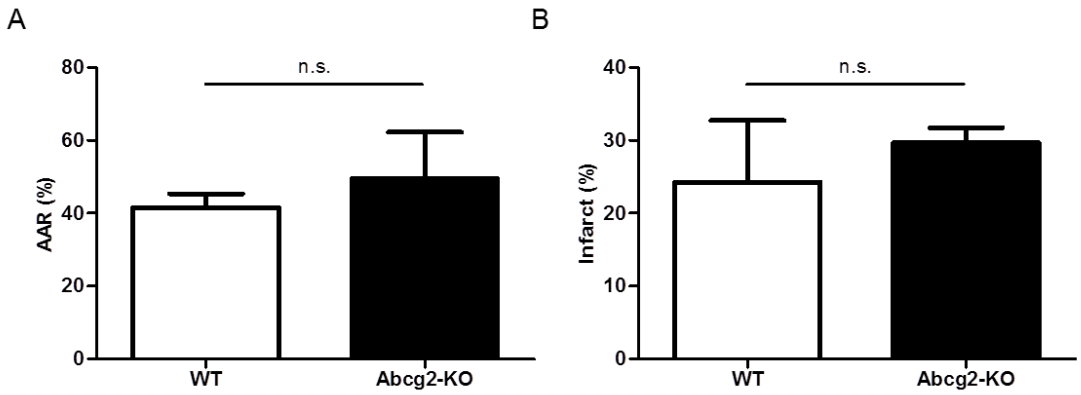

Figure 41: Abcg2-KO mice do not exhibit differences in A) infarct area at risk (AAR) or B) infarct size 24 hours post-injury. Data are mean ± s.e.m.

In order to confirm that the initial injury was consistent between the two groups, microsphere injection and TTC staining were performed 24 hours post-injury as described in the materials and methods section. As expected, there were no significant differences between the two groups in both area at risk (AAR) and initial infarct (Figure 41).

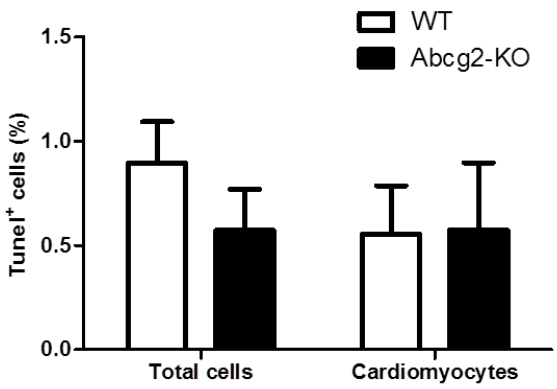

Figure 42: WT and Abcg2-KO mice do not exhibit differences in cell death 4 days post-MI. Data are mean ± s.e.m.

As mentioned earlier, Abcg2 plays a protective role against cell death in CSP cells *in vitro*. To test whether Abcg2 has a similar role *in vivo*, WT and Abcg2-KO heart sections were stained for Tunel. Surprisingly, no differences were observed between the two groups in cardiomyocyte or total cell death (Figure 42). However, the *in vivo* effect of the lack of Abcg2 on the population of CSP cells could not be determined by immuno-histochemical staining due to lack of appropriate CSP identification markers.

ABCG2-KO MICE EXHIBIT SIMILAR CAPILLARY DENSITY WITH WT MICE ONE WEEK POST-MI

In order to investigate whether the phenotype observed post-MI could be attributed to decreased oxygenation of the cardiac tissue, the density and size of capillaries with a diameter less than 10μm were measured. No differences were observed between WT and Abcg2-KO samples in number of capillaries per μm^2 in both infarct border and remote area. However, Abcg2-KO hearts demonstrated smaller capillaries compared to WT (Figure 43).

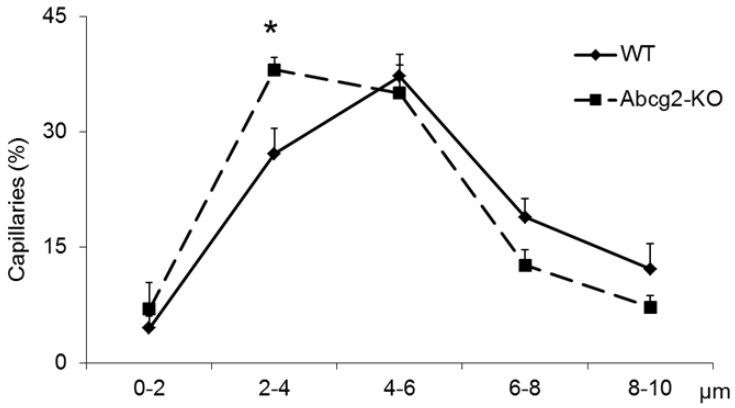

Figure 43: Abcg2-KO mice demonstrate smaller capillaries 4 days post-MI. Data are mean ± s.e.m. *: $p<0.05$ vs WT.

The old dogma supporting that the heart is a static post-mitotic organ with no self-renewal ability has been widely refuted by several pioneering studies demonstrating the presence of resident cardiac progenitor/stem cells and cardiac regeneration. The main focus of my thesis is the study of the role of Abcg2 in the homeostasis of cardiac progenitor cells in order to delineate the mechanisms regulating cardiac regeneration. Thus, my next goal was to examine the effect of Abcg2 in cardiomyocyte replenishment and tissue repair

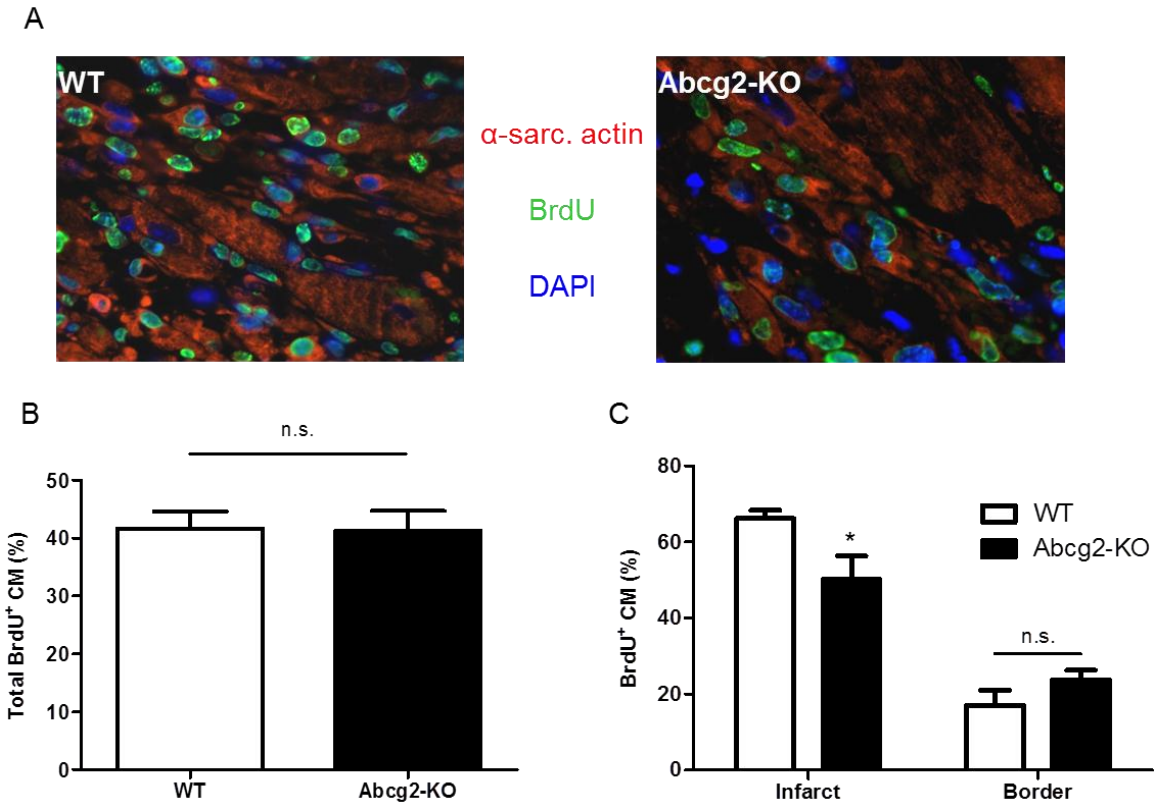

Figure 44: New myocyte formation following MI. A) Representative fluorescent microscopy images of WT and Abcg2-KO cardiac tissue sections stained for α-sarc. actin (red), and BrdU (green). B) No differences are observed in new myocyte $BrdU^+$ cardiomyocytes between WT and Abcg2-KO hearts in the infarct/border zone. C) Analysis of infract and border areas separately. Data are mean ± s.e.m. *: $p<0.05$ vs WT.

in the setting of MI injury. After MI, proliferating inflammatory cells infiltrate the tissue, hence, a large number of BrdU positive non-cardiomyocytes were observed in all MI samples mainly in the infarct / border zone. For the purpose of my study only BrdU positive cardiomyocytes were considered. Cross sections of the entire tissue (remote, border and infarct areas) were examined for the presence of BrdU and α-sarcomeric actinin double positive cells, however all BrdU positive cardiomyocytes were found in the infarct / border zone of MI samples. Surprisingly, WT and Abcg2-KO hearts did not demonstrate any differences in the percentage of BrdU positive cardiomyocytes in the infarct / border zone (Figure 44B). When the two areas were analyzed separately, a small but significant decrease was revealed in the amount of BrdU positive cardiomyocytes in the infarct area of Abcg2-KO hearts (Figure 44C). All BrdU and α-sarcomeric actinin double positive cells were small in size compared to BrdU negative α-sarcomeric positive cells indicating that the double positive cells are newly generated cardiomyocytes (Figure 44A).

The possibility of BrdU positivity being due to DNA repair was excluded since according to the literature in this case the nuclei should demonstrate a punctuated staining. All the cells that were taken into consideration presented a uniform nuclear BrdU staining.

LACK OF ABCG2 HINDERS THE PROLIFERATIVE RESPONSE OF CSP CELLS POST-MI

The generation of new cardiomyocytes can be attributed to either the proliferation of existing cardiomyocytes or the differentiation of progenitor cells. As mentioned above, all the BrdU positive myocytes were small in size (~25-75μm^2) compared to the average cardiomyocyte cross-section size (~200-600μm^2). Therefore, it is most likely that the BrdU

positive cardiomyocytes observed were generated from differentiating progenitors. Careful analysis of CSP cells post-MI revealed a significant increase of CSP cell numbers in both WT and Abcg2-KO hearts compared to sham operated animals (Figure 45). However, Abcg2-KO mice exhibited lower cell numbers compared to WT. As previously shown by Ki67 staining [74] WT CSP cells exhibited an increased proliferation rate post-MI compared to sham controls as evidence by BrdU staining of sorted CSP cells. Interestingly, Abcg2-KO CSP cells did not demonstrate a similar proliferative response post-MI. On the contrary, BrdU positive Abcg2-KO cells were modestly increased post-MI compared to sham animals (Figure 45).

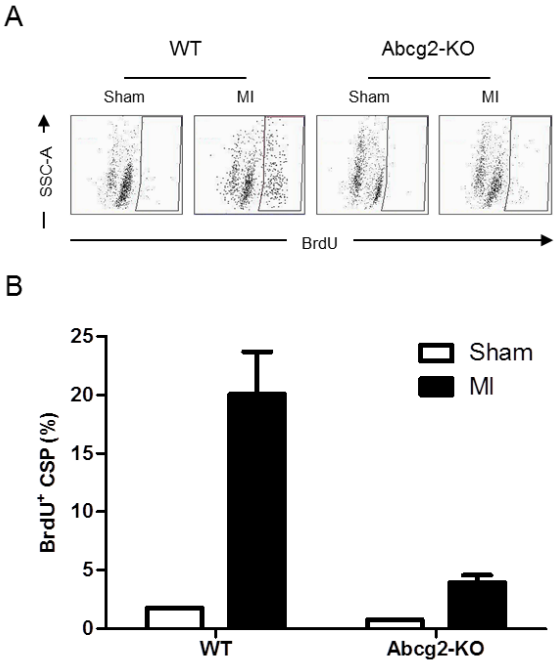

Figure 45: A) Representative plots of flow cytometric analysis for $BrdU^+$ CSP. B) WT CSP cells exhibit increased proliferative capacity post-MI while Abcg2-KO CSP have a moderate increase. Data are mean ± s.e.m.

CSP CELL SURFACE MARKER EXPRESSION PROFILE CHANGES DURING DEVELOPMENT

Following the observation that CSP cell numbers are dynamically regulated during development, I sought to further characterize these cells in different developmental stages. CSP cells from neonatal (P3) and embryonic (E15.5) mouse hearts exhibited a completely different cell surface marker expression profile than the adult CSP cells. Namely, the majority of embryonic CSP cells were $CD31^{+}/Sca^{-}$ (78%), neonatal CSP were predominantly $Sca1^{-}/CD31^{-}$ (83%) while approximately 70% of adult CSP were $Sca1^{+}/CD31^{+}$ (Figure 46).

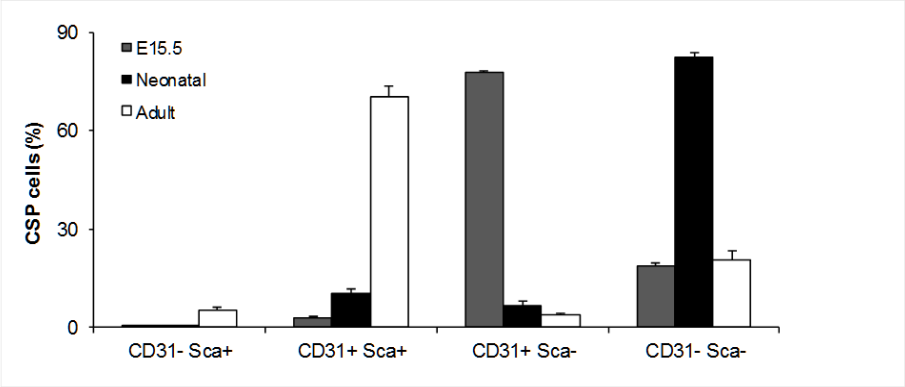

Figure 46: CSP cell surface marker expression profile during development. Flow cytometric analysis of embryonic (E15.5), neonatal and adult CSP. Data are mean ± s.e.m. *: $p<0.05$ vs WT.

As shown earlier, neonatal CSP cells express high levels of Abcg2. I therefore hypothesized that CSP cells have increased proliferation capacity at birth. Indeed, Ki67 staining of freshly isolated cells revealed that a high percentage of neonatal CSP cells are actively cycling (~40%) compared to adult cells (~10%) (Figure 47).

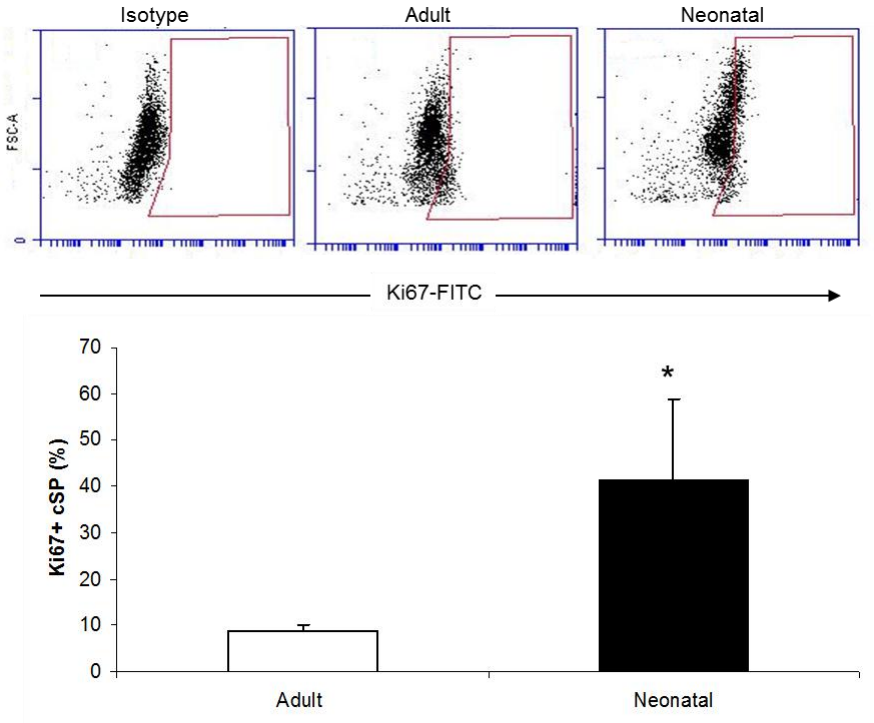

Figure 47: Neonatal CSP are cycling *in vivo*. Flow cytometric analysis of adult and neonatal CSP stained for Ki67. Data are mean ± s.e.m. *: $p<0.05$.

NEONATAL CSP CELLS LOSE THEIR PROLIFERATIVE POTENTIAL IN CULTURE

My next step was to expand neonatal CSP cells for further study. Surprisingly, neonatal CSP cells almost completely lost their proliferative capacity in culture rendering their manipulation very difficult (Figure 48A). Similarly, embryonic CSP cells were also unable to be expanded. In an effort to ameliorated culture conditions, embryonic stem cell medium was used to culture adult and neonatal CSP cells. However, neonatal CSP cells were not able to grow in these conditions either (Figure 48B).

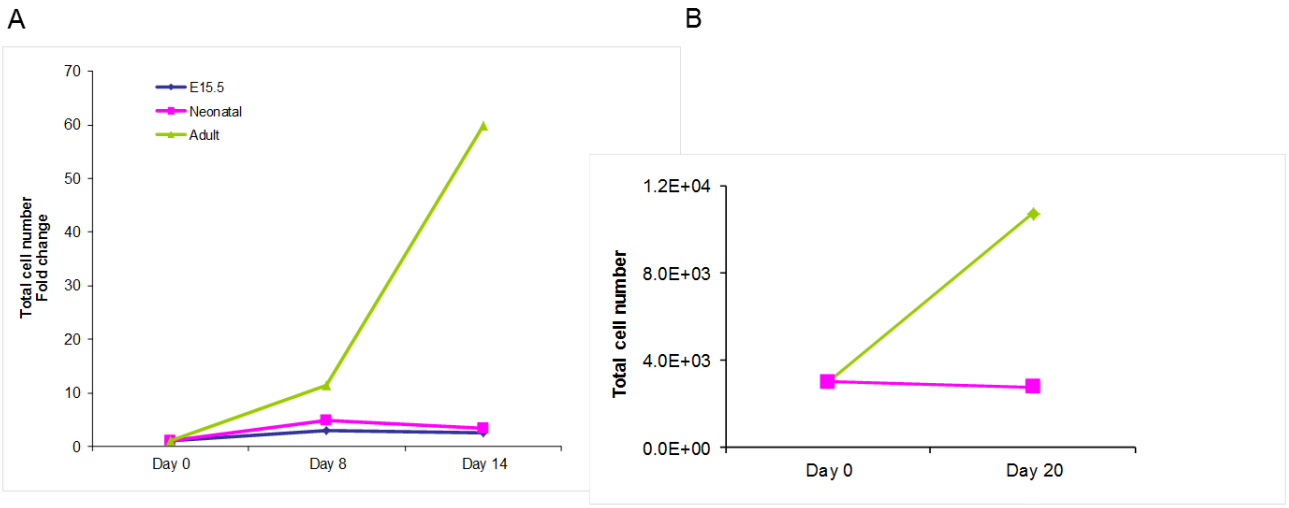

Figure 48: Neonatal CSP lose their proliferative capacity *in vitro*. A) Proliferation assays of embryonic (E15.5) neonatal and adult CSP. B) Expansion of adult and neonatal CSP in ESC medium. Data are mean ± s.e.m. *: $p<0.05$ vs adult.

NEONATAL CSP CELLS EXHIBIT INCREASED DIFFERENTIATION CAPACITY

To assess the differentiation potential of CSP cells from different developmental stages, cells were isolated from adult and neonatal WT FVB-GFP mice and co-cultured with

neonatal rat cardiomyocytes (NRVM). Interestingly, neonatal CSP cells demonstrated a significantly higher cardiomyogenic capacity compared to adult (Figure 49).

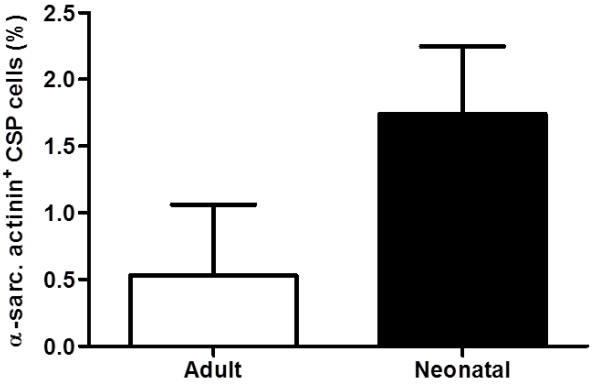

Figure 49: Neonatal CSP exhibit increased differentiation capacity. Cardiomyogenic differentiation of CSP co-cultured with NRVM. Data are mean ± s.e.m. *: $p<0.05$.

DISCUSSION

It is now widely accepted that the heart, a previously considered terminally-differentiated organ, possesses regenerative potential [2, 7, 45, 188]. The identification of adult cardiac stem cells and their use for the treatment of cardiovascular diseases has recently provided encouraging results and opened new horizons in the cardiovascular field [48]. Thorough characterization of the biological processes and molecular mechanisms regulating cardiac stem cell homeostasis is needed now more than ever to fully exploit their regenerative potential.

Since the initial identification of SP cells from bone marrow, the side population phenotype has been commonly used to isolate progenitor cells from a variety of tissues including the heart. In BMSP cells the ATP-binding cassette transporter Abcg2 has been identified as the sole determinant of the SP phenotype. However, its contribution to the cardiac side population as well as its physiologic role in the regulation of CSP cell homeostasis is currently unknown.

In this context, the work encompassing my thesis focused primarily on the role of the ATP-binding cassette transporter Abcg2 in regulating cardiac side population progenitor cells homeostasis both *in vitro* and *in vivo*. In addition to demonstrating an age-dependent contribution of Abcg2 to the CSP phenotype, my work reveals for the first time that Abcg2 regulates CSP progenitor cell cycle, survival and asymmetric division. Furthermore, I provide evidence suggesting a protective role for Abcg2 in the heart following injury.

Isolation of side population cells is based on their ability to efflux the Hoechst dye through the action of ABC-transporters. In BMSP, although both Abcg2 and Mdr1a/b are expressed, the efflux ability is solely attributed to Abcg2 since lack of the transporter leads to BMSP depletion [89, 119]. Since this initial report, Abcg2 was found to be enriched in stem/progenitor cells from various tissues and has become a general marker of stem cells and in particular of side population cells. However, the contribution of Abcg2 to the cardiac SP phenotype remains elusive.

Martin et al, demonstrated persistent expression of Abcg2 in the developing and adult heart [71]. Moreover, gene array analysis revealed significant up-regulation of Abcg2 in CSP compared to main population cells. The authors by using FTC, a so-called specific inhibitor for Abcg2, concluded that Abcg2 is the molecular determinant of CSP cells similar to BMSP [71]. In accordance with this data, my work confirms that Abcg2 is expressed in CSP cells and that FTC is able to inhibit the SP phenotype. However, CSP analysis in mice with genetic deletion of Abcg2 (Abcg2-KO) revealed a detectable although reduced CSP population. This population was sensitive to the known SP inhibitor verapamil as well as to ATP-depletion and FTC. Moreover, CSP analysis in mice with genetic deletion of Mdr1a/b revealed a complete elimination of CSP tail indicating that Abcg2 is not sufficient to mediate the SP phenotype in the heart and that Mdr1a/b is the molecular determinant of the adult CSP. To verify this discrepancy I followed two approaches. First I introduced an internal control to the Hoechst staining by the mixing samples with WT GFP cells. This GFP-mixing experiment confirmed that no error had occurred during cell counting and that the results obtained were not due to over- or under-staining of the CSP cells with Hoechst. The second

approach was to verify the specificity of FTC. For this purpose, I incubated Mdr1 over-expressing cells with FTC and demonstrated that the SP phenotype was blocked. Although several reports have demonstrated FTC specificity in inhibiting Abcg2-mediated efflux [183-185], our results indicate that FTC function could be dependent on the experimental conditions used such as cell type, substrate type and concentration.

Interestingly, my results further revealed a dynamic age-dependent contribution of Abcg2 and Mdr1a/b to the CSP phenotype. Namely, the role of Mdr1a/b as a mediator of the CSP phenotype is limited to the adult hearts while Abcg2 is the mediator in early post-natal stages. The contribution of each transporter is accompanied with changes in gene expression during development with Abcg2 being up-regulated in neonatal CSP and down-regulated in adult, while Mdr1a/b expression is minimal in neonatal and markedly increases in adult CSP. This finding could suggest that CSP cells have different origin from BMSP since Mdr1a/b-KO mice have normal BMSP levels but completely lack CSP. In line with this speculation, CSP cells were found to be negative for the hematopoietic marker CD45 (Table 1). These data are in accordance with previous findings indicating that BMSP cells home to the heart only following myocardial infarction and contribute to the CSP phenotype by approximately 25% [74].

My results suggest that there is no universal ABC-transporter that defines the SP phenotype but rather that the microenvironment and developmental stage are the factors that determine the relative contribution of the transporters. This conclusion is further supported by SP analysis in the mammary gland where Abcg2 and Mdr1 have complementary roles [120].

Age-dependent characterization of CSP cells

In addition to differences in ABC-transporter expression, CSP cells from different developmental stages exhibited altered surface marker expression profile as well as proliferation and differentiation capacity. Whether there is a connection between differential expression of Sca1 and CD31 and the increased proliferation observed in neonatal CSP cells *in vivo* compared to adult requires further examination. Interestingly, expanded neonatal CSP cells lose their proliferative advantage and become more cardiogenic. It is likely that neonatal CSP cells are more primitive progenitor cells compared to adult and while exiting the cardiac niche they lose the signals required for their maintenance in a proliferative state and they start to differentiate. Supporting the notion of neonatal CSP cells being more primitive it has recently been proposed that neonatal mouse hearts (injury at day 1) are able to completely regenerate lost tissue within one week after birth [189]. In line with this report, in mice during early post-natal life there is an increase in cardiomyocyte number until one week after birth when the cardiomyocyte number reaches a plateau [190, 191]. This increase could be attributed to proliferation of existing cardiomyocytes as well as differentiation of progenitor cells. The inability of adult hearts to regenerate efficiently following injury could be the result of a deterioration of progenitor cell function (ie proliferation, regenerative capacity) either due to intrinsic mechanisms or environmental cues. In order to delineate the signaling pathways promoting progenitor cell differentiation during cardiac development as well as the molecules inhibiting similar responses in the adult heart, miRNA and mRNA microarray analysis of CSP cells from different developmental stages as well as following MI is currently underway.

ABCG2 REGULATES CSP CELL PROLIFERATION THROUGH ITS EFFLUX FUNCTION

Abcg2 has been previously associated with proliferation in stem/progenitor cells as well as various cancer cell lines. However, its role in regulating CSP cell proliferation is currently unknown. Through various methodologies, my work reveals that Abcg2 confers a proliferative advantage to CSP cells. Gain- and loss-of-function approaches demonstrated that lack of Abcg2 compromises CSP cell proliferation while its over-expression increases CSP cell numbers. These results agree with studies in bone marrow cells where over-expression of Abcg2 resulted in increased SP numbers [89] as well as with data from cancer cell lines where Abcg2 expression was associated with highly proliferative cells [121, 122].

My work further demonstrates that the transporter function of Abcg2 is required to mediate its effects on CSP cell proliferation. Similar to previous reports [187], K85M mutation efficiently abolished Abcg2 efflux capacity without affecting protein expression. Moreover, CSP cells expressing the mutant form exhibited similar proliferation capacity with control mock-expressing cells. These results suggest that the export of one or several substrates of Abcg2 is required for CSP proliferation. Therefore, it is reasonable to speculate that in Abcg2-eficient CSP cells, an unknown factor (possibly a metabolite or toxin) accumulates in the cytoplasm and inhibits proliferation. Further studies are required to identify the molecules mediating this effect. For this purpose experiments identifying the metabolic profile of WT and Abcg2-KO CSP cells are underway. Both extra-cellular/secreted and intra-cellular metabolites will be analyzed by mass spectrometry.

Further dissecting the effects of Abcg2 on CSP cell proliferation, my work revealed that Abcg2-KO CSP cells exhibit defective cell cycle progression. Through several methodologies such as immuno-cytochemical staining for cell cycle markers (pH3, BrdU), DNA content analysis (propidium iodide) as well as more elaborate methods such as the FUCCI indicators, my results indicate that lack of Abcg2 prolongs the cell cycle and particularly the transition from G1 to S phase.

Moreover, the FUCCI experiments revealed that the majority of Abcg2-KO CSP cells was negative for the two cell cycle probes while only a small fraction of WT CSP appeared negative. It is known that cells appear as negative following cytokinesis or exit from the cell cycle. For WT CSP cells it is reasonable to suggest that negative cells represent newly separated daughter cells since the increase in the percentage of this population is relative to the increase in cells in S-G2-M. On the other hand, based on the decreased proliferation capacity as well as the delayed progression through the cycle observed in Abcg2-KO CSP cells, the possibility for the negative fraction to represent cells that have just completed cytokinesis is highly unlikely. This hypothesis was further confirmed by live cell imaging. Additional experiments are required to establish whether the negative fraction of Abcg2-KO CSP cells represents cells in G0. Staining for pyronin-y to distinguish cells in G0 and G1 phases, or labeling for Ki67 that marks cells in all cell cycle phases except G0 would provide a definitive confirmation.

ABCG2 PLAYS A PROTECTIVE ROLE IN CSP CELLS

In addition to the increased proliferation, my data show that CSP cells expressing Abcg2 are protected from apoptotic and necrotic cell death in both normal and oxidative stress conditions. These results are in agreement with previously reported studies in both cancer and normal cells that have established Abcg2 as a protective protein [100-102, 111]. Notably, the large majority of compounds exported by Abcg2 have been found to have toxic effects [192]. Similar to CSP cells, Abcg2-KO hematopoietic stem cells were found to be more sensitive to cell death under hypoxic conditions [112]. Interestingly, the increased cell death was attributed to the inability of Abcg2-KO cells to export heme further supporting the importance of Abcg2 efflux function [112]. Likewise, microvascular endothelial cells lacking Abcg2 expression exhibit accumulation of protopotphyrin IX and increased cell death [126]. Moreover, in mouse embryonic fibroblast Abcg2 over-expression promoted the production of low levels of reactive oxygen species which resulted in preconditioning and protection of the cells from H_2O_2 induced cell death [114]. It is noteworthy that the Abcg2 promoter region has several putative hypoxia-response elements and that both HIF-1α and HIF-2α have been suggested to bind and up-regulate Abcg2 expression.

My work further suggests that lack of Abcg2 in CSP cells promotes DNA damage. Several key players of the DNA damage response pathway were significantly up-regulated indicating that Abcg2-KO CSP cells have severe defects. This result further supports the delay in cell cycle progression observed in Abcg2-KO CSP cells. Additionally, DNA damage and inability to repair could be responsible for cell cycle prolongation and exit and could explain the fraction of cells negative for both FUCCI cell cycle probes. Experiments such as

detection of phospho-histone H2A.X, a protein activated by DNA damage and required for DNA fragmentation during apoptosis, are necessary to further support my findings.

ABCG2 REGULATES ASYMMETRIC CELL DIVISION AND CARDIOMYOGENIC COMMITMENT OF CSP CELLS

Several reports have suggested a regulatory role for G1 cell cycle phase length in stem/progenitor cell function [165-171] . Cells with high self-renewal ability such as embryonic stem cells have short G1 phase that is significantly prolonged with differentiation during development [171]. Similarly, in adult neural stem cells inhibition of G1 cell cycle kinases resulted in neurogenesis [166] while shortening of G1 promoted progenitor cell expansion through symmetric divisions [175]. Such data led to the formulation of the "cell cycle length hypothesis" supporting that by increasing their cell cycle length, cells allow the production and proper positioning of cell fate determinants within the cell. My data are consistent with this notion. In addition to the prolonged G1 phase, Abcg2-KO CSP cells undergo primarily asymmetric cell division as evidenced by asymmetric partitioning of the cell fate determinants α-adaptin and numb. However, the fate of the CSP cell inheriting the fate determinants remains to be determined. Studies in drosophila have suggested that the cell that inherits numb will acquire a differentiation fate [143]. Co-expression analyses of fate determinants and cardiac differentiation markers will provide a definitive answer. Moreover, live cell imaging of cell division would allow tracking of fate determinants and visualization of the cell decisions. The identification of mitochondria asymmetric partitioning during cell division provides a useful tool for such experiments [193, 194]. Labeling of mitochondria with mitotracker dyes could bypass the need for the use of fate determinant reporter constructs.

The molecular mechanism by which Abcg2 regulates the asymmetric division and the cell cycle duration of CSP cells still remains unclear. Among other DNA-damage responsive genes, the stress sensor p53 was found to be up-regulated in Abcg2-KO CSP cells. Several studies have reported a key role for p53 in the regulation of asymmetric cell kinetics [158-163]. Induction of p53 expression in epithelial stem cells, as well as restoration of p53 levels in p53-deficient fetal fibroblasts resulted in a switch from symmetric cell divisions to asymmetric divisions [158, 159]. Furthermore, stabilization of p53 expression in ErbB2 mammary cancer stem cells that are characterized by reduced p53 expression, promoted their asymmetric division [162]. Regulation of asymmetric cell kinetics by p53 has been proposed to occur through down-regulation of the rate-limiting enzyme for guanine nucleotide synthesis, IMPDH (inosine 5'-monophosphate dehydrogenase) [160, 164]. Abcg2 is a membrane transporter primarily responsible for the cytoplasmic clearance of cytotoxic compounds [195]. It is likely that in cells lacking Abcg2, the accumulation of toxic compounds may promote stress-induced DNA damage and p53 activation and therefore an increase in p53-induced asymmetric division. Additional studies are required to address the direct role of Abcg2 in asymmetric cell division of CSP cells.

The definition of stem cell asymmetric division is the generation of one stem cell (self renewal) and a committed cell within one division cycle. Likewise, my data reveal that in addition to the predominance of asymmetric division, Abcg2-KO CSP cells exhibit increased cardiomyogenic differentiation capacity. This finding is consistent with work from hematopoietic and retinal stem cells where over-expression of Abcg2 led to increased cell expansion and adversely affected their lineage commitment [65, 89, 196]. The mechanism regulating the changes in Abcg2 expression during proliferation and

differentiation remains unclear. More recently, Zong et al identified three Abcg2 isoforms (E1A, E1B and E1C) differing in their 5'UTR sequence and proposed that in different hematopoietic developmental stages the differential expression of these isoforms controls Abcg2 levels. Namely, E1A isoform was primarily expressed in mouse HSCs whereas in erythroid cells, E1B was the predominant form [197].

My work has shown that Abcg2 promotes CSP cell proliferation and more particularly cell cycle progression and at the same time represses their asymmetric division and differentiation. These data suggest that regulation of Abcg2 expression is a key factor in the maintenance of cardiac stem/progenitor cell pool. This notion is further highlighted by the finding that Abcg2 plays a protective role against DNA damage and cell death. In this context, the prevalence of asymmetric divisions in Abcg2-KO cells could promote in addition to cell commitment, the asymmetric segregation of cytotoxic molecules such as misfolded proteins to one daughter cell that would get eliminated thus allowing stem cell self-renewal [155, 156].

The observation that Abcg2-KO mice develop normally and exhibit a normal cardiac phenotype [198] implies that under physiological conditions, efficient functional compensation exists. Therefore, my *in vivo* work focused on the investigation of the impact of Abcg2 inhibition under myocardial injury conditions. My data reveal data that Abcg2 deficiency leads to increased mortality post-MI accompanied by cardiac hypertrophy and significantly larger infarcts compared to WT animals. These data are in complete agreement with recently published work by Higashikuni et al in Abcg2-KO female mice [126, 127]. The authors observed increased mortality four to six days post-MI due to cardiac rupture and increased cardiac hypertrophy and infarct size [126]. Moreover, in pressure-overload induced cardiac hypertrophy Abcg2-KO animals exhibited decreased capillary density and size and exacerbated oxidative stress and inflammation [126]. In my study, cardiac rupture was observed rarely. This could be due to the different gender of animals used. Indeed female gender is one of the risk factors of cardiac rupture following MI [199, 200].

Furthermore, consistent with the aforementioned reports, Abcg2-KO hearts were found to have smaller capillaries suggesting inefficient oxygenation of the tissue. Based on my *in vitro* data and a number of reports, Abcg2 acts as a pro-survival factor, however, no differences in total cell and cardiomyocyte death were observed between WT and Abcg2-KO mice post-MI. Further experiments need to be performed in order to elucidate the specific cell type mostly affected by Abcg2 deficiency. A possible target could be endothelial cells since lack of Abcg2 impairs survival of microvascular endothelial cells in oxidative stress conditions [126].

In line with my *in vitro* data, my work further demonstrates that Abcg2-KO animals exhibit cardiac regenerative capacity in the infarct area four days post-MI albeit at a smaller extent compared to WT. Moreover, in CSP cells, lack of Abcg2 resulted in major inhibition of their proliferative response following MI. These results are in agreement with the increased asymmetric division and cardiomyogenic differentiation observed in Abcg2-KO CSP and lead to the hypothesis that although Abcg2 deficient CSP cells are markedly decreased post-MI their cardiomyogenic potential is such that allows significant regeneration of the lost tissue. The difference in newly formed cardiomyocytes between WT and Abcg2-KO mice is marginal while the difference observed in CSP cell proliferation is quite striking. It can be speculated that following injury WT CSP cells undergo primarily symmetric divisions and thus increase in number while Abcg2-KO cells divide asymmetrically and contribute more efficiently to the regeneration of the lost tissue. However, four days post-MI is a very short period to observe significant contribution of regeneration to cardiac repair. Therefore, the increased mortality observed in Abcg2-KO mice cannot be explained by the lack of progenitor cells. Further experiments, including generation of smaller infarct, or the choice of different injury model such as pressure overload (TAC) or ischemia reperfusion that would result in milder insult, would allow the study of the animals for several weeks following injury and provide more insightful information regarding cardiac regeneration. It is noteworthy, that one week following a one hour ischemia-reperfusion injury did not reveal any differences in cardiac function between WT and Abcg2-KO animals. However, Abcg2-KO animals demonstrated increased regenerative potential.

Based on the effect of Abcg2 *in vivo* in the MI setting, it is reasonable to suggest that manipulation of Abcg2 expression following injury could permit an initial enrichment of the

progenitor cell pool (high Abcg2 expression) and subsequent regeneration of the lost tissue (inhibition of Abcg2 expression).

CONCLUSIONS

Overall my work on Abcg2 reveals a previously unappreciated player in the regulation of cardiac stem cell biology and cardiac regeneration. Further investigation of the complex role of this transporter will contribute to our understanding of cardiac regeneration and will provide additional knowledge towards the development of stem cell-based therapies for cardiovascular diseases. Moreover, understanding the function of Abcg2 is of great significance in cancer research. Abcg2 is a cancer drug transporter up-regulated in several forms of cancer. The regulation of symmetric and asymmetric division by Abcg2 could be a subject of further investigation since deregulated asymmetric division in cancer stem cells can result in cancer formation [157].

My work introduces Abcg2 as multi-functional protein affecting several aspects of cellular biology. Moreover, the large variety of substances transported by Abcg2 reflects its involvement in a multitude of cellular processes. The manipulation of Abcg2 expression could be an efficient approach in stem cell therapy for cardiac failure patients. Autologous stem cell transplantation for patients with cardiac injury requires stem cell expansion in large numbers in a short period of time. Activation of Abcg2 in culture would allow the rapid expansion of the cells while inhibition of the transporter's expression before re-implantation would activate differentiation. However, extensive work and characterization of the exact function of Abcg2 is imperative before moving to the clinic. The identification of metabolites transferred by Abcg2 responsible for its action in CSP cells is of outmost importance not only for cardiovascular research but also for stem cell research in general as

well as for the cancer field. The possibility to mimic the function of Abcg2 through pharmacological means would provide an easier, safer and inexpensive therapeutic alternative.

REFERENCES

1. Sakaue-Sawano, A., et al., *Visualizing spatiotemporal dynamics of multicellular cell-cycle progression.* Cell, 2008. **132**(3): p. 487-98.
2. Bergmann, O., et al., *Evidence for cardiomyocyte renewal in humans.* Science, 2009. **324**(5923): p. 98-102.
3. Bunting, K., *ABC transporters as phenotypic markers and functional regulators of stem cells.* Stem cells (Dayton, Ohio), 2002. **20**(1): p. 11-31.
4. van Herwaarden, A. and A. Schinkel, *The function of breast cancer resistance protein in epithelial barriers, stem cells and milk secretion of drugs and xenotoxins.* Trends in pharmacological sciences, 2006. **27**(1): p. 10-16.
5. Konstam, M., et al., *Left ventricular remodeling in heart failure: current concepts in clinical significance and assessment.* JACC. Cardiovascular imaging, 2011. **4**(1): p. 98-206.
6. Pfister, O., et al., *CD31- but Not CD31+ cardiac side population cells exhibit functional cardiomyogenic differentiation.* Circulation research, 2005. **97**(1): p. 52-113.
7. Beltrami, A., et al., *Evidence that human cardiac myocytes divide after myocardial infarction.* The New England journal of medicine, 2001. **344**(23): p. 1750-1757.
8. Chang, K., C. Wang, and H. Wang, *Balancing self-renewal and differentiation by asymmetric division: insights from brain tumor suppressors in Drosophila neural stem cells.* BioEssays : news and reviews in molecular, cellular and developmental biology, 2012. **34**(4): p. 301-311.
9. Mathers, C., T. Boerma, and D. Ma Fat, *Global and regional causes of death.* British medical bulletin, 2009. **92**: p. 7-39.
10. Roger, V.r., et al., *Heart disease and stroke statistics--2012 update: a report from the American Heart Association.* Circulation, 2012. **125**(1).
11. Shah, A. and D. Mann, *In search of new therapeutic targets and strategies for heart failure: recent advances in basic science.* Lancet, 2011. **378**(9792): p. 704-716.
12. Foody, J., M. Farrell, and H. Krumholz, *beta-Blocker therapy in heart failure: scientific review.* JAMA : the journal of the American Medical Association, 2002. **287**(7): p. 883-892.
13. Cohn, J., *The management of chronic heart failure.* The New England journal of medicine, 1996. **335**(7): p. 490-498.
14. Morice, M.-C., et al., *Outcomes in patients with de novo left main disease treated with either percutaneous coronary intervention using paclitaxel-eluting stents or coronary artery bypass graft treatment in the Synergy Between Percutaneous Coronary Intervention with TAXUS and Cardiac Surgery (SYNTAX) trial.* Circulation, 2010. **121**(24): p. 2645-2698.

15. Parolari, A., et al., *Performance of EuroSCORE in CABG and off-pump coronary artery bypass grafting: single institution experience and meta-analysis.* European heart journal, 2009. **30**(3): p. 297-601.
16. Athanasuleas, C., et al., *Surgical ventricular restoration in the treatment of congestive heart failure due to post-infarction ventricular dilation.* Journal of the American College of Cardiology, 2004. **44**(7): p. 1439-1484.
17. Van Bommel, R., et al., *Critical appraisal of the use of cardiac resynchronization therapy beyond current guidelines.* Journal of the American College of Cardiology, 2010. **56**(10): p. 754-816.
18. Kirklin, J., et al., *The Fourth INTERMACS Annual Report: 4,000 implants and counting.* The Journal of heart and lung transplantation : the official publication of the International Society for Heart Transplantation, 2012. **31**(2): p. 117-143.
19. Pagani, F., et al., *Autologous skeletal myoblasts transplanted to ischemia-damaged myocardium in humans. Histological analysis of cell survival and differentiation.* Journal of the American College of Cardiology, 2003. **41**(5): p. 879-967.
20. Murry, C., et al., *Skeletal myoblast transplantation for repair of myocardial necrosis.* The Journal of clinical investigation, 1996. **98**(11): p. 2512-2535.
21. Menasche, P., et al., *The Myoblast Autologous Grafting in Ischemic Cardiomyopathy (MAGIC) trial: first randomized placebo-controlled study of myoblast transplantation.* Circulation, 2008. **117**(9): p. 1189-1389.
22. Dimmeler, S., J. Burchfield, and A. Zeiher, *Cell-based therapy of myocardial infarction.* Arteriosclerosis, thrombosis, and vascular biology, 2008. **28**(2): p. 208-224.
23. Abdel-Latif, A., et al., *Adult bone marrow-derived cells for cardiac repair: a systematic review and meta-analysis.* Archives of internal medicine, 2007. **167**(10): p. 989-1086.
24. Joggerst, S. and A. Hatzopoulos, *Stem cell therapy for cardiac repair: benefits and barriers.* Expert reviews in molecular medicine, 2009. **11**.
25. Chien, K. and E. Olson, *Converging pathways and principles in heart development and disease: CV@CSH.* Cell, 2002. **110**(2): p. 153-215.
26. Agah, R., et al., *Adenoviral delivery of E2F-1 directs cell cycle reentry and p53-independent apoptosis in postmitotic adult myocardium in vivo.* The Journal of clinical investigation, 1997. **100**(11): p. 2722-2730.
27. Soonpaa, M., et al., *Cardiomyocyte DNA synthesis and binucleation during murine development.* The American journal of physiology, 1996. **271**(5 Pt 2): p. 9.
28. Soonpaa, M. and L. Field, *Assessment of cardiomyocyte DNA synthesis in normal and injured adult mouse hearts.* The American journal of physiology, 1997. **272**(1 Pt 2): p. 6.
29. Cheng, W., et al., *Down-regulation of the IGF-1 system parallels the attenuation in the proliferative capacity of rat ventricular myocytes during postnatal development.* Laboratory investigation; a journal of technical methods and pathology, 1995. **72**(6): p. 646-701.
30. Marino, T., et al., *Proliferating cell nuclear antigen in developing and adult rat cardiac muscle cells.* Circulation research, 1991. **69**(5): p. 1353-1413.

31. Dowell, R. and R. McManus, *Pressure-induced cardiac enlargement in neonatal and adult rats. Left ventricular functional characteristics and evidence of cardiac muscle cell proliferation in the neonate.* Circulation research, 1978. **42**(3): p. 303-313.
32. Macdonald, R. and G. Mallory, *Autoradiography using tritiated thymidine. Detection of new cell formation in rat tissues.* Laboratory investigation; a journal of technical methods and pathology, 1959. **8**: p. 1547-1609.
33. Kajstura, J., et al., *The IGF-1-IGF-1 receptor system modulates myocyte proliferation but not myocyte cellular hypertrophy in vitro.* Experimental cell research, 1994. **215**(2): p. 273-356.
34. Anversa, P. and J. Kajstura, *Ventricular myocytes are not terminally differentiated in the adult mammalian heart.* Circulation research, 1998. **83**(1): p. 1-15.
35. Beltrami, A., et al., *Adult cardiac stem cells are multipotent and support myocardial regeneration.* Cell, 2003. **114**(6): p. 763-839.
36. Laugwitz, K.-L., et al., *Postnatal isl1+ cardioblasts enter fully differentiated cardiomyocyte lineages.* Nature, 2005. **433**(7026): p. 647-700.
37. Messina, E., et al., *Isolation and expansion of adult cardiac stem cells from human and murine heart.* Circulation research, 2004. **95**(9): p. 911-932.
38. Oh, H., et al., *Cardiac progenitor cells from adult myocardium: homing, differentiation, and fusion after infarction.* Proceedings of the National Academy of Sciences of the United States of America, 2003. **100**(21): p. 12313-12321.
39. Parmacek, M. and J. Epstein, *Pursuing cardiac progenitors: regeneration redux.* Cell, 2005. **120**(3): p. 295-303.
40. Kajstura, J., et al., *Cardiomyogenesis in the adult human heart.* Circulation research, 2010. **107**(2): p. 305-320.
41. Hierlihy, A.e., et al., *The post-natal heart contains a myocardial stem cell population.* FEBS letters, 2002. **530**(1-3): p. 239-282.
42. Zhou, B., et al., *Epicardial progenitors contribute to the cardiomyocyte lineage in the developing heart.* Nature, 2008. **454**(7200): p. 109-122.
43. Blume-Jensen, P. and T. Hunter, *Oncogenic kinase signalling.* Nature, 2001. **411**(6835): p. 355-420.
44. Urbanek, K., et al., *Stem cell niches in the adult mouse heart.* Proceedings of the National Academy of Sciences of the United States of America, 2006. **103**(24): p. 9226-9257.
45. Linke, A., et al., *Stem cells in the dog heart are self-renewing, clonogenic, and multipotent and regenerate infarcted myocardium, improving cardiac function.* Proceedings of the National Academy of Sciences of the United States of America, 2005. **102**(25): p. 8966-9037.
46. Bearzi, C., et al., *Human cardiac stem cells.* Proceedings of the National Academy of Sciences of the United States of America, 2007. **104**(35): p. 14068-14141.
47. Dawn, B., et al., *Cardiac stem cells delivered intravascularly traverse the vessel barrier, regenerate infarcted myocardium, and improve cardiac function.* Proceedings of the National Academy of Sciences of the United States of America, 2005. **102**(10): p. 3766-3837.

48. Bolli, R., et al., *Cardiac stem cells in patients with ischaemic cardiomyopathy (SCIPIO): initial results of a randomised phase 1 trial.* Lancet, 2011. **378**(9806): p. 1847-1904.
49. Wang, X., et al., *The role of the sca-1+/CD31- cardiac progenitor cell population in postinfarction left ventricular remodeling.* Stem cells (Dayton, Ohio), 2006. **24**(7): p. 1779-1867.
50. Matsuura, K., et al., *Adult cardiac Sca-1-positive cells differentiate into beating cardiomyocytes.* The Journal of biological chemistry, 2004. **279**(12): p. 11384-11475.
51. Smits, A., et al., *Human cardiomyocyte progenitor cells differentiate into functional mature cardiomyocytes: an in vitro model for studying human cardiac physiology and pathophysiology.* Nature protocols, 2009. **4**(2): p. 232-275.
52. Makkar, R., et al., *Intracoronary cardiosphere-derived cells for heart regeneration after myocardial infarction (CADUCEUS): a prospective, randomised phase 1 trial.* Lancet, 2012. **379**(9819): p. 895-1799.
53. Moretti, A., et al., *Multipotent embryonic isl1+ progenitor cells lead to cardiac, smooth muscle, and endothelial cell diversification.* Cell, 2006. **127**(6): p. 1151-1216.
54. Ye, J., et al., *Sca-1+ cardiosphere-derived cells are enriched for Isl1-expressing cardiac precursors and improve cardiac function after myocardial injury.* PloS one, 2012. **7**(1).
55. Cai, C.-L., et al., *A myocardial lineage derives from Tbx18 epicardial cells.* Nature, 2008. **454**(7200): p. 104-112.
56. Asakura, A. and M. Rudnicki, *Side population cells from diverse adult tissues are capable of in vitro hematopoietic differentiation.* Experimental hematology, 2002. **30**(11): p. 1339-1384.
57. Summer, R., et al., *Side population cells and Bcrp1 expression in lung.* American journal of physiology. Lung cellular and molecular physiology, 2003. **285**(1): p. 104.
58. Behbod, F., et al., *Transcriptional profiling of mammary gland side population cells.* Stem cells (Dayton, Ohio), 2006. **24**(4): p. 1065-1139.
59. Kotton, D., A. Fabian, and R. Mulligan, *A novel stem-cell population in adult liver with potent hematopoietic-reconstitution activity.* Blood, 2005. **106**(5): p. 1574-1654.
60. Rivier, F.o., et al., *Role of bone marrow cell trafficking in replenishing skeletal muscle SP and MP cell populations.* Journal of cell science, 2004. **117**(Pt 10): p. 1979-2067.
61. Hishikawa, K., et al., *Musculin/MyoR is expressed in kidney side population cells and can regulate their function.* The Journal of cell biology, 2005. **169**(6): p. 921-929.
62. Alison, M., *Tissue-based stem cells: ABC transporter proteins take centre stage.* The Journal of pathology, 2003. **200**(5): p. 547-597.
63. Patrawala, L., et al., *Highly purified CD44+ prostate cancer cells from xenograft human tumors are enriched in tumorigenic and metastatic progenitor cells.* Oncogene, 2006. **25**(12): p. 1696-2404.

64. Fang, D., et al., *A tumorigenic subpopulation with stem cell properties in melanomas.* Cancer research, 2005. **65**(20): p. 9328-9365.
65. Scharenberg, C., M. Harkey, and B. Torok-Storb, *The ABCG2 transporter is an efficient Hoechst 33342 efflux pump and is preferentially expressed by immature human hematopoietic progenitors.* Blood, 2002. **99**(2): p. 507-519.
66. Singh, S., et al., *Identification of human brain tumour initiating cells.* Nature, 2004. **432**(7015): p. 396-797.
67. Ponti, D., et al., *Isolation and in vitro propagation of tumorigenic breast cancer cells with stem/progenitor cell properties.* Cancer research, 2005. **65**(13): p. 5506-5517.
68. Ricci-Vitiani, L., et al., *Identification and expansion of human colon-cancer-initiating cells.* Nature, 2007. **445**(7123): p. 111-116.
69. Sandstedt, J., et al., *Left atrium of the human adult heart contains a population of side population cells.* Basic research in cardiology, 2012. **107**(2): p. 255.
70. Alfakir, M., et al., *The temporal and spatial expression patterns of ABCG2 in the developing human heart.* International journal of cardiology, 2012. **156**(2): p. 133-141.
71. Martin, C., et al., *Persistent expression of the ATP-binding cassette transporter, Abcg2, identifies cardiac SP cells in the developing and adult heart.* Developmental biology, 2004. **265**(1): p. 262-337.
72. Pfister, O., et al., *Isolation of resident cardiac progenitor cells by Hoechst 33342 staining.* Methods in molecular biology (Clifton, N.J.), 2010. **660**: p. 53-116.
73. Oyama, T., et al., *Cardiac side population cells have a potential to migrate and differentiate into cardiomyocytes in vitro and in vivo.* The Journal of cell biology, 2007. **176**(3): p. 329-370.
74. Mouquet, F.d.r., et al., *Restoration of cardiac progenitor cells after myocardial infarction by self-proliferation and selective homing of bone marrow-derived stem cells.* Circulation research, 2005. **97**(11): p. 1090-1092.
75. Oikonomopoulos, A., et al., *Wnt signaling exerts an antiproliferative effect on adult cardiac progenitor cells through IGFBP3.* Circ Res, 2011. **109**(12): p. 1363-74.
76. Christoforou, N. and J. Gearhart, *Stem cells and their potential in cell-based cardiac therapies.* Progress in cardiovascular diseases, 2007. **49**(6): p. 396-809.
77. Yamashita, J., et al., *Flk1-positive cells derived from embryonic stem cells serve as vascular progenitors.* Nature, 2000. **408**(6808): p. 92-98.
78. Kehat, I., et al., *Electromechanical integration of cardiomyocytes derived from human embryonic stem cells.* Nature biotechnology, 2004. **22**(10): p. 1282-1291.
79. Gimond, C., S. Marchetti, and G. PagΓ¨s, *Differentiation of mouse embryonic stem cells into endothelial cells: genetic selection and potential use in vivo.* Methods in molecular biology (Clifton, N.J.), 2006. **330**: p. 303-332.
80. Singla, D., et al., *Transplantation of embryonic stem cells into the infarcted mouse heart: formation of multiple cell types.* Journal of molecular and cellular cardiology, 2006. **40**(1): p. 195-395.
81. Min, J.-Y., et al., *Long-term improvement of cardiac function in rats after infarction by transplantation of embryonic stem cells.* The Journal of thoracic and cardiovascular surgery, 2003. **125**(2): p. 361-370.

82. Yamanaka, S., *A fresh look at iPS cells.* Cell, 2009. **137**(1): p. 13-20.
83. Takahashi, K., et al., *Induction of pluripotent stem cells from adult human fibroblasts by defined factors.* Cell, 2007. **131**(5): p. 861-933.
84. Kim, J., et al., *Pluripotent stem cells induced from adult neural stem cells by reprogramming with two factors.* Nature, 2008. **454**(7204): p. 646-696.
85. Okita, K., et al., *Generation of mouse-induced pluripotent stem cells with plasmid vectors.* Nature protocols, 2010. **5**(3): p. 418-446.
86. Okita, K., et al., *Generation of mouse induced pluripotent stem cells without viral vectors.* Science (New York, N.Y.), 2008. **322**(5903): p. 949-1002.
87. Mehta, A., et al., *Pharmacological response of human cardiomyocytes derived from virus-free induced pluripotent stem cells.* Cardiovascular research, 2011. **91**(4): p. 577-663.
88. Goodell, M., et al., *Isolation and functional properties of murine hematopoietic stem cells that are replicating in vivo.* The Journal of experimental medicine, 1996. **183**(4): p. 1797-2603.
89. Zhou, S., et al., *The ABC transporter Bcrp1/ABCG2 is expressed in a wide variety of stem cells and is a molecular determinant of the side-population phenotype.* Nature medicine, 2001. **7**(9): p. 1028-1062.
90. Dean, M. and R. Allikmets, *Complete characterization of the human ABC gene family.* Journal of bioenergetics and biomembranes, 2001. **33**(6): p. 475-484.
91. Dean, M. and T. Annilo, *Evolution of the ATP-binding cassette (ABC) transporter superfamily in vertebrates.* Annual review of genomics and human genetics, 2005. **6**: p. 123-165.
92. Dean, M., A. Rzhetsky, and R. Allikmets, *The human ATP-binding cassette (ABC) transporter superfamily.* Genome research, 2001. **11**(7): p. 1156-1222.
93. Gillet, J.-P., T. Efferth, and J. Remacle, *Chemotherapy-induced resistance by ATP-binding cassette transporter genes.* Biochimica et biophysica acta, 2007. **1775**(2): p. 237-299.
94. Quazi, F. and R. Molday, *Lipid transport by mammalian ABC proteins.* Essays in biochemistry, 2011. **50**(1): p. 265-355.
95. Chen, Z.-Q., et al., *The essential vertebrate ABCE1 protein interacts with eukaryotic initiation factors.* The Journal of biological chemistry, 2006. **281**(11): p. 7452-7459.
96. Kerr, I., *Sequence analysis of twin ATP binding cassette proteins involved in translational control, antibiotic resistance, and ribonuclease L inhibition.* Biochemical and biophysical research communications, 2004. **315**(1): p. 166-239.
97. Tyzack, J., et al., *ABC50 interacts with eukaryotic initiation factor 2 and associates with the ribosome in an ATP-dependent manner.* The Journal of biological chemistry, 2000. **275**(44): p. 34131-34140.
98. Woodward, O., A. KГ¶ttgen, and M. KГ¶ttgen, *ABCG transporters and disease.* The FEBS journal, 2011. **278**(18): p. 3215-3240.
99. Ambudkar, S., et al., *Biochemical, cellular, and pharmacological aspects of the multidrug transporter.* Annual review of pharmacology and toxicology, 1999. **39**: p. 361-459.

100. Miyake, K., et al., *Molecular cloning of cDNAs which are highly overexpressed in mitoxantrone-resistant cells: demonstration of homology to ABC transport genes.* Cancer research, 1999. **59**(1): p. 8-21.
101. Allikmets, R., et al., *A human placenta-specific ATP-binding cassette gene (ABCP) on chromosome 4q22 that is involved in multidrug resistance.* Cancer research, 1998. **58**(23): p. 5337-5346.
102. Doyle, L., et al., *A multidrug resistance transporter from human MCF-7 breast cancer cells.* Proceedings of the National Academy of Sciences of the United States of America, 1998. **95**(26): p. 15665-15735.
103. Litman, T., et al., *Use of peptide antibodies to probe for the mitoxantrone resistance-associated protein MXR/BCRP/ABCP/ABCG2.* Biochimica et biophysica acta, 2002. **1565**(1): p. 6-22.
104. Ozvegy, C., et al., *Functional characterization of the human multidrug transporter, ABCG2, expressed in insect cells.* Biochemical and biophysical research communications, 2001. **285**(1): p. 111-118.
105. Ozvegy, C., A.s. VΓ˘radi, and B.z. Sarkadi, *Characterization of drug transport, ATP hydrolysis, and nucleotide trapping by the human ABCG2 multidrug transporter. Modulation of substrate specificity by a point mutation.* The Journal of biological chemistry, 2002. **277**(50): p. 47980-48070.
106. Kage, K., et al., *Dominant-negative inhibition of breast cancer resistance protein as drug efflux pump through the inhibition of S-S dependent homodimerization.* International journal of cancer. Journal international du cancer, 2002. **97**(5): p. 626-656.
107. Xu, J., et al., *Characterization of oligomeric human half-ABC transporter ATP-binding cassette G2.* The Journal of biological chemistry, 2004. **279**(19): p. 19781-19790.
108. Rocchi, E., et al., *The product of the ABC half-transporter gene ABCG2 (BCRP/MXR/ABCP) is expressed in the plasma membrane.* Biochemical and biophysical research communications, 2000. **271**(1): p. 42-48.
109. Jonker, J., et al., *Role of breast cancer resistance protein in the bioavailability and fetal penetration of topotecan.* Journal of the National Cancer Institute, 2000. **92**(20): p. 1651-1657.
110. Doyle, L. and D. Ross, *Multidrug resistance mediated by the breast cancer resistance protein BCRP (ABCG2).* Oncogene, 2003. **22**(47): p. 7340-7398.
111. Polgar, O., R. Robey, and S. Bates, *ABCG2: structure, function and role in drug response.* Expert opinion on drug metabolism & toxicology, 2008. **4**(1): p. 1-16.
112. Krishnamurthy, P., et al., *The stem cell marker Bcrp/ABCG2 enhances hypoxic cell survival through interactions with heme.* The Journal of biological chemistry, 2004. **279**(23): p. 24218-24243.
113. Woodward, O., et al., *Identification of a urate transporter, ABCG2, with a common functional polymorphism causing gout.* Proceedings of the National Academy of Sciences of the United States of America, 2009. **106**(25): p. 10338-10380.
114. Martin, C., et al., *Hypoxia-inducible factor-2alpha transactivates Abcg2 and promotes cytoprotection in cardiac side population cells.* Circulation research, 2008. **102**(9): p. 1075-1156.

115. Liadaki, K., et al., *Side population cells isolated from different tissues share transcriptome signatures and express tissue-specific markers.* Experimental cell research, 2005. **303**(2): p. 360-434.
116. Kajstura, J., et al., *Cardiac stem cells and myocardial disease.* Journal of molecular and cellular cardiology, 2008. **45**(4): p. 505-518.
117. Stolzing, A. and A. Scutt, *Age-related impairment of mesenchymal progenitor cell function.* Aging cell, 2006. **5**(3): p. 213-237.
118. Goswami, S., N. Maulik, and D. Das, *Ischemia-reperfusion and cardioprotection: a delicate balance between reactive oxygen species generation and redox homeostasis.* Annals of medicine, 2007. **39**(4): p. 275-364.
119. Zhou, S., et al., *Bcrp1 gene expression is required for normal numbers of side population stem cells in mice, and confers relative protection to mitoxantrone in hematopoietic cells in vivo.* Proceedings of the National Academy of Sciences of the United States of America, 2002. **99**(19): p. 12339-12383.
120. Jonker, J., et al., *Contribution of the ABC transporters Bcrp1 and Mdr1a/1b to the side population phenotype in mammary gland and bone marrow of mice.* Stem cells (Dayton, Ohio), 2005. **23**(8): p. 1059-1124.
121. Patrawala, L., et al., *Side population is enriched in tumorigenic, stem-like cancer cells, whereas ABCG2+ and ABCG2- cancer cells are similarly tumorigenic.* Cancer research, 2005. **65**(14): p. 6207-6226.
122. Chen, Z., et al., *Suppression of ABCG2 inhibits cancer cell proliferation.* International journal of cancer. Journal international du cancer, 2010. **126**(4): p. 841-892.
123. Zhou, S., et al., *Increased expression of the Abcg2 transporter during erythroid maturation plays a role in decreasing cellular protoporphyrin IX levels.* Blood, 2005. **105**(6): p. 2571-2577.
124. Meissner, K., et al., *The ATP-binding cassette transporter ABCG2 (BCRP), a marker for side population stem cells, is expressed in human heart.* The journal of histochemistry and cytochemistry : official journal of the Histochemistry Society, 2006. **54**(2): p. 215-236.
125. Solbach, T., et al., *ATP-binding cassette transporters in human heart failure.* Naunyn-Schmiedeberg's archives of pharmacology, 2008. **377**(3): p. 231-274.
126. Higashikuni, Y., et al., *The ATP-binding cassette transporter BCRP1/ABCG2 plays a pivotal role in cardiac repair after myocardial infarction via modulation of microvascular endothelial cell survival and function.* Arteriosclerosis, thrombosis, and vascular biology, 2010. **30**(11): p. 2128-2163.
127. Higashikuni, Y., et al., *The ATP-binding cassette transporter ABCG2 protects against pressure overload-induced cardiac hypertrophy and heart failure by promoting angiogenesis and antioxidant response.* Arteriosclerosis, thrombosis, and vascular biology, 2012. **32**(3): p. 654-715.
128. Knoblich, J., *Mechanisms of asymmetric stem cell division.* Cell, 2008. **132**(4): p. 583-680.
129. Morrison, S. and J. Kimble, *Asymmetric and symmetric stem-cell divisions in development and cancer.* Nature, 2006. **441**(7097): p. 1068-1142.
130. Gonczy, P., *Mechanisms of asymmetric cell division: flies and worms pave the way.* Nature reviews. Molecular cell biology, 2008. **9**(5): p. 355-421.

131. Wright, D., et al., *Cyclophosphamide/granulocyte colony-stimulating factor causes selective mobilization of bone marrow hematopoietic stem cells into the blood after M phase of the cell cycle.* Blood, 2001. **97**(8): p. 2278-2363.
132. Roeder, I. and R. Lorenz, *Asymmetry of stem cell fate and the potential impact of the niche.* Stem Cell Reviews and Reports, 2006.
133. Scadden, D., *The stem-cell niche as an entity of action.* Nature, 2006. **441**(7097): p. 1075-1084.
134. Schofield, R., *The relationship between the spleen colony-forming cell and the haemopoietic stem cell.* Blood cells, 1978. **4**(1-2): p. 7-32.
135. Hsu, Y.-C. and E. Fuchs, *A family business: stem cell progeny join the niche to regulate homeostasis.* Nature reviews. Molecular cell biology, 2012. **13**(2): p. 103-117.
136. Lo Celso, C., et al., *Live-animal tracking of individual haematopoietic stem/progenitor cells in their niche.* Nature, 2009. **457**(7225): p. 92-98.
137. Kiel, M., et al., *SLAM family receptors distinguish hematopoietic stem and progenitor cells and reveal endothelial niches for stem cells.* Cell, 2005. **121**(7): p. 1109-1130.
138. Barker, N., et al., *Identification of stem cells in small intestine and colon by marker gene Lgr5.* Nature, 2007. **449**(7165): p. 1003-1010.
139. Tumbar, T., et al., *Defining the epithelial stem cell niche in skin.* Science (New York, N.Y.), 2004. **303**(5656): p. 359-422.
140. Urbanek, K., et al., *Stem cell niches in the adult mouse heart.* Proc Natl Acad Sci U S A, 2006. **103**(24): p. 9226-31.
141. Rhyu, M., L. Jan, and Y. Jan, *Asymmetric distribution of numb protein during division of the sensory organ precursor cell confers distinct fates to daughter cells.* Cell, 1994. **76**(a65f1489-9f33-7b95-1b79-0a69cc7a55f6): p. 477-568.
142. Couturier, L., N. Vodovar, and F. Schweisguth, *Endocytosis by Numb breaks Notch symmetry at cytokinesis.* Nature cell biology, 2012. **14**(f9656ea7-9f36-3a04-2432-0abee8f0bc13): p. 131-140.
143. Smith, C., et al., *aPKC-mediated phosphorylation regulates asymmetric membrane localization of the cell fate determinant Numb.* The EMBO journal, 2007. **26**(9f435a4d-3e00-6b79-6cae-0a78a7e5e4be): p. 468-548.
144. Berdnik, D., et al., *The endocytic protein alpha-Adaptin is required for numb-mediated asymmetric cell division in Drosophila.* Developmental cell, 2002. **3**(2): p. 221-252.
145. Song, Y. and B. Lu, *Notch Signaling Modulator Numb's Interaction with Ξ±-Adaptin Regulates Endocytosis of Notch Pathway Components and Cell Fate Determination of Neural Stem Cells.* The Journal of biological chemistry, 2012.
146. Goldstein, B. and I. Macara, *The PAR proteins: fundamental players in animal cell polarization.* Developmental cell, 2007. **13**(44cee11e-db20-ce7a-9b14-0ae54732205f): p. 609-631.
147. Atwood, S., et al., *Cdc42 acts downstream of Bazooka to regulate neuroblast polarity through Par-6 aPKC.* Journal of cell science, 2007. **120**(bb2902a1-3647-3b41-2c23-0ae5a8859d42): p. 3200-3206.
148. Siegrist, S. and C. Doe, *Microtubule-induced cortical cell polarity.* Genes & development, 2007. **21**(5): p. 483-579.

149. Xu, J., et al., *Polarity reveals intrinsic cell chirality.* Proceedings of the National Academy of Sciences of the United States of America, 2007. **104**(22): p. 9296-9596.
150. Chen, J., J. Lippincott-Schwartz, and J. Liu, *Intracellular spatial localization regulated by the microtubule network.* PloS one, 2012. **7**(4).
151. Nteliopoulos, G. and M. Gordon, *Protein segregation between dividing hematopoietic progenitor cells in the determination of the symmetry/asymmetry of cell division.* Stem cells and development, 2012.
152. Ting, S., et al., *Asymmetric segregation and self-renewal of hematopoietic stem and progenitor cells with endocytic Ap2a2.* Blood, 2012. **119**(11): p. 2510-2532.
153. Poulson, N. and T. Lechler, *Asymmetric cell divisions in the epidermis.* International review of cell and molecular biology, 2012. **295**: p. 199-431.
154. Williams, S., et al., *Asymmetric cell divisions promote Notch-dependent epidermal differentiation.* Nature, 2011. **470**(7334): p. 353-361.
155. Rujano, M.a., et al., *Polarised asymmetric inheritance of accumulated protein damage in higher eukaryotes.* PLoS biology, 2006. **4**(12).
156. Tyedmers, J., A. Mogk, and B. Bukau, *Cellular strategies for controlling protein aggregation.* Nature reviews. Molecular cell biology, 2010. **11**(11): p. 777-865.
157. Reya, T., et al., *Stem cells, cancer, and cancer stem cells.* Nature, 2001. **414**(6859): p. 105-116.
158. Sherley, J., P. Stadler, and D. Johnson, *Expression of the wild-type p53 antioncogene induces guanine nucleotide-dependent stem cell division kinetics.* Proceedings of the National Academy of Sciences of the United States of America, 1995. **92**(1): p. 136-176.
159. Rambhatla, L., et al., *Cellular Senescence: Ex Vivo p53-Dependent Asymmetric Cell Kinetics.* Journal of biomedicine & biotechnology, 2001. **1**(1): p. 28-65.
160. Rambhatla, L., et al., *Immortal DNA strand cosegregation requires p53/IMPDH-dependent asymmetric self-renewal associated with adult stem cells.* Cancer research, 2005. **65**(8): p. 3155-3216.
161. Sherley, J., *Asymmetric cell kinetics genes: the key to expansion of adult stem cells in culture.* TheScientificWorldJournal, 2002. **2**: p. 1906-1927.
162. Cicalese, A., et al., *The tumor suppressor p53 regulates polarity of self-renewing divisions in mammary stem cells.* Cell, 2009. **138**(6): p. 1083-1178.
163. Huh, Y., et al., *SACK-Expanded Hair Follicle Stem Cells Display Asymmetric Nuclear Lgr5 Expression With Non-Random Sister Chromatid Segregation.* Scientific reports, 2011. **1**: p. 176.
164. Sherley, J., *Guanine nucleotide biosynthesis is regulated by the cellular p53 concentration.* The Journal of biological chemistry, 1991. **266**(36): p. 24815-24843.
165. Orford, K. and D. Scadden, *Deconstructing stem cell self-renewal: genetic insights into cell-cycle regulation.* Nature reviews. Genetics, 2008. **9**(2): p. 115-143.
166. Calegari, F. and W. Huttner, *An inhibition of cyclin-dependent kinases that lengthens, but does not arrest, neuroepithelial cell cycle induces premature neurogenesis.* Journal of cell science, 2003. **116**(Pt 24): p. 4947-5002.

167. Salomoni, P. and F. Calegari, *Cell cycle control of mammalian neural stem cells: putting a speed limit on G1.* Trends in cell biology, 2010. **20**(5): p. 233-276.
168. Orihara-Ono, M., et al., *Downregulation of Notch mediates the seamless transition of individual Drosophila neuroepithelial progenitors into optic medullar neuroblasts during prolonged G1.* Developmental biology, 2011. **351**(1): p. 163-238.
169. Tsunekawa, Y., et al., *Cyclin D2 in the basal process of neural progenitors is linked to non-equivalent cell fates.* The EMBO journal, 2012. **31**(8): p. 1879-1971.
170. Calegari, F., *CyclinD2 at the edge: splitting up cell fate.* EMBO J, 2012. **31**(8): p. 1850-2.
171. Malumbres, M., *Physiological relevance of cell cycle kinases.* Physiological reviews, 2011. **91**(3): p. 973-1980.
172. Calegari, F., et al., *Selective lengthening of the cell cycle in the neurogenic subpopulation of neural progenitor cells during mouse brain development.* J Neurosci, 2005. **25**(28): p. 6533-8.
173. Takahashi, T., R.S. Nowakowski, and V.S. Caviness, Jr., *The cell cycle of the pseudostratified ventricular epithelium of the embryonic murine cerebral wall.* J Neurosci, 1995. **15**(9): p. 6046-57.
174. Lukaszewicz, A., et al., *G1 phase regulation, area-specific cell cycle control, and cytoarchitectonics in the primate cortex.* Neuron, 2005. **47**(3): p. 353-64.
175. Lange, C., W. Huttner, and F. Calegari, *Cdk4/cyclinD1 overexpression in neural stem cells shortens G1, delays neurogenesis, and promotes the generation and expansion of basal progenitors.* Cell stem cell, 2009. **5**(3): p. 320-351.
176. Cottage, C., et al., *Cardiac progenitor cell cycling stimulated by pim-1 kinase.* Circulation research, 2010. **106**(5): p. 891-1792.
177. Sundararaman, B., et al., *Asymmetric Chromatid Segregation in Cardiac Progenitor Cells Is Enhanced by Pim-1 Kinase.* Circulation research, 2012.
178. Dzeja, P., et al., *Developmental enhancement of adenylate kinase-AMPK metabolic signaling axis supports stem cell cardiac differentiation.* PloS one, 2011. **6**(4).
179. Jain, M., et al., *Cell therapy attenuates deleterious ventricular remodeling and improves cardiac performance after myocardial infarction.* Circulation, 2001. **103**(14): p. 1920-7.
180. Tang, X.L., et al., *Intracoronary administration of cardiac progenitor cells alleviates left ventricular dysfunction in rats with a 30-day-old infarction.* Circulation, 2010. **121**(2): p. 293-305.
181. Pfister, O. and R. Liao, *Pump to survive: novel cytoprotective strategies for cardiac progenitor cells.* Circ Res, 2008. **102**(9): p. 998-1001.
182. Bunting, K.D., et al., *Enforced P-glycoprotein pump function in murine bone marrow cells results in expansion of side population stem cells in vitro and repopulating cells in vivo.* Blood, 2000. **96**(3): p. 902-9.
183. Honjo, Y., et al., *Acquired mutations in the MXR/BCRP/ABCP gene alter substrate specificity in MXR/BCRP/ABCP-overexpressing cells.* Cancer Res, 2001. **61**(18): p. 6635-9.

184. Robey, R.W., et al., *A functional assay for detection of the mitoxantrone resistance protein, MXR (ABCG2).* Biochim Biophys Acta, 2001. **1512**(2): p. 171-82.
185. Garimella, T.S., et al., *Plasma pharmacokinetics and tissue distribution of the breast cancer resistance protein (BCRP/ABCG2) inhibitor fumitremorgin C in SCID mice bearing T8 tumors.* Cancer Chemother Pharmacol, 2005. **55**(2): p. 101-9.
186. Helson, L., et al., *A saturation threshold for taxol cytotoxicity in human glial and neuroblastoma cells.* Anticancer Drugs, 1993. **4**(4): p. 487-90.
187. Henriksen, U., U. Gether, and T. Litman, *Effect of Walker A mutation (K86M) on oligomerization and surface targeting of the multidrug resistance transporter ABCG2.* Journal of cell science, 2005. **118**(Pt 7): p. 1417-1443.
188. Hsieh, P., et al., *Evidence from a genetic fate-mapping study that stem cells refresh adult mammalian cardiomyocytes after injury.* Nature medicine, 2007. **13**(8): p. 970-974.
189. Porrello, E.R., et al., *Transient regenerative potential of the neonatal mouse heart.* Science, 2011. **331**(6020): p. 1078-80.
190. Li, F., et al., *Rapid transition of cardiac myocytes from hyperplasia to hypertrophy during postnatal development.* J Mol Cell Cardiol, 1996. **28**(8): p. 1737-46.
191. Laflamme, M.A. and C.E. Murry, *Heart regeneration.* Nature, 2011. **473**(7347): p. 326-35.
192. Krishnamurthy, P. and J. Schuetz, *Role of ABCG2/BCRP in biology and medicine.* Annual review of pharmacology and toxicology, 2006. **46**: p. 381-791.
193. Staiber, W., *Asymmetric distribution of mitochondria and of spindle microtubules in opposite directions in differential mitosis of germ line cells in Acricotopus.* Cell Tissue Res, 2007. **329**(1): p. 197-203.
194. Kashatus, D.F., et al., *RALA and RALBP1 regulate mitochondrial fission at mitosis.* Nat Cell Biol, 2011. **13**(9): p. 1108-15.
195. Huls, M., F.G. Russel, and R. Masereeuw, *The role of ATP binding cassette transporters in tissue defense and organ regeneration.* J Pharmacol Exp Ther, 2009. **328**(1): p. 3-9.
196. Bhattacharya, S., et al., *Maintenance of retinal stem cells by Abcg2 is regulated by notch signaling.* J Cell Sci, 2007. **120**(Pt 15): p. 2652-62.
197. Zong, Y., *Expression of Mouse Abcg2 mRNA during Hematopoiesis Is Regulated by Alternative Use of Multiple Leader Exons and Promoters.* Journal of Biological Chemistry, 2006. **281**.
198. Jonker, J., et al., *The breast cancer resistance protein protects against a major chlorophyll-derived dietary phototoxin and protoporphyria.* Proceedings of the National Academy of Sciences of the United States of America, 2002. **99**(24): p. 15649-15703.
199. Moreno, R., et al., *Primary angioplasty reduces the risk of left ventricular free wall rupture compared with thrombolysis in patients with acute myocardial infarction.* J Am Coll Cardiol, 2002. **39**(4): p. 598-603.

200. Yip, H.K., et al., *Cardiac rupture complicating acute myocardial infarction in the direct percutaneous coronary intervention reperfusion era.* Chest, 2003. **124**(2): p. 565-71.

Chapter 4

Isolation of Resident Cardiac Progenitor Cells by Hoechst 33342 Staining

Otmar Pfister, Angelos Oikonomopoulos, Konstantina-Ioanna Sereti, and Ronglih Liao

Abstract

Cardiac resident stem/progenitor cells are critical to the cellular and functional integrity of the heart by maintaining myocardial cell homeostasis. Given their central role in myocardial biology, resident cardiac progenitor cells have become a major focus in cardiovascular research. Identification of putative cardiac progenitor cells within the myocardium is largely based on the presence or absence of specific cell surface markers. Additional purification strategies take advantage of the ability of stem cells to efficiently efflux vital dyes such as Hoechst 33342. During fluoresence activated cell sorting (FACS) such Hoechst-extruding cells appear to the side of Hoechst-dye retaining cells and have thus been termed side population (SP) cells. We have shown that cardiac SP cells that express stem cell antigen 1 (Sca-1) but not CD31 are cardiomyogenic, and thus represent a putative cardiac progenitor cell population. This chapter describes the methodology for the isolation of resident cardiac progenitor cells utilizing the SP phenotype combined with stem cell surface markers.

Key words: Hoechst 33342, FACS, Side population (SP), Cardiac progenitor cells

1. Introduction

The identification of resident cardiac stem cells with the potential to differentiate into multiple cardiac cell lineages has added an important new dimension to myocardial biology. In order to properly study cardiac stem cells, reliable methods for the identification and isolation of putative cardiac stem cells are crucial. Over the last 5 years several isolation protocols have been published (1–5). Most of these protocols rely on the presence of stem-cell associated cell surface markers including stem cell antigen 1 (Sca-1), the receptor for cytokine stem cell factor, steel factor (c-kit), as well as the ATP-binding cassette (ABC) transporters

Randall J. Lee (ed.), *Stem Cells for Myocardial Regeneration: Methods and Protocols*, Methods in Molecular Biology, vol. 660,
DOI 10.1007/978-1-60761-705-1_4,

Mdr1 and Abcg2, and the absence of cell-lineage markers, including lineage, CD45, and CD31, among others (2, 4–7). While enzymatic tissue digestion potentially alters the expression of cell surface markers via cleavage (e.g., c-kit), ABC-transporter activity is not affected by the digestion process (5).

Functionally, ABC-transporter activity can be conveniently and reliably assessed by challenging cells with the DNA-binding dye Hoechst 33342 (8, 9). Upon Hoechst 33342 exposure, ABC-transporter-competent cells efficiently clear the fluorescent dye Hoechst 33342, thereby becoming "Hoechst-low." Putative stem cells are thus identified as the cellular fraction with the lowest Hoechst fluorescence intensity during fluorescence-activated cell sorting (FACS) (8). As Hoechst-low cells characteristically appear to the side of Hoechst dye retaining cells in the FACS profile, Hoechst-low cells have traditionally been termed side population (SP) cells. ABC-transporter activity is ATP and calcium dependent, thus, blocking of the ATP-binding site by the calcium channel blocker verapamil abolishes the Hoechst-efflux phenomenon. Hence, verapamil is commonly used to document the specificity of the SP pattern during FACS analysis (10).

Utilizing Hoechst 33342 dye staining to identify mononuclear cells containing stem cell activity was first introduced by Goodell et al. (8). In their seminal work, the authors demonstrated that Hoechst-extruding SP cells isolated from bone marrow are enriched in hematopoietic stem cell properties. Subsequently, the SP phenotype has been used to isolate stem/progenitor cells successfully from various solid tissues (10). We have modified the protocol by Goodell et al. and established a protocol exclusively for the isolation of SP cells from adult myocardium (5). The myocardium contains a subset of cardiac progenitor cells that express the ABC transporters Abcg2 and Mdr1 necessary for Hoechst-extrusion (Fig. 1). In fact, the Hoechst efflux ability, i.e., SP phenotype, of cardiac SP cells is regulated by both Abcg2 and Mdr1 in an age-dependent fashion (11). Thus, developmental status and age might significantly impact the yield and phenotype of cardiac SP cells. To further isolate the stem/progenitors with higher cardiomyogenic potential, we have combined SP isolation techniques with immunostaining for Sca-1 and CD31 to select for Sca-1+/CD31– cardiac SP, a sub population of cardiac SP cells with enriched cardiomyogenic potential (5).

2. Materials

2.1. Enzymatic Digestion of Murine Hearts

1. Collagenase B, lyophilizate (Roche Applied Science). The final concentration for the digestion is 0.1%. Store dry at 4°C and protected from light.

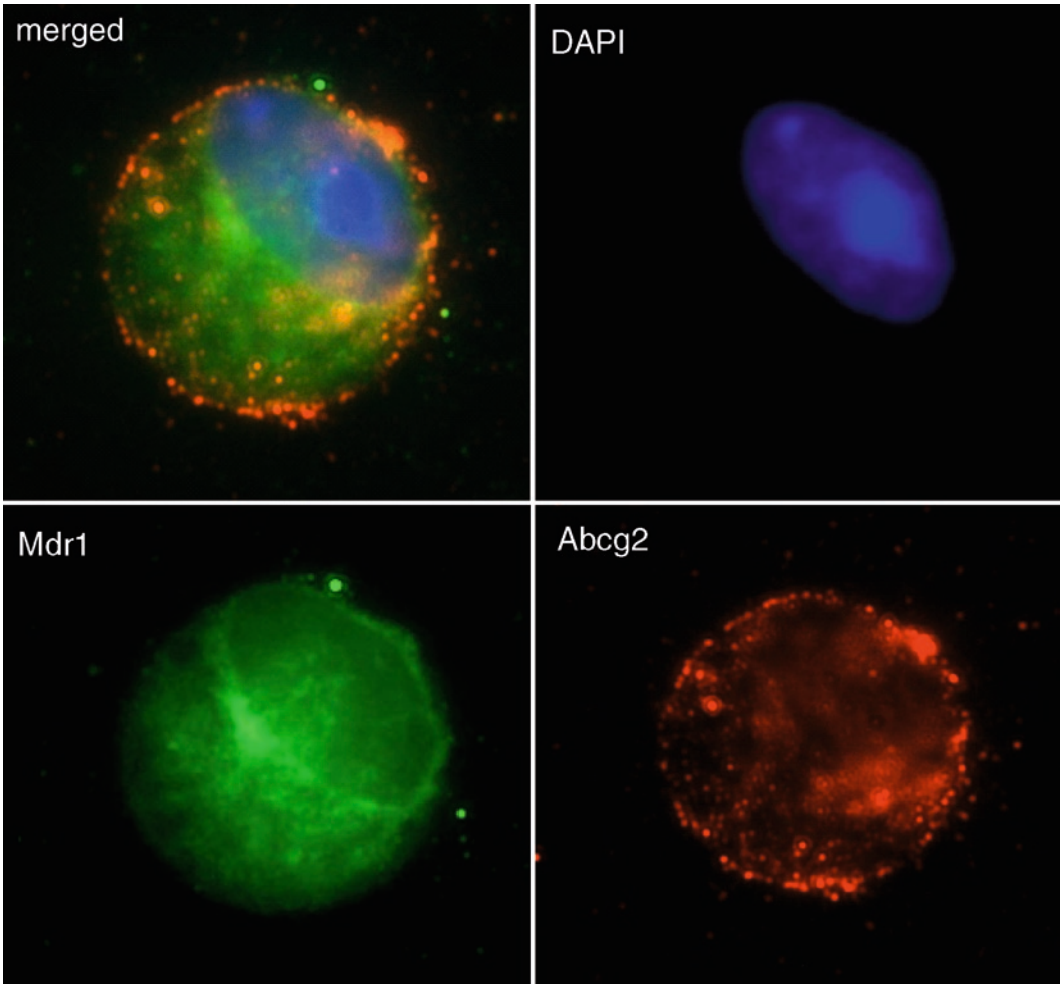

Fig. 1. Cardiac SP cells expressing Abcg2 and Mdr1. Freshly isolated cardiac SP cells stained for Mdr1 (*green*) and Abcg2 (*red*). The nuclei were stained with DAPI (*blue*).

2. Dispase II, lyophilizate (Roche Applied Science). The final concentration for the digestion is 2.4 U/ml in 5.56 mM glucose, 138 mM NaCl, 5.4 mM KCl, and 4.16 mM $NaHCO_3$.
3. $CaCl_2$. The final concentration for the digestion is 2.5 mM.
4. Hanks Balanced Salt Solution (HBSS) buffer: HBSS (Invitrogen) supplemented with 2% fetal bovine serum (GIBCO) and 10 mM HEPES.

2.2. Hoechst 33342 Incubation

1. Hoechst 33342 (Sigma Aldrich) dissolved in water at a final concentration of 1 mg/ml, filter sterilized.
2. High glucose Dulbecco's Modified Eagle's Medium (DMEM) buffer: DMEM (Cellgro) supplemented with 2% fetal bovine serum (GIBCO) and 10 mM HEPES.
3. Verapamil (Sigma) 5 mM stock solution in 95% ethanol.

2.3. Cell Surface Antigen Staining

1. HBSS buffer: Hanks Balanced Salt Solution (HBSS) (Invitrogen) supplemented with 2% fetal bovine serum (GIBCO) and 10 mM HEPES.
2. Sca-1 antibody: Phycoerythrin (PE) conjugated rat antimouse (BD Pharmingen). Isotype control PE Rat IgG2a, κ (BD Pharmingen).
3. CD31 antibody: Allophycocyanin (APC) conjugated rat antimouse (BD Pharmingen). Isotype control APC Rat IgG2a, κ (BD Pharmingen).
4. Flow cytometers: MoFlo (Cytomation, Inc). FACSAria (BD Bioscience).

2.4. FACS Analysis and Sorting

1. FACS tubes (BD Pharmingen).
2. Filters (40 μm and 70 μm, BD Pharmingen).
3. Propidium iodide (PI) (Sigma) is dissolved in water at 200 μg/ml and stored in small aliquots at −20°C. PI is used at a final concentration of 2 μg/ml.

3. Methods

This Hoechst SP cell purification protocol was established for the isolation of murine cardiac SP progenitor cells from C57Bl/6 and FVB mice. It is important to note that total cardiac SP cell yield, as well as the proportion of Sca-1+/CD31− cardiac SP cells, is age dependent with higher SP cell numbers in neonatal hearts compared to adult hearts (5). According to our experience with the aforementioned mouse strains, an average of 0.8 ± 0.2% cardiac SP cells can be expected in mice 10–12 weeks of age.

As the ability to discriminate Hoechst low SP cells is based on an active biological process, namely the energy dependent efflux of Hoechst 33342 by the ABC-transporters Abcg2 and Mdr1 (11), careful attention must be applied to the staining conditions in order to obtain an optimal resolution for the FACS profile. Correct Hoechst concentration, accurate cell counting, exact staining time, and staining temperature are critical. In order to prohibit further dye efflux after the staining process, it is crucial to keep the cells at 4°C until the FACS analysis is performed.

3.1. Enzymatic Digestion of Murine Hearts

1. Make fresh digestion buffer containing 0.1% Collagenase B, 2.4 U/ml Dispase II, $CaCl_2$ 2.5 mM. Prewarm this digestion buffer in a 37°C water bath prior to use. Utilize 5 ml digestion buffer per mouse-heart. For pooled hearts digestion, calculate the total amount of digestion buffer accordingly (Note that for optimal digestion, it is best to pool no more than four hearts).

2. Anesthetize the mouse with pentobarbital (65 mg/kg body weight i.p.). Note that alternative methods of anesthesia can be used in accordance with the individual Institutional Animal Care and Use Committee's guidelines and approval. Once the mouse is fully anesthetized, wipe the chest region gently with 70% ethanol. Cut the rib cage to expose the thoracic cavity. Open the thorax to expose the heart and flush the heart with 10 ml PBS. Use forceps to lift and cut the heart out and then place the heart immediately on ice in a culture dish containing cold PBS to wash away any residual blood.
3. After washing, remove all PBS and place the hearts in a 60×15 mm culture dish. Trim away the great vessels and atria. Cut the hearts with sterile scissors into small pieces and further mince with a sterile razor blade. Add 5 ml digestion buffer per heart for single heart digestion or 20 ml per four hearts for pooled hearts digestion. Thoroughly homogenate the minced cardiac tissue in digestion buffer by passing through a 2 ml pasteur pipette multiple times. Incubate at 37°C for 30 min and ensure that the tissue is entirely submerged in the digestion buffer. During the 30 min incubation time, pass the tissue homogenate through the pasteur pipette one more time about 15 min into the incubation period in order to disrupt connective tissue.
4. Following 30 min of incubation, stop the enzymatic reaction by diluting the digestion buffer with equal volumes of cold HBSS buffer, and filter through a 70 μm filter. Centrifuge at 530 g for 5 min at 4°C and carefully remove the supernatant. Resuspend the cells in the same HBSS buffer as described previously followed by filtering cells again through a 40 μm filter. Take 10–20 μl of this cell suspension and count the mononucleated cells with a haemocytometer. Note that cell counting is the most crucial step of the entire isolation procedure and one must be sure to not include erythrocytes in the total cell count. Any counting errors that might occur in the cell counting will lead to the incorrect Hoechst dye/total cell number ratio in the subsequent Hoechst staining. We find an average number of 3–5×10^6 cardiomyocyte-depleted mononucleated cells per heart from a ~10-week-old C57Bl/6 mouse.

3.2. Hoechst Incubation

As the Hoechst staining procedure is temperature sensitive, it is of utmost importance to ensure that the water bath is set precisely at 37°C. Temperature fluctuations during incubation should be avoided if possible.

1. Centrifuge the cell suspension at 530 g for 5 min at 4°C and carefully remove the supernatant. Resuspend the cells at 10^6 cardiomyocyte- and erythrocyte-depleted (Notes 1 and 2)

mononucleated cells per ml in prewarmed (37°C) DMEM buffer (DMEM buffer refers to the DMEM media containing FBS and HEPES as described in Subheading 2.2 above) and add Hoechst 33342 to a final concentration of 1 μg/ml (Note 3). Mix the cells and Hoechst dye well and place the tubes in a 37°C water bath protected from light for exactly 90 min. It is important to ensure that the temperature in each tube is maintained precisely at 37°C. During the 90-min incubation time period, gently shake the tubes in order to remix the cell suspension every 15 min.

2. Always prepare a negative control sample by including verapamil (50 μM) during the entire Hoechst staining procedure. Verapamil blocks the ABC-transporter dependent Hoechst dye efflux and thus will serve to distinguish Hoechst retaining cells from SP cells upon FACS analysis. Because this negative control sample determines the threshold of the respective SP gate, it is an essential element of the SP analysis and should be included in each staining protocol.
3. After the 90 min incubation time, stop the reaction by placing the tubes on ice and spin the cells down at 530 g for 5 min at 4°C. Remove the supernatant and resuspend cells in cold HBSS buffer. Wash cells twice with cold HBSS buffer. At this point, samples are ready for FACS analysis or for surface marker staining (for details see the section below) for additional subpopulation selection or analysis. It is important to note that from this point onward all further manipulations should be performed at 4°C (on ice).

3.3. Cell Surface Antigen Staining

After the last washing step (step 3 in the section described above), resuspend cells at 10^6 cells per 100 μl cold HBSS buffer and stain with PE-conjugated rat antimouse antibody reactive to Sca-1 and APC-conjugated rat antimouse antibody reactive to CD31 at a concentration of 1/100. Incubate samples in the dark for 30 min at 4°C. After incubation, wash cells twice in cold HBSS buffer and proceed with FACS analysis. Propidium iodide (PI) (2 μg/ml) or 7-AAD (7-Amino-actinomycin D) (0.25 μg/10^6 cells) is added to each sample prior to FACS analysis to exclude dead cells.

3.4. FACS Analysis

FACS can be performed in any commercially available flow cytometer equipped with ultraviolet (UV) laser with the capacity to excite at 350 nm and to collect emissions at 450 and 650 nm. We have satisfactory experience with several different flow cytometers including MoFlo and FACSAria equipped with triple lasers. The availability of an UV laser to excite the Hoechst dye is a prerequisite for performing Hoechst dye efflux analysis. Hoechst dye is excitable at the wavelength of 350 nm (UV range) and its

dual emission fluorescence is measured at 450–480 nm (Hoechst blue) and 650–680 nm (Hoechst red). A long pass dichroic mirror is used to separate the emission wavelengths. Note that the precise excitation and emission wavelengths may differ slightly depending on the setup of the given instrumentation, though it should fall within the excitation and emission spectrum of Hoechst 33342 dye. It is recommended to consult with an experienced FACS operator and the user manual of each flow cytometer (Note 4).

For those with limited experience in FACS and/or SP cell isolation, it is recommended to perform dose-dependent studies with various concentrations of Hoechst 33342 dye to cell number ratio. This dose-dependent experiment in combination with verapamil will help to determine the optimal concentration of Hoechst dye per given cell number. During the analysis and/or sorting, it is recommended that samples be kept on ice to maintain the quality of the specimen. Moreover, PI or 7-AAD positive cells represent nonviable cells, and should be excluded from the subsequent analysis by proper gating. As showed in Fig. 2, the percentage of Hoechst low or negative cells increases as the Hoechst concentration is lowered (Fig. 2a–c). This phenomenon is due to intrinsic Hoechst efflux abilities of ABC-transporters. When the Hoechst concentration is much lower than the capacity of ABC-transporters, Hoechst low cells or SP profile is artificially increased, whereas, when the Hoechst concentration exceeds the efflux capacity of ABC-transporters, the cells appearing as Hoechst low decrease drastically, leading to an incorrect SP profile. As such, Hoechst dose-dependent studies in combination with verapamil will aid in determining an optimal Hoechst/cell number ratio. Using this method, we find that 1 μg/ml Hoechst is the best concentration (Fig. 2b) to obtain a SP profile that can completely be inhibited by verapamil (Fig. 2e), with a lower or higher Hoechst concentration leading to understaining and overstaining, respectively.

Once the optimal Hoechst concentration has been selected, SP cells may be obtained as described below.

1. Nonviable or dead cells are excluded by displaying PI or 7-AAD (vertical axis) versus forward scatter parameters. Then, the Hoechst Blue versus Red profile is displayed, with Blue on the vertical axis (405 BP filter) and Red (660 LP filter) on the horizontal axis on linear scale. For voltage adjustments, it is important to put detectors in linear mode. Voltages are adjusted in a way that contaminating erythrocytes are located in the lower left corner and the bulk of nonerythrocytes are centered (Fig. 3). Once such a profile is displayed, draw a gate excluding erythrocytes and display the gate in a new window. For cardiac SP analysis, we recommend to collect

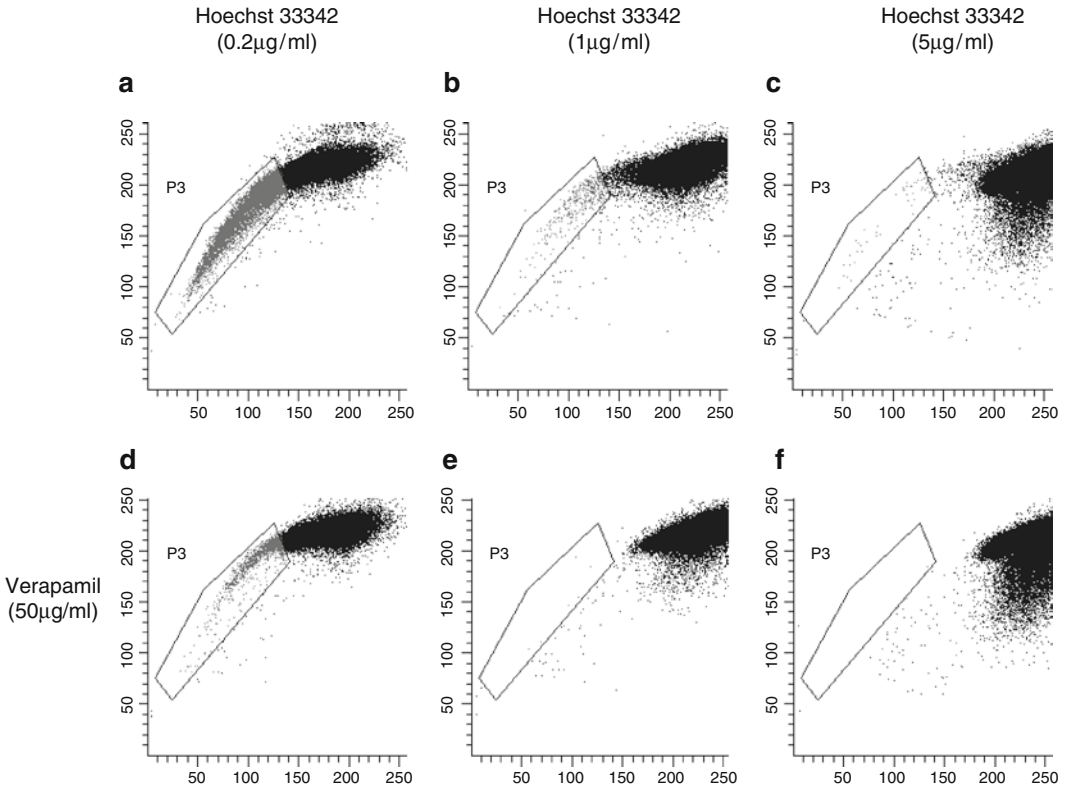

Fig. 2. (**a–e**) Titration of the optimal Hoechst/cell number ratio. Characteristic FACS dot-plot of Hoechst-stained cardiac cells with Hoechst red fluorescence on the horizontal and Hoechst blue fluorescence on the vertical axis. The boxed area depicts the region of Hoechst-low side population (SP) cells. The number of Hoechst-extruding SP cells within the boxed area is directly dependent on the Hoechst-concentration (Hoechst/cell number ratio). An inappropriately low Hoechst/cell number ratio (understaining) leads to an excess in SP cells (**a**) because of nonspecificity as demonstrated by the incomplete inhibition of the SP phenotype after coincubation with the ABC-transporters inhibitor verapamil (**d**). An inappropriately high Hoechst/cell number ratio (overstaining) overwhelms the ability of ABC-transporters and thus, dramatically reduces the percentage of SP cells (**c** + **f**). The optimal Hoechst/cell number ratio provides a robust SP population (**b**) that is entirely inhibited after coincubation with verapamil (**e**).

a minimum of 100,000 events within this gate. With optimal resolution, the cardiac SP profile should appear as shown in Fig. 2b, with SP cells located in the boxed area.

2. Confirm the specificity of the SP profile using the negative control (sample coincubated with verapamil and Hoechst). In this sample, no cells should appear in the boxed area (Fig. 2e).
3. After confirming the right position of the SP gate, sort SP cells in desired media. The SP population can be further purified or analyzed by staining with various surface markers. PE-conjugated rat antimouse antibody reactive to Sca-1 and APC-conjugated rat antimouse antibody reactive to CD31 at a concentration of 1/100 have previously been used by our laboratory.

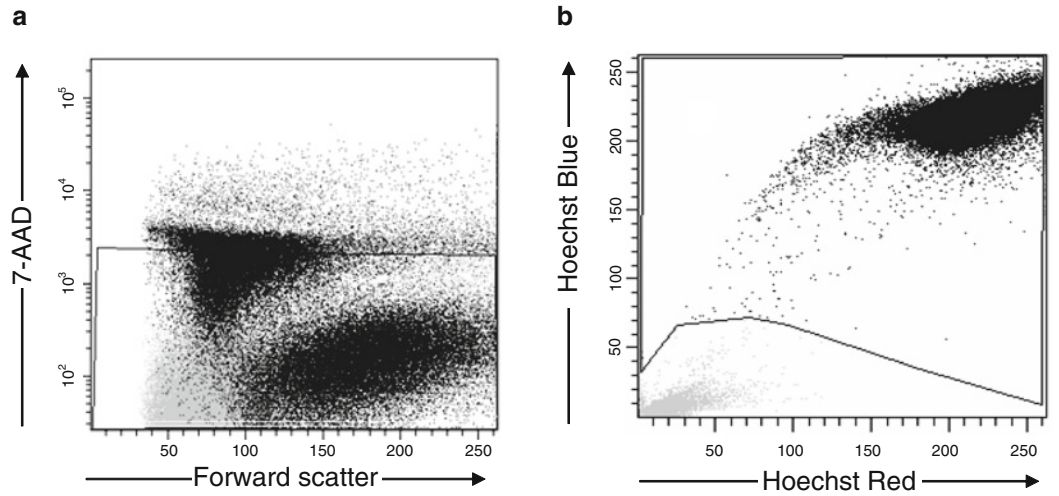

Fig. 3. Separation of Hoechst-stained cardiac cells from nonstained erythrocytes. For separation of Hoechst-stained cardiac cells from Hoechst-negative erythrocytes voltage of FACS detectors should be adjusted in linear mode in a way that contaminating erythrocytes are located in the lower left corner and the bulk of nonerythrocytes (Hoechst-stained cardiac cells) are centered.

Incubate samples in the dark for 30 min at 4°C. FACS analysis is preformed following the incubation and washout. Within the SP gate (boxed area), one can further display the expression of Sca-1 and CD31, alone or in combination, in a new dot plot with APC on the vertical axis and PE on the horizontal axis as shown in Fig. 4.

4. Notes

1. In our hands, the combination of collagenase B and dispase II reliably digests all mature cardiomyocytes, thus the resulting cardiac cell suspension is free from contaminating cardiomyocytes and no additional purification is needed. Other groups have used different digestion protocols, using pronase (2) for tissue digestion followed by a 30–70% Percoll gradient to remove residual cardiomyocytes to obtain cardiomyocyte-free cardiac cell suspensions for cardiac SP cell analysis.
2. Red blood cell lysis buffer or Ficoll gradient can be used to remove excess red blood cells.
3. As cell counting may vary quite a bit among users, 1 μg/ml Hoechst should not be the generalized concentration for everyone. Therefore, it is necessary to perform Hoechst dose-dependent curves in combination with verapamil to

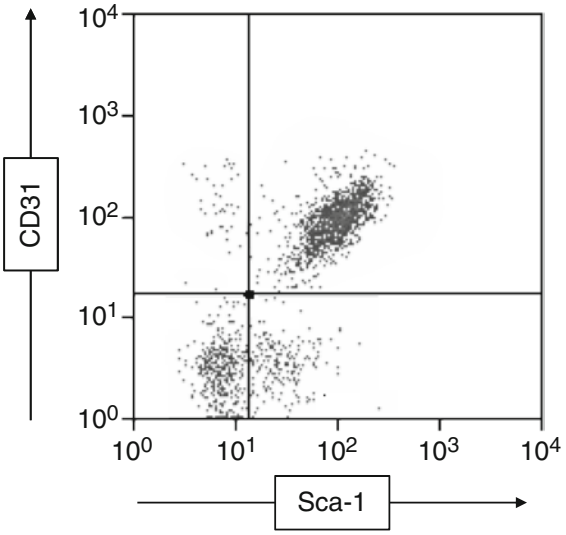

Fig. 4. Further purification by cell surface antigen staining. Subpopulations of cardiac SP cells according to Sca-1/CD31 staining. FACS analysis of cardiac SP cells following Sca-1 and CD31 labeling demonstrating that Sca-1+/CD31+ represent the majority, and Sca-1+/CD31– the minority of total cardiac SP cells.

determine the optimal Hoechst/cell number ratio per ml solution.

4. For the best results, it is recommended to work with low differential pressures and low velocities during FACS analysis.

Acknowledgments

This work was supported by NIH grants HL71775, HL86967, HL73756, HL 88533, and HL93148. The authors would like to thank Mr. Darragh Cullen for technical assistance. Mr. Grigoriy Losyev at BWH Cardiovascular FACS Core is acknowledged for assistance with cell sorting.

References

1. Laugwitz, K. L., Moretti, A., Lam, J., Gruber, P., Chen, Y., Woodard, S., Lin, L. Z., Cai, C. L., Lu, M. M., Reth, M., Platoshyn, O., Yuan, J. X., Evans, S., and Chien, K. R. (2005) Postnatal isl1+ cardioblasts enter fully differentiated cardiomyocyte lineages, *Nature 433*, 647–653.
2. Martin, C. M., Meeson, A. P., Robertson, S. M., Hawke, T. J., Richardson, J. A., Bates, S., Goetsch, S. C., Gallardo, T. D., and Garry, D. J. (2004) Persistent expression of the ATP-binding cassette transporter, Abcg2, identifies cardiac SP cells in the developing and adult heart, *Dev Biol 265*, 262–275.
3. Messina, E., De Angelis, L., Frati, G., Morrone, S., Chimenti, S., Fiordaliso, F., Salio, M., Battaglia, M., Latronico, M. V., Coletta, M., Vivarelli, E., Frati, L., Cossu, G., and Giacomello, A. (2004) Isolation and expansion of adult cardiac stem cells from human and murine heart, *Circ Res 95*, 911–921.
4. Oh, H., Bradfute, S. B., Gallardo, T. D., Nakamura, T., Gaussin, V., Mishina, Y.,

Pocius, J., Michael, L. H., Behringer, R. R., Garry, D. J., Entman, M. L., and Schneider, M. D. (2003) Cardiac progenitor cells from adult myocardium: homing, differentiation, and fusion after infarction, *Proc Natl Acad Sci U S A 100*, 12313–12318.

5. Pfister, O., Mouquet, F., Jain, M., Summer, R., Helmes, M., Fine, A., Colucci, W. S., and Liao, R. (2005) $CD31^-$ but Not $CD31^+$ cardiac side population cells exhibit functional cardiomyogenic differentiation, *Circ Res 97*, 52–61.
6. Beltrami, A. P., Barlucchi, L., Torella, D., Baker, M., Limana, F., Chimenti, S., Kasahara, H., Rota, M., Musso, E., Urbanek, K., Leri, A., Kajstura, J., Nadal-Ginard, B., and Anversa, P. (2003) Adult cardiac stem cells are multipotent and support myocardial regeneration, *Cell 114*, 763–776.
7. Hierlihy, A. M., Seale, P., Lobe, C. G., Rudnicki, M. A., and Megeney, L. A. (2002) The post-natal heart contains a myocardial stem cell population, *FEBS Lett 530*, 239–243.
8. Goodell, M. A., Brose, K., Paradis, G., Conner, A. S., and Mulligan, R. C. (1996) Isolation and functional properties of murine hematopoietic stem cells that are replicating in vivo, *J Exp Med 183*, 1797–1806.
9. Zhou, S., Schuetz, J. D., Bunting, K. D., Colapietro, A. M., Sampath, J., Morris, J. J., Lagutina, I., Grosveld, G. C., Osawa, M., Nakauchi, H., and Sorrentino, B. P. (2001) The ABC transporter Bcrp1/ABCG2 is expressed in a wide variety of stem cells and is a molecular determinant of the side-population phenotype, *Nat Med 7*, 1028–1034.
10. Challen, G. A., and Little, M. H. (2006) A side order of stem cells: the SP phenotype, *Stem Cells 24*, 3–12.
11. Pfister, O., Oikonomopoulos, A., Sereti, K. I., Sohn, R. L., Cullen, D., Fine, G. C., Mouquet, F., Westerman, K., and Liao, R. (2008) Role of the ATP-binding cassette transporter Abcg2 in the phenotype and function of cardiac side population cells, *Circ Res 103*, 825–835.

Circulation Research
JOURNAL OF THE AMERICAN HEART ASSOCIATION

Wnt Signaling Exerts an Antiproliferative Effect on Adult Cardiac Progenitor Cells Through IGFBP3

Angelos Oikonomopoulos, Konstantina-Ioanna Sereti, Frank Conyers, Michael Bauer, Annette Liao, Jian Guan, Dylan Crapps, Jung-Kyu Han, Hanhua Dong, Ahmad F. Bayomy, Gabriel C. Fine, Karen Westerman, Travis L. Biechele, Randall T. Moon, Thomas Force and Ronglih Liao

Circ Res. 2011;109:1363-1374; originally published online October 27, 2011;
doi: 10.1161/CIRCRESAHA.111.250282
Circulation Research is published by the American Heart Association, 7272 Greenville Avenue, Dallas, TX 75231

Print ISSN: 0009-7330. Online ISSN: 1524-4571

Wnt Signaling Exerts an Antiproliferative Effect on Adult Cardiac Progenitor Cells Through IGFBP3

Angelos Oikonomopoulos, Konstantina-Ioanna Sereti, Frank Conyers, Michael Bauer, Annette Liao, Jian Guan, Dylan Crapps, Jung-Kyu Han, Hanhua Dong, Ahmad F. Bayomy, Gabriel C. Fine, Karen Westerman, Travis L. Biechele, Randall T. Moon, Thomas Force, Ronglih Liao

Rationale: **Recent work in animal models and humans has demonstrated the presence of organ-specific progenitor cells required for the regenerative capacity of the adult heart. In response to tissue injury, progenitor cells differentiate into specialized cells, while their numbers are maintained through mechanisms of self-renewal. The molecular cues that dictate the self-renewal of adult progenitor cells in the heart, however, remain unclear.**

Objective: **We investigate the role of canonical Wnt signaling on adult cardiac side population (CSP) cells under physiological and disease conditions.**

Methods and Results: **CSP cells isolated from C57BL/6J mice were used to study the effects of canonical Wnt signaling on their proliferative capacity. The proliferative capacity of CSP cells was also tested after injection of recombinant Wnt3a protein (r-Wnt3a) in the left ventricular free wall. Wnt signaling was found to decrease the proliferation of adult CSP cells, both in vitro and in vivo, through suppression of cell cycle progression. Wnt stimulation exerted its antiproliferative effects through a previously unappreciated activation of insulin-like growth factor binding protein 3 (IGFBP3), which requires intact IGF binding site for its action. Moreover, injection of r-Wnt3a after myocardial infarction in mice showed that Wnt signaling limits CSP cell renewal, blocks endogenous cardiac regeneration and impairs cardiac performance, highlighting the importance of progenitor cells in maintaining tissue function after injury.**

Conclusions: **Our study identifies canonical Wnt signaling and the novel downstream mediator, IGFBP3, as key regulators of adult cardiac progenitor self-renewal in physiological and pathological states. (*Circ Res*. 2011;109:1363-1374.)**

Key Words: cardiac side population cells ■ Wnt signaling ■ cardiac regeneration ■ stem cells ■ proliferation

Accumulating evidence over the past decade in both humans and animal models has documented the presence of endogenous progenitor cells in adult myocardium.[1–6] In response to local tissue injury, cardiac progenitor cells differentiate into specialized cells, while the pool of progenitor cells is maintained, in part, through self-renewal and enhanced proliferation.[7,8] However, the molecular cues and signaling pathways that dictate the homeostasis of adult progenitor cells and in particular their self-renewal, in physiological and pathological states, remain unclear.

Wnt ligands constitute a family of 19 secreted glycoproteins that act as key regulators of cellular function during development, adulthood, and disease.[9,10] Several reports have proposed time and context dependent roles for Wnt signaling in cardiogenesis and progenitor cell biology.[11] Studies in chick and Xenopus embryos have demonstrated that inhibition of Wnt signaling is required for cardiac differentiation,[12,13] whereas Wnt signaling has also been found to promote cardiomyogenesis in Drosophila and embryonic carcinoma P19 cells.[14,15] Moreover, early in gastrulation, Wnt ligands activate a cardiac differentiation program, whereas at later stages they act as potent inhibitors of the cardiomyogenic differentiation.[16,17] Recent genetic studies have demonstrated that the canonical Wnt signaling cascade promotes the

Original received June 15, 2011; revision received October 14, 2011; accepted October 20, 2011. In September 2011, the average time from submission to first decision for all original research papers submitted to *Circulation Research* was 16 days.

From the Cardiovascular Division, the Department of Medicine, Brigham and Women's Hospital, Harvard Medical School, Boston, MA (A.O., K.-I.S., F.C., M.B., A.L., J.G., D.C., J.-K.H., H.D., A.F.B., G.C.F., R.L.); University of Crete Medical School, Heraklion, Greece (A.O., K.-I.S.); Hepatic Surgery Centre, Tongji Hospital, and Huazhong University of Science and Technology, Wuhan, China (H.D.); University of Washington School of Medicine, Seattle, WA (A.F.B., G.C.F.); the Department of Anesthesia, Perioperative and Pain Medicine, Brigham and Women's Hospital, Boston, MA (K.W.); Howard Hughes Medical Institute, the Department of Pharmacology, and Institute for Stem Cell and Regenerative Medicine, University of Washington School of Medicine, Seattle, WA (T.L.B., R.T.M.); and the Center for Translational Medicine and the Cardiology Division, Thomas Jefferson University Hospital, Philadelphia, PA (T.F.).

Correspondence to Ronglih Liao, PhD, Cardiac Muscle Research Laboratory, Cardiovascular Division, Department of Medicine, Brigham and Women's Hospital, Harvard Medical School, 77 Avenue Louis Pasteur, NRB 431, Boston, MA 02115. E-mail rliao@rics.bwh.harvard.edu

Circulation Research **is available at http://circres.ahajournals.org** **DOI: 10.1161/CIRCRESAHA.111.250282**

Non-standard Abbreviations and Acronyms	
CSP	cardiac side population
IGF	insulin growth factor
IGFBP3	insulin growth factor binding protein 3
MI	myocardial infarction
SP	side population

proliferation of neonatal and embryonic Isl-1$^+$ cardiac progenitors in vitro and in vivo.[18–20] Little is known, however, regarding the role of Wnt signals in modulating adult progenitor cell populations.

Side population (SP) cells were initially identified based on their unique ability to efflux the DNA binding dye Hoechst 33342,[21] and were found to retain the long-term regenerative potential of bone marrow. Subsequently, SP cells were identified in various adult tissues/organs including adult myocardium.[22] Cardiac SP (CSP) cells are enriched in Sca1 but do not express c-kit or Isl-1.[6] More importantly, CSP cells are found to be capable of differentiation into functional cardiac myocytes in vitro or in vivo after myocardial infarction (MI).[6,23–25] We demonstrate that in contrast to previous work in embryonic or early postnatal stem cells, Wnt signaling negatively regulates the proliferation of adult CSP progenitor cells, both in vitro and in vivo, through suppression of cell cycle progression. Moreover, Wnt activation exerts its antiproliferative effects through a previously unappreciated activation of IGFBP3, which is found to require intact IGF binding site for its action. Importantly, activation of Wnt signaling was found to limit CSP cell renewal after MI, impair endogenous regenerative capacity, and worsen post-MI structural and functional remodeling. Overall, our study represents the first investigation of the role of canonical Wnt pathway in the homeostasis of adult cardiac progenitor cells in both physiological and pathological states and highlights the importance of cardiac progenitor cells in maintaining tissue function after injury.

Methods

An expanded Methods section describing all procedures and protocols is available in the Online Data Supplement at http://circres.ahajournals.org.

Animals

C57BL/6J male and female mice (8–12 weeks old) were purchased from Jackson Laboratory (Jackson East, MP 15). All animal procedures and handling were performed under the guidelines of Harvard Medical School, the Longwood Medical Area Institutional Animal Care and Use Committee (IACUC), and the National Society for Medical Research. MI was generated in C57BL/6J female mice as previously described.[26] MI size was estimated using histological imaging of three transverse myocardial sections (base, midpapillary, and apex) after staining with Masson trichrome, as previously described.[27]

Intramyocardial Injection of Recombinant Wnt3a or Recombinant IGFBP3

Ten microliters of recombinant Wnt3a (r-Wnt3a, 400 ng) or recombinant IGFBP3 (r-IGFBP3) proteins (1000 ng) (R&D) or vehicle (PBS) was given by intramyocardial injection into 3 sites of the left ventricular free wall of nonsurgically operated female mice (r-Wnt3a) or into the infarct/border zone area of mice immediately after MI (r-Wnt3a or r-IGFBP3).

Heart Fixation and Histology

One day after echocardiographic measurements, animals were euthanized and hearts were fixed at an end-diastolic pressure of 5 mm Hg, using a Langendorff apparatus. For details, see Methods in the Online Data Supplement.

Echocardiography

Echocardiography was performed 1 day before MI and 7 days after MI using a high-resolution, high-frequency digital imaging system (Vevo 2100, VisualSonics), as previously described.[28] For details, see Methods in the Online Data Supplement.

FACS Analysis

FACS was performed using a FACSAria (Becton Dickinson, BD) equipped with 3 lasers (488 nm, 633 nm, 355 nm). Hoechst 33342 dye was excited by an UV (355 nm) laser. Acquired data were analyzed by FACSDIVA software (BD Biosciences).

RNA Isolation and RT-PCR

RNA was extracted from CSP cells using Trizol reagent (Invitrogen) followed by RNeasy Mini Kit (Qiagen). Genomic DNA was removed using Turbo-DNA free kit (Ambion). cDNA was generated using a reverse transcription synthesis kit (Bio-Rad) and RT-PCR was performed in a MyiQ cycler (Bio-Rad). Primer sequences are available on request.

Luciferase Assays

Luciferase activity was measured using a dual luciferase kit (Promega). Cell lysates were prepared from trypsinized CSP cells and used to determine the values of *Firefly* and *Renilla* luciferases, with a 20/20^n Luminometer (Turner Biosystems).

Statistical Analysis

Statistical differences were evaluated using 1-way ANOVA analysis and Student unpaired *t* test, using GraphPad Prism (Version 5.03). Data are presented as mean±SEM. A probability value ≤ 0.05 was considered statistically significant.

Results

Wnt3a Negatively Regulates the Growth Potential of CSP Cells Both In Vitro and In Vivo

Given the context dependency of Wnt signaling, we examined the role of Wnt signals in mediating the proliferative capacity of adult CSP cells. Under unstimulated conditions, application of recombinant SFRP2 (Soluble Frizzled-related Protein 2), a known Wnt antagonist,[29] did not affect the proliferation capacity of CSP cells in vitro, suggesting that Wnt activity in baseline CSP cells in vitro is relatively low (Online Figure I). Treatment of CSP cells with increasing doses of Wnt3a-conditioned medium (Wnt3a-CM) resulted in a gradual activation of the canonical Wnt signaling pathway, as assessed by a T-cell factor-controlled luciferase reporter assay[30] and a respective decrease in CSP cell number, in comparison to vehicle-conditioned medium treated cells (Figure 1A and 1B). A similar decrease in cell proliferation in response to activation of canonical Wnt signaling was also observed in CSP cells treated with recombinant Wnt3a protein (r-Wnt3a) (Figure 1C and 1D). Likewise, BIO ((2′Z, 3′E)-6-

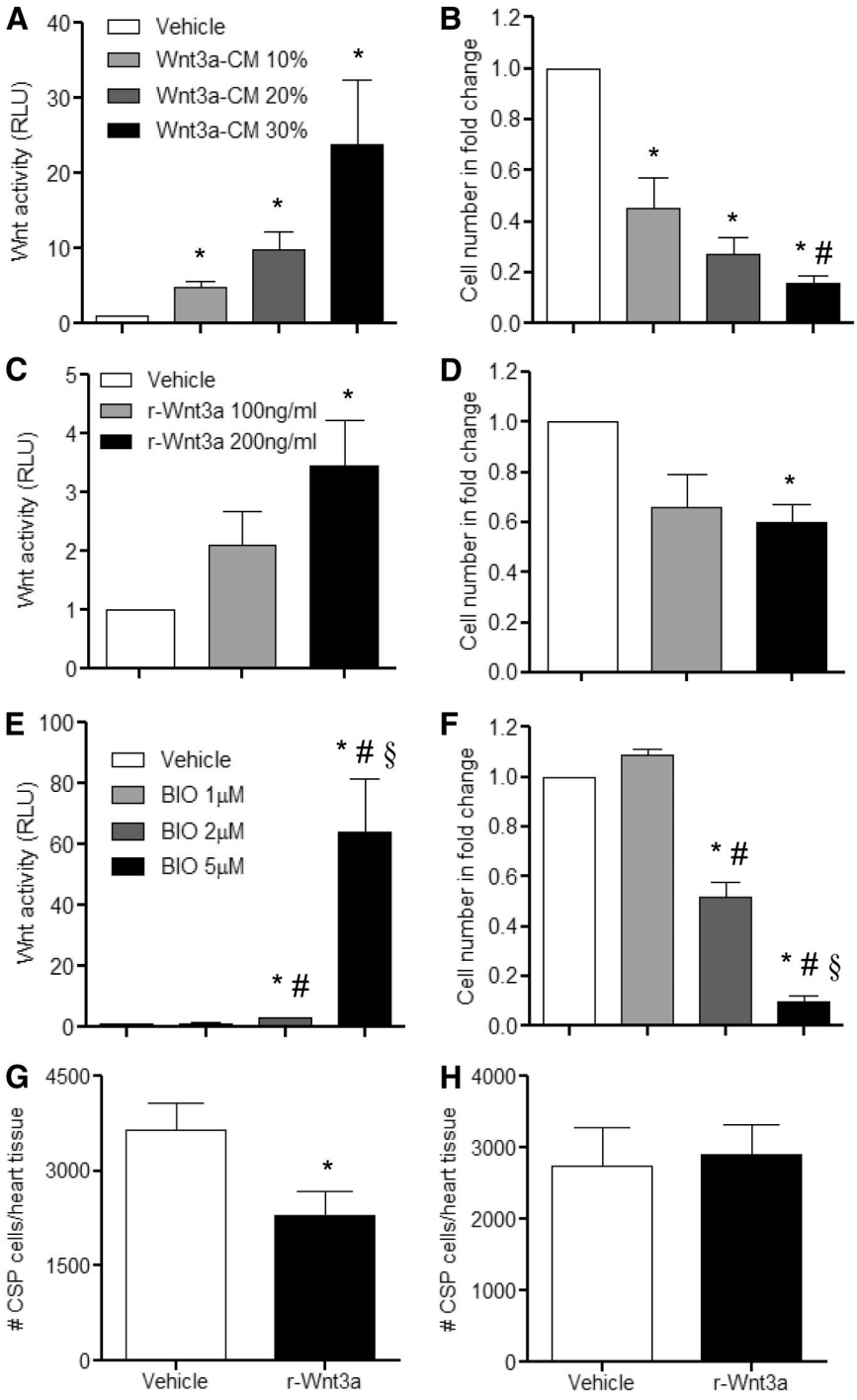

Figure 1. Canonical Wnt signaling pathway mediates antigrowth effects on CSP cells. Treatment of CSP cells with increasing concentrations of **A**, Wnt3a-CM (n=3); **C**, r-Wnt3a (n=3); and **E**, BIO (n=6) activated the canonical Wnt signaling pathway, as measured by the T-cell factor–luciferase reporter assay. Corresponding proliferation assays using the same dosages of **B**, Wnt3a-CM (n=4); **D**, r-Wnt3a (n=4); and **F**, BIO (n=6) revealed decreased growth capacity of CSP cells. T-cell factor–luciferase activity is measured in relative light units (RLU). Analysis of CSP cell number in **G**, the vehicle- or r-Wnt3a-injected areas (left ventricular free wall) (vehicle, n=14; r-Wnt3a, n=16), and in **H**, the remote areas from the injection sites (atria, septum, right ventricle) (vehicle, n=12; r-Wnt3a, n=13). Data are mean±SEM. *$P \leq 0.05$ all samples to respective vehicle, #$P \leq 0.05$, Wnt 10% to Wnt 30%; BIO, 1 μmol/L to BIO 2 μmol/L and BIO 5 μmol/L; §$P \leq 0.05$, BIO 2 μmol/L to BIO 5 μmol/L. Cell number in fold change presented in **B**, **D**, and **F** is normalized to respective vehicle group.

Bromoindirubin-3′-oxime), a GSK-3 inhibitor, caused a comparable decline in CSP cell number with corresponding activation of the Wnt pathway (Figure 1E and 1F). We further examined the antiproliferative effects of Wnt signaling on CSP cells in vivo, with direct intramyocardial injection of r-Wnt3a protein into the LV free wall of normal adult mouse hearts. Injection of r-Wnt3a substantially reduced the number of CSP cells (Figure 1G) in the injected area relative to vehicle, whereas the number of CSP cells remote to the injection site (atria, septum and right ventricle) remained unchanged (Figure 1H).

Wnt3a Directly Alters the Cell Cycle Progression of Adult CSP Cells

To further investigate the antiproliferative effect of canonical Wnt signaling on CSP cells, we examined the effect of Wnt3a on cell cycle progression in CSP cells. Treatment of CSP cells with Wnt3a-CM led to a drastic reduction of cells residing in the cell cycle S phase, as evidenced by decreased BrdU incorporation (Figure 2A through 2C). Moreover, activation of canonical Wnt signaling decreased the fraction of CSP cells residing in the cell cycle M phase, as shown by immunostaining for the phosphorylated form of histone H3

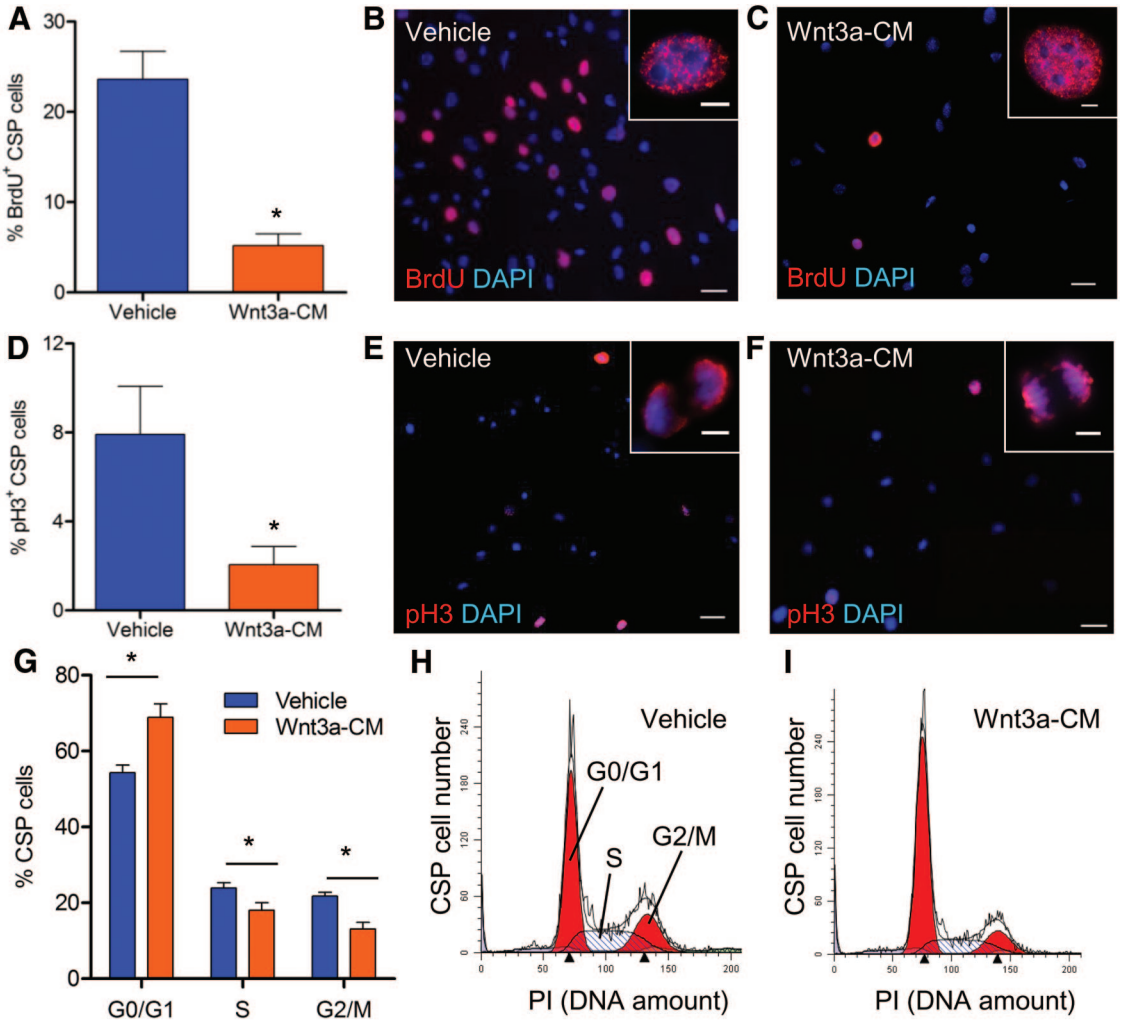

Figure 2. Activation of the canonical Wnt signaling pathway in CSP cells blocks cell cycle progression. Immunocytochemical analysis of **A**, BrdU incorporation (n=5), and **D**, expression of p-H3 (n=4) in CSP cells, after treatment with Wnt3a-conditioned medium (Wnt3a-CM) or vehicle. Representative images of (**B** and **C**) $BrdU^+$ and (**E** and **F**) $p\text{-}H3^+$ CSP cells, in low (scale bars, 50 μm) and high magnification (**inset**, scale bars, 5 μm). **G**, Flow cytometric analysis of CSP cells stained with propidium iodide (PI) (n=4). Representative examples of PI analysis after treatment with vehicle (**H**) or Wnt3a-CM (**I**). Data are mean±SEM. *$P \leq 0.05$.

(p-H3) (Figure 2D through 2F). The altered cell cycle profile in Wnt3a-CM–treated CSP cells was further tested by direct measurement of DNA content with propidium iodide staining. As demonstrated in Figure 2G through 2I, Wnt3a-CM treatment considerably increased the amount of cells residing in G0/G1-cell cycle phases while decreasing the fraction of cells residing in S- and G2/M-cell cycle phases, in comparison to vehicle treated CSP cells.

To further clarify the role of Wnt signaling in the regulation of CSP cell cycle progression, we examined the expression pattern of known cell cycle regulator genes. Consistent with the impaired proliferative capacity, treatment of CSP cells with Wnt3a-CM, in comparison to vehicle, downregulated the expression of several positive cell-cycle regulators including Ki67, PCNA, and Brca2, while upregulating negative cell-cycle regulators such as Gadd45a and p16 (Cdkn2a), within 8 hours (Online Table I). Notably, this gene expression pattern persisted throughout later time points and was accompanied by further downregulation of additional cell cycle regulators, including c-myb, Ccnf, Ccnb1, Cdk4, Mcm3, Mcm2, Cdc25a, Brca1, and Wee1 (Online Table I). These findings suggest that canonical Wnt stimulation impairs the proliferation of adult cardiac progenitor cells potentially through modulation of cell-cycle regulators.

IGFBP3 Is Upregulated in Response to Activated Wnt Signaling in CSP Cells

Using an RT-PCR-based array to monitor several key intracellular signaling pathways, we sought to identify possible mediators for the antiproliferative action of Wnt signaling. Several genes previously identified to be associated with Wnt signaling activation (Wnt2, Tcf7, Lef1) and with cell-cycle regulation (p16) were found to be significantly upregulated in Wnt3a-CM–treated CSP cells in comparison to vehicle-treated cells (Online Figure II, A, and Online Table II). Interestingly, among those genes examined, IGFBP3 exhibited the most robust upregulation with Wnt activation, increasing more than 40-fold (Online Figure II, A). Furthermore, IGFBP3 gene expression was upregulated by Wnt3a-CM in CSP cells in a time-dependent manner (Figure

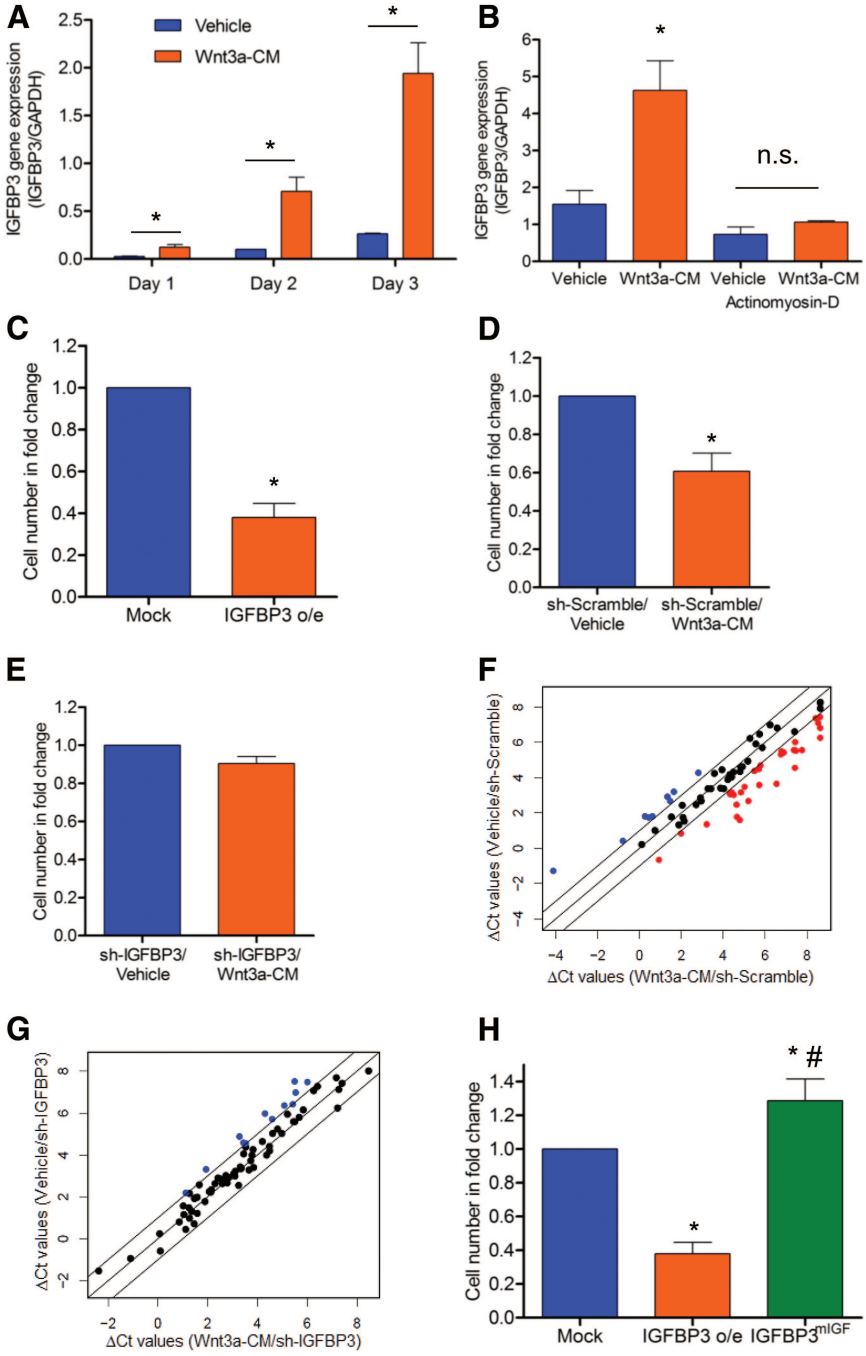

Figure 3. IGFBP3 mediates antiproliferative effects of the Wnt signaling pathway on CSP cells. A, Time course gene expression analysis of IGFBP3 in CSP cells after treatment with vehicle or Wnt3a-CM (n=3). **B**, IGFBP3 gene expression analysis in CSP cells after pretreatment with Actinomyosin-D (30 minutes) and subsequent application of vehicle or Wnt3a-CM (24 hours) (n=3). **C**, Proliferation assay of mock and IGFBP3 (IGFBP3 o/e)-infected CSP cells (n=5). Proliferation assay of sh-Scramble (**D**) and sh-IGFBP3-infected (**E**) CSP cells (n=4) after treatment with vehicle or Wnt3a-CM. Scatterplot analysis of the ΔCt values of cell cycle–related genes, in sh-Scramble (**F**) and sh-IGFBP3-infected (**G**) CSP cells, after treatment with vehicle or Wnt3a-CM for 5 days. Outer diagonal lines indicate 2-fold changes. **Black**, **blue**, **and red circles** represent unchanged, upregulated, and downregulated genes after Wnt activation, respectively. **H**, Proliferation assay of mock, IGFBP3 o/e, and IGFBP3^{mIGF}-infected CSP cells (n=3). Data are mean±SEM. *P≤0.05 to respective vehicle or mock, #P≤0.05 IGFBP3^{mIGF} to IGFBP3 o/e. Cell number in fold change presented in **B**, **C**, **D**, and **G** was normalized to respective vehicle or mock.

3A). Consistent to the increased gene expression, IGFBP3 protein levels were found increased in CSP cells treated with Wnt3a-CM (Online Figure II, B). To examine whether increased IGFBP3 was derived from de novo transcription, stabilization of IGFBP3 mRNA, or by alternative mechanisms, CSP cells were treated with actinomyosin-D, an inhibitor of de novo transcription. Actinomyosin-D abolished Wnt-mediated upregulation of IGFBP3, suggesting that the IGFBP3 induction after Wnt3a treatment was mediated predominantly by transcriptional mechanisms (Figure 3B). These experiments identify IGFBP3 as a potential mediator of Wnt3a signaling in adult cardiac progenitor cells.

IGFBP3 Is Sufficient to Inhibit the Proliferative Capacity of CSP Cells

To test whether the expression of IGFBP3 was sufficient to mimic the antiproliferative effects of Wnt3a, we constructed a lentiviral-vector overexpressing IGFBP3 (IGFBP3 o/e) in CSP cells (Online Figure III). We found that the proliferative capacity of CSP cells overexpressing IGFBP3 was markedly decreased (Figure 3C). Consistent with this observation, overexpression of IGFBP3 resulted in a cell cycle gene expression pattern similar to that of canonical Wnt signaling, with approximately 80% of examined genes (66 genes of a total of 84 genes tested) similarly regulated in both experi-

mental conditions (Online Table III). Overall, our data suggest that IGFBP3 acts as a mediator of Wnt signaling that is sufficient to recapitulate the phenotypic response to Wnt activation in CSP cells.

IGFBP3 Is Required for Wnt3a-Mediated Antiproliferative Effects in CSP Cells

To determine whether IGFBP3 is required for the antiproliferative effects of Wnt3a, we decreased IGFBP3 protein expression in CSP cells by using lentiviral-mediated expression of a shRNA targeting IGFBP3 (sh-IGFBP3) (Online Figure IV) before Wnt activation. Scramble-infected (sh-Scramble) CSP cells treated with Wnt3a-CM exhibited decreased proliferation (Figure 3D), similar to uninfected cells. In contrast, silencing of IGFBP3 prevented Wnt-mediated inhibition of CSP cell proliferation (Figure 3E). To further investigate the role of IGFBP3 in mediating the antiproliferative effects of Wnt signaling at the gene level, we compared the expression profile of cell cycle-related genes in sh-Scramble and sh-IGFBP3 CSP cells after treatment with vehicle or Wnt3a-CM. In sh-Scramble CSP cells, 40 of the 75 (53%) expressed cell-cycle related genes were altered (upregulated or downregulated) by more than 2-fold after treatment with Wnt3a-CM (Figure 3F and Online Table IV), including upregulation of cell-cycle inhibitors (Cdkn2a and Cdkn1a) and downregulation of positive mediators of cell-cycle progression (Ccna2, Ccnb1, E2f3, Ki67, PCNA, Mcm2, Mcm3, Mcm4, and Wee1). In sh-IGFBP3 CSP cells, only 12 of the 75 examined cell cycle regulators (16%) were altered by more than 2-fold after treatment with Wnt3a-CM (Figure 3G and Online Table IV). In sh-IGFBP3–infected CSP cells, Wnt signaling did not result in altered expression of negative cell-cycle regulators and even upregulated the expression of several positive regulators (Ccna2, Ccnb1, Wee1). Overall, our data suggest that silencing of IGFBP3 results in normalization of cell cycle gene expression in response to Wnt signaling activation and that IGFBP3 is necessary for the antiproliferative effects of Wnt3a activation in adult CSP cells.

Integrity of IGF-Binding Site Is Required for the Antiproliferative Effect of IGFBP3 on CSP Cells

IGFBP3 is an abundant circulating IGF-binding protein and acts as a modulator of cell survival, cell proliferation, and cell metabolism through IGF-dependent or IGF-independent mechanisms.[31] IGFBP3 is known to bind IGFs both in vitro and in vivo.[31] IGF-1 is a potent stimulant of several cell types including adult cardiac stem cells.[32] We found that IGF-1 stimulates CSP cell proliferation in vitro (Online Figure V, A). However, the expression of IGF-1 receptors did not change after Wnt3a treatment (Online Figure V, B and C). To determine whether IGF binding to IGFBP3 is required for the antiproliferative effect of IGFBP3, we overexpressed wild-type IGFBP3 or mutated IGFBP3 with loss of the IGF binding site ($IGFBP3^{mIGF}$) in CSP cells.[33] Overexpression of wild-type IGFBP3 decreased cell proliferation, whereas overexpression of $IGFBP3^{mIGF}$ increased cell division (Figure 3H), suggesting that the IGF binding site is critical for the antiproliferative function of IGFBP3 in CSP cells.

Administration of r-Wnt3a Protein After MI Diminishes the Pool of Endogenous Cardiac Progenitors

After cardiac injury, CSP cell pools are acutely depleted and later renewed, in part, through enhanced proliferation of local CSP cells.[26] Given the context and cell-type dependency of Wnt activation in response to cardiac injury, we measured Wnt-related genes in CSP cells isolated from the myocardium 1, 3, and 7 days after coronary ligation. Using a Wnt pathway focused gene array, we established that Wnt-related genes were downregulated in CSP cells early after MI and continued to decline over 7 days. Conversely, a corresponding increase in Wnt pathway inhibitor genes was detected (Figure 4A through 4C and Online Tables V through VIII). During this early post-MI period, CSP proliferation increased, as shown by BrdU labeling (Figure 4D). To determine whether activation of Wnt signaling may inhibit the growth capacity of CSP cells after tissue injury, r-Wnt3a was injected into the infarct and border zone of mouse hearts after MI. Injection of r-Wnt3a after MI upregulated Wnt target genes, including Ccnd1, Tcf7, Lef-1, and Wnt3a (Figure 5A), confirming the activation of canonical Wnt in vivo. Administration of r-Wnt3a resulted in a significant reduction in CSP cell number in the region of injection (Figure 5B) but did not alter CSP cell number in areas remote to the injection site (atria, right ventricle and septum) relative to vehicle treated animals (Figure 5C). To further determine whether the Wnt-mediated decrease in CSP pools alters myocardial regeneration after MI, we determined the formation of new cardiomyocytes by pulsing BrdU, a thymidine analog, through Alzet mini-osmotic pumps for a period of 1 week. BrdU-positive cardiomyocytes were found to reside primarily in the infarct and border zone areas of the injured myocardium (Figure 6A) and were significantly decreased after r-Wnt3a administration compared with vehicle injected counterparts (Figure 6B), suggesting an impairment in new cardiomyocyte generation. Notably, the majority of BrdU-positive cardiomyocytes were smaller in size in both r-Wnt3a and vehicle-injected hearts as compared with nondividing, BrdU-negative cardiomyocytes (Figure 6C). A representative cluster of BrdU-positive cardiomyocytes located in the infarct/border zone area is presented in Online Figure VI. Our data show that activation of Wnt signaling pathway diminishes the endogenous repair mechanisms of the heart after MI.

Administration of Wnt or IGFBP3 Adversely Affects Post-MI Cardiac Remodeling

We further determined whether diminished CSP pools and myocardial regeneration after MI influence the development of adverse cardiac remodeling. One week after MI, heart weight/body weight (Figure 7A) and infarct size (Figure 7B) were significantly increased with r-Wnt3a injection. Moreover, injection of r-Wnt3a protein and impaired myocardial regeneration were associated with decreased intraventricular septal wall thickness, increased left ventricular chamber dimension, and impaired cardiac performance, marked by reduced ratio of fractional shortening and fractional area change, compared with vehicle-injected mice (Figure 7C through 7F). Taken together, our data suggest that activation

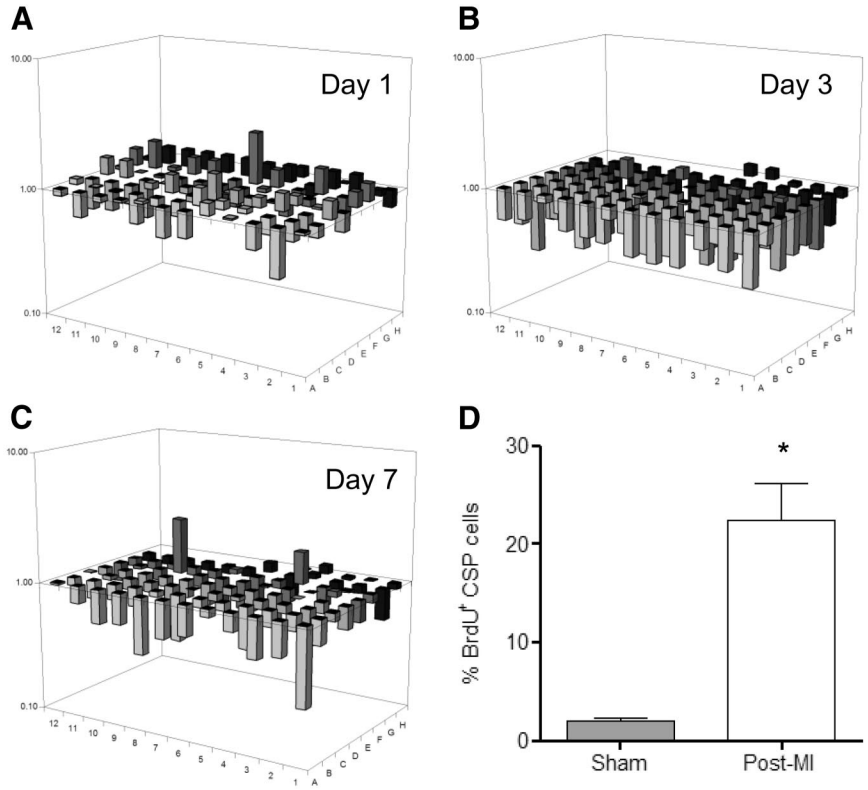

Figure 4. Wnt signaling pathway expression profile in CSP cells after MI. Three-dimensional diagrams show expression profile of Wnt signaling-related genes in CSP cells at 1 day after MI (**A**), 3 days after MI (**B**), and 7 days after MI (**C**) (n=3). The gene corresponding to each bar can be found in Online Table VIII. The position (well) A1 in (**A** through **C**) is located in the bottom right corner of each diagram. **D**, Analysis of CSP cell proliferation (BrdU incorporation assay) at 4 days after MI (n=3). Data are mean±SEM. *$P \leq 0.05$.

of Wnt signaling worsens the post-MI structural and functional remodeling. Similarly, administration of r-IGFBP3 into the infarct/border zone area acutely after coronary artery occlusion resulted in a decrease in intraventricular septal thickness and an increase in left ventricular chamber dimension, as well as a corresponding reduction in LV fractional shortening and fractional area change (Figure 8A through 8D). Collectively, these data suggest that IGFBP3 mimics the

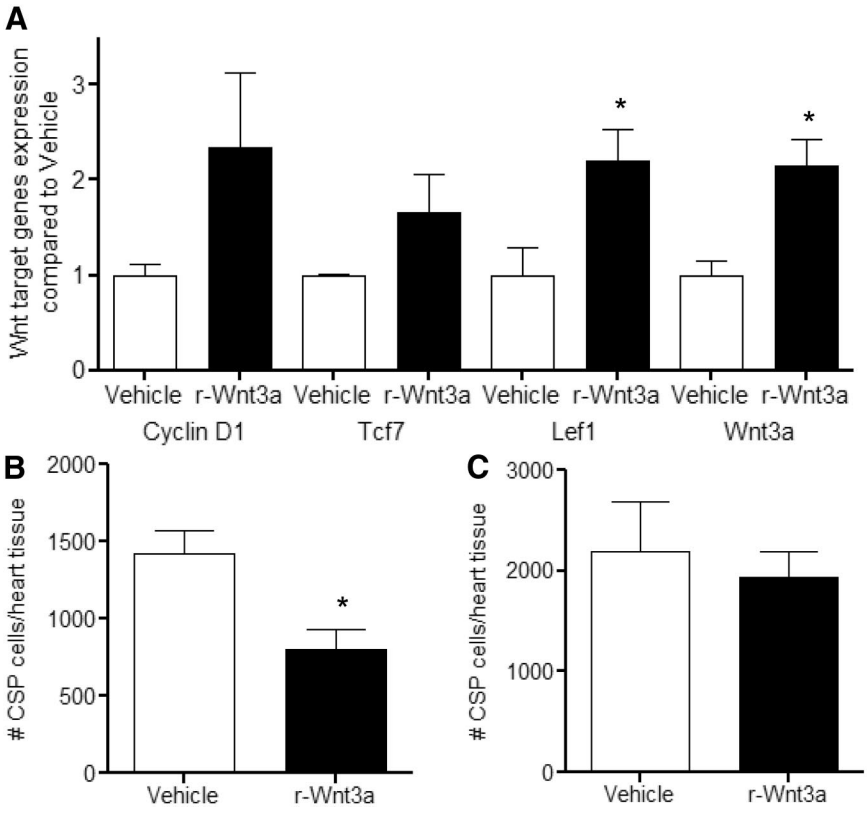

Figure 5. Administration of r-Wnt3a protein decreases the amount of CSP cells after MI. A, Gene expression analysis of Wnt target genes (Cyclin-D1, Tcf7, Lef1, and Wnt3a) in the infarct/border zone area (injection site) after intramyocardial injection of r-Wnt3a protein (n=3). Analysis of CSP cell number 3 days after MI, in **B**, the infarct/border zone area (injection site), and **C**, the remote areas (atria, septum, right ventricle) of vehicle-injected or r-Wnt3a–injected hearts (vehicle, n=10, and r-Wnt3a, n=9). Data are mean±SEM. *$P \leq 0.05$.

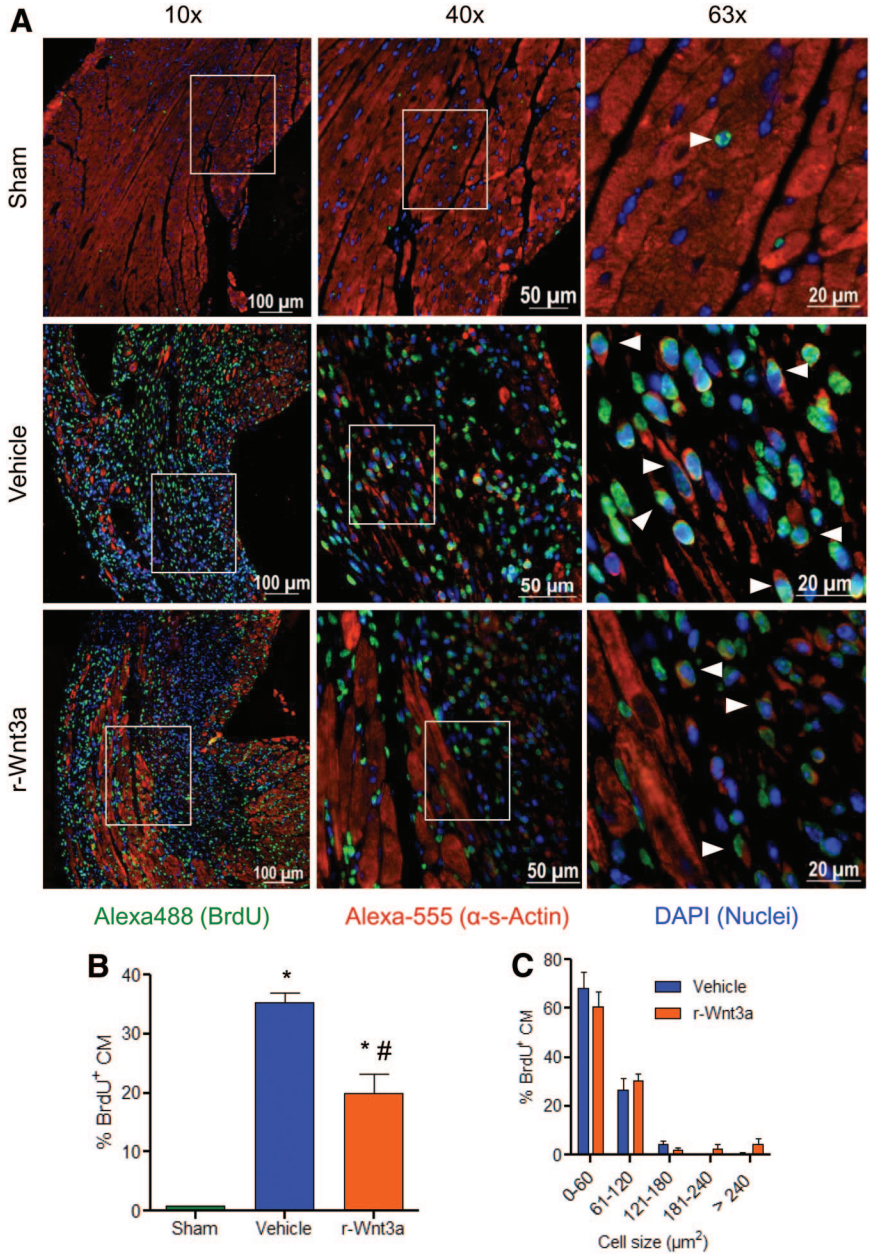

Figure 6. Injection of r-Wnt3a after MI inhibits the formation of new cardiomyocytes (CM). A, Representative fluorescent microscope images of BrdU$^+$ CM located in the infarct/border zone area 1 week after MI, presented in low (10×), medium (40×), and high (63×) magnification power. **White arrowheads**, shown in 63× magnification, indicate BrdU$^+$ CM. **B**, Quantification of BrdU incorporation in CM at 1 week after MI in sham (n=3), vehicle-injected (n=5), and r-Wnt3a–injected (n=4) hearts. **C**, Cell size distribution frequency of BrdU$^+$ CM in the infarct/border zone area of vehicle (n=3) and r-Wnt3a–injected (n=4) animals. Data are mean±SEM. *P≤0.05, all samples to sham; #P≤0.05, r-Wnt3a to vehicle.

effects of r-Wnt3a on cardiac function in the presence of ischemic myocardial injury.

Discussion

Detailed knowledge of the molecular cues that regulate progenitor cell fate decisions in physiological and pathological states is of the utmost importance for achieving the overarching goal of therapeutic cardiac regeneration. Wnt signaling is a pivotal factor in the regulation of organogenesis from embryonic development to aging, as well as in various disease conditions.[9,10] Although Wnt signaling is undoubtedly established to be critical for cardiogenesis during cardiac development,[11] its role in adult cardiac progenitor cells and post-MI remodeling remains poorly understood. In this study, we define the role of canonical Wnt signaling in regulating the function of adult cardiac progenitor cells in vitro and in vivo. Furthermore, we identify a previously unknown link between canonical Wnt signaling and IGFBP3 and demonstrate an important role for IGFBP3 in mediating Wnt signaling effects in adult cardiac progenitor cells. Last, our study emphasizes the functional significance of adult cardiac progenitor cells in tissue regeneration after cardiac injury such as MI.

The antiproliferative effects of Wnt signaling on CSP cells appear to be mediated through its negative effects on the cell cycle progression. Activation of Wnt signaling leads to accumulation of CSP cells in the early nonproliferating G0/G1 cell-cycle phases, while altering substantially the expression profile of various cell cycle regulators. In contrast, prior reports suggest that Wnt signaling potentiates the expansion of embryonic and neonatal Isl-1$^+$ cardiac progenitor cells.[18–20] The distinct response of CSP cells to Wnt

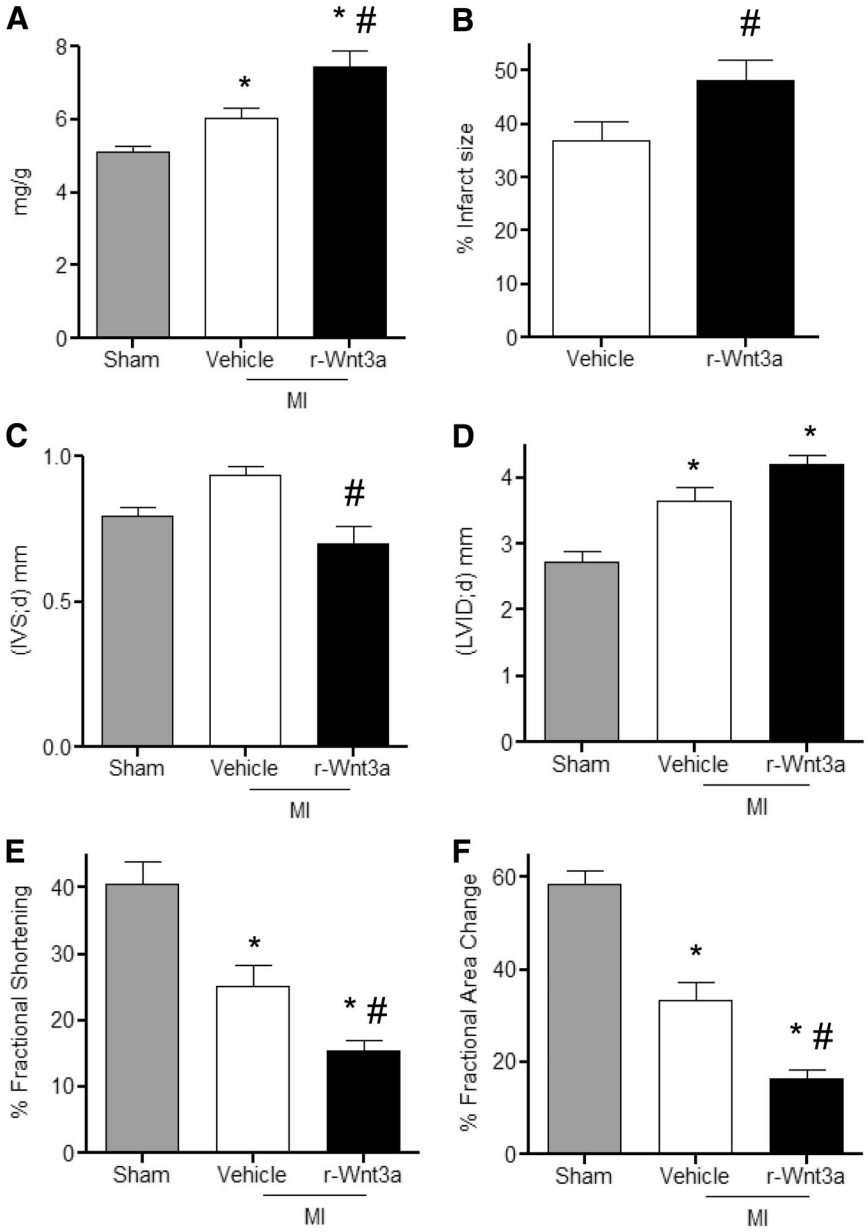

Figure 7. Administration of r-Wnt3a after MI leads to impaired cardiac performance. **A**, Quantification of heart weight–to–body weight ratios in sham (n=8), vehicle-injected (n=12), and r-Wnt3a–injected animals (n=12). **B**, Measurement of infarct size in vehicle and r-Wnt3a–injected hearts (n=8). Echocardiographic assessment of **C**, intraventricular septal thickness in diastole (IVS;d); **D**, left ventricular internal dimension in diastole (LVID;d); **E**, fractional shortening; and **F**, fractional area change (sham, n=7; vehicle, n=9; r-Wnt3a, n=10). All measurements were performed at 1 week after MI. Data are mean±SEM. *$P \leq 0.05$, all samples to sham; #$P \leq 0.05$, r-Wnt3a to vehicle.

signals in adult versus embryonic progenitor cells probably is due to intrinsic differences of each cell type and to the highly time and context dependent nature of Wnt signaling.[11,17] The milieu-dependent role of Wnt signaling is also supported by recent evidence in the cancer biology field. Although Wnt signaling is associated with oncogenic transformation, it has recently been suggested that activation of Wnt signaling may decrease proliferation in melanoma cancerous cells.[34]

Further, we demonstrated that IGFBP3 is transcriptionally upregulated by Wnt signaling and that it is the critical determinant of the antiproliferative effects of Wnt on CSP cells. Importantly, this phenomenon depends on a functional IGF binding site in IGFBP3. Analysis of the IGFBP3 gene promoter sequence has revealed a number of conserved transcriptional factor binding sites for factors such as REPIN1, MYOD1, and NFATC.[35–37] ChIP-chip and ChIP-seq experiments have recognized a number of other transcriptional factors that may bind to the promoter region of IGFBP3.[38] Recent reports suggest IGFBP5 is a potential target of Wnt-mediated transcriptional activity.[39,40] Among the members of the IGFBP family, IGFBP3 has a high structural and functional resemblance to IGFBP5,[41,42] raising the possibility that IGFBP3 is upregulated in CSP cells through a direct Wnt-mediated transcriptional mechanism.

The role of IGFBP proteins in the adult myocardium is largely unknown. The insulin-like growth factor axis (ratio of IGF-1 to IGFBP3) has been introduced as a predictor of clinical outcomes in heart failure patients.[43] Moreover, mice overexpressing IGFBP3 exhibited cardiac organomegaly.[44] More recently, a direct link between cardiomyogenesis, IGFBP proteins, and Wnt signaling was identified.[45] IGFBP4 increases the cardiomyogenic differentiation of P19CL6 cells and embryonic stem cells through inhibition of canonical Wnt.[45] However, IGFBP4 activates Wnt/β-catenin transcrip-

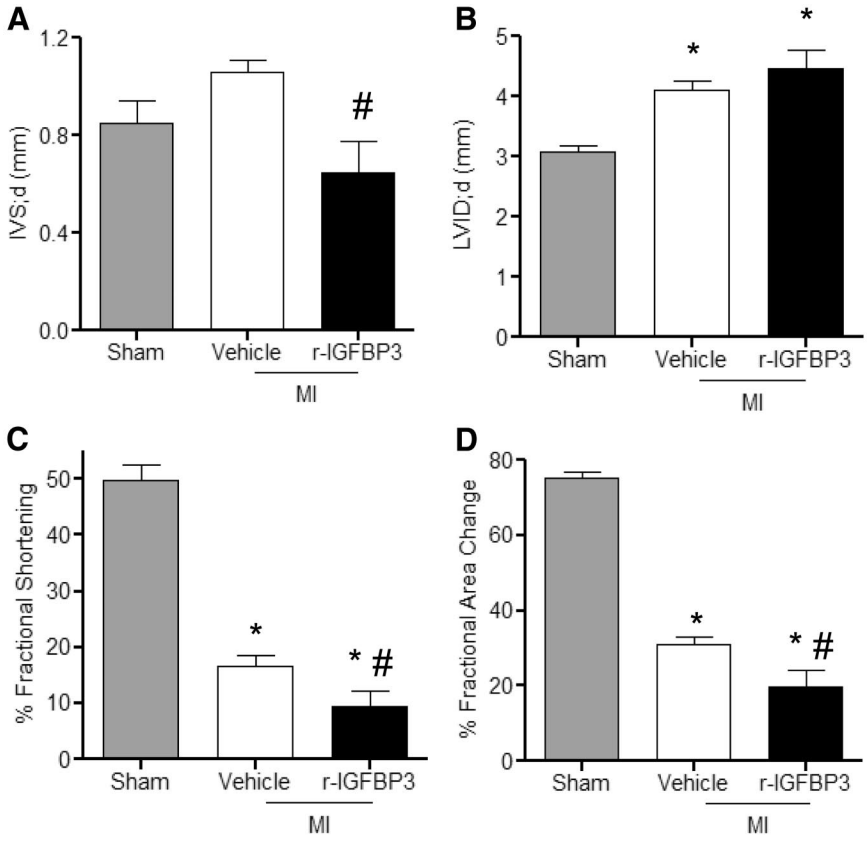

Figure 8. Administration of r-IGFBP3 after MI compromises cardiac function. Echocardiographic assessment of **A**, intraventricular septal thickness in diastole (IVS;d); **B**, left ventricular internal dimension in diastole (LVID;d); **C**, fractional shortening; and **D**, fractional area change (sham, n=3; vehicle, n=6; r-IGFBP3, n=6). All measurements were performed at 1 week after MI. Data are mean±SEM. *$P \leq 0.05$, all samples to sham; #$P \leq 0.05$, r-IGFBP3 to vehicle.

tional activity in a renal cancer cell line.[46] Thus, a context-dependent and cell type–dependent specificity may define the interaction between IGFBP proteins and Wnt.

Activation of Wnt signaling decreases resident cardiac progenitor cell renewal and negatively affects the myocardial response to infarction. SFRP1 and SFRP2, 2 well-documented Wnt signaling inhibitors, exert a potent cardioprotective effect after ischemic myocardial injury.[47–50] Similarly, depletion of β-catenin attenuates post-MI cardiac remodeling and improves animal survival by stimulating the resident cardiac stem cell pool.[51] Wnt signaling has been reported to be enhanced within the infarct-border zone, but Wnt activation was limited to endothelial cells, smooth muscle cells, $CD31^+/Sca1^+$ cells, $c\text{-}kit^+/CD45^+$ cells, and fibroblasts.[52,53] Results from the current study, however, indicate that Wnt pathway genes were decreased in CSP cells isolated from the infarcted heart, whereas Wnt inhibitors, such as SFRP2, increased. Consistent with this observation, we found that CSP cell proliferation was enhanced early after MI. Conversely, activation of Wnt signaling in CSP cells through the delivery of recombinant Wnt protein decreased the number of CSP cells. On the basis of in vitro data, it is reasonable to speculate that downregulation of Wnt signaling in CSP cells may promote the proliferation of CSP cells after cardiac injury. In addition to the effects on cardiac progenitor cells, r-Wnt3a may influence other cell types, including cardiomyocytes. Indeed, we found that r-Wnt3a leads to an increase in cardiomyocyte death (Online Figure VII, A), but no change is observed in cell death when all cardiac cells are considered (Online Figure VII, B). Importantly, recombinant Wnt3a results in an increase in heart weight–to–body weight ratio, although cardiomyocyte cross-sectional area remains unchanged. These results do not exclude an increase in myocyte length, which may contribute to the expansion in cavitary volume (Online Figure VIII). Although we cannot exclude that Wnt affects other cell types, our findings point to a potential interaction between impaired progenitor cell function and negative outcome after MI. Importantly, future research is necessary to determine those cell types which underlie the in vivo effects of recombinant Wnt administration and whether targeting Wnt may be a viable therapeutic option.

In summary, our work reveals a novel role of Wnt signaling pathway in adult cardiac progenitor cells and shows that canonical Wnt ligands compromise the self-renewal properties of CSP cells in vitro and in vivo. This phenomenon, in turn, may lead to impaired cardiac recovery after ischemic injury. Furthermore, we have identified a previously unrecognized link between Wnt signaling and IGFBP3, which together regulate cardiac progenitor cell function. Canonical Wnt contributes to negative left ventricular remodeling by interfering with the endogenous myocardial regeneration. Understanding the molecular signals that modulate tissue homeostasis and repair is important for the design of novel therapeutic strategies for the failing heart.

Acknowledgments

We thank G. Losyev at the Cardiovascular FACS Core for assistance with SP cells sorting, S. Ngoy at the Cardiovascular Physiology Core for mouse surgery, and C. Mbah for assistance with echocardiogra-

phy measurements. We also thank B. Jiang and members of Liao laboratory for discussion.

Sources of Funding

This study was supported in part by NIH grants (HL086967, HL093148, and HL099173) to R.L. and American Heart Association fellowship awards to A.O. (predoctoral) and J.-K.H. and M.B. (postdoctoral). G.F. and A.F.B. are supported by the Sarnoff Cardiovascular Research Foundation.

Disclosures

None.

References

1. Beltrami AP, Barlucchi L, Torella D, Baker M, Limana F, Chimenti S, Kasahara H, Rota M, Musso E, Urbanek K, Leri A, Kajstura J, Nadal-Ginard B, Anversa P. Adult cardiac stem cells are multipotent and support myocardial regeneration. *Cell*. 2003;114:763–776.
2. Laugwitz KL, Moretti A, Lam J, Gruber P, Chen Y, Woodard S, Lin LZ, Cai CL, Lu MM, Reth M, Platoshyn O, Yuan JX, Evans S, Chien KR. Postnatal isl1+ cardioblasts enter fully differentiated cardiomyocyte lineages. *Nature*. 2005;433:647–653.
3. Messina E, De Angelis L, Frati G, Morrone S, Chimenti S, Fiordaliso F, Salio M, Battaglia M, Latronico MV, Coletta M, Vivarelli E, Frati L, Cossu G, Giacomello A. Isolation and expansion of adult cardiac stem cells from human and murine heart. *Circ Res*. 2004;95:911–921.
4. Oh H, Bradfute SB, Gallardo TD, Nakamura T, Gaussin V, Mishina Y, Pocius J, Michael LH, Behringer RR, Garry DJ, Entman ML, Schneider MD. Cardiac progenitor cells from adult myocardium: homing, differentiation, and fusion after infarction. *Proc Natl Acad Sci U S A*. 2003;100:12313–12318.
5. Bearzi C, Rota M, Hosoda T, Tillmanns J, Nascimbene A, De Angelis A, Yasuzawa-Amano S, Trofimova I, Siggins RW, Lecapitaine N, Cascapera S, Beltrami AP, D'Alessandro DA, Zias E, Quaini F, Urbanek K, Michler RE, Bolli R, Kajstura J, Leri A, Anversa P. Human cardiac stem cells. *Proc Natl Acad Sci U S A*. 2007;104:14068–14073.
6. Pfister O, Mouquet F, Jain M, Summer R, Helmes M, Fine A, Colucci WS, Liao R. Cd31- but not cd31+ cardiac side population cells exhibit functional cardiomyogenic differentiation. *Circ Res*. 2005;97:52–61.
7. Bergmann O, Bhardwaj RD, Bernard S, Zdunek S, Barnabe-Heider F, Walsh S, Zupicich J, Alkass K, Buchholz BA, Druid H, Jovinge S, Frisen J. Evidence for cardiomyocyte renewal in humans. *Science*. 2009;324:98–102.
8. Hsieh PC, Segers VF, Davis ME, MacGillivray C, Gannon J, Molkentin JD, Robbins J, Lee RT. Evidence from a genetic fate-mapping study that stem cells refresh adult mammalian cardiomyocytes after injury. *Nat Med*. 2007;13:970–974.
9. Chien AJ, Conrad WH, Moon RT. A Wnt survival guide: from flies to human disease. *J Invest Dermatol*. 2009;129:1614–1627.
10. Cohen ED, Tian Y, Morrisey EE. Wnt signaling: an essential regulator of cardiovascular differentiation, morphogenesis and progenitor self-renewal. *Development*. 2008;135:789–798.
11. Gessert S, Kuhl M. The multiple phases and faces of Wnt signaling during cardiac differentiation and development. *Circ Res*. 2010;107:186–199.
12. Marvin MJ, Di Rocco G, Gardiner A, Bush SM, Lassar AB. Inhibition of Wnt activity induces heart formation from posterior mesoderm. *Genes Dev*. 2001;15:316–327.
13. Schneider VA, Mercola M. Wnt antagonism initiates cardiogenesis in xenopus laevis. *Genes Dev*. 2001;15:304–315.
14. Nakamura T, Sano M, Songyang Z, Schneider MD. A Wnt- and beta-catenin-dependent pathway for mammalian cardiac myogenesis. *Proc Natl Acad Sci U S A*. 2003;100:5834–5839.
15. Wu X, Golden K, Bodmer R. Heart development in drosophila requires the segment polarity gene wingless. *Dev Biol*. 1995;169:619–628.
16. Naito AT, Shiojima I, Akazawa H, Hidaka K, Morisaki T, Kikuchi A, Komuro I. Developmental stage-specific biphasic roles of Wnt/beta-catenin signaling in cardiomyogenesis and hematopoiesis. *Proc Natl Acad Sci U S A*. 2006;103:19812–19817.
17. Ueno S, Weidinger G, Osugi T, Kohn AD, Golob JL, Pabon L, Reinecke H, Moon RT, Murry CE. Biphasic role for Wnt/beta-catenin signaling in cardiac specification in zebrafish and embryonic stem cells. *Proc Natl Acad Sci U S A*. 2007;104:9685–9690.
18. Cohen ED, Wang Z, Lepore JJ, Lu MM, Taketo MM, Epstein DJ, Morrisey EE. Wnt/beta-catenin signaling promotes expansion of isl-1-positive cardiac progenitor cells through regulation of FGF signaling. *J Clin Invest*. 2007;117:1794–1804.
19. Qyang Y, Martin-Puig S, Chiravuri M, Chen S, Xu H, Bu L, Jiang X, Lin L, Granger A, Moretti A, Caron L, Wu X, Clarke J, Taketo MM, Laugwitz KL, Moon RT, Gruber P, Evans SM, Ding S, Chien KR. The renewal and differentiation of isl1+ cardiovascular progenitors are controlled by a Wnt/beta-catenin pathway. *Cell Stem Cell*. 2007;1:165–179.
20. Bu L, Jiang X, Martin-Puig S, Caron L, Zhu S, Shao Y, Roberts DJ, Huang PL, Domian IJ, Chien KR. Human isl1 heart progenitors generate diverse multipotent cardiovascular cell lineages. *Nature*. 2009;460:113–117.
21. Goodell MA, Brose K, Paradis G, Conner AS, Mulligan RC. Isolation and functional properties of murine hematopoietic stem cells that are replicating in vivo. *J Exp Med*. 1996;183:1797–1806.
22. Challen GA, Little MH. A side order of stem cells: the sp phenotype. *Stem Cells*. 2006;24:3–12.
23. Hierlihy AM, Seale P, Lobe CG, Rudnicki MA, Megeney LA. The post-natal heart contains a myocardial stem cell population. *FEBS Lett*. 2002;530:239–243.
24. Oyama T, Nagai T, Wada H, Naito AT, Matsuura K, Iwanaga K, Takahashi T, Goto M, Mikami Y, Yasuda N, Akazawa H, Uezumi A, Takeda S, Komuro I. Cardiac side population cells have a potential to migrate and differentiate into cardiomyocytes in vitro and in vivo. *J Cell Biol*. 2007;176:329–341.
25. Pfister O, Oikonomopoulos A, Sereti KI, Sohn RL, Cullen D, Fine GC, Mouquet F, Westerman K, Liao R. Role of the ATP-binding cassette transporter abcg2 in the phenotype and function of cardiac side population cells. *Circ Res*. 2008;103:825–835.
26. Mouquet F, Pfister O, Jain M, Oikonomopoulos A, Ngoy S, Summer R, Fine A, Liao R. Restoration of cardiac progenitor cells after myocardial infarction by self-proliferation and selective homing of bone marrow-derived stem cells. *Circ Res*. 2005;97:1090–1092.
27. Jain M, DerSimonian H, Brenner DA, Ngoy S, Teller P, Edge AS, Zawadzka A, Wetzel K, Sawyer DB, Colucci WS, Apstein CS, Liao R. Cell therapy attenuates deleterious ventricular remodeling and improves cardiac performance after myocardial infarction. *Circulation*. 2001;103:1920–1927.
28. Bauer M, Cheng S, Jain M, Ngoy S, Theodoropoulos C, Trujillo A, Lin FC, Liao R. Echocardiographic speckle-tracking-based strain imaging for rapid cardiovascular phenotyping in mice. *Circ Res*. 2011;108:908–916.
29. Jones SE, Jomary C. Secreted frizzled-related proteins: searching for relationships and patterns. *Bioessays*. 2002;24:811–820.
30. Biechele TL, Moon RT. Assaying beta-catenin/TCF transcription with beta-catenin/TCF transcription-based reporter constructs. *Methods Mol Biol*. 2008;468:99–110.
31. Yamada PM, Lee KW. Perspectives in mammalian igfbp-3 biology: local vs systemic action. *Am J Physiol Cell Physiol*. 2009;296:C954–C976.
32. D'Amario D, Cabral-Da-Silva MC, Zheng H, Fiorini C, Goichberg P, Steadman E, Ferreira-Martins J, Sanada F, Piccoli M, Cappetta D, D'Alessandro DA, Michler RE, Hosoda T, Anastasia L, Rota M, Leri A, Anversa P, Kajstura J. Insulin-like growth factor-1 receptor identifies a pool of human cardiac stem cells with superior therapeutic potential for myocardial regeneration. *Circ Res*. 2011;108:1467–1481.
33. Buckway CK, Wilson EM, Ahlsen M, Bang P, Oh Y, Rosenfeld RG. Mutation of three critical amino acids of the n-terminal domain of IGF-binding protein-3 essential for high affinity IGF binding. *J Clin Endocrinol Metab*. 2001;86:4943–4950.
34. Chien AJ, Moore EC, Lonsdorf AS, Kulikauskas RM, Rothberg BG, Berger AJ, Major MB, Hwang ST, Rimm DL, Moon RT. Activated Wnt/beta-catenin signaling in melanoma is associated with decreased proliferation in patient tumors and a murine melanoma model. *Proc Natl Acad Sci U S A*. 2009;106:1193–1198.
35. Lu XF, Jiang XG, Lu YB, Bai JH, Mao ZB. Characterization of a novel positive transcription regulatory element that differentially regulates the insulin-like growth factor binding protein-3 (igfbp-3) gene in senescent cells. *J Biol Chem*. 2005;280:22606–22615.
36. Paquette J, Bessette B, Ledru E, Deal C. Identification of upstream stimulatory factor binding sites in the human igfbp3 promoter and potential implication of adjacent single-nucleotide polymorphisms and responsiveness to insulin. *Endocrinology*. 2007;148:6007–6018.
37. Schweighofer B, Testori J, Sturtzel C, Sattler S, Mayer H, Wagner O, Bilban M, Hofer E. The Vegf-induced transcriptional response comprises

gene clusters at the crossroad of angiogenesis and inflammation. *Thromb Haemost*. 2009;102:544–554.
38. McCabe CD, Spyropoulos DD, Martin D, Moreno CS. Genome-wide analysis of the homeobox c6 transcriptional network in prostate cancer. *Cancer Res*. 2008;68:1988–1996.
39. Baurand A, Zelarayan L, Betney R, Gehrke C, Dunger S, Noack C, Busjahn A, Huelsken J, Taketo MM, Birchmeier W, Dietz R, Bergmann MW. Beta-catenin downregulation is required for adaptive cardiac remodeling. *Circ Res*. 2007;100:1353–1362.
40. Chen Y, Guo Y, Ge X, Itoh H, Watanabe A, Fujiwara T, Kodama T, Aburatani H. Elevated expression and potential roles of human sp5, a member of sp transcription factor family, in human cancers. *Biochem Biophys Res Commun*. 2006;340:758–766.
41. Burger AM, Leyland-Jones B, Banerjee K, Spyropoulos DD, Seth AK. Essential roles of igfbp-3 and igfbp-rp1 in breast cancer. *Eur J Cancer*. 2005;41:1515–1527.
42. Hwa V, Oh Y, Rosenfeld RG. The insulin-like growth factor-binding protein (IGFBP) superfamily. *Endocr Rev*. 1999;20:761–787.
43. Watanabe S, Tamura T, Ono K, Horiuchi H, Kimura T, Kita T, Furukawa Y. Insulin-like growth factor axis (insulin-like growth factor-I/insulin-like growth factor-binding protein-3) as a prognostic predictor of heart failure: association with adiponectin. *Eur J Heart Fail*. 2010;12:1214–1222.
44. Murphy LJ, Molnar P, Lu X, Huang H. Expression of human insulin-like growth factor-binding protein-3 in transgenic mice. *J Mol Endocrinol*. 1995;15:293–303.
45. Zhu W, Shiojima I, Ito Y, Li Z, Ikeda H, Yoshida M, Naito AT, Nishi J, Ueno H, Umezawa A, Minamino T, Nagai T, Kikuchi A, Asashima M, Komuro I. Igfbp-4 is an inhibitor of canonical Wnt signalling required for cardiogenesis. *Nature*. 2008;454:345–349.
46. Ueno K, Hirata H, Majid S, Tabatabai Z, Hinoda Y, Dahiya R. Igfbp-4 activates the Wnt/beta-catenin signaling pathway and induces m-cam expression in human renal cell carcinoma. *Int J Cancer*. 2011;129:2360–2369.
47. Alfaro MP, Pagni M, Vincent A, Atkinson J, Hill MF, Cates J, Davidson JM, Rottman J, Lee E, Young PP. The Wnt modulator sfrp2 enhances mesenchymal stem cell engraftment, granulation tissue formation and myocardial repair. *Proc Natl Acad Sci U S A*. 2008;105:18366–18371.
48. Mirotsou M, Zhang Z, Deb A, Zhang L, Gnecchi M, Noiseux N, Mu H, Pachori A, Dzau V. Secreted frizzled related protein 2 (sfrp2) is the key akt-mesenchymal stem cell-released paracrine factor mediating myocardial survival and repair. *Proc Natl Acad Sci U S A*. 2007;104:1643–1648.
49. Bergmann MW. Wnt signaling in adult cardiac hypertrophy and remodeling: lessons learned from cardiac development. *Circ Res*. 2010;107:1198–1208.
50. Barandon L, Couffinhal T, Ezan J, Dufourcq P, Costet P, Alzieu P, Leroux L, Moreau C, Dare D, Duplaa C. Reduction of infarct size and prevention of cardiac rupture in transgenic mice overexpressing frza. *Circulation*. 2003;108:2282–2289.
51. Zelarayan LC, Noack C, Sekkali B, Kmecova J, Gehrke C, Renger A, Zafiriou MP, van der Nagel R, Dietz R, de Windt LJ, Balligand JL, Bergmann MW. Beta-catenin downregulation attenuates ischemic cardiac remodeling through enhanced resident precursor cell differentiation. *Proc Natl Acad Sci U S A*. 2008;105:19762–19767.
52. Aisagbonhi O, Rai M, Ryzhov S, Atria N, Feoktistov I, Hatzopoulos AK. Experimental myocardial infarction triggers canonical Wnt signaling and endothelial-to-mesenchymal transition. *Dis Model Mech*. 2011;4:469–483.
53. Oerlemans MI, Goumans MJ, van Middelaar B, Clevers H, Doevendans PA, Sluijter JP. Active Wnt signaling in response to cardiac injury. *Basic Res Cardiol*. 2010;105:631–641.

Novelty and Significance

What Is Known?

- Cardiac side population (CSP) cells represent an endogenous pool of progenitor cells in the adult heart.
- The molecular mechanisms that dictate the homeostasis and cell fate of CSP cells remain elusive.
- Wnt signals are key molecules that govern cardiac development and proliferation of embryonic stem cells, though their role in regulating adult cardiac progenitor cells remains unknown.

What New Information Does This Article Contribute?

- Activation of Wnt signaling pathway negatively regulates the proliferation capacity of adult CSP cells and compromises the endogenous regenerative capacity of the heart after myocardial infarction.
- Wnt stimulation exerts its antiproliferative effects through a previously unappreciated transcriptional activation of insulin-like growth factor binding protein 3 (IGFBP3).

Designing novel therapeutic approaches to modulate the endogenous regenerative capacity of the failing heart represents a desirable, although challenging, task. Understanding the basic mechanisms that control homeostasis of cardiac precursors, such as CSP cells, is of fundamental importance in achieving this goal. The Wnt signaling pathway is a key modulator of cardiac development and a major factor that determines cell fate, particularly in embryonic stem cell populations. However, the role of Wnt signaling in adult cardiac progenitor cells remains unclear. Our work reveals an antiproliferative effect for Wnt signaling in adult CSP cells through a previously unappreciated transcriptional interaction with IGBFP3 and direct regulation of CSP cell cycle progression. After cardiac injury in vivo, Wnt signaling is downregulated in CSP cells with corresponding increase in CSP cell proliferation. Increasing Wnt stimulation after myocardial infarction in CSP cells compromises the endogenous regenerative capacity of the heart and is associated with worsening of cardiac remodeling. Our findings demonstrate that canonical Wnt signaling is a potent modulator of endogenous adult cardiac progenitor cells and suggest that modulation of Wnt signaling or IGFBP3 may could be an effective therapeutic strategy for promoting cardiac regeneration.

Circulation Research
JOURNAL OF THE AMERICAN HEART ASSOCIATION

Role of the ATP-Binding Cassette Transporter *Abcg2* in the Phenotype and Function of Cardiac Side Population Cells

Otmar Pfister, Angelos Oikonomopoulos, Konstantina-Ioanna Sereti, Regina L. Sohn, Darragh Cullen, Gabriel C. Fine, Frédéric Mouquet, Karen Westerman and Ronglih Liao

Circ Res. 2008;103:825-835; originally published online September 11, 2008;
doi: 10.1161/CIRCRESAHA.108.174615
Circulation Research is published by the American Heart Association, 7272 Greenville Avenue, Dallas, TX 75231

Print ISSN: 0009-7330. Online ISSN: 1524-4571

Role of the ATP-Binding Cassette Transporter *Abcg2* in the Phenotype and Function of Cardiac Side Population Cells

Otmar Pfister,* Angelos Oikonomopoulos,* Konstantina-Ioanna Sereti,* Regina L. Sohn, Darragh Cullen, Gabriel C. Fine, Frédéric Mouquet, Karen Westerman, Ronglih Liao

Abstract—Recently, the side population (SP) phenotype has been introduced as a reliable marker to identify subpopulations of cells with stem/progenitor cell properties in various tissues. We and others have identified SP cells from postmitotic tissues, including adult myocardium, in which they have been suggested to contribute to cellular regeneration following injury. SP cells are identified and characterized by a unique efflux of Hoechst 33342 dye. *Abcg2* belongs to the ATP-binding cassette (ABC) transporter superfamily and constitutes the molecular basis for the dye efflux, hence the SP phenotype, in hematopoietic stem cells. Although *Abcg2* is also expressed in cardiac SP (cSP) cells, its role in regulating the SP phenotype and function of cSP cells is unknown. Herein, we demonstrate that regulation of the SP phenotype in cSP cells occurs in a dynamic, age-dependent fashion, with *Abcg2* as the molecular determinant of the cSP phenotype in the neonatal heart and another ABC transporter, *Mdr1,* as the main contributor to the SP phenotype in the adult heart. Using loss- and gain-of-function experiments, we find that *Abcg2* tightly regulates cell fate and function. Adult cSP cells isolated from mice with genetic ablation of *Abcg2* exhibit blunted proliferation capacity and augmented cell death. Conversely, overexpression of *Abcg2* is sufficient to enhance cell proliferation, although with a limitation of cardiomyogenic differentiation. In summary, for the first time, we reveal a functional role for *Abcg2* in modulating the proliferation, differentiation, and survival of adult cSP cells that goes beyond its distinct role in Hoechst dye efflux. **(*Circ Res*. 2008;103:825-835.)**

Key Words: *Abcg2* ■ *Mdr1* ■ progenitor cells ■ proliferation ■ SP cells

Recently, the side population (SP) phenotype has been introduced as a reliable marker to identify subpopulations of cells with stem/progenitor cell properties in various tissues including the heart.[1] On the molecular level, the SP phenotype is linked to the presence of ATP-binding cassette (ABC) transporters with the ability to efficiently efflux the DNA binding dye Hoechst 33342.[2] This ABC transporter–dependent Hoechst efflux phenomenon confers the characteristic fluorescent-activated cell sorting (FACS) profile of SP cells as a Hoechst-low "side population" located to the periphery of the Hoechst-high main population.[2]

Among the various members of the ABC transporter superfamily, *Abcg2* (also referred to as breast cancer resistance protein 1 [*Bcrp1*]) and *Mdr1* (also referred to as P-glycoprotein [*p-gp*] or *Abcb1*) have been shown to efficiently efflux Hoechst 33342 and thereby confer the SP phenotype.[3] Although both transporters are highly expressed in bone marrow (BM)SP cells, studies performed in mice with targeted disruption of the *Mdr1a* and *Mdr1b* genes, the murine homologs of the human Abcb1/Mdr1 gene, demonstrated that *Abcg2* is the sole molecular determinant of the SP phenotype in hematopoietic stem cells.[4] Moreover, *Abcg2* expression is conserved in SP cells from a wide range of tissues including blood, gonad, lung, skeletal muscle and the retina, suggesting an important role of *Abcg2* in stem cells.[4–7]

We and others have characterized SP cells isolated from adult myocardium.[8–11] These cardiac (c)SP cells are phenotypically distinct from BMSP cells, in that they are not hematopoietic but exhibit the potential to differentiate into functional cardiomyocytes.[10] As in SP cells from the bone marrow, *Abcg2* is expressed in SP cells from the heart.[9] The contribution of *Abcg2* to the cSP phenotype and its biological significance in cSP progenitor cells, however, remain unknown. In this study, we find that the contribution of *Abcg2* to the SP phenotype in the heart exists in an age-dependent manner, with *Abcg2* as the molecular determinant of the SP phenotype in the neonatal heart and *Mdr1* as the basis for the SP phenotype in the adult heart. In addition, we demonstrate

Original received February 25, 2008; revision received August 27, 2008; accepted August 28, 2008.

From the Cardiac Muscle Research Laboratory (O.P., A.O., K.-I.S., R.L.S., D.C., G.C.F., F.M., R.L.), Cardiovascular Division, Department of Medicine; and Department of Anesthesia (K.W.), Brigham and Women's Hospital, Harvard Medical School, Boston, Mass; School of Medicine (A.O., K.-I.S.), University of Crete, Greece; and University of Washington School of Medicine (G.C.F.), Seattle. Present address for O.P.: Myocardial Research, Department of Biomedicine, and Division of Cardiology, University Hospital Basel, Switzerland. Present address for F.M.: Cardiologie C, Lille University Hospital, France.

*These authors contributed equally to this work.

Correspondence to Dr Ronglih Liao, Division of Cardiology, Department of Medicine, Brigham and Women's Hospital, Harvard Medical School, 77 Ave Louis Pasteur, NRB 431, Boston, MA 02115. E-mail rliao@rics.bwh.harvard.edu

Circulation Research **is available at http://circres.ahajournals.org** **DOI: 10.1161/CIRCRESAHA.108.174615**

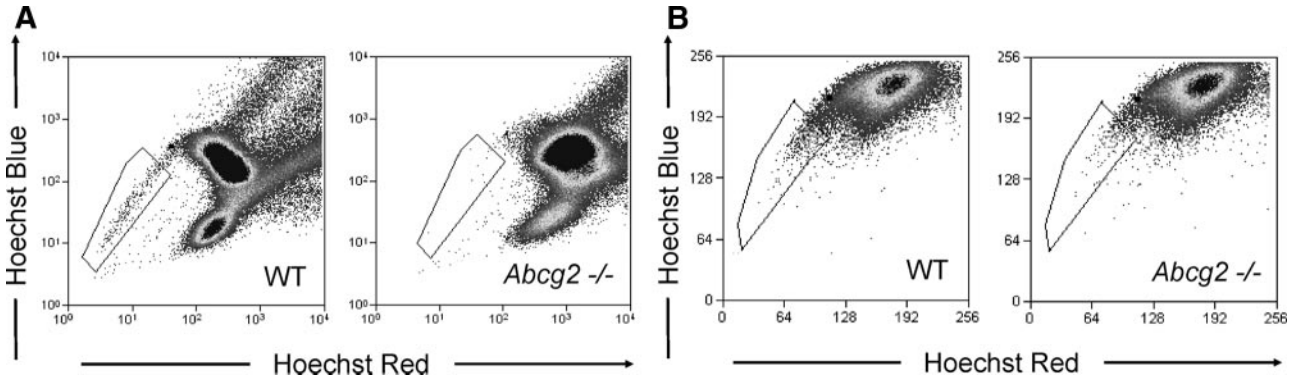

Figure 1. The role of *Abcg2* in mediating the SP cell phenotype in bone marrow and cardiac cells. FACS analyses carried out on Hoechst-stained bone marrow and cardiac cells from WT and *Abcg2*$^{-/-}$ mice. Hoechst-extruding SP cells are located in the boxed area. Compared to WT cells, bone marrow cells from *Abcg2*$^{-/-}$ mice lack a detectable SP cell population (A), whereas cardiac cells from *Abcg2*$^{-/-}$ mice exhibit a clearly detectable SP cell population (B).

that *Abcg2* plays a crucial role in the maintenance of cSP progenitor cells by promoting cell proliferation and survival, while inhibiting lineage commitment. Intriguingly, for the first time, we reveal a functional role of *Abcg2* in modulating proliferation, differentiation, and survival of cSP cells that goes beyond its distinct role of Hoechst dye efflux.

Materials and Methods

Animals

Male mice with genetic ablation of *Abcg2* (*Abcg2*$^{-/-}$) or *Mdr1a/b* (*Mdr1a/b*$^{-/-}$) were purchased from Taconic (catalog nos. 002767-M and 001487-MM; Germantown, NY). Age-matched FVB mice were also purchased from Taconic to serve as wild-type (WT) control. Mice were studied at postnatal day (p)3, p14, and p21 and between 8 and 12 weeks of age (adult). All animal studies strictly adhered to the guidelines of the Harvard Medical School, the Institutional Animal Care and Use Committee of the Longwood Medical Area, and the National Society for Medical Research.

Cardiac and BMSP Cell Preparation

Cardiomyocyte-depleted mononuclear cell suspensions were prepared as previously described to obtain cSP cells.[10] (For details, see the expanded Materials and Methods section in the online data supplement, available at http://circres.ahajournals.org.) BMSP cells were isolated form the tibia and femur as previously described.[1]

Cell Viability Assay

Cell death was determined by an annexin V kit (Abcam) using FACS analysis, and cell viability was determined by CellTiter-Glo and CellTiter-Blue (Promega) using a luminescence/fluorescence plate reader, respectively, according to the instructions of the manufacturer.

cSP Expansion and Lentiviral Infection

Freshly isolated cSP cells were cultured in expansion medium (α-MEM culture medium supplemented with 20% FBS, 2 mmol/L L-glutamine, and 1% penicillin/streptomycin). Vector pSPORT1 (American Type Culture Collection vector no. 10471063) was enzymatically digested with *Bam*HI, and the resulting Abcg2 cDNA was blunted and subsequently cloned into the HPV-422 lentivirus vector (kindly provided by Dr P. Allen, Brigham and Women's Hospital, Harvard Medical School, Boston, Mass). The bicistronic vector HPV-422 encodes the Abcg2 and IRES-GFP under the promoter EF1a. WT cSP cells from passage 4 to 6 were infected with the *Abcg2*-IRES-GFP lentivirus, and 48 hours postinfection green fluorescent protein–positive (GFP^{+}) cSP cells were sorted and further expanded. Culture medium was replaced every 72 hours.

Proliferation Assays

The proliferative capacity of cSP cells was determined in expanded passage 4 to 6 cSP cells using total cell number, expression of Ki67 and phospho-histone H_3, total protein, and total DNA. For detailed protocols, see the online data supplement.

Cardiomyogenic Differentiation Capacity

The role of *Abcg2* in regulating the ability of cSP cells to undergo cardiomyogenic differentiation was determined in our established coculture system.[10] cSP cells were transfected with GFP-expressing lentivirus, and cocultures were stained for α-sarcomeric actinin (Sigma). (For details, see the online data supplement.)

Statistical Analysis

Statistical differences between groups were evaluated using Student's unpaired *t* test or ANOVA, as appropriate. All data are presented as means±SEM. A probability value of <0.05 was considered statistically significant.

Results

Abcg2 Regulates the SP Phenotype in cSP Cells in an Age-Dependent Manner

Given published data suggesting that *Abcg2* is the sole molecular determinant of the SP cell phenotype in bone marrow cells, we first sought to determine whether *Abcg2* also regulates the SP phenotype in cardiac cells. To establish the role of *Abcg2* in mediating the SP cell phenotype, bone marrow and cardiac cell suspensions were isolated from 8- to 12-week-old age-matched mice with genetic ablation of *Abcg2* (*Abcg2*$^{-/-}$) and WT counterparts. FACS analysis of bone marrow cell suspensions from *Abcg2*$^{-/-}$ mice demonstrated a complete lack of BMSP cells (WT: 0.20±0.05%; *Abcg2*$^{-/-}$: 0.02±0.02%) compared to WT mice, suggesting that *Abcg2* is indeed required for conferring the SP phenotype in bone marrow cells (Figure 1A). In contrast, cSP cells from *Abcg2*$^{-/-}$ hearts revealed a clearly detectable, although significantly reduced, SP population (WT: 0.8±0.1%; *Abcg2*$^{-/-}$: 0.46±0.1%) (Figure 1B).

To confirm the correct FACS gating of SP cells (Figure 2A and 2B), we used 2 potent inhibitors of ABC transporters, verapamil and fumitremorgin C (FTC). Treatment of cells with verapamil or FTC completely abolished the SP cell band in both WT and *Abcg2*$^{-/-}$ cardiac cell suspensions (Figure 2C and 2F). To further verify that Hoechst dye efflux in *Abcg2*$^{-/-}$

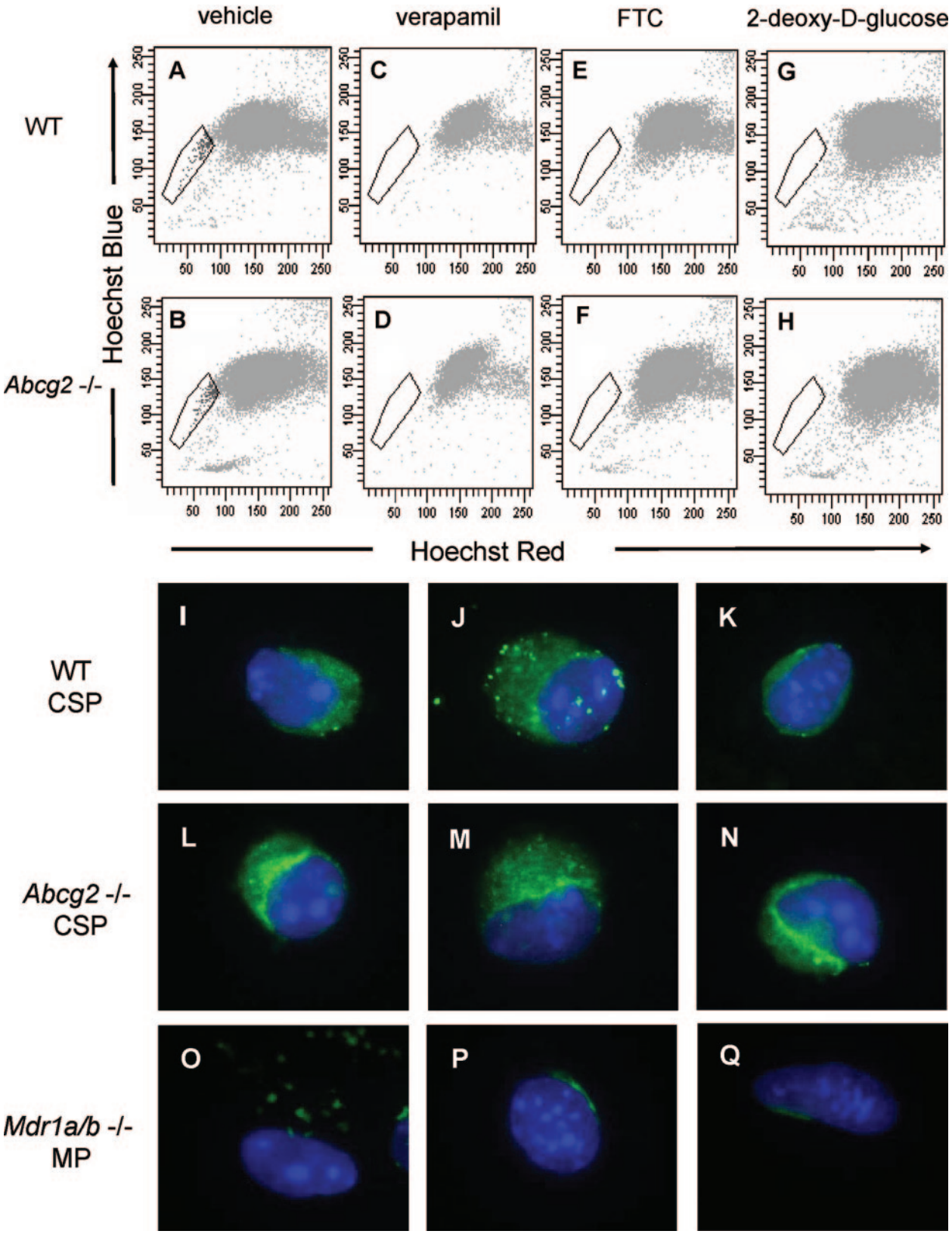

Figure 2. Hoechst dye efflux in *Abcg2*$^{-/-}$ cardiac cells is mediated by ATP-dependent ABC transporter function. FACS analyses of Hoechst-stained cardiac cells from WT and *Abcg2*$^{-/-}$ mice pretreated with either vehicle (A and B), the ABC transporter inhibitors verapamil (C and D), or FTC (E and F) or after ATP depletion with 2-deoxy-D-glucose (G and H). Similar to WT cardiac cells, inhibition of ABC-transporter function, as well as ATP depletion, completely abolishes the SP phenotype in *Abcg2*$^{-/-}$ cardiac cells, indicating that dye efflux in *Abcg2*$^{-/-}$ cardiac cell suspensions is mediated via ABC transporter activity. Immunocytochemical analysis demonstrates the expression of *Mdr1a/b* in freshly isolated WT and *Abcg2*$^{-/-}$ cSP cells (I through N). The lack of *Mdr1a/b* expression seen in *Mdr1a/b*$^{-/-}$ main population (MP) cells serves as negative control (O through Q).

Table. Cell Surface Marker Expression in WT and *Abcg2*$^{-/-}$ Cardiac SP Cells

Surface Marker	WT (%)	*Abcg2*$^{-/-}$ (%)
Sca-1	90±1	89±2
CD31	80±2	79±3
CD45	≤1	≤1

hearts was mediated via ABC transport, cardiac cell suspensions were preincubated with 2-deoxyglucose to deplete ATP and thereby inactivate ATP-dependent transporter function. Depletion of ATP also resulted in a complete loss of SP cells in both WT and *Abcg2*$^{-/-}$ cell suspensions, indicating that dye efflux in *Abcg2*$^{-/-}$ cell suspensions is indeed mediated in an ATP-dependent manner (Figure 2G and 2H).

We and others have previously shown that cSP cells express high levels of stem cell antigen 1 (Sca-1) and moderate levels of CD31 but lack the pan-hematopoietic marker CD45.[10] To further immunophenotypically characterize *Abcg2*$^{-/-}$ cSP cells, we compared the expression of cell surface markers, Sca-1, CD31 and CD45, in *Abcg2*$^{-/-}$ and WT cSP cells using FACS analysis. As shown in the Table, deficiency of *Abcg2* did not alter the expression pattern of Sca-1, CD31, and CD45, as compared to WT cSP cells, further suggesting that lacking *Abcg2* does not alter the expression pattern of major cell surface markers in adult cSP cells.

In addition to *Abcg2*, another member of the ABC transporter superfamily, the P-glycoprotein *Mdr1*, has been demonstrated to exhibit the capacity to efflux the Hoechst 33342 dye.[12] We therefore hypothesized that *Mdr1* may be involved in the regulation of the cSP phenotype in the adult heart. Quantitative RT-PCR analysis (Figure I in the online data supplement) and immunocytochemistry (Figure 2I through 2Q) in WT and *Abcg2*$^{-/-}$ cSP cells confirmed the expression of *Mdr1a* and *Mdr1b* genes and proteins independent of the expression of *Abcg2*.

To determine the contribution of *Mdr1* to the Hoechst 33342 efflux phenotype in the adult heart, cSP cells were isolated from hearts of adult mice with targeted disruption of *Mdr1a/b* genes. Strikingly, *Mdr1a/b*$^{-/-}$ hearts exhibited a severe depletion of cSP (Figure 3A). In contrast, bone marrow from *Mdr1a/b*$^{-/-}$ animals exhibited normal BMSP cell numbers (data not shown). To ensure that the limited number of cSP cells observed in *Mdr1a/b*$^{-/-}$ hearts was not attributable to experimental variables, in particular Hoechst concentration, cell ratio, and staining duration, we used an internal control by mixing 1 part of cardiomyocyte-depleted mononuclear cells ubiquitously expressing enhanced green fluorescent protein (GFP$^+$ control cells) with 3 parts of non-GFP, *Mdr1a/b*$^{-/-}$, or WT cardiomyocyte-depleted mononuclear cells (Figure 3B). Indeed, analysis of these cell mixtures revealed almost exclusively GFP$^+$ cells among the cSP cells (>98%), with no significant contribution from *Mdr1a/b*$^{-/-}$ cells to the SP band, thereby confirming the severely impaired Hoechst efflux capacity in *Mdr1a/b*$^{-/-}$ cSP cells (Figure 3B). In contrast, 1:3 cell mixtures of GFP$^+$ control cells and WT cardiac cells revealed only ≈25% GFP$^+$ control cells within the SP cell population, confirming the dye efflux competence of WT cardiac cells (Figure 3B).

Whereas *Abcg2* is enriched in early neonatal cSP cells, its expression level is markedly decreased postnatally.[9] To determine whether ABC-transporter expression in the heart is age-dependent, quantitative RT-PCR analysis for *Abcg2* and *Mdr1a/b* was performed in neonatal and adult mouse hearts. These analyses confirmed profound downregulation of *Abcg2* gene expression in the adult cSP cells as compared to the neonatal cSP cells. In contrast, *Mdr1a/b* expression levels demonstrated a reverse pattern with low expression in the neonatal cSP cells and high expression in the adult cSP cells (supplemental Figure II). To determine whether *Abcg2* and *Mdr1a/b* mediate the SP phenotype in cSP cells in an age-dependent manner, cSP cells were isolated from *Abcg2*$^{-/-}$, *Mdr1a/b*$^{-/-}$, and age-matched WT mice at p3, p14, and p21 and 8 to 12 weeks (adult) of age (Figure 4A through 4D). In contrast to adult hearts, early postnatal (p3) *Abcg2*$^{-/-}$ hearts demonstrated almost no detectable cSP cells, whereas a similar number of SP cells was observed in *Mdr1a/b*$^{-/-}$ and WT hearts (Figure 4A). The lack of Hoechst dye efflux was confirmed in cSP cells from *Abcg2*$^{-/-}$ hearts at p3 using GFP-mixing studies, similar to those described above (data not shown). A gradual decrease in cSP cells from p3 (9.4±1.2%) to adulthood (0.8±0.1%) was noted in WT hearts. *Abcg2*$^{-/-}$ hearts, however, demonstrated a gradual increase in cSP cells from day 3 postnatally (0.18±0.1%) to adult (0.46±0.1%) and thereafter maintained cSP cell levels into adulthood. The opposite profile was observed in *Mdr1a/b*$^{-/-}$ hearts, with cSP cell numbers dropping dramatically within the first 3 weeks of postnatal life and being barely detectable in adulthood. Taken together, these data demonstrate that the cSP cell phenotype is mediated by *Abcg2* and *Mdr1a/b* in an age-dependent fashion.

Abcg2 Regulates cSP Cell Proliferation

Expression of *Abcg2* has been associated with cellular proliferation in cancer cell lines.[13] Using gain- and loss-of-function approaches, we investigated the role of *Abcg2* in the regulation of cSP cell proliferation. cSP cells isolated from adult age-matched *Abcg2*$^{-/-}$ and WT mouse hearts were subjected to proliferation assays. As shown in Figure 5A, the proliferation capacity, as determined by total cell number, was markedly decreased in cSP cells lacking *Abcg2*. Consistent with the decrease in cell proliferation, the expression of the cell cycle markers Ki67 that identifies cells in G_1, S, G_2, and M phases (Figure 5B) and phospho-histone H_3 (Figure 5C and 5D) that identifies cells in M phase were decreased by ≈50% and ≈70%, respectively, in *Abcg2*$^{-/-}$ cSP cells when compared to WT cSP cells. Likewise, total protein and DNA content were significantly decreased in *Abcg2*$^{-/-}$ cSP cells cultured in the expansion media, thus further supporting impaired cell proliferation seen in *Abcg2*$^{-/-}$ cSP cells (Figure 5E and 5F). Conversely, the proliferation capacity was significantly enhanced in cSP cells following overexpression of *Abcg2* via lentiviral-mediated gene transfer, with an increase in both total cell number (Figure 5G) and expression of Ki67 (data not shown) as compared to WT cSP cells.

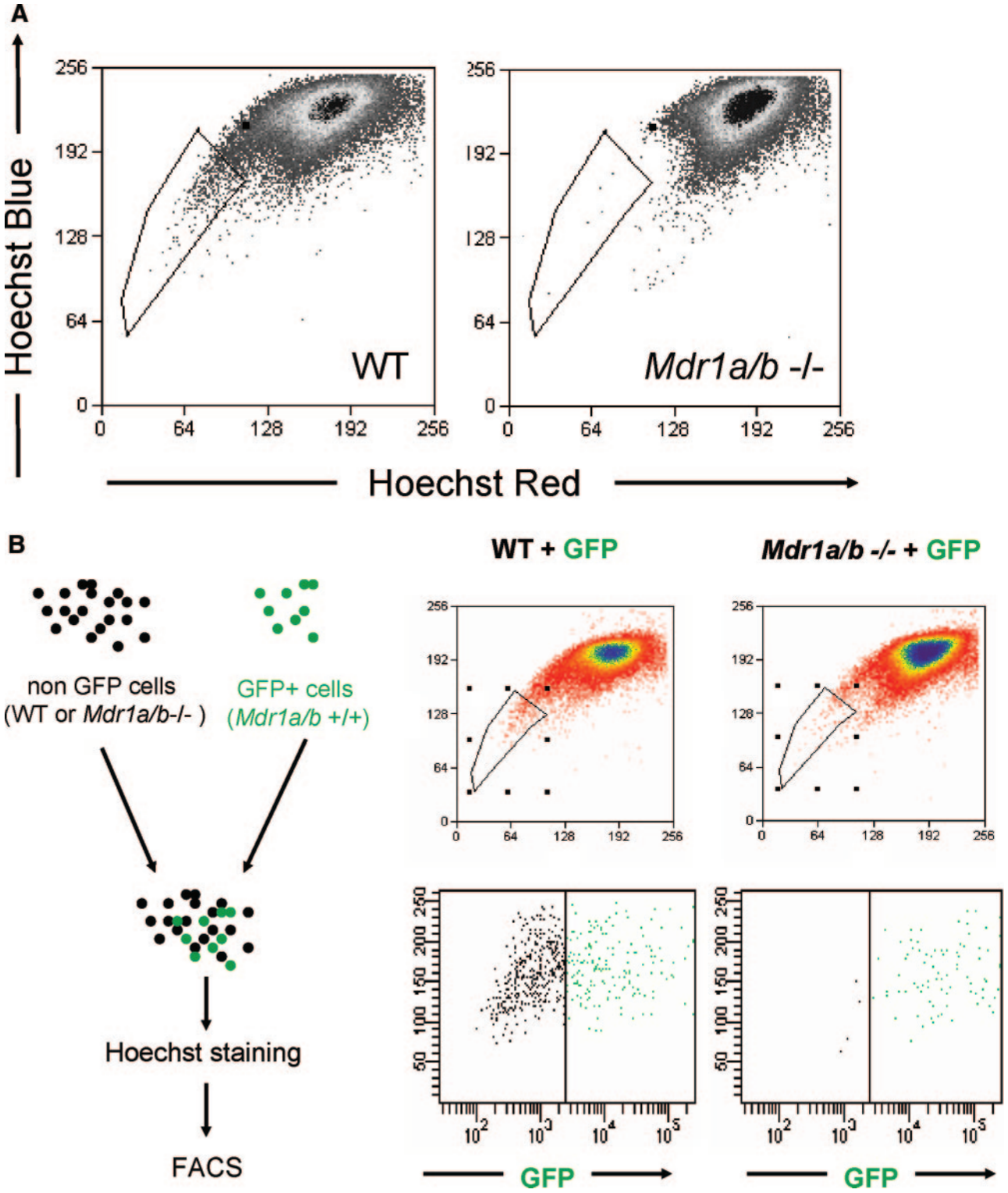

Figure 3. The ABC transporter *Mdr1a/b* mediates the Hoechst efflux phenotype of cSP cells in the adult heart. SP cell analyses of cardiac cells from WT and *Mdr1a/b*$^{-/-}$ mice. A, Compared to WT cells, *Mdr1a/b*$^{-/-}$ mononuclear cells almost completely lack cSP cells. B, SP cell analyses of cell mixtures containing 1 part of WT mononuclear cells expressing GFP and 3 parts of either WT or *Mdr1a/b*$^{-/-}$ mononuclear cells not expressing GFP. In cell mixtures containing WT cells, GFP^{+} cells account for ≈25% of total SP cells, thus reflecting the 1:3 ratio of the cell mixture. In cell mixtures containing GFP^{+} control and *Mdr1a/b*$^{-/-}$ cells, however, SP cells are almost exclusively GFP-positive, implicating a dominant role of *Mdr1a/b* in the mediation of the cSP cell phenotype in adult hearts.

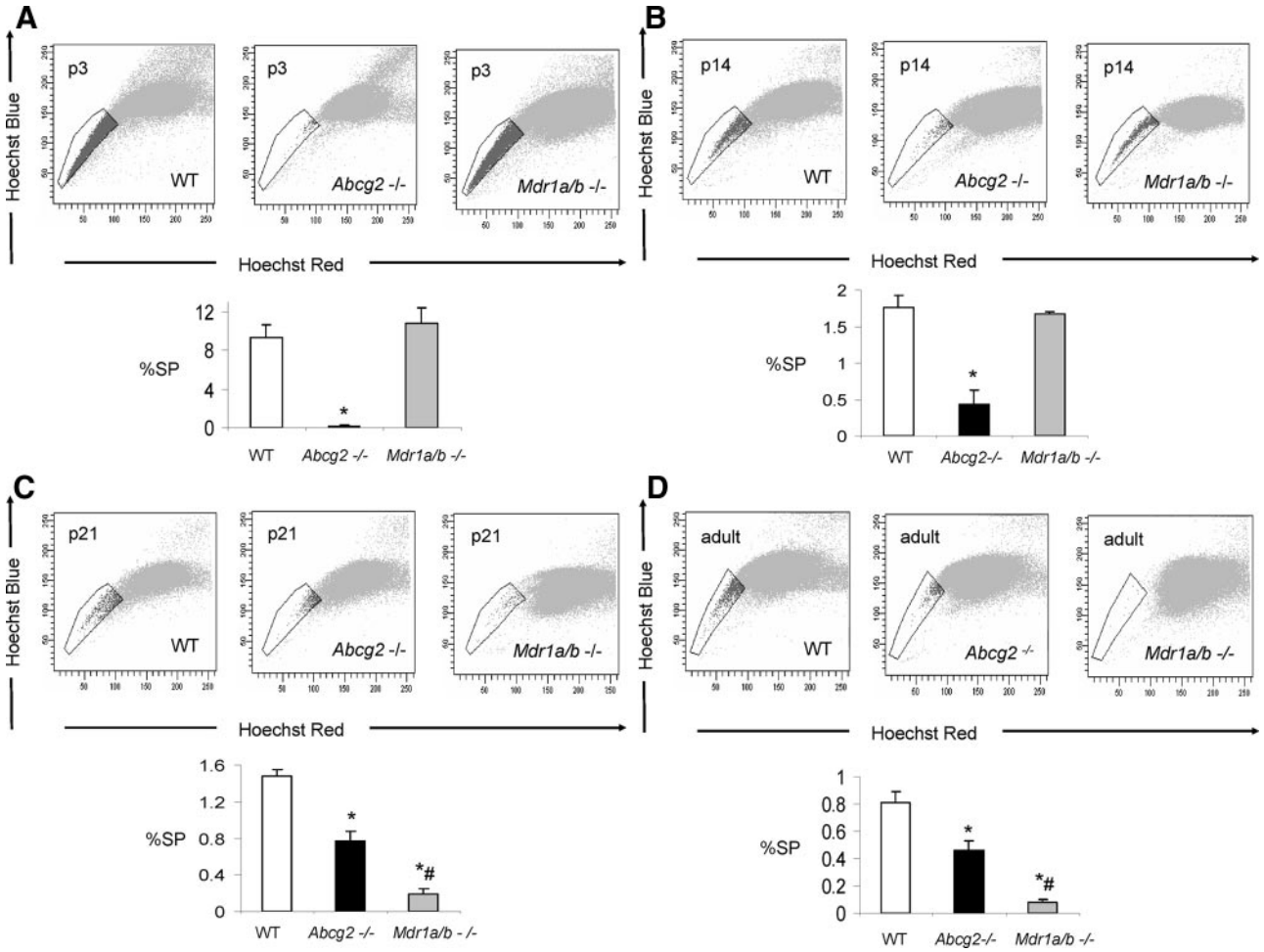

Figure 4. Age-dependent regulation of the cSP phenotype by *Abcg2* and *Mdr1a/b*. SP cell analyses of cardiac cells isolated from *Abcg2*$^{-/-}$, *Mdr1a/b*$^{-/-}$, and age-matched WT mice at p3, p14, and p21 and 8 to 12 weeks (adult) (A through D). A gradual decrease in cSP cells from early postnatal life through adulthood is evident in WT hearts. In contrast to WT hearts, early postnatal (p3) *Abcg2*$^{-/-}$ hearts demonstrate almost no detectable cSP cells, whereas similar numbers of SP cells are observed between *Mdr1a/b*$^{-/-}$ and WT hearts (A). During postnatal development, *Abcg2*$^{-/-}$ hearts demonstrate a steady increase in cSP cells from early postnatal into early adulthood (A through C) and maintain significant SP cell numbers throughout adulthood (D), whereas SP cell numbers of *Mdr1a/b*$^{-/-}$ hearts dramatically drop within the first 3 weeks of postnatal life and are barely detectable in adulthood (B through D).

Taken together, these data demonstrate a functional role of *Abcg2* in facilitating proliferation of cSP cells.

Regulation of cSP Cell Survival by *Abcg2*

Emerging evidence also suggests that *Abcg2* may play a critical role in protecting primitive cells from cellular injury.[14,15] To date, it is unclear whether *Abcg2* also exerts cell protective effects on cSP cells. To determine whether *Abcg2* is implicated in cSP cell survival, we first assessed apoptosis and necrosis in cSP cells under normal culture conditions using annexin V and propidium iodide staining, respectively. As illustrated in Figure 6A and 6B, even under normal culture conditions, significantly elevated numbers of both apoptotic and necrotic cells were observed in cSP cells lacking *Abcg2* as compared to WT cells. In addition, cell viability assays measuring cellular metabolic capacity by means of ATP quantitation (CellTiter-Glo, Promega) or conversion of the redox dye resazurin to the fluorescent end product resorufin (CellTiter-Blue, Promega) demonstrated significantly decreased metabolic capacity in *Abcg2*$^{-/-}$ cSP cells (Figure 6C and 6D), thus further confirming impaired viability.

Because oxidative stress is a common mediator of cell death in myocardial injury of various causes, we further investigated oxidative stress–induced cell death in WT and *Abcg2*$^{-/-}$ cSP cells after exposing cSP cell cultures to 200 μmol/L H_2O_2. In this model, oxidative stress–induced cell death was significantly higher in cSP cells lacking *Abcg2* as compared to WT cSP cells (Figure 6E). Taken together, our data indicate a protective role of *Abcg2* in cSP cells under normal culture (21% O_2) and H_2O_2-induced oxidative stress conditions.

Overexpression of *Abcg2* Impairs the Ability of cSP Cells to Undergo Cardiomyogenic Differentiation

Regulation of proliferation and differentiation maintains progenitor cell homeostasis. We have found that *Abcg2* is an essential regulator of cSP cell proliferation. We next sought to determine whether *Abcg2* mediates cardiomyogenic differentiation of cSP cells. Using a previously described coculture

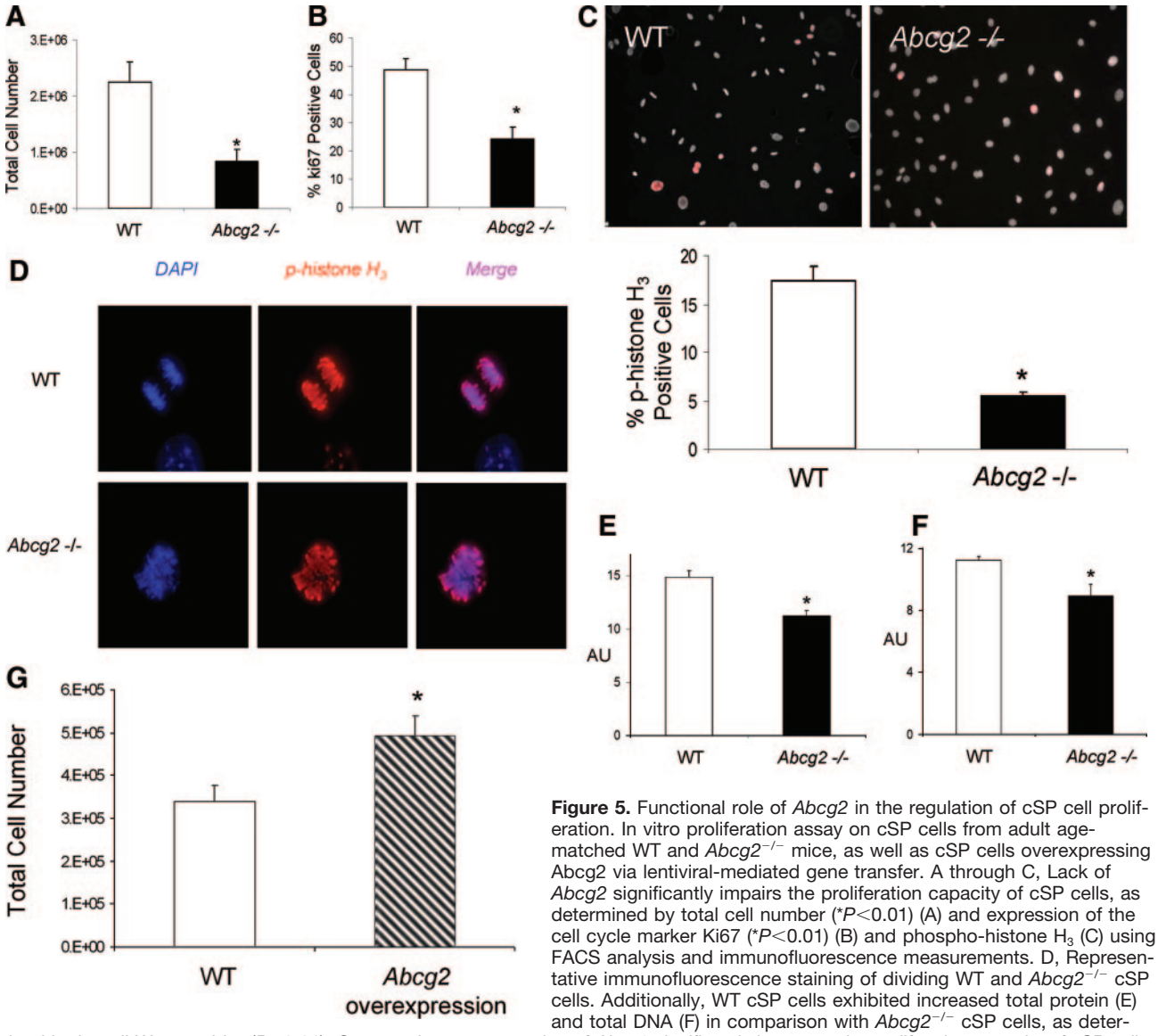

Figure 5. Functional role of *Abcg2* in the regulation of cSP cell proliferation. In vitro proliferation assay on cSP cells from adult age-matched WT and *Abcg2*$^{-/-}$ mice, as well as cSP cells overexpressing Abcg2 via lentiviral-mediated gene transfer. A through C, Lack of *Abcg2* significantly impairs the proliferation capacity of cSP cells, as determined by total cell number (*$P<0.01$) (A) and expression of the cell cycle marker Ki67 (*$P<0.01$) (B) and phospho-histone H_3 (C) using FACS analysis and immunofluorescence measurements. D, Representative immunofluorescence staining of dividing WT and *Abcg2*$^{-/-}$ cSP cells. Additionally, WT cSP cells exhibited increased total protein (E) and total DNA (F) in comparison with *Abcg2*$^{-/-}$ cSP cells, as determined by in-cell Western blot ($P<0.01$). Conversely, overexpression of *Abcg2* significantly increases the proliferation capacity of cSP cells in terms of (G) total cell number ($P<0.05$).

system with adult rat cardiomyocytes, cardiomyogenic differentiation was assessed in WT and *Abcg2*$^{-/-}$ cSP cells, as well as in *Abcg2*-overexpressing cSP cells (Figure 7A through 7I). To track the cell fate of cells in coculture, cSP cells were infected with lentivirus expressing GFP. Genetic deficiency of *Abcg2* did not limit the cardiomyogenic differentiation of cSP cells (Figure 7D through 7F). Overexpression of *Abcg2* via lentiviral-mediated gene transfer significantly decreased cardiomyogenic differentiation of cSP cells (Figure 7G through 7I). Moreover, overexpression of *Abcg2* maintained cSP cells in a proliferative state even under conditions promoting cardiomyogenic differentiation.

Discussion

Since the first isolation of BMSP cells more than a decade ago,[2] the SP phenotype has been widely used to identify stem/progenitor cells in various tissues.[2,7,16–19] More recently, the ABC transporter *Abcg2* has been identified as the sole molecular determinant of the SP phenotype in bone marrow cells.[4] However, the role of ABC transporters in the regulation of SP phenotype and function of cSP cells remains unknown. Herein, we demonstrate not only a dynamic, age-dependent regulation of the cSP phenotype by *Abcg2* but also a functional role of *Abcg2* in modulating proliferation, differentiation, and survival of cSP cells that goes beyond its distinct role in Hoechst dye efflux.

Role of *Abcg2* in Conferring the SP Phenotype in the Heart

Although *Abcg2* and *Mdr1* are both expressed in hematopoietic stem cells identified by the SP phenotype, *Abcg2* was shown to be the sole molecular determinant of the SP phenotype in bone marrow cells.[4] These findings in the bone marrow led to the assumption that *Abcg2* may also be

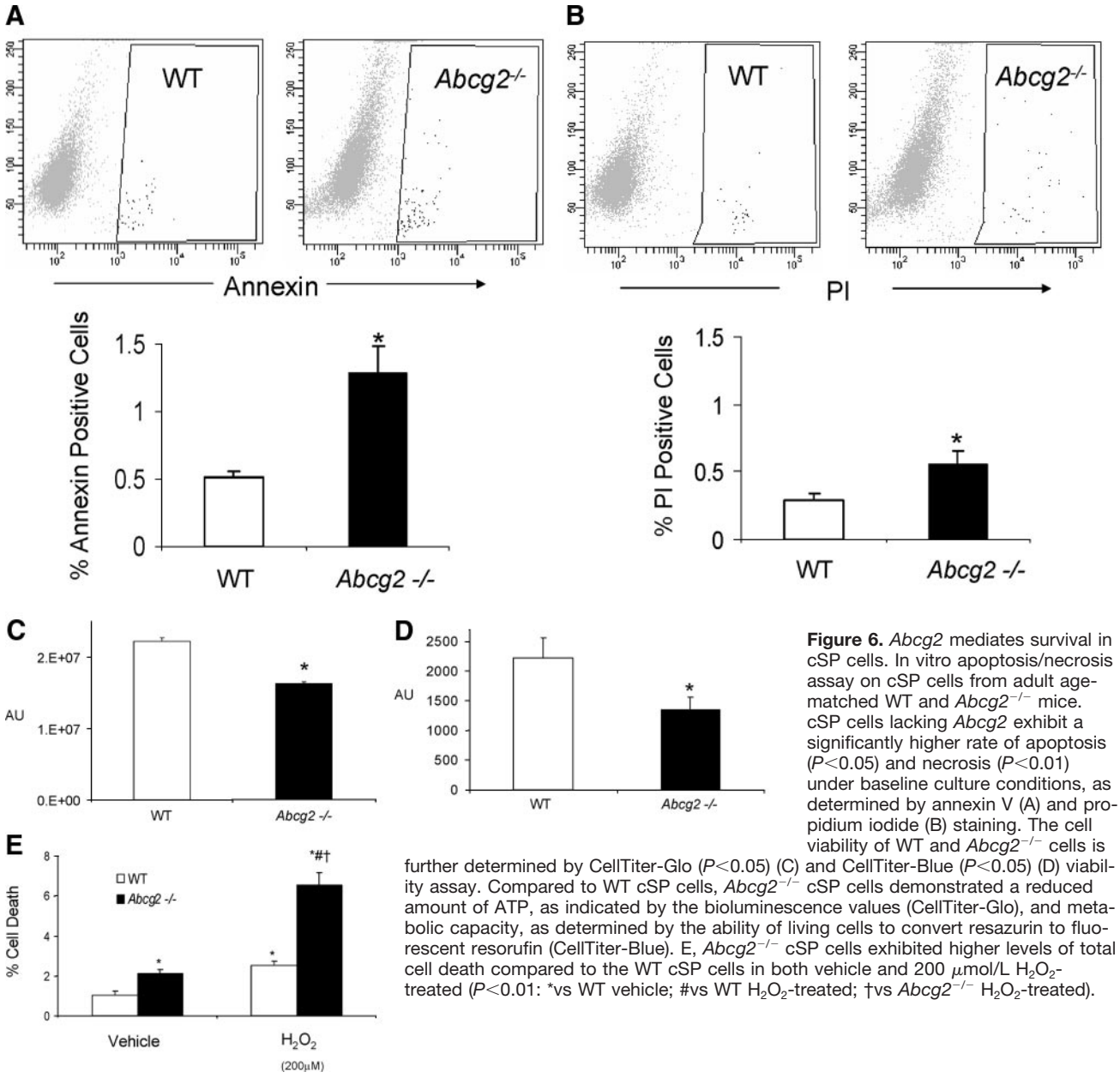

Figure 6. *Abcg2* mediates survival in cSP cells. In vitro apoptosis/necrosis assay on cSP cells from adult age-matched WT and *Abcg2*$^{-/-}$ mice. cSP cells lacking *Abcg2* exhibit a significantly higher rate of apoptosis ($P<0.05$) and necrosis ($P<0.01$) under baseline culture conditions, as determined by annexin V (A) and propidium iodide (B) staining. The cell viability of WT and *Abcg2*$^{-/-}$ cells is further determined by CellTiter-Glo ($P<0.05$) (C) and CellTiter-Blue ($P<0.05$) (D) viability assay. Compared to WT cSP cells, *Abcg2*$^{-/-}$ cSP cells demonstrated a reduced amount of ATP, as indicated by the bioluminescence values (CellTiter-Glo), and metabolic capacity, as determined by the ability of living cells to convert resazurin to fluorescent resorufin (CellTiter-Blue). E, *Abcg2*$^{-/-}$ cSP cells exhibited higher levels of total cell death compared to the WT cSP cells in both vehicle and 200 μmol/L H_2O_2-treated ($P<0.01$: *vs WT vehicle; #vs WT H_2O_2-treated; †vs *Abcg2*$^{-/-}$ H_2O_2-treated).

responsible for the dye efflux observed in SP cells isolated from other tissues, particularly given the preferential expression pattern of *Abcg2* in SP cells as compared to main population cells. Similar to their expression in bone marrow, *Abcg2* and *Mdr1* were shown to be expressed in the heart, although their contribution to the cSP phenotype remained to be elucidated. Using mouse models with targeted gene ablation of either *Abcg2* or *Mdr1*, we demonstrate that the cSP cell phenotype is not governed by a single ABC transporter but rather is regulated in an age-dependent manner by both *Abcg2* and *Mdr1*. Our findings show that during early postnatal development, *Abcg2* represents the main transporter responsible for dye efflux in cardiac cells and thus constitutes the molecular basis for the SP phenotype in the neonatal and early postnatal heart. This is in accordance with the role of *Abcg2* in bone marrow–derived cells and may indicate that cSP cells of the early postnatal heart share phenotypic characteristics of bone marrow–derived SP cells. Whether cSP cells developmentally originate from blood-borne cells, however, remains to be determined. It is important to point out that our present data provide no evidence to either support or dispute such notion. Prior data from our laboratory using labeled bone marrow transplantation, however, suggest that extracardiac stem cells only contribute to the maintenance of resident cSP cell pools following injury, with little role in the maintenance of cSP cell numbers under normal physiological conditions.[20]

Although our results agree with previous reports of persistent *Abcg2* expression in cSP cells throughout adulthood,[9] we find that the contribution of *Abcg2* to the SP phenotype diminishes in the adult heart. Our results show that very limited cSP cells can be detected in early neonatal *Abcg2*$^{-/-}$ hearts, with

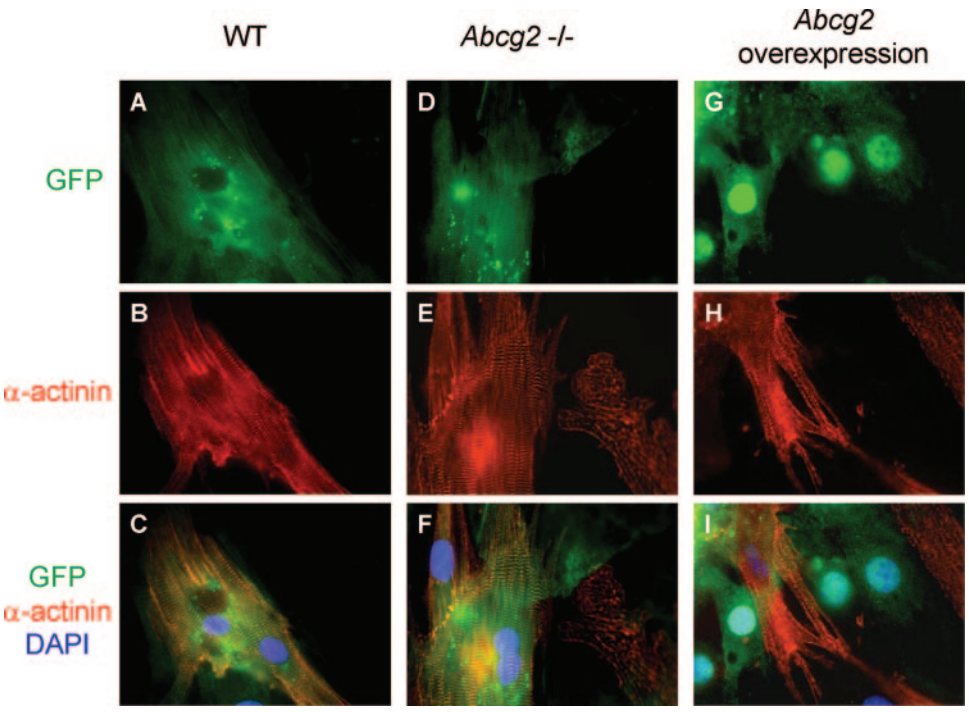

Figure 7. *Abcg2* overexpression prevents cardiomyogenic differentiation of cSP cells. Fluorescence images of WT (A through C), *Abcg2*$^{-/-}$ (D through F), and *Abcg2*-overexpressing (G through I) cSP cells in coculture with adult rat cardiomyocytes. Green fluorescence corresponds to GFP expression that identifies respective cSP cells (upper row). Red fluorescence corresponds to the expression of α-actinin, a marker of cardiomyogenic differentiation (middle row). Merged images show areas of colocalization of GFP and α-actinin in yellow (bottom row). In this differentiation assay, lack of *Abcg2* does not limit the cardiomyogenic differentiation of cSP cells, as demonstrated by α-actinin expression and appearance of clearly organized sarcomeric structures in differentiated *Abcg2*$^{-/-}$ cSP cells (D through F), similar to that seen in WT cells (A through C). *Abcg2* overexpression, however, prevents cSP cells from undergoing cardiomyogenic differentiation, as demonstrated by lack of α-actinin expression in *Abcg2*-overexpressing cSP cells cocultured with cardiomyocytes (G through I).

clearly detectable cSP cells in adult *Abcg2*$^{-/-}$ hearts, albeit at a lower total number as compared to WT hearts. These *Abcg2*$^{-/-}$ cSP cells are sensitive to verapamil, FTC, and 2-deoxyglucose treatment, thus suggesting that their Hoechst-extruding ability is mediated through another ABC transporter. Analyses of mice completely lacking *Mdr1* identified the P-glycoprotein as the essential ABC transporter for Hoechst efflux in adult cSP cells. It is important to note that the putative *Abcg2* inhibitor FTC, which was previously shown to have no effect on *Mdr1*-mediated mitoxantrone efflux in mitoxantrone-resistance-selected human colon carcinoma cell lines,[21] did inhibit *Mdr1*-mediated Hoechst efflux in cSP cells, suggesting that the specificity of FTC may depend on the cell type and the substrate.

Interestingly, this regulatory role of *Mdr1* in the cSP phenotype is limited to cSP cells from mice older than 3 weeks of age, with limited contribution of *Mdr1* to the SP phenotype in early neonatal mouse hearts. Although the origin of cardiac stem/progenitor cells and their relationship with bone marrow–derived stem cells remains speculative at this time, our data suggest that BMSP cells do not significantly contribute to the maintenance of cSP cells under physiological conditions, as evidenced by the lack of SP cells in adult *Mdr1a/b*$^{-/-}$ hearts, whereas *Mdr1a/b*$^{-/-}$ bone marrow contains normal SP cells. Thus, the present data are consistent with our previous findings demonstrating that BMSP cells only contribute to the maintenance of cSP cells following cardiac injury such as myocardial infarction.[20]

Our data dispute the perception that a single universal ABC transporter is responsible for the SP phenotype and suggest that developmental status and local microenvironment dictate the relative contribution of ABC transporters to the SP phenotype at the given tissue. In line with this observation is the recent demonstration of contribution of both *Mdr1* and *Abcg2* transporters to the SP phenotype in mammary glands.[22]

Role of *Abcg2* in Regulating the Function of cSP Cells

Abcg2 has been found to be highly expressed in various proliferating stem/progenitor cells and tumor cell lines, although its role in the regulation of SP cell proliferation and differentiation remains unknown. Using gain- and loss-of function approaches, we demonstrate that overexpression of *Abcg2* is sufficient to increase the proliferative capacity of cSP cells, whereas lack of *Abcg2* expression markedly impairs their expandability in vitro. The marked decrease in cells being in M phase of the cell cycle, as measured by phospho-histone H_3 expression, suggests that the absence of *Abcg2* may hamper cell cycle progression. This association of *Abcg2* expression with cell proliferation is in line with the findings in cancer cells, where *Abcg2* identified mainly fast cycling tumor progenitor cells.[13] Our data provide convincing evidence demonstrating that *Abcg2* may play a functional role in regulating the proliferation capacity of cSP cells, although the precise mechanisms are unknown. Further investigation, therefore, is warranted to dissect the molecular mechanisms by which *Abcg2* facilitates the cell cycle progression in cardiac progenitor cells.

In addition to enhancing cell proliferation, we show that *Abcg2* expression is necessary for protecting cSP cells from undergoing apoptosis and necrosis, specifically under condi-

tions of increased oxidative stress. A similar prosurvival effect of *Abcg2* was identified in trophoblast and hematopoietic stem cells.[14,23] Moreover, Martin et al recently demonstrated that expression of *Abcg2* induced low levels of oxidative stress in C2C12 myoblasts, which resulted in upregulation of cytoprotective and oxidative stress pathways.[15] The cytoprotective effect of such *Abcg2*-mediated ROS preconditioning was also confirmed in mouse embryonic fibroblasts that displayed reduced oxidative stress–induced cell death, when transfected with *Abcg2*.[15] Our data are in complete agreement with this concept by demonstrating increased tolerance of oxidative stress in *Abcg2*-competent WT cSP cells as compared to cSP cells lacking *Abcg2*.

Consistent with the notion that *Abcg2* maintains progenitor cells in a proliferative stage and is downregulated during lineage-specific differentiation, overexpression of *Abcg2* prevented cSP cells from undergoing cardiomyogenic differentiation. Our data are supported by the recently published work in hematopoietic and retinal stem cells demonstrating highly regulated *Abcg2* expression during stem cell differentiation with a sharp decline during lineage commitment.[4,5] In contrast, overexpression of *Abcg2* blocks the differentiation of hematopoietic and retinal stem cells, indicating a functional role of *Abcg2* in the maintenance of the stem cell pool.[4,5] In both cell types, overexpression of *Abcg2* leads to increased cell expansion and adversely affects their lineage commitment.

We have shown that overexpression of *Abcg2* not only promotes proliferation and survival of cSP cells but, at the same time, also inhibits cellular differentiation. Taken together, our data suggest that *Abcg2* is essential to the fate and function of cSP cells. As such, the tight regulation of *Abcg2* expression may be critical for maintaining progenitor cells in either a proproliferative or prodifferentiation state. Moreover, such regulation may be especially essential following tissue injury, during which a rapid increase in cSP cell proliferation is observed to replenish tissue SP cell pools.[20] Dysregulation of *Abcg2* expression may also result in uncontrolled cell growth or cell death. To date, the exact mechanism by which *Abcg2* prevents stem cells from lineage commitment remains to be elucidated. Considering the primary function of *Abcg2* as a detoxifying transmembrane pump, however, it is tempting to speculate that active extrusion of key molecules of the differentiation-promoting pathway might be involved in this process.

In summary, our study highlights the importance of *Abcg2* in regulating the function and homeostasis of cSP cells that goes beyond its traditional role as dye efflux transporter. Manipulation of *Abcg2* expression and function may be of particular importance in promoting cardiac regeneration following injury by both endogenous and exogenously delivered cSP cells. Given the role of *Abcg2* in the proliferation of cancer cells, as well as cSP cells, there is great potential for cardiac toxicity with emerging chemotherapeutic agents specifically targeting *Abcg2*. Further investigation into the role of *Abcg2* in cSP cells is of clinical importance to limit cancer drug–induced cardiac toxicity and to promote cardiac regeneration.

Acknowledgments

We thank Drs Richard C. Mulligan and Alejandro B. Balazs for help in the purification of SP cells and for useful discussions. Grigoriy Losyev at the Brigham and Women's Hospital Cardiovascular and Laura B. Prickett at the Massachusetts General Hospital FACS Cores are acknowledged for assistance with cell sorting.

Sources of Funding

This work was supported by NIH grants HL71775, HL86967, HL73756, and HL 88533 (to R.L.). A.O. and G.C.F. were supported by an American Heart Association Northeast Affiliate Predoctoral Fellowship and a Sarnoff Cardiovascular Research Foundation Fellowship, respectively.

Disclosures

None.

References

1. Challen GA, Little MH. A side order of stem cells: the SP phenotype. *Stem Cells*. 2006;24:3–12.
2. Goodell MA, Brose K, Paradis G, Conner AS, Mulligan RC. Isolation and functional properties of murine hematopoietic stem cells that are replicating in vivo. *J Exp Med*. 1996;183:1797–1806.
3. Bunting KD. ABC transporters as phenotypic markers and functional regulators of stem cells. *Stem Cells*. 2002;20:11–20.
4. Zhou S, Schuetz JD, Bunting KD, Colapietro AM, Sampath J, Morris JJ, Lagutina I, Grosveld GC, Osawa M, Nakauchi H, Sorrentino BP. The ABC transporter Bcrp1/ABCG2 is expressed in a wide variety of stem cells and is a molecular determinant of the side-population phenotype. *Nat Med*. 2001;7:1028–1034.
5. Bhattacharya S, Das A, Mallya K, Ahmad I. Maintenance of retinal stem cells by Abcg2 is regulated by notch signaling. *J Cell Sci*. 2007;120:2652–2662.
6. Lassalle B, Bastos H, Louis JP, Riou L, Testart J, Dutrillaux B, Fouchet P, Allemand I. 'Side Population' cells in adult mouse testis express Bcrp1 gene and are enriched in spermatogonia and germinal stem cells. *Development*. 2004;131:479–487.
7. Summer R, Kotton DN, Sun X, Ma B, Fitzsimmons K, Fine A. Side population cells and Bcrp1 expression in lung. *Am J Physiol Lung Cell Mol Physiol*. 2003;285:L97–L104.
8. Hierlihy AM, Seale P, Lobe CG, Rudnicki MA, Megeney LA. The post-natal heart contains a myocardial stem cell population. *FEBS Lett*. 2002;530:239–243.
9. Martin CM, Meeson AP, Robertson SM, Hawke TJ, Richardson JA, Bates S, Goetsch SC, Gallardo TD, Garry DJ. Persistent expression of the ATP-binding cassette transporter, Abcg2, identifies cardiac SP cells in the developing and adult heart. *Dev Biol*. 2004;265:262–275.
10. Pfister O, Mouquet F, Jain M, Summer R, Helmes M, Fine A, Colucci WS, Liao R. CD31- but Not CD31+ cardiac side population cells exhibit functional cardiomyogenic differentiation. *Circ Res*. 2005;97:52–61.
11. Oyama T, Nagai T, Wada H, Naito AT, Matsuura K, Iwanaga K, Takahashi T, Goto M, Mikami Y, Yasuda N, Akazawa H, Uezumi A, Takeda S, Komuro I. Cardiac side population cells have a potential to migrate and differentiate into cardiomyocytes in vitro and in vivo. *J Cell Biol*. 2007;176:329–341.
12. Bunting KD, Zhou S, Lu T, Sorrentino BP. Enforced P-glycoprotein pump function in murine bone marrow cells results in expansion of side population stem cells in vitro and repopulating cells in vivo. *Blood*. 2000;96:902–909.
13. Patrawala L, Calhoun T, Schneider-Broussard R, Zhou J, Claypool K, Tang DG. Side population is enriched in tumorigenic, stem-like cancer cells, whereas ABCG2+ and ABCG2− cancer cells are similarly tumorigenic. *Cancer Res*. 2005;65:6207–6219.
14. Krishnamurthy P, Ross DD, Nakanishi T, Bailey-Dell K, Zhou S, Mercer KE, Sarkadi B, Sorrentino BP, Schuetz JD. The stem cell marker Bcrp/ABCG2 enhances hypoxic cell survival through interactions with heme. *J Biol Chem*. 2004;279:24218–24225.
15. Martin CM, Ferdous A, Gallardo T, Humphries C, Sadek H, Caprioli A, Garcia JA, Szweda LI, Garry MG, Garry DJ. Hypoxia-inducible factor-

2alpha transactivates Abcg2 and promotes cytoprotection in cardiac side population cells. *Circ Res*. 2008;102:1075–1081.
16. Behbod F, Xian W, Shaw CA, Hilsenbeck SG, Tsimelzon A, Rosen JM. Transcriptional profiling of mammary gland side population cells. *Stem Cells*. 2006;24:1065–1074.
17. Hishikawa K, Marumo T, Miura S, Nakanishi A, Matsuzaki Y, Shibata K, Ichiyanagi T, Kohike H, Komori T, Takahashi I, Takase O, Imai N, Yoshikawa M, Inowa T, Hayashi M, Nakaki T, Nakauchi H, Okano H, Fujita T. Musculin/MyoR is expressed in kidney side population cells and can regulate their function. *J Cell Biol*. 2005;169:921–928.
18. Kotton DN, Fabian AJ, Mulligan RC. A novel stem-cell population in adult liver with potent hematopoietic-reconstitution activity. *Blood*. 2005; 106:1574–1580.
19. Rivier F, Alkan O, Flint AF, Muskiewicz K, Allen PD, Leboulch P, Gussoni E. Role of bone marrow cell trafficking in replenishing skeletal muscle SP and MP cell populations. *J Cell Sci*. 2004;117: 1979–1988.
20. Mouquet F, Pfister O, Jain M, Oikonomopoulos A, Ngoy S, Summer R, Fine A, Liao R. Restoration of cardiac progenitor cells after myocardial infarction by self-proliferation and selective homing of bone marrow-derived stem cells. *Circ Res*. 2005;97:1090–1092.
21. Rabindran SK, He H, Singh M, Brown E, Collins KI, Annable T, Greenberger LM. Reversal of a novel multidrug resistance mechanism in human colon carcinoma cells by fumitremorgin C. *Cancer Res*. 1998;58: 5850–5858.
22. Jonker JW, Freeman J, Bolscher E, Musters S, Alvi AJ, Titley I, Schinkel AH, Dale TC. Contribution of the ABC transporters Bcrp1 and Mdr1a/1b to the side population phenotype in mammary gland and bone marrow of mice. *Stem Cells*. 2005;23:1059–1065.
23. Evseenko DA, Murthi P, Paxton JW, Reid G, Emerald BS, Mohankumar KM, Lobie PE, Brennecke SP, Kalionis B, Keelan JA. The ABC transporter BCRP/ABCG2 is a placental survival factor, and its expression is reduced in idiopathic human fetal growth restriction. *FASEB J*. 2007;21: 3592–3605.